ELLIS HORWOOD BOOKS IN MINING AND MINERAL RESOURCES ENGINEERING

MECHANICAL ACTIVATION OF MINERALS BY GRINDING

pulverizing and morphology of particles

A. Z. Juhász and L. Opoczky

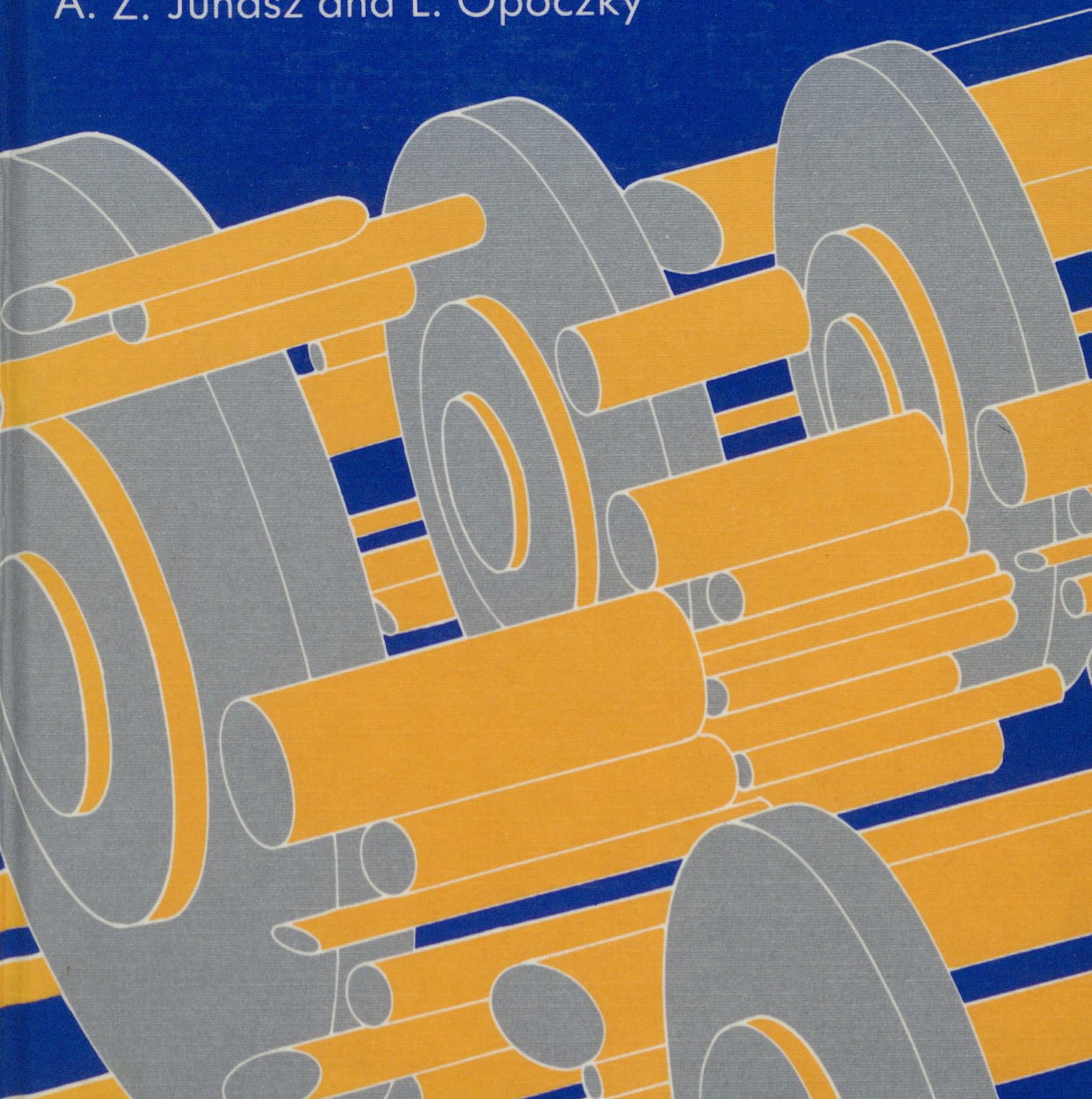

Mechanical Activation of Minerals by Grinding: Pulverizing and Morphology of Particles

10002

Mechanical Activation of Minerals by Grinding: Pulverizing and Morphology of Particles

A. Z. JUHÁSZ, Prof. D.Sc.
Veszprém University of Chemical Engineering
Veszprém, Hungary

and

L. OPOCZKY, Prof. D.Sc.
Central Research and Design Institute for
Silicate Industry
Budapest, Hungary

AKADÉMIAI KIADÓ · BUDAPEST 1990

MTA
KIK
0 00003 83294 3

674937

This is a revised version of the Hungarian
Szilikátok mechanikai aktiválása finomőrléssel, published by Akadémiai Kiadó

This monograph is published by Ellis Horwood Limited in the series "Mining and Mineral Resources Engineering"

Translated by M. NÓGRÁDI, D.Sc.

Translation editor M. P. JONES, Ph.D.

MAGYAR
TUDOMÁNYOS AKADÉMIA
KÖNYVTÁRA

ISBN 963 05 5329 5

© *A. Z. Juhász and L. Opoczky 1990*
© *English translation—M. Nógrádi 1990*

M. TUD. AKADÉMIA KÖNYVTÁRA
Könyvleltár. 3943/19. 90 sz.

Joint edition published by
Akadémiai Kiadó, Budapest, Hungary
and
Ellis Horwood Limited Publishers
Market Cross House, Cooper Street, Chichester, West Sussex, England

All rights reserved. No part of this book may be reproduced by any means or transmitted, or translated into machine language without the written permission of the publisher.

Printed in Hungary by Akadémiai Kiadó és Nyomda Vállalat, Budapest

CONTENTS

Preface 9

Chapter 1 11

1. General features of mechanical activation 11

1.1. The scope of mechano-chemistry 11
1.2. Mechanical activation by fine grinding 12
1.3. Modes of mechanical activation 13
Symbols in Chapter 1 15
References 15

Chapter 2 17

2. Characterisation and methods of examination of disperse systems 17

2.1. Characterisation of the bulk structure of solid disperse systems by the SPV system 17
2.2. Study of disperse systems 20
2.2.1. Determination of particle size 20
2.2.2. Particle size distribution 23
2.2.3. Specific surface area 28
2.2.3.1. Methods for determining specific surface 28
2.2.3.2. Determining specific surface on the basis of permeability 30
2.2.3.3. Methods of measuring specific surface by adsorption ... 33
2.2.4. Measurement of pore size and its distribution 36
2.2.5. Stability of bulk and compaction work 38
2.3. Methodology of investigating mechano-chemical phenomena 39
Symbols in Chapter 2 40
References 42

Chapter 3 44

3. Changes in the structure and in the chemical reactivity of solids due to deformation and fracture 44

3.1. Macroscopic phenomena in solids induced by mechanical load 44
3.1.1. Some basic phenomena of stress analysis 44
3.1.2. Chemical phenomena accompanying deformation and fracture 49
3.2. Structural changes associated with deformation 52
3.2.1. Deformation of ideal crystals 52
3.2.2. Deformation of real crystals 58
3.2.3. Deformation of polycrystalline materials 65
3.2.4. Deformation of amorphous materials 65
3.3. Fracture 67
3.4. Electrical and luminous phenomena triggered by mechanical activation 74
Symbols in Chapter 3 74
References 75

Chapter 4 77

4. The process of fine grinding 77

4.1. Material characteristics relevant during comminution 77
4.1.1. Hardness (microhardness) 77
4.1.2. A concept study of grindability 79
4.1.3. Physico-mechanical characteristics and grindability of clinker minerals and cement clinkers 83
4.2. The process of grinding and the interaction of particles 88
4.2.1. Stages of grinding. Aggregation and agglomeration 89
4.2.2. Fine grinding and equilibrium states 101
4.2.3. Mechanism of particle interactions 105
4.3. Energy requirements during grinding 110
4.4. The role of the medium in fine grinding 114
4.4.1. The effect of the medium on the mechanical properties of solid bodies 114
4.4.2. Effect of medium on grinding 118
4.4.3. Mechanism of action of grinding aids 124
Symbols in Chapter 4 138
References 140

Chapter 5 147

5. Structural changes and mechano-chemical reactions induced by fine grinding 147

5.1. Changes in the crystal structure 151

5.2. Mechano-chemical reactions 155
5.2.1. Homogeneous mechano-chemical reactions 155
5.2.2. Mechano-chemical dissociation 157
5.2.3. Mechano-chemical decomposition of organic and silicate polymers. Surface activation 161
5.2.4. Mechano-chemical reactions between gases and solids 163
5.2.5. Mechano-chemical reactions between liquids and solids 164
5.2.6. Mechano-chemical reactions between solids 165
5.2.7. Mechano-chemical reactions combined with capillary condensation 166
5.2.8. Chemi-hesion and the overlapping effect 168
5.3. Effect of mechano-chemical activation on the physico-chemical and technological properties of silicates and other materials used in the silicate industry 170
5.3.1. Examples of changes in crystal structure 170
5.3.2. Examples of solubility changes 193
5.3.3. Examples of changes in high temperature reactions 195
5.3.4. Examples of the modification of cation-exchange capacity 197
5.3.5. Improving the hydration capacity of βC_2S by fine grinding 200
5.3.6. Enhancement of activity achieved by fine grinding hydraulites, industrial wastes, and raw materials of the cement industry 202
5.3.7. Changes in the dielectric properties 203
5.3.8. Effect of grinding on clay–water systems 204
Symbols in Chapter 5 206
References 207

Chapter 6 214

6. Equipment for fine grinding and the problem of mechanical activation 214

6.1. Ball mills 214
6.2. Vibration mills 217
6.3. Jet mills 220
6.4. The attritor mill 222
6.5. Disintegrators 222
6.6. Planetary mills 225
Symbols in Chapter 6 226
References 226

Subject index 229

PREFACE

Current textbooks define grinding usually as a purely mechanical operation. This would only be correct if grinding were nothing other than size reduction. However, at present a large body of experimental facts is available which proves that grinding, first of all fine grinding, involves physico-chemical changes which affect the intrinsic properties of material and which cannot be explained adequately by the reduction of particle size only. These accompanying phenomena, affecting either the specific surface or the structure of a material, and eventually also its chemical composition, are all associated with an increase of the free energy of the system. Grinding can therefore be discussed in general terms as a method of mechanical activation. The subject matter of our book is the discussion of structural and chemical transformations elicited by mechanical effects during grinding. Its topic is therefore part of the more comprehensive field of mechano-chemistry. Apart from literature sources, a substantial portion of the experimental results are from our own investigations, and one of our objectives was the systematization of information gained from both sources. Although our interest was centred on silicates, other materials were also drawn into the discussion if they helped the understanding of more general phenomena or assisted their clear presentation.

The authors

Chapter 1

1. GENERAL FEATURES OF MECHANICAL ACTIVATION

1.1. THE SCOPE OF MECHANO-CHEMISTRY

The term "mechano-chemistry" was first used by Wilhelm Ostwald in his book "Handbuch der allgemeinen Chemie" [1]. He regarded mechano-chemistry as an independent discipline of chemistry, similar to thermo- and electrophoto-chemistry etc., and he defined it as the study of chemical transformations induced by gravitational and kinetic energy, as well as by energies connected with changes in the volume, surface and shape of materials.

Smekal [2] used the term "mechanical activation" to describe those processes which were effected by mechanical energy and which involved an increase in the chemical reactivity of the system, but without altering its chemical composition. According to Peters, however [3], "mechano-chemical reactions" are transformations which are accompanied by changes in the chemical composition of the system through the action of mechanical energy. Hüttig [4] considered mechano-chemistry to be the study of correlations between chemical bonding and mechanical strength. Thiessen–Meyer–Heinicke [5] defined mechano-chemistry as a part of chemistry dealing with all such physico-chemical changes of material as are induced by mechanical energy. The special case when such changes are generated by friction in solids may, according to Heinicke, be called tribo-chemistry [6]. Essentially similar definitions of mechano-chemistry were also given by many other authors [7–15].

In our view mechano-chemistry comprises those structural and physico-chemical changes (as well as the chemical reactions) which are induced in solids by deformation, disintegration and dispersion as a result of application of mechanical energy, or which are the consequence of such actions.

Systematic studies on mechanical activation, including mechano-chemistry and tribo-chemistry, were initiated in the late fifties and have since been conducted in several countries.

In Hungary the first publications on this subject were published in the late sixties [16–21] and were based mainly on the works of Beke on fine grinding [22]. In writing this book we leaned on the available literature and on our own experience collected over the years in the fields of fine grinding, mechanical activation and mechano-chemistry [23–24].

1.2. MECHANICAL ACTIVATION BY FINE GRINDING

Mechano-chemical phenomena proceeding during mechanical dispersion of solids have a special importance within the defined broader scope of our topic.

The most common method of producing dispersed systems is by mechanical disintegration, i.e. grinding. In mineral dressing and in various technological processes of the silicate industry fine grinding is of prime importance and fine powders, including silicate minerals, have a wide field of application. Over the years many attempts have been made to achieve non-mechanical size reduction but these methods have not yet found their way into practice.

The most direct result of grinding is the reduction of particle size, but in finely ground material other, more profound changes affecting the surface as well as the chemical, physico-chemical and structural properties may also take place.

Chemical changes occurring during grinding have been recognised for a long time. Peters [3] drew attention to a work published in 1894 by Carey Lea [32] in which the dissociation of the chlorides and iodides of Ag, Au, Pt and Hg during grinding were described. It has been known for long in paper manufacturing that the reactivity of cellulose can be enhanced by size reduction. This is accompanied by the degradation of cellulose molecules and the concurrent appearance of reactive radicals. Several publications deal with the increased reactivity of metals on deformation and with reactions and transformations of natural and synthetic macro-molecules, explosives, and other organic and inorganic compounds under the action of mechanical forces.

The transformations induced in solids by grinding are complex and, therefore, it may be useful to distinguish between primary and secondary mechano-chemical processes [25].

Primary processes are those which increase the free energy of the system and enhance the reactivity and activity of the ground product. If primary processes result in measurable changes in the physico-chemical parameters of the system then the process is called mechanical activation.

Primary processes include the deformation and disintegration of the particles of dispersed systems effected by mechanical action, as well as the shock-like increase of their temperature due to fracture. Other primary processes include certain internal changes caused directly by deformation and by thermal shock, such as the formation and translocation of lattice defects, polymorphous transformations, formation of supercooled liquids, some chemical reactions, etc.

In solids which are activated by mechanical energy some spontaneous transformations may take place which decrease the free energy of the system. Such changes may be considered as secondary processes.

Secondary mechano-chemical processes may proceed both during grinding (in the deformation period or during momentary intervals between mechanical actions) and after the completion of grinding, provided the circumstances favour such transformations.

Examples for some typical secondary processes include:

—interaction between the particles of a dispersed system resulting in an increase of particle size. Two stages of secondary processes accompanying fine grinding and

involving an increase of particle size can be distinguished: aggregation following relatively short grinding periods (in other words the weak and reversible adhesion of particles due to van der Waals—primarily London—dispersion forces) and agglomeration following, in general, longer grinding times or mechanical activation characterised by a very compact, irreversible adhesion of the particles (co-crystallisation, fusion, mechano-chemical reactions) in which chemical bonding may also play a role [20, 26, 27];

—spontaneous re-arrangement of the surface layer in order to relieve surface tension [28];

—interaction between the surfaces of particles and extraneous molecules which result in a decrease of the free energy of those surfaces (adsorption and chemisorption of gases, vapours, surface active agents, etc.). Theory and experimental studies by Rehbinder [29], and also by Hungarian researchers, show that these very reactions may serve as a means of suppressing interactions between particles and promote mechanical activation [21, 30, 31];

—chemical reactions between the particles being ground. This is usually a complex sequence of partial reactions which cannot, therefore, be regarded as a simple solid phase reaction between two particles [3, 5, 32–34];

—re-crystallisation and/or re-arrangement of the atomic structure of the activated particles. As a consequence, a metastable modification of a particle which had previously been amorphous can often be observed. De-activation by internal re-arrangement of originally amorphous systems, or of systems which become amorphous on activation, can also be observed [35];

—the overlapping effect, i.e. a decrease in the chemical potential, and especially of the reactivity, of the remaining free surfaces due to mutual attachment of surfaces and of active sites on the surfaces [36].

1.3. MODES OF MECHANICAL ACTIVATION

In general terms, grinding can be defined as work expended against the bonding energy of crystalline solids; where bonding energy is defined as the theoretical amount of energy necessary to remove the atoms or ions of the dispersed system from each other to infinite distance. In dispersed systems the bonding energies of atoms inside the particles are different from those which characterise the surface atoms or ions, and the bonding energy of a dispersed system of unit mass has to be divided into an internal term ($n_i e_i$) and a surface term ($n_s e_s$). Thus;

$$E = n_i e_i + n_s e_s = (n - n_s) e_i + n_s e_s = n e_i - n_s (e_i - e_s). \qquad (1)$$

In this equation $ne_i = E_u$ is the bonding energy in the non-dispersed system (in a perfect crystal this is the lattice energy); $n_s(e_i - e_s) = E_s = e_\gamma a_s$ is the energy representing surface forces that are not neutralised by neighbouring atoms; in other words it is the surface free energy (E_s) which is the product of the specific surface free energy e_γ and the specific surface (a_s); $n = n_i + n_s$ is the number of atoms in the system (n_i is the number of internal atoms, n_s is the number of surface atoms).

After replacements:

$$E = E_u - e_\gamma a_s. \tag{2}$$

The change in bonding energy after grinding:

$$\Delta E = \Delta E_u - \Delta(e_\gamma a_s) = \eta_z W_z. \tag{3}$$

Where W_z is the input of work during grinding and η_z is the efficiency of grinding. (Efficiency is defined as the ratio of the change in bonding energy and the input of grinding work.)

If grinding, as an activation process by mechanical energy, is characterised by the change of bonding energy as shown in equation (3), then it is of no consequence how it was caused during the absorption of mechanical energy. In fact, however, more or less distinct partial processes can be recognised as functions of grinding time:

(a) If, on grinding, only the specific surface is altered, then

$$\eta_z W_z = \Delta E = -e_\gamma \Delta a_s. \tag{4}$$

When η_z is constant, equation (4) is in accordance with Rittinger's equation [37].

(b) If both the specific surface and the specific surface free energy change, then we arrive at the equation for grinding work suggested by Smekal [2]:

$$\eta_z W_z = \Delta E = -\Delta(e_\gamma a_s). \tag{5}$$

(In Smekal's view the result of grinding is the change of surface free energy.)

(c) Finally, if the increase of specific surface and specific surface free energy are accompanied by a decrease of lattice energy (i.e. where deformation of the

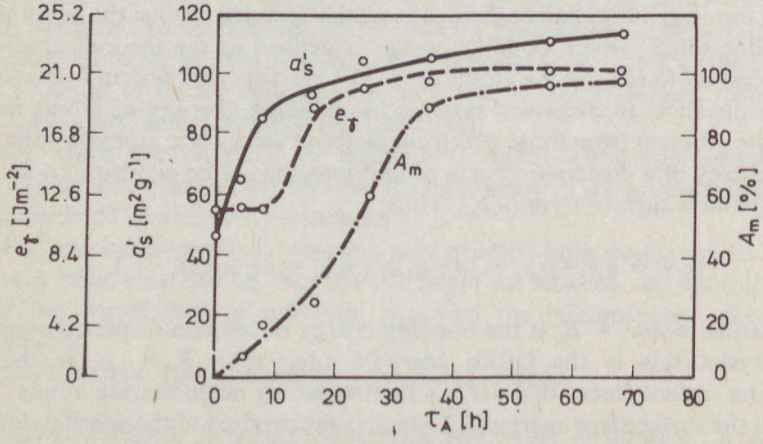

Fig. 1.1. Correlation of the "total" specific surface (a'_s), the potential of water adsorption (e_γ), amorphisation (A_m) and grinding time (τ_A) [17]

crystal lattice takes place or the material becomes amorphous), then we arrive at the general equation (3).

We may, therefore, distinguish the following extreme situations:

—mechanical dispersion,
—surface activation, and
—mechano-chemical (structural) activation.

In real grinding processes complete separation of these partial processes is not possible since they overlap and proceed concurrently. For example, when kaolin is dry ground in a vibration mill (Fig. 1.1), then, during the initial period the main change is the increase in specific surface. In the second period adsorption potential, as measured by the adsorption of water, also increases; in the third period far-reaching amorphisation of the crystal lattice can also be observed, i.e. the lattice energy is decreased [17].

The state and the technological value of a dispersed system produced by fine grinding is determined by an array of physical and physico-chemical characteristics, such as degree of dispersion, particle size distribution, the structure of particle surface and other chemical and physical features. The appearance, degree, and character of the changes depend on the grinding properties of the material and on the technological conditions applied.

SYMBOLS IN CHAPTER 1

n number of atoms
n_i number of internal atoms
n_s number of surface atoms
e_i bonding energy of internal atoms
e_s bonding energy of surface atoms
E bonding energy
E_u bonding energy of non-dispersed system (for an ideal crystal lattice energy)
E_s surface free energy
e_γ specific surface free energy
W_z grinding work
a_s "external" specific surface
a'_s "total" specific surface
τ_A grinding time
A_m degree of amorphisation
η_z efficiency of grinding

REFERENCES

[1] Ostwald, W.: *Handbuch der allgemeinen Chemie. Vol. 1*, Akad. Verlagsanstalt, Leipzig 1919
[2] Smekal, A. G.: in *Proceedings of the International Symposium on the Reactivity of Solids* (ed. Hedvall, J. A.). Cotenburg 1952
[3] Peters, K.: *1. Europ. Symp. Zerkleinern* (ed. Rumpf, H.). Verlag Chemie, Weinheim, VDI Verlag, Düsseldorf 1962

[4] Hüttig, G. R.: in *Handbuch der Katalyse. Vol. IV; Heterogene Katalyse. Vol. III* (ed. Schwab, G. M.). Springer, Wien 1943
[5] Thiessen, P. A., Meyer, K., Heinicke, G.: *Grundlagen der Tribochemie*. Akademie Verlag, Berlin 1967
[6] Heinicke, G.: *Tribochemistry*. Akademie Verlag, Berlin 1984
[7] Hedvall, J.: *Einführung in die Festkörperchemie*. Friedrich Vieweg u. Sohn, Braunschweig 1952
[8] Rasch, R.: *Ber. Dtsch. Keram. Ges.* **40,** 635 (1963)
[9] Schrader, R., Tetzner, G.: *Silikattechnik*, **22,** 11 (1971)
[10] Szántho E.: *MTA Műszaki Tudományok Oszt. Közleményei*, **38,** 191 (1967)
[11] Kubo, T.: *Introduction to Mechanochemistry* (in Japanese). Kagaku Dojin, Tokyo 1971
[12] Boldyrev, V. V., Meyer, K.: *Festkörperchemie*. VEB Deutscher Verlag für Grundstoffindustrie, Leipzig 1973
[13] (Hodakov, G. S.) Г. С. Ходаков: *Физика измельчения*. Физматгиз, Москва 1979
[14] (Avvakumov, E. G.) Е. Г. Аввакумов: *Механические методы активации химических процессов*. 2-е изд. Сиб. отделение АН СССР Наука, Новосибирск 1986
[15] Lin, I. J., Nadiv, S., Grodzian, D. J. M.: *Mineral Sci. Eng.*, **7,** 313 (1975)
[16] Juhász, Z.: *Építőanyag*, **17,** 419 (1965)
[17] Juhász, Z.: *MTA Kémiai Közlemények*, **31,** 227 (1969)
[18] Juhász, Z.: Mechanochemical activation of silicate minerals (in Hungarian). Ph.D. thesis, Budapest 1969
[19] Opoczky, L.: *Építőanyag*, **18,** 41 (1966)
[20] Beke, B., Opoczky, L.: *Dechema Monographien. Vol. 57*, Verlag Chemie, Weinheim 1967
[21] Opoczky, L.: Investigation of grinding processes of the cement clinker and intensifying them by grinding aids (in Hungarian). Ph.D. thesis, Budapest 1968
[22] Beke, B.: *Principles of Comminution* (in Hungarian). Akadémiai Kiadó, Budapest 1963
[23] Juhász, Z.: Mechanical activation of raw materials in industry of building materials (in Hungarian). DSc thesis, Budapest 1979
[24] Opoczky, L.: Fine grinding processes of brittle materials in silicate industry (in Hungarian). DSc thesis, Budapest 1982
[25] Juhász, Z.: *Aufbereitungs-Technik*, **10,** 558 (1974)
[26] Opoczky, L.: *Powder Technol.*, **17,** 1 (1977)
[27] Opoczky, L.: *MTA Kémiai Közlemények*, **48,** 235 (1977)
[28] Rehbinder, P. A., Chodakow, G. S.: *Silikattechnik*, **13,** 200 (1962)
[29] (Rehbinder, P. A.) П. А. Ребиндер: *Доклады на VI. съезде физиков*. Госиздат, Москва 1928; *Физико-химическая механика*. Изд-во АН СССР, Москва 1958
[30] Opoczky, L.: *Építőanyag*, **21,** 188 (1969)
[31] Opoczky, L.: *Építőanyag*, **27,** 284 (1975)
[32] Carey Lea, M.: *Phil. Mag. & J. Sci.*, **37,** 470 (1894)
[33] Juhász, Z.: *MTA Kémiai Közlemények*, **43,** 225 (1975)
[34] Menyhárt-Kocsis, M., Domsa, K.: *MTA Kémiai Közlemények*, **35,** 9 (1971)
[35] Schrader, R., Hoffmann, B.: *Z. anorg. u. allgem. Chem.*, **369,** 41 (1969)
[36] Juhász, Z., Tímár, M., Adamis, Z.: *Építőanyag*, **29,** 327 (1977)
[37] Rittinger, P. R.: *Lehrbuch der Aufbereitungskunde*. Ernst u. Korn, Berlin 1867

Chapter 2

2. CHARACTERISATION AND METHODS OF EXAMINATION OF DISPERSE SYSTEMS

The selection and development of suitable techniques of characterisation is of fundamental importance for the study of disperse systems obtained by fine grinding. For a comprehensive description of the ground product it is recommended that different methods of examination be applied in parallel. The following set of characteristics may give direct or indirect information about the physical and physico-chemical states of the product:

—degree of dispersion (specific surface);
—particle size distribution;
—morphology of the product and of the particles, respectively;
—surface structure of particles, and the physical and chemical properties connected with them.

The methods and instruments used for determining the degree of dispersion of a ground product are varied and are adequately covered by the literature [1–10]. In the field of mechano-chemistry methods which have been either borrowed from other areas or have been specifically developed for this field are applied [11–20].

In this section we define some basic concepts and present our own approach which has been developed for describing the internal structures of disperse systems [21]. This is followed by a discussion of the methods available for determining some basic characteristics of disperse systems, such as degree of dispersion, particle size distribution, specific surface, etc.

2.1. CHARACTERISATION OF THE BULK STRUCTURE OF SOLID DISPERSE SYSTEMS BY THE SPV SYSTEM

Solid–disperse systems—based on common features of their microstructure—are classified [21] as follows:

Dense solid bodies (denoted by S). Their true density ϱ and bulk density calculated from the mass and geometry ($\varrho_s = \varrho$) are equal. Their volume is made up additively

from the specific volumes of phases dispersed in each other:

$$\frac{m}{\varrho} = \sum_{i=1}^{i} \frac{m_i}{\varrho_i}$$

Porous bodies (denoted by SP) have their own shape and are formed by a solid, continuous (i.e. non-disperse) skeleton and a porous capillary system formed by this skeleton. Their bulk density is lower than their true density ($\varrho_s < \varrho$).

Dense particle bulks (denoted by SV) are composed partly of a disperse skeleton, formed by random or ordered aggregation of particles, and partly from a cavity system formed by this skeleton. This bulk has no shape of its own and its shape can be modified by small forces. The true density is larger than the bulk density ($\varrho_B < \varrho$).

It is evident, however, that these three groups represent extreme cases. The intermediate, transitional systems (denoted by SPV) are common. These, in turn, can again be divided into two groups:

(a) Porous bodies with a disperse skeleton: such bodies have a discontinuous solid skeleton consisting of particles and are produced by compression grinds.
(b) Porous disperse bulks: such bulks have particles with both open and closed pores and are obtained, for example, by grinding porous bodies.

Since it is difficult to draw a line between these two groups, it is more appropriate to regard them as members of a single structural type, taking into consideration the stability of the structure, that is, the resistance of the structure to external forces. In this respect bulks resistant to external forces are coherent, whilst systems with less resistant bulk structures are incoherent bulks. From the same point of view one can distinguish between voids and pores. One part of the cavity system can be easily varied by external forces; this is the void system. The rest of the cavities behave against external forces as a constituent part of the disperse skeleton; this is called the pore system. (For a method of determining bulk-stability cf., Section 2.2.5.)

The bulk density ϱ_B of porous bulks is less than the average density of the particles ϱ_s. Therefore,

$$\varrho_B < \varrho_s < \varrho.$$

The porous bulk (bulk with a cavity system formed partly by the voids between the particles and partly by the pores within the particles) can be regarded as a general model of grinds. Bulks containing dense particles represent an extreme case with zero particle porosity. Ground materials will be regarded, therefore, as porous bulks (SPV).

Following this line of thought, compactness v_s was selected as a first approximation for a quantitative description of the internal structure of porous bulks. Compactness is the ratio of the dense part in a unit volume of the bulk. The pore system and the void system are characterised by porosity v_p and voids v_v. The following equation applies to these volumes:

$$v_s + v_p + v_v = 1. \qquad (1)$$

For this reason the state of porous bulks can be represented by a ternary diagram ("SPV system") see Fig. 2.1. The sides of this triangle are scaled in v_S, v_P, and v_V units, hence dense particle bulks, porous bodies, and porous bulks are located on side SV, side SP, and inside the SPV triangle, respectively.

The main changes of state of ground materials are clearly represented by the SPV system.

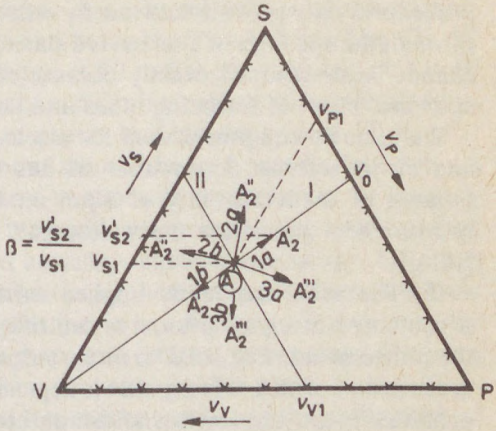

Fig. 2.1. State of porous bulk in the SPV (compactness–porosity–voids) system. Some changes of state of ground material represented in the SPV system [21]

(1) If a straight line I is drawn through a point A_1 representing a state, and through the vertex V of triangle SPV, this base-line will intercept side SP at v_0, which is the particle porosity. If the material is subjected to such external or internal forces that its bulk structure changes from A_1 to A_2 ($=A'_2, A''_2, A'''_2$), then this transition is illustrated by the vector A_1–A_2. If only the void system of the bulk is changed, e.g. by a simple increase or decrease of compactness, or a change of particle size distribution, then point A_2 lies on base-line I (arrows 1a and 1b). If, in turn, particle porosity decreases, then point A''_2 representing the transition is located above the base-line (arrows 2a and 2b). The reason for a decrease of particle porosity can be either the opening up of some pores (pore to void transition) or an increase of compactness of the disperse skeleton, for example by sintering or by agglomeration [22].

If the transformation is characterised by an increase in particle porosity, e.g. by aggregation of particles (void to pore transformation) or by the formation of pores due to chemical reactions or to skeleton-forming sintering, then point A'''_2, representing the final stage, is under the base-line (arrows 3a and 3b).

(2) A second base-line (II) can be drawn through points A_1 and v_{v1}. Point A_2, representing the final stage, may lie to the left or to the right of this base-line according to the increase (arrows b) or decrease (arrows a) of void system volume, as a result of processes bringing about the transition. The decrease might be the result of agglomeration.

The transition can also be characterised by the compaction factor which involves the compactness of the starting and final stages:

$$\beta = \frac{v_{s2}}{v_{s1}} = \frac{\varrho_{B2}}{\varrho_{B1}}. \tag{2}$$

2.2. STUDY OF DISPERSE SYSTEMS

2.2.1. DETERMINATION OF PARTICLE SIZE

(a) The simplest method of particle size determination is dry, or wet screening. Various standardised screen sets are used in different countries. "Classical" screening procedures only provide statistically reliable results above 45 μm. However, passage through the openings of a screen is a statistical process, and the end-point of screening cannot be determined exactly because of aggregation of fines on the screen. The statistical effect of screening takes into account non-spherical particle shapes.

Well-known equipment used for mechanical screening include shaking, vibrating, and air-jet screens. Screen-analysis has lost some of its importance recently, but because of the availability of 5 μm mesh microsieves and the automation of the measurement procedure the widespread revival of this technique can be expected [10, 23].

(b) The most frequently applied method of particle size determination is sedimentation in a gravitational or centrifugal field of force. The basis of the method is the phenomenon that solid particles suspended in a fluid fall, after a short period of acceleration, with a velocity that is dependent upon particle size. Sedimentation rates achieved by gravity, for Reynolds numbers smaller than 0.2, and the diameter of the particles, can be calculated from Stokes' law:

$$d = \sqrt{\frac{18\eta}{\varrho - \varrho_0} \frac{h}{\tau g}}, \tag{3}$$

where d is the equivalent spherical diameter of the particle, g the gravitational acceleration, ϱ and ϱ_0 the densities of particle and medium, η the dynamic viscosity of the medium, τ the settling period, h the settling height (measured from the surface of the medium to the settling depth). The lower detection limit of the method is about 1 μm.

With sedimentation in a centrifugal field the diameter of a particle can be calculated by the following formula [24]:

$$d = \sqrt{\frac{18\eta \ln \frac{r}{r_a}}{(\varrho - \varrho_0)\omega^2 \tau}} \tag{4}$$

where ω is the angular velocity, r the distance of the particle from the axis of rotation, r_a the initial distance from that axis (if $\tau = 0$, $r_a = r$). The lower detection limit is about 0.05 μm. In practice both methods suffer from incomplete dispersion of the sample in the medium and from the difficulty of avoiding coagulation during settling. Some practical hints are given in papers by Bernhardt [25, 26], who reviewed the use of anticoagulants and peptizers.

The following instruments are used most frequently in measurements performed in a gravitational field: Robinson–Köhn [27] and Andreasen pipettes (both in its original

form [28, 29] and in its modified form [30]), and sedimentation balances [31], e.g. the Sartorius balance. In addition to these classical instruments the following methods are widely used: photo-sedimentometers and scanning photo-sedimentometers based on the absorption of light (in the particle range 100 to 2 μm) [24, 32–36], X-ray- and scanning X-ray sedimentometers based on the absorption of X-rays (particle sizes 1 to 2 μm) [24, 37] and laser sedimentometers based on the absorption of a laser beam (particle sizes of 1 μm). The laser instrument is equipped with a programmable counting desk and the time of an analysis can be as short as 10 min. The CILAS instruments are capable of operating in the range of 0.1 to 600 μm with ranges 0.1 to 50 and 1 to 600 μm selectable. For further details concerning particle size determination in a centrifugal field and its instruments see papers by Leschonski et al. [9].

(c) There are some procedures which count the numbers of particles in fractions within given size limits [38–41]. Either direct methods of measurement or imaging methods can be used. Earlier imaging methods were carried out with optical microscopes fitted with measuring scales, but nowadays electron microscopy, TV raster techniques and computers extend the possibilities of these methods. These methods have undoubted advantages over others in that they give a direct impression, not only of the size of the particles, but also of their shape and internal morphology. Electron microscopy provides a means of counting particles smaller than 1 μm. Time-consuming counting and measuring procedures can be partly or fully automated or computerised by using TV raster techniques. The results obtained by counting are different—in terms of mass—from those arrived at by screening or sedimentation.

(d) The size of individual, mostly submicroscopic crystals, can be determined by X-ray diffractometry by measuring the widths of diffraction lines. Line-broadening can be caused not only by changes in the size of crystallites (5 to 200 nm), but also by changes in the crystalline structure of the material and by amorphisation. These effects can be distinguished by mathematical methods [16, 42, 44].

If the crystal structure of the particles does not change during grinding, then the size of crystallites (Λ) can be calculated by Laue's formula as follows:

$$\Lambda = \frac{\lambda R k}{\beta_i \cos \vartheta}, \tag{5}$$

where λ is the wavelength of X-ray, R the radius of the goniometer, k the Scherrer factor [43] (0.89–1.0), β_i the integral width of X-ray line, and ϑ the Bragg angle. Laue [42] suggested that the integral width of the X-ray lines be measured to determine crystallite size, i.e. measure the width of a rectangle having an area equal to the area under the line and a height equal to the maximum intensity. However, for simplicity, the half-widths of X-ray lines are generally used, since the integral width and the half-width are very similar (see Fig. 2.2).

If, in addition to the size of crystallites, the crystal structure also changes under the effect of mechanical forces, then both will effect the X-ray lines. Kochendörfer [16] pointed out that the two effects can be distinguished by studying line-broadening as a function of diffraction angle.

Crystallite size (Λ) and crystal lattice distortion ($\Delta a/a_0$) can be determined

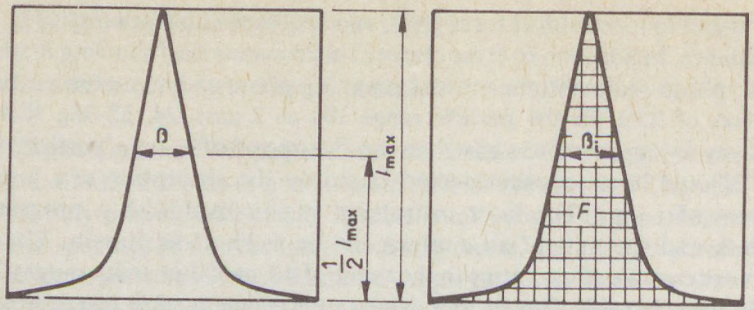

Fig. 2.2. Half-height width and integral width of X-ray lines. β—half-height width; I_{max}—maximum intensity of line; β_i—integral width of line (β_i—F/I_{max}, where F is the surface integral)

separately by measuring the average widths of two X-ray lines having different diffraction angles (ϑ_1 and ϑ_2).

If $\beta_v > 2\beta_T$, then

$$\Lambda = \frac{k\lambda R(\beta_2 \cos \vartheta_2 \sin \vartheta_2 - \beta_1 \cos \vartheta_1 \sin \vartheta_1)}{\beta_1 \beta_2 \cos \vartheta_1 \cos \vartheta_2 (\sin \vartheta_2 - \sin \vartheta_1)} \tag{6}$$

and

$$\frac{\Delta a}{a_0} = \frac{\lambda(\beta_2 \cos \vartheta_2 - \beta_1 \cos \vartheta_1)}{\Lambda(\beta_2 \cos \vartheta_2 \sin \vartheta_2 - \beta_1 \cos \vartheta_1 \sin \vartheta_2)}, \tag{7}$$

where β_T is the broadening of the lines due to the change of crystallite size, β_v the same effect for crystal lattice distortion. Other notations used in Eqs (6) and (7) are the same as in Eq. (5).

If $\beta_T = \beta_v$, then for β_v:

$$\beta_v = \frac{\Delta a}{a_0} \operatorname{tg} \vartheta.$$

The following formula can be used to determine the number of lattice defects created by mechanical dispersion provided that $\vartheta_1 > \vartheta_2$ and $(\vartheta_2 - \vartheta_1) > 10° \vartheta$ [11, 45]:

$$\bar{\mu} = \pm \sqrt{\ln Q \frac{\lambda^2}{16\pi^2(\sin^2 \vartheta_2 - \sin^2 \vartheta_1)}}, \tag{8}$$

where $Q = Q_x/Q_0$ is the ratio of diffraction angles and intensities.

2.2.2. PARTICLE SIZE DISTRIBUTION

Much of the information about the actual physical state of a grind can be gained from its particle size distribution. Three kinds of distribution functions are used to describe this distribution: the Gaudin–Schuhmann–Andreev [46–48], the Rosin–Rammler–Sperling–Bennett [49–51], and the Kolmogorov [52] functions. For detailed discussion of these functions see Beke [53], Leschonski et al. [54], and Schubert [55].

(a) The Gaudin–Schuhmann–Andreev equation (in the range $0 \leqslant x \leqslant x_{max}$):

$$D(x) = (x/x_{max})^m, \tag{9}$$

where D is the mass fraction of the ground product passing a screen with an opening of size x, while x_{max} and m are constants. The above equation, when plotted on log–log paper, gives a straight line:

$$\log D = m \log x - m \log x_{max}. \tag{10}$$

The slope of this straight line (m) was denoted by Schuhmann as the scattering module. By replacing x by x_{max} we get $D = 1$, that is x_{max} is the largest particle size of the distribution, or it is the sieve size through which all particles pass. Beyond $D = 1$ the distribution function becomes meaningless.

A typical particle size distribution curve of a cement mixture is shown in Fig. 2.3. It can be seen that for both large and small values of D, the measuring points are rather off the straight line. (In the figure, the passing fraction is given in percent.) The Gaudin–Schuhmann–Andreev distribution curve is, therefore, only valid for medium particle sizes.

(b) Experience shows that the empirical equation of Rosin, Rammler, and Sperling, or its modification by Bennett (the RRSB equation), can be conveniently applied to characterise the particle size distributions of ground products used in the silicate industry (cement, limestone, quartz, etc.).

$$1 - D(x) = R(x) = \exp[-(x/\bar{x})^n], \tag{11}$$

where R is the mass fraction retained on a screen with an opening x, x the grain size (the aperture size of the screen), $\bar{x}$ and n are constants. The RRSB function can be rewritten as follows:

$$\ln \ln (1/R) = n \ln x - n \ln \bar{x} + \ln \ln e = n \ln x + \text{const}. \tag{12}$$

This relation can be plotted as a straight line in a coordinate system made up from a log scale abscissa and an ordinate for $1/R$ in a double logarithmic scale (the RRSB

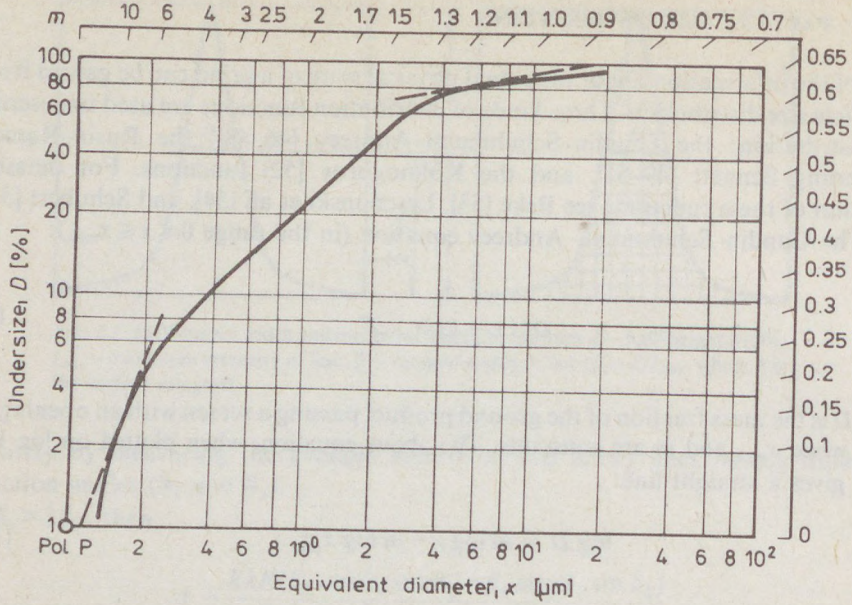

Fig. 2.3. Particle size distribution of a cement grind represented on the Gaudin–Schuhmann–Andreev plot [53]

chart). The slope of the straight line is n. The latter is intercepted at particle size x by the horizontal line representing $100/e = 36.8\%$ oversize. Size $\bar{x}$ is the fineness number and n is the uniformity coefficient. When calculated using logarithmic arguments, n is

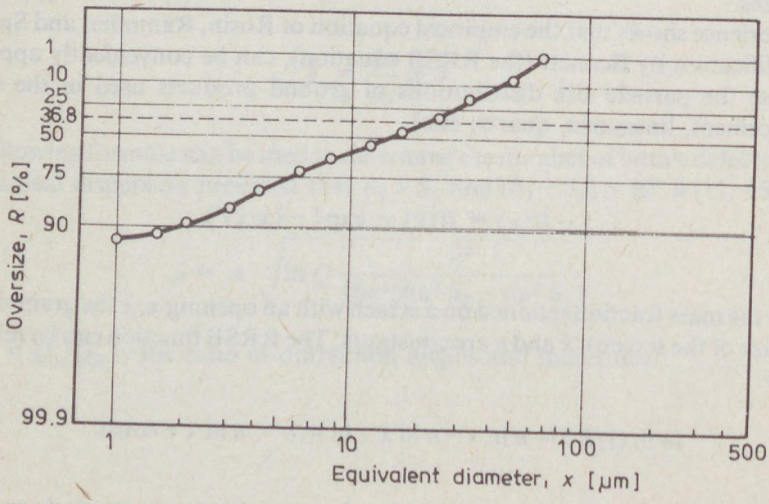

Fig. 2.4. Particle size distribution of a cement grind represented on the RRSB plot [77]

inversely proportional to the scatter of the distribution and it is, therefore, an important statistical characteristic [56]. Recently, Smirnov [57] introduced a "third" constant into the RRSB equation.

In Figure 2.4 the particle size distribution of ground cement clinker is plotted on an RRSB chart. Data obtained with a laser granulometer were evaluated with the aid of a computer program for fitting experimental data to the RRSB equation and for providing both parameters (n and $\bar{x}$) as well as the correlation coefficient (r).

Experimental data:

Equivalent diameter, x [μm]	Oversize, R [%]	Undersize, D [%]
1.0	93.3	6.7
1.5	92.5	7.5
2.0	90.5	9.5
3.0	86.8	13.2
4.0	80.6	19.4
6.0	72.6	27.4
8.0	64.3	35.7
12.0	55.4	44.6
16.0	44.1	55.9
24.0	31.2	68.8
32.0	18.1	91.9
48.0	6.9	93.1
64.0	1.1	98.9
96.0	0	100.0
128.0	0	100.0
192.0	0	100.0

Results of evaluation:

$r =$ 0.9959 (correlation coefficient)
$n =$ 1.0087 (uniformity coefficient)
$\bar{x} =$ 18.3274 (fineness number)

The RRSB equation:

$$R(x) = 1 - D(x) = \exp\left(-(x/18.3274)^{1.0087}\right)$$

(c) The general form of Kolmogorov's log–normal distribution function is:

$$D(x) = \Phi\left[\ln\left(\frac{x}{x_{50}}\right)^{-s}\right], \tag{13}$$

where $D(x)$ is the passing fraction (the mass fraction of a ground product passing through a screen with an opening of size x), x the particle size (the opening of the screen), Φ the Gaussian error integral, and x_{50} and s are constants.

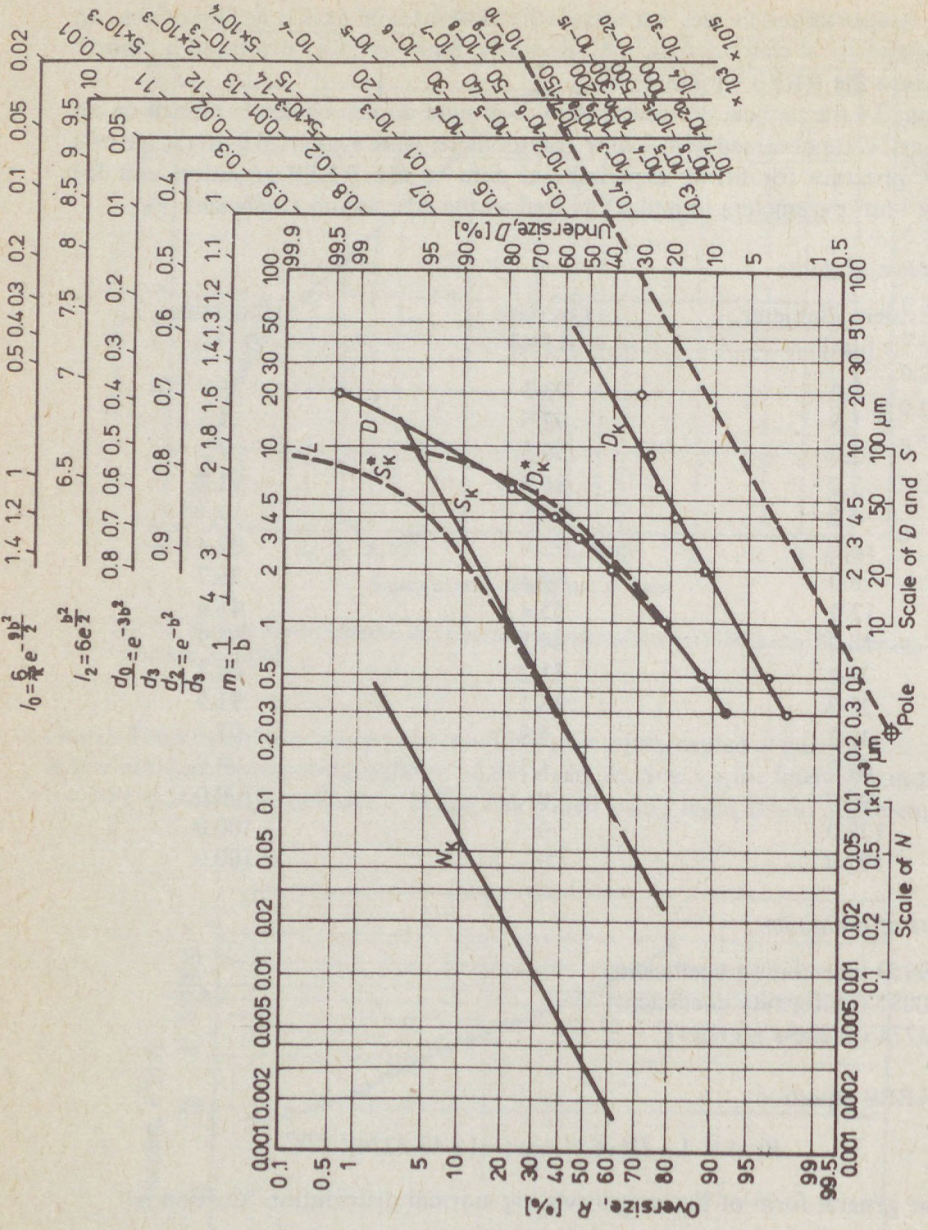

Fig. 2.5. Particle size distribution of a cement grind represented on a Fáy–Zhelev's plot [59]. D_K^* and S_K^* represent the mass and surface distributions pertinent to the balanced re-normalized distributions D_K and S_K when cut at $L = 100$ µm. Coding of side scales: $m = 1/b$ slope of re-normalized particle structure straight line; $d_2/d_3 = e^{-b^2}$ ratio of surface and mass medians, $d_0/d_3 = e^{-3b^2}$ ratio of particle number and mass medians, $l_2 = Fd_3 = 6e^{b^2/2}$ is the second order and $l_0 = Nd_0^3 = 6/\pi e^{-9b^2/2}$ the zero order invariant

The log–normal distribution can be plotted as a straight line in a co-ordinate system having a log scale abscissa and an ordinate scaled according to the Gaussian error integral. The slope of the straight line is s and the median value $x = x_{50}$ corresponds to an ordinate of 50%.

Calculation of the parameters of the log–normal distribution poses no problems from a mathematical point of view; therefore, it is frequently used for particle size determination. Numerical examples of the application of log–normal distributions can be found in papers by Leschonski et al. [9]. In reality the log–normal distribution generally fails to represent the particle size distribution of ground products. Experimental data usually follow an upward curve deviating from the straight line.

The possibilities of straightening the curve were first discussed by Gebelein [58] and later by Fáy and Zhelev [59] who supposed that the upward deviation of the curve might be attributed to classification during grinding, namely to a truncation at the upper particle limit. The re-normalised log–normal distribution introduced by Fáy and Zhelev closely approximates the real particle size distribution of ground products and it is also suitable for calculating certain characteristics of the grind (specific surface area, particle number). The Fáy–Zhelev chart is shown in Fig. 2.5. For the sake of completeness it must be mentioned that there are distribution functions with three constant parameters, the best known among them being the one proposed by Svensson [60].

In conclusion, it may be stated that there is no function of general validity and no function should be given absolute priority over the others.

In mechanical grinding processes various forces act upon materials of most diverse properties and disperse systems with a large variety of particle size distributions are produced. In each case it is a matter of judgement which distribution function furnishes the best approach to the actual particle size distribution.

For a further analysis of distribution functions we need to introduce two additional concepts; the frequency function and specific surface area.

The results of screening and sedimentation are usually given in the form of a series of discrete values but by regarding particle size as a random variable, the distribution is usually represented as a continuous function giving ratios that are smaller than, or

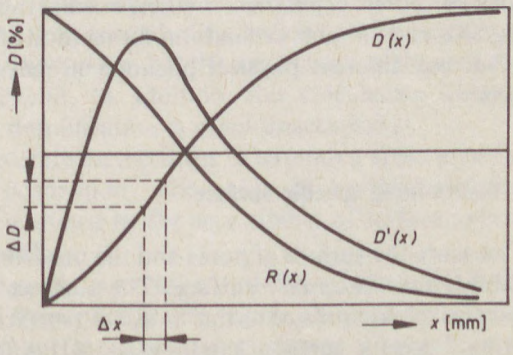

Fig. 2.6. $D(x)$ undersize curve, $R(x)$ oversize curve, $D'(x)$ frequency curve [53]

greater than, the given particle size. In this way we arrive at the $D(x)$ (passing) and $R(x)$ (residue) functions (see Fig. 2.6). The $D(x)$ passing function gives the mass of particles smaller than size x related to the total mass, while $R(x)$ yields the same set of values for particles greater than size x; that is, $R(x)+D(x)$ equals 1. Therefore, the relative mass ΔD of the size fraction of width Δx can be read as the difference of ordinates. At an infinitely small Δx value we arrive at the following frequency function:

$$\frac{\mathrm{d}D(x)}{\mathrm{d}x} = -\frac{\mathrm{d}R(x)}{\mathrm{d}x} = D'(x) \tag{14}$$

which gives the probability of the occurrence of particle size x.

2.2.3. SPECIFIC SURFACE AREA

In a physico-chemical sense only those particles have a surface where a distinction can be made between atoms or molecules situated within and those at the surface of the particle. Inner atoms or molecules are surrounded from all directions by neighbours belonging to the same phase; that is, they have a complete coordination sphere. Atoms situated at a surface are in contact with atoms of another phase from at least one direction; therefore, these atoms constitute the geometrical surface of the particle. The smallest set of spheres fulfilling this condition consists of 13 spheres having the same diameter (one inner sphere surrounded by 12 surface spheres). If atoms are considered as spheres having the same diameter of about 3×10^{-1} nm, then a particle of the smallest surface will have a diameter of 1 nm, corresponding to 10^3 m^2 g^{-1} specific surface area.

Although the concept of surface can be clearly defined from a geometrical, or even from a physico-chemical point of view, in practice, the numerical definition of the specific surface of ground material poses several difficulties. The determination of specific surface is straightforward if the system consists of solid particles of regular geometrical shape (e.g. spheres). If, however, the particles have an irregular shape and an uneven surface with bays, protrusions, splinters etc. and, in addition, there are surfaces inside the particles (pores, capillaries, cavities, cracks) then the definition of surface becomes ambiguous and its value depends on the method of its determination. Measuring methods that use different physical phenomena may measure different elements of the surface.

2.2.3.1. Methods for determining specific surface

If a method does not measure the surface of pores and the unevenness of the surface, then it can only establish the "external" surface. The surfaces of pores and the unevenness of the outer surface is expressed as the "internal" surface. The sum of these two surfaces is the "total" specific surface. Koglin et al. [61] differentiated "total", "external", and "internal" surface by considering the character of the interface between the solid phase and the continuous fluid phase.

According to our simple classification, the surface areas of porous bodies and dense particle bulks are given by the pore/solid boundary a_{SP} and void/solid boundary a_{SV}, respectively, whilst the total surface area of porous bulks is given by the sum of the "internal" surface of pores and the "external" surface of voids:

$$a_s = a_{SP} + a_{SV}. \tag{15}$$

With the ground products used in the silicate industry the "internal" surface is, in most cases, an order of magnitude larger than the "external" surface and the latter has little influence on the value of the "total" surface. Therefore, the two terms are often used in the same sense. The following methods can be used for determining specific surface:

(a) If the particle size distribution function is known and the particles are considered to be spherical, then the specific surface can be calculated by the following formula:

$$a_s = \frac{6}{\varrho}\sum\frac{\Delta D}{x} = \frac{6}{\varrho}\int_0^\infty \frac{D'(x)}{x}\,\mathrm{d}x, \tag{16}$$

where ϱ is the density and ΔD the relative amount of a fraction of width Δx.

Unfortunately, none of the functions that describe particle size distributions discussed in Section 2.2.2 is suitable for calculating specific surface. The value obtained according to the Gaudin–Schuhmann–Andreev equation depends on the value of m. If $m > 1$ the upper, if $m < 1$ the lower limit of integration provides the real value, while with $m = 1$ the value is indefinite. Similarly, the surface calculated with the aid of the RRSB equation depends on the value of the uniformity factor (n). With $n \leqslant 1$ the equation becomes meaningless and with small values of n unrealistically large specific surface values are obtained [62]. It is only the log–normal distribution that gives a finite surface with any small value of particle size (i.e. $x_{\min} = 0$) and at any value of s, but the results obtained in this way are mostly smaller by an order of magnitude than the real value. Taking the lower limit of integration as zero is, however, a contradiction of our knowledge about the structure of matter.

A re-normalized log–normal distribution may, in principle, be suitable for calculating the specific surface, but the uncertainty of the reduction factor makes such the calculation difficult. In addition, this calculation assumes that particles are spherical and this simplification is often unacceptable.

(b) The most accurate methods for determining specific surface area are based on gas and vapour adsorption. The value of "total" surface yielded by such a measurement is determined by the accessibility of surface unevennesses and pores to the adsorbed molecules.

(c) For a bulk of particles having a well-defined shape the "external" surface can be directly calculated from particle size values obtained by microscopy.

(d) Photometric surface area measurement (turbidimetry) is based on the dependence of light transmission of a suspension of particles on the surface of solid particles, since their surfaces absorb and reflect light. The lower detection limit of

conventional instruments is the wavelength of light, i.e. approximately 1 μm. In practice, photometric surface measurement is only used above 1 μm particle size [61, 63, 64].

(e) For a bulk of particles the specific surface can be determined from the flow rate of a fluid passing through (permeability), provided that we know the porosity of that bulk.

Methods based on permeability and adsorption will be discussed in more detail below.

2.2.3.2. Determining specific surface on the basis of permeability

The principle of determining specific surface by measuring permeability is that the pressure drop of a fluid flowing through a bed of porous material can be correlated with the surface area of the medium passed.

In principle, two states of flow can be distinguished, i.e. continuous flow and Knudsen diffusion.

If the mean free path of the fluid (l_0) is negligibly small as compared to the size of the capillaries (d) then flow is continuous and Knudsen's number ($K = l_s/d$) is smaller than 1.

If the mean free path of gas molecules is longer than the size of the capillaries we are faced with Knudsen diffusion (pore diffusion) and Knudsen's number is $K \gg 1$.

At sufficiently low pressure Knudsen diffusion dominates. In air at atmospheric pressure the mean free path of molecules is about 0.1 μm and Knudsen's number characteristic of continuous flow ($K \leqslant 0.01$) is associated with a pore diameter of $d \geqslant 10$ μm. This limit, taking porosity $\varepsilon = 0.5$, corresponds to an average particle size of approximately 10 μm and a specific surface of approximately 6000 cm^{-1}. If the specific surface exceeds this value then gas flow at atmospheric pressure proceeds in the intermediate range between continuous flow and Knudsen diffusion. At $K > 10$ diffusion is of the pure Knudsen type. This occurs when $d < 10$ μm and the pressure is less than 133 Pa [9].

Accordingly, measurement methods based on two different principles are generally applied:

(a) When measurements based on continuous flow are carried out it is important that the conditions for laminar flow ($Re < 0.6$) are observed. Specific surface per unit volume of the bed of particles can be calculated by the Kozeny–Carman equation [65]:

$$a_s^2 = \frac{1}{k} \frac{\varepsilon^3}{(1-\varepsilon)^2} \frac{1}{\eta} \frac{A}{L} \frac{\Delta p}{V}, \tag{17}$$

where V is the volume of fluid passing per unit time, L the thickness of the bed, ε the porosity of the bed, A the cross section of the bed, Δp the pressure drop, η the viscosity of the fluid, and k a constant depending on the shape of the pores.

From the above equation a constant characteristic that applies only for the bulk of the particles can be separated.

$$K = \frac{1}{k} \frac{\varepsilon^3}{a_s^2(1-\varepsilon)^2}. \tag{18}$$

This is the permeability factor and it depends essentially on the particle size distribution and on the shape of the particles in the bed. Although often applied, the "form factor" value $K=5$ is not always valid [66]. According to measurements by Rumpf and Gupte et al. [67, 68], $\varepsilon^{4.55}/(1-\varepsilon)$ is more realistic than the value given by $\varepsilon^3/(1-\varepsilon)^2$. This problem will be discussed later.

In commercial instruments the fluid is generally air.

(b) In methods based on diffusion the specific surface can be calculated from the pressure drop Δp that causes flow and from the diffusion coefficient N, knowing the porosity, by means of the Derjagin–Talaev correlation [69]:

$$a_s = \frac{24}{13}\sqrt{\frac{2}{\pi}}\,\varepsilon^2 \frac{1}{\sqrt{MRT}}\frac{A}{L}\frac{\Delta p}{N}, \tag{19}$$

where R is the gas constant and M the molecular mass. Orr's instrument that measures the permeability of helium is operated on this principle [70].

Surface area values established by Knudsen diffusion and sorption methods are approximately the same, excluding the internal surface of pores.

(c) The surface areas of porous bodies and powder bulks are calculated from experimental permeability data, using simple structural models and assuming simplified flow conditions. The model used is a cluster of parallel, uniform capillaries, through which the gases flow, following the same rules as in a powder bulk, having the same specific surface (see upper row of Table 2.1) [21].

Table 2.1. Basic equations, substitutions and permeability for SV and SPV models [21]

Model	Basic equation	Substitutions	Permeability
SV 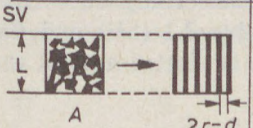 $v_S+v_V=1$ $(v_P=0)$ $\varepsilon=v_V$	$q=n\dfrac{r^4\pi^2\Delta p}{k\eta L}$	$\dfrac{nr^2\pi L}{AL}=\varepsilon=1-\dfrac{m}{AL\varrho}$ $\dfrac{\varepsilon}{a}=r$ $a=(1-\varepsilon_{PV})\varrho a_s$	$D_p=\dfrac{\varepsilon^2_{PV}}{(1-\varepsilon_{PV})^2\varrho^2 a_s^2 k}$
SPV 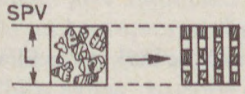 $v_S+v_P+v_V=1$ $\varepsilon=v_V+v_P$	$q=n\dfrac{r_V^4\pi\Delta p}{k\eta L}$	$\dfrac{nr_V^2\pi L}{AL}=v_V=1-\dfrac{m}{AL\varrho_0}$ $\dfrac{v_V}{a_V}=r_V$ $a_V=(1-v_V)\varrho_0 a_s^0$	$D_p=\dfrac{v_V^3}{(1-v_V)^2\varrho_0^2(a_s^0)k\eta}$

A	cross-section of the powder sample	Δp	pressure drop on the layer
a_s	surface area of the powder	q	flow rate (of gas)
a_{SV}	surface area of the void system	r	radius of a capillary, hydrodynamic radius
a_{SP}	surface area of the porous system	a_s'	"total" specific surface
D_p	permeability	a_s^0	"virtual" void/gas interface
k	shape factor (=5)	ε	bulk porosity
L	layer thickness, or length of capillaries	η	viscosity of the gas
m	mass of the sample	ϱ	density
n	number of capillary columns	ϱ_0	apparent density

It is supposed that the gas flow follows the Hagen–Poiseuille rule in every capillary channel. This supposition—with the substitutions given in Table 2.1—leads to a relationship between the permeability D_P and surface area, from which the specific surface can be calculated.

It is evident, however, that this model is valid only for bulks of dense particles (SV), and that only the cavity system of the bulk as a whole takes part in gas conduction. The void volume v_V is identical to the bulk porosity ε; that is, to the volume fraction of the whole void system. If a system does not correspond to these conditions, a new model, applicable to porous bulks (SPV), must be introduced according to the second row of Table 2.1. This structural model is a cluster containing "through" channels as well as pores which are inactive with respect to flow. This cluster consists of capillaries having non-dense walls. Permeability measurements are useful only for determining the surface of "through" channels but are not useful for measuring the surfaces of closed pores.

In real systems, not only are the closed pores inactive but parts of the void system might also be inactive with respect to the flow. This may either be because there are voids closed by particles in the bulk or some voids are so narrow that the gas flow does not follow the Hagen–Poiseuille law but corresponds to the much slower Knudsen diffusion.

This latter factor complicates the evaluation of results and, therefore, only a "virtual surface area" a_s^0 can be determined from permeability measurements.

The structural model given in the second row of Table 2.1 applies to ground material of SPV-type only if the apparent particle density ϱ_0 is known. This is calculated from the measured permeability data according to the following considerations:

Let us prepare several layers having different degrees of compactness from SPV-type ground material and measure the permeability of the layers at each compaction step. First, the structural model given in the upper row of Table 2.1 (SV) and the corresponding equation are applied. If the permeability D_P is plotted against the "porosity number" X where

$$X = X_{PV} = \frac{\varepsilon^3}{(1-\varepsilon)^2} \tag{20}$$

then a single straight line is obtained. This only applies if changes of the bulk in the SPV system are also on a single base-line; i.e. if there are no voids to pores or "active void" to "inactive void" transitions occurring during compaction. In addition, the gas flow should follow the Hagen–Poiseuille rule at every step of compaction in the whole active void system, and compaction should be nearly uniform along the whole length of the bulk.

Moreover, the straight line D_P versus $X = X_{PV}$ may have two different forms. In one case, the extrapolation of the experimental line goes through the origin (Fig. 2.7, line *1*). It is evident that this result holds true only in the extreme case of a truly SV-type bulk. (The Carman–Lea or other permeability-based methods of surface area measurement are applicable in such cases).

In the other instance the extrapolation of the experimental straight line intersects the X-axis at an X_0 value (Fig. 2.7, line *2*). At this fictitious point X_0 permeability is zero,

and an "active" pore system no longer exists. Therefore, the bulk porosity contains only an "inactive" cavity system, and so in Eq. (21)

$$X_0 = \frac{v_0^3}{(1-v_0)^2}, \tag{21}$$

v_0 is regarded as a virtual particle porosity, the value of which is determined by the simple extrapolation given above.

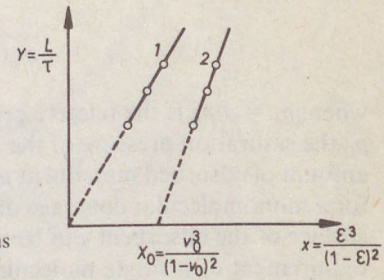

Fig. 2.7. The two different forms of experimental lines: D_p versus X [21]

Bulks with different compactness are represented in the SPV system as points along the base-line $v - v_0$ (Fig. 2.1). The apparent density can also be calculated from v_0:

$$\varrho_0 = (1 - v_0)\varrho \tag{22}$$

and the structural model according to the lower row of Table 2.1 can be applied. The "virtual" specific surface a_s^0 can also be calculated.

One should, however, use both a_s^0 and v_0 for the characterisation of bulk structure. The "degree of de-aggregation" defined as

$$\delta = \frac{a_s^0}{a_s'} \tag{23}$$

might give additional information. The "total" surface area a_s' should be determined by an appropriate adsorption method. δ is equal to 1 only for SV-type systems; in any other case (SPV) δ is less than 1.

2.2.3.3. Methods of measuring specific surface by adsorption

These methods are all based on the assumption that, under well-defined conditions, the amount of adsorbed material is proportional to the surface area.

Determinations are carried out by recording adsorption isotherms. These are curves which correlate equilibrium gas or vapour pressures (for solutions equilibrium concentrations) with the amount of adsorbed material. The shapes of such isotherms vary according to the nature of the adsorbing material and the adsorbate. Brunauer et al. [71] distinguished five main types of isotherms (BDDT classification). Among the mathematical descriptions of the various isotherms the best known, and the most

important for surface area measurement, is the BET-equation [72]. This is used for calculating the adsorption capacities corresponding to the monomolecular coverage of the adsorbing material from the adsorption isotherms. Once the surface requirement of the adsorbed molecule is known, the specific surface can be calculated.

The BET-equation is only applicable for calculating the specific surface below the critical temperature of the adsorbed gas, in the relative pressure range of $0.05 < p/p_0 < 0.25$, and for isotherms of type II and IV. The linearised form of the equation is:

$$\frac{p_r}{m_n(1-p_r)} = \frac{1}{m_m c} + \frac{c-1}{m_m c}, \tag{24}$$

where $p_r = p/p_0$ is the relative pressure, p the actual equilibrium adsorption pressure, p_0 the saturation pressure of the adsorbate at the temperature of the isotherm, m_n the amount of adsorbed material at p_r relative pressure, m_m the amount of material needed for a monomolecular coverage of the adsorbent, and c the BET constant. The specific surface of the adsorbent can be calculated by m_m and in the knowledge of the surface requirement of a single molecule (f_m).

With silicates the most commonly used adsorbates are argon, nitrogen, and water vapour, but other gases and vapours are not uncommon. The determination of f_m is crucial in this method and for liquid nitrogen at 77.4 K it is generally taken as 0.162 nm². The surface requirement of other gases is determined by comparison with nitrogen and the accepted values are: argon (at 77.4 K) 0.138, crypton 0.202, and water 0.106 nm².

Some comments are needed on the use of water vapour for the determination of specific surfaces of cement clinker, clinker minerals, and ground products prepared therefrom.

Although opinions somewhat diverge [73] in this respect, Powers and Brownyard and others [74–76] established that water vapour is suitable for the above mentioned purpose. According to the BDDT notation, the isotherms are of type II and exhibit an

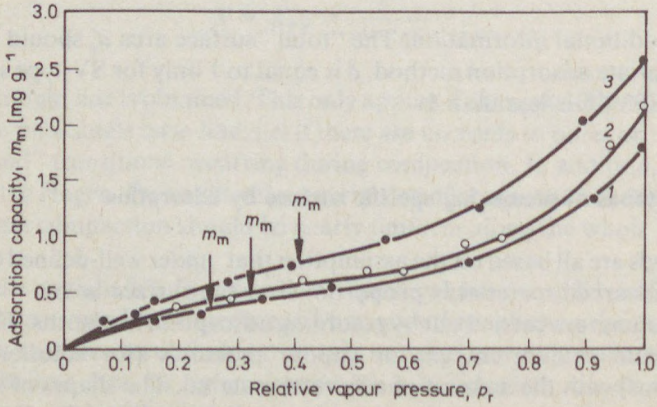

Fig. 2.8. Isotherms of the adsorption of water vapour on β-dicalcium silicate samples ground for different periods (τ_A): *1*—2 h, *2*—10 h, *3*—90 h [77]

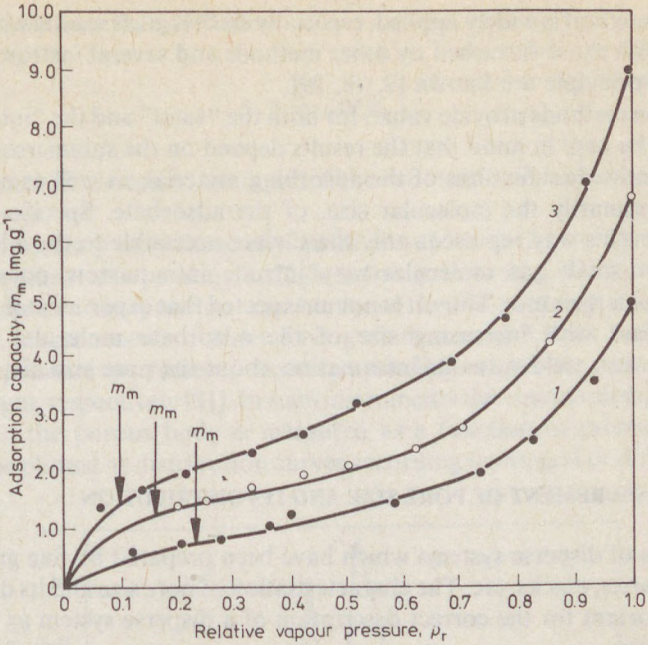

Fig. 2.9. Isotherms of the adsorption of water vapour on limestone ground for different periods (τ_A): *1*—1 h, *2*—5 h, *3*—10 h [77]

inflexion. To the left of the inflexion, i.e. in the domain of smaller vapour content, adsorption of water vapour into the surface of particles is mainly of a physical character, while on the right-hand side of the inflexion capillary condensation in the fine pores of the adsorbent and chemical bonding also play a role.

The adsorption isotherms of water vapour on β-dicalcium silicate and limestone ground for different periods are shown in Figs 2.8 and 2.9.

The adsorption isotherms of β-dicalcium silicates, sample nos. *1* and *2* (Fig. 2.8), are practically coincident up to $p_r = 0.8$ and the values for monomolecular adsorption capacity (m_m) are also very similar. The isotherm for sample *3* runs above the first two and indicates that, after prolonged grinding, monomolecular coverage develops at higher vapour pressure. This implies weaker bonding between surface and water molecules; in other words, a decrease of surface activity. Capillary condensation only sets in at relative pressures $p_r \geqslant 0.75$.

For ground samples of limestone (Fig. 2.9) monomolecular coverage develops at $p_r = 0.10$–0.15; capillary condensation starts at $p_r \geqslant 0.6$ and is more pronounced than with β-dicalcium silicate.

The application of water vapour as adsorbate for specific surface measurement is especially interesting for such products, e.g. ground cement clinker, which come into contact with water when they are used. In this case the determination of the surface able to contact water ("active surface") allows one to draw some conclusions about the quality of the product.

The BET-method is widely applied, especially since it gives results which are in good agreement with those furnished by other methods and several instruments operating on the BET-principle are known [9, 78, 79].

Adsorption methods provide values for both the "total" and the "internal" surfaces but it has to be kept in mind that the results depend on the submicroscopic structure and on the individual features of the adsorbing material, as well as on the chemical properties, primarily the molecular size, of the adsorbate. Specific surface values determined in this way represent only the surface accessible to the adsorbate and, it is clear, that small gas molecules may intrude into narrow pores that cannot accommodate larger ones. Thus, it is not unexpected that experimental specific surface values decrease with increasing size of the adsorbate molecule. However, this phenomenon can yield valuable information about the pore size distribution of the adsorbents.

2.2.4. MEASUREMENT OF PORE SIZE AND ITS DISTRIBUTION

The particles of disperse systems which have been prepared by fine grinding contain pores, capillaries, cracks, etc. The characterisation of pore size and its distribution is at least as important for the correct description of a disperse system as particle size or specific surface.

In terms of capillary condensation of vapours, pores are generally classified according to the following size ranges: micropores 1.5 to 20 nm, intermediate pores 20 to 100 nm, and macropores over 100 nm [9]. The basis of this classification is the applicability of Kelvin's equation, which is of limited validity in the micropore range.

The Kelvin (Thomson) equation correlates the tension of vapour in equilibrium with liquid phases having a curved (p) and a normal flat surface (p_0):

$$p = p_0 \exp\left[-\frac{2\sigma V \cos\theta}{RT}\left(\frac{1}{c_1} + \frac{1}{c_2}\right)\right], \tag{25}$$

where σ is the surface tension of the liquid, V its molar volume, while c_1 and c_2 are the main curvatures of the surface. This expression is only correct if the dependence of σ on curvature is negligible.

For a spherical surface the equation takes the form:

$$-RT \ln \frac{p}{p_0} = \frac{2\sigma V \cos\theta}{r}, \tag{26}$$

where R is the gas constant and r the radius of the sphere.

An important physical characteristic of pore systems is the size distribution of pores. If we assume cylindrical capillaries then their equivalent radius can be determined by porosimetry (penetrometry).

The basic principle of this method is the determination of the pressure at which a liquid that does not "wet" the walls of the capillaries (usually mercury) intrudes, or can

be forced, to enter into the capillaries:

$$p = \frac{2\sigma}{r} \cos \theta, \tag{27}$$

where σ is the surface tension of the liquid, θ the "contact" angle of wetting, and r the radius of the pore.

At a given pressure p only those capillaries for which $r > 2\sigma \cos \theta / p$ are filled.

Mercury porosimeters operating at high or low pressure are available. In a high-pressure porosimeter the pressure can be varied in the range of 0.1 to 200 MPa permitting the measurement of pores having diameters of 7.5 μm to 3.75 nm [80], while for low pressure instruments the corresponding ranges are 4 to 200 kPa and 200 μm to 3.5 μm, respectively [81]. In such instruments the volume change of mercury in contact with the porous body is measured as a function of pressure. The data obtained can be plotted as distribution curves according to integral or differential pore sizes.

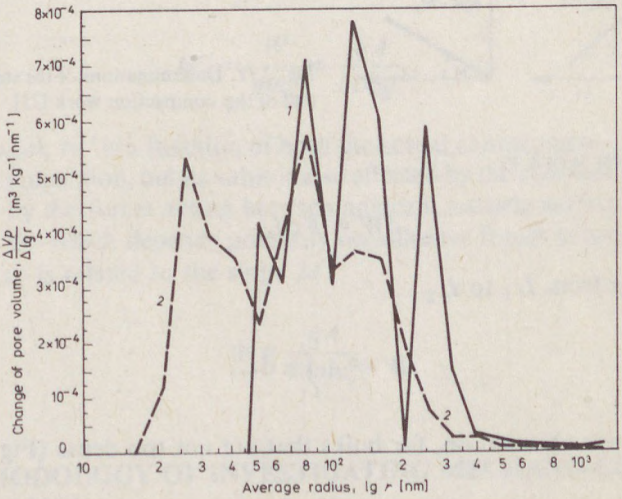

Fig. 2.10. Pore distribution curves of clinker. *1*—prepared by a wet process; *2*—prepared by a dry process [77]

Figure 2.10 shows the differential pore distribution curves of two cement clinkers manufactured in Hungary. It is apparent that clinkers manufactured by dry and wet processes have different distributions by pore size and have a wide range of pore sizes. Since pores, acting as "defect sites" have a significant influence on the fracture of particles and the pore distribution curves provide valuable information about the grindability of a given material.

There are also methods which apply wetting liquids, e.g. water, for determining pore sizes: these methods are useful in the pore size ranges of 1 μm to 200 μm [11, 81].

It should be noted, however, that the real distribution of pore size may significantly deviate from that calculated by assuming cylindrical pores. Difficulties may arise

especially with closed, "ink-pot" shaped pores. The volume of such pores is determined by removing mercury from the pores by gradually decreasing the pressure. In this way, a hysteresis curve is obtained along the V–P curve from which the volume of closed pores can be inferred.

2.2.5. STABILITY OF BULK AND COMPACTION WORK

The method of studying grinds compacted stepwise, as described above, can be extended to the determination of compaction work [21]. The compacting operation should be carried out in a cylinder with a piston, as shown in Fig. 2.11(a) and the compacting force F and the compacting pressure $\sigma' = F/A$ necessary to obtain each compaction step (i.e. layer thickness L) should be measured.

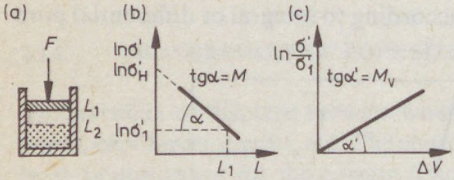

Fig. 2.11. Determinations of the stability of "bulks" and of the compaction work [21]

The compaction work is

$$dW = F\,dL. \tag{28}$$

By compacting from L_1 to L_2

$$W = A\int_{L_1}^{L_2} \sigma\,dL. \tag{29}$$

According to our observation, for bulks that are not too dense (Fig. 2.11(b)),

$$\ln\sigma' = ML + \ln\sigma'_H, \tag{30}$$

where $\ln\sigma_H$ and M are constants; the latter is negative and can be determined experimentally (Fig. 2.11(b)). The height L_1 of a bulk compacted by a pressure of $\sigma'_1 = 1$ MPa can also be obtained from the experimental curve. The compactness of this bulk is

$$v_{s1} = \frac{m}{AL_1\varrho} = \frac{\varrho_{B1}}{\varrho}, \tag{31}$$

where m is the mass of the sample and A the cross section of the sample holder.

By agreement, grinds compacted with $\sigma'_1 = 1$ MPa pressure are regarded as references with respect to further compaction.

Base-line II in the SPV system intersects base-line I at v_{s1} (Fig. 2.1, point A_1). The bulk structure of different grinds can be compared according to the intersection, i.e. the

"reference point". Starting from this point, the displacement of the piston—as seen in Fig. 2.11(a)—is $\Delta L = L_1 - L$. A modified equation is

$$\sigma^{\cdot} = \sigma^{\cdot}_1 \exp(M\Delta L). \tag{32}$$

The slope of the straight line is

$$M = \frac{1}{\Delta L} \ln \frac{\sigma^{\cdot}}{\sigma^{\cdot}_1}. \tag{33}$$

Compaction work is given, therefore, as

$$W = A\sigma^{\cdot}_1 \int_0^L \exp(M\Delta L)\, \mathrm{d}(\Delta L) = \frac{\sigma^{\cdot} A}{M}. \tag{34}$$

Compaction work referred to 1 m² of "active" surface area is given as

$$W' = \frac{W}{ma_s^0} = \frac{\sigma A}{Mma_s^0}. \tag{35}$$

Compaction work W' is a function of both the actual compactness of the bulk and of the degree of compaction, but its value is also affected by the position of the particles in the bulk and by the forces acting between adjacent particle surfaces.

Bulk stability Φ—which depends primarily on adhesive forces between particles in incoherent bulks—is related to the slope M:

$$\Phi = \frac{\sigma A}{Mma_s^0}. \tag{36}$$

2.3. METHODOLOGY OF INVESTIGATING MECHANO-CHEMICAL PHENOMENA

Mechano-chemical reactions and changes in the crystal structure induced by fine grinding can be investigated by the following methods [11, 82]:

—quantitative and qualitative evaluation of crystallinity, crystallite size, lattice defects, and amorphisation by X-ray crystallography;
—chemical analysis; X-ray fluorescence analysis;
—differential thermal analysis (DTA–DTG) for determining the decomposition temperature of carbonates, the loss of crystal water from hydrates, etc.;
—determination of density, in order to follow polymorphic transformations;
—determination of free enthalpy by measuring heat of dissolution;
—metallographic methods of observing the changes;
—magnetic equilibrium and magnetohydrostatic methods to follow changes in the magnetic properties induced by grinding;

—Mössbauer spectroscopy to detect changes in the crystal structure at atomic level, determination of solid phase reactions, etc.;
—electron microscopy for the recognition of new crystal structures, detection of nucleation, crystal growth, crystallite morphology, translations, and cleavages;
—infrared adsorption spectroscopy for the study of prototropy in minerals and crystals;
—electron microprobe studies to determine the composition of phases and the distribution of elements on the interfaces;
—Auger-electron spectroscopy for determining mineral composition on the fracture surface;
—visual examination for the detection of mechano-chemical reactions by colour changes;
—determination of dielectric constant;
—studies on ion-exchange capacity;
—other physical methods (NMR, EPR) for the detection of lattice defects generated by fine grinding, etc.

Examples of the application of the individual methods will be presented in Chapter 5 dealing with mechano-chemical reactions.

SYMBOLS IN CHAPTER 2

ϱ	true density, density
ϱ_s	bulk density of dense solid bodies
ϱ_0	density of the medium, apparent density
m	mass
M	molecular mass
ϱ_B	bulk density of bulks
v_p	porosity
v_v	voids
v_s	compactness
v_0	particle porosity, "virtual particle porosity"
d	equivalent spherical diameter, size of capillaries
g	gravitational acceleration
η	dynamic viscosity
τ	settling time
h	settling height
ω	angular velocity
r	distance of particles from the axis of rotation
r_a	initial distance
Λ	size of crystallites
λ	wavelength of X-ray
R	radius of goniometer
k	Scherrer factor
β_i	integral width of X-ray line

ϑ	Bragg angle
$\Delta a/a_0$	crystal lattice distortion
Q	ratio of diffraction angles and intensities
D	undersize
x	particle size (mesh size)
x_{max}	maximum particle size of range
m	constant
R	oversize
R	gas constant
n	uniformity coefficient
n	number of capillary columns
$\bar{x}$	fineness number
r	correlation coefficient
Φ	Gaussian error integral
s, k	constant
x_{50}	constant
a_s	specific surface, "external" specific surface
a'_s	"total" specific surface
a_B	"total" surface of the bulk
a_{SP}	surface of pore/solid boundary
a_{SV}	surface of void/solid boundary
a_s^0	virtual void/gas boundary
l_0	mean free path of fluid
v	volume of fluid
L	thickness of the bed
ε	porosity of the bed
A	cross section of the bed
ΔP	pressure drop
N	diffusion coefficient
M	molecular mass
K, k	shape factor, Knudsen's number
q	flow rate
p_r	relative pressure
m_n	amount of adsorbed material
f_m	surface requirement of a single molecule
c_1, c_2	main curvatures of the surface
σ	surface tension of the liquid
θ	angle of wetting (contact angle)
F	compacting force
$\sigma\cdot$	compacting pressure
W	compaction work
Φ	bulk stability
δ	degree of de-aggregation
m_m	amount of adsorbed material needed for a monomolecular coverage

REFERENCES

[1] (Romashov, G. I.) Г. И. Ромашов: *Основные принципы и методы определения состава пылей.* Изд-во ЛИОТ, Ленинград 1938

[2] (Figurovskij, N. A.) Н. А. Фигуровский: *Седиментометрический анализ.* Изд-во АН СССР, Москва 1948

[3] *The Analyst (London)*, **88,** (1044) 156 (1963)

[4] Lauer, O.: *Feinheitsmessungen an technischen Stäuben,* Alpine AG, Augsburg 1963

[5] Gál, S.: *Die Methodik der Wasserdampf-Sorptionsmessungen.* Springer, Berlin 1967

[6] Rumpf, H., Alex, W., Johne, R.. *Ber. Bunsenges. Phys. Chem.*, **71,** 253 (1967)

[7] (Hodakov, G. S.) Г. С. Ходаков: *Основные методы дисперсионного анализа порошков.* Стройиздат, Москва 1968

[8] Batel, W.: *Einführung in die Korngrössenmesstechnik.* 3rd ed. Springer, Berlin 1971.

[9] Leschonski, K., Alex, W., Koglin, B.: *Chem. Ing. Tech.* **46,** 23, 101, 289, 387, 477, 563, 641, 729, 821, 901, 984 (1974) **47,** 21, 97 (1975)

[10] Lauer, O.: *Verfahrenstechnik,* **2,** 99 (1968)

[11] Juhász, Z. (ed.): Autorenkollektiv. Untersuchungsmethoden zur Charakterisierung mechanisch aktivierter Festkörper. *BME Tudományos Közlemények,* **13,** KÖZDOK, Budapest 1978

[12] (Boldirev, V. V.) В. В. Болдырев: *Наука* (Сибирское отдел. АН СССР), **64** (1983)

[13] Ziegler, G.: *Keram. Z.,* **33,** 602 (1981)

[14] Schrader, R.: *Die Technik,* **24,** 89 (1969)

[15] Schneider, U.: *Aachener Blätter,* **16,** 71 (1966)

[16] Kochendörfer, A.: *Z. Kristallogr.,* **105,** 393 (1944)

[17] Tetzner, G.: Beitrage zur Mechanochemie. Ph. D. thesis, Freiberg 1964

[18] Patzak, I.: *Ber. Dtsch. Keram. Ges.,* **43,** 77 (1966)

[19] Ohlberg, S. M., Strickler, D. W.: *J. Am. Ceram. Soc.,* **45,** 170 (1962)

[20] Heegn, H., Bernhardt, C., Gottschalk, J., Husemann, K.: *Chem. Tech.,* **26,** 696 (1974)

[21] Juhász, Z.: *Powder Technol.,* **42,** 123 (1985)

[22] Opoczky, L.: *Powder Technol.,* **17,** 1 (1977)

[23] Joos, E.: *Staub,* **25,** 540 (1965)

[24] Otto, H. J.: *Chemie-Anlagen u. Verfahren,* **9,** 104 (1977)

[25] Bernhardt, C.: *Flüssigkeiten und Zusatz-Stoffe für die Sedimentationsanalyse.* Forschungsinstitut für Aufbereitung, Freiberg 1973

[26] Bernhardt, C.: *Freiberger Forschungshefte,* **A533,** 47 (1974)

[27] Robinson, G. W.: *J. agric. Sci.,* **12,** 306 (1922)

[28] Andreasen, A. H. M.: *Kolloidchem. Beih.,* **27,** 405 (1928)

[29] Andreasen, A. H. M., Lundberg, J.: *Ber. Dtsch. Keram. Ges.,* **11,** 312 (1930)

[30] Leschonski, K.: *Staub-Reinhalt, Luft,* **22,** 475 (1962)

[31] Oden, S.: *Kolloid-Z.,* **18,** 33 (1915)

[32] Johne, R.: *Staub-Reinhalt. Luft,* **23,** 269 (1963)

[33] Kurz, M. P., Johne, R.: *Powder Technol.,* **3,** 83 (1969–70)

[34] Allen, T.: *Powder Technol.,* **2,** 133 (1968)

[35] Rose, H. E.: *Engineering,* **169,** 405 (1950)

[36] Rose, H. E., Lloyd, H. B.: *Soc. Chem. Ind.,* **65,** 65 (1946)

[37] Hendrix, W. P., Orr, C jun.: *Proc. Conf. on Particle Size Analysis, Bradford 1970.* 147/157. Soc. Anal. Chem., London 1970

[38] Langer, G.: *Powder Technol.,* **6,** 5 (1972)

[39] Schleusener, A. S.: *J. Air Pollution Control Assoc.,* **19,** 40 (1969)

[40] Borho, K.: *Staub-Reinhalt. Luft,* **30,** 479 (1970)

[41] Binek, B.: *Staub-Reinhalt, Luft,* **30,** 468 (1970)

[42] Laue, M.: *Z. Kristallogr.,* **64,** 115 (1926)

[43] Scherrer, P.: *Nachrichten Akad. Wiss. Göttingen Math. Phys.,* **2,** 96 (1918)

[44] Neff, M.: *Grundlagen und Anwendung der Röntgen-Feinstruktur-Analyse.* R. Oldenbourg, München 1962

[45] Fricke, R., Gwinner, E.: *Z. Phys. Chem. (Wiesbaden),* **183,** 165 (1939)

[46] Gaudin, A. M.: *Trans. Am. Inst. Mining Met., Petrol Eng.,* **73,** 253 (1926)

[47] Schuhmann, R.: *Trans. Am. Inst. Mining Met. Eng. tech. Publ.* 1189 (1940), *Trans. AIME,* **217,** 22 (1960)
[48] (Andreev, S. E., Tovarov, V. V., Perov, V. A.) С. Е. Андреев, В. В. Товаров, В. А. Перов: *Закономерности измельчения и исчисления гранулометрического состава.* Металлургиздат, Москва 1959
[49] Rosin, P., Rammler, E., Sperling, K.: *Bericht 52 des Reichskohlenrates. Vol. 1,* 30, Berlin 1933
[50] Rammler, E.: *Beih. Z. VDI, Verfahrenstechnik,* **5,** 101 (1937)
[51] Bennett, I. G.: *J. Inst. Fuel,* **10,** 23 (1936)
[52] (Kolmogorov, A. N.) А. Н. Колмогоров: *Доклады АН СССР,* серия **XXXI,** 99 (1941)
[53] Beke, B.: *Principles of Comminution.* Akadémiai Kiadó, Budapest 1964
[54] Leschonski, K., Alex, W., Koglin, B.: *Chem. Ing. Tech.* **46,** 101 (1974)
[55] Schubert, H.: *Aufbereitung fester mineralischer Rohstoffe.* Vol. 1, 3rd ed. VEB Deutscher Verlag für Grundstoffindustrie, Leipzig 1975
[56] Beke, B.: *Műszaki Tudomány,* **44,** 83 (1971)
[57] Smirnov, S.: *Aufbereitungs-Techn.,* **16,** 308 (1975)
[58] Gebelein, H.: *Chem. Ing. Tech.,* **28,** 773 (1956)
[59] Fáy, Gy., Zhelev, B.: *Energ. & Atomtech.* **13,** 333 (1960); *Építőanyag,* **13,** 382 (1961)
[60] Svensson, I.: *Trans. Roy. Inst. Technol. (Stockholm),* **88** (1955)
[61] Koglin, B., Leschonski, K., Alex, W.: *Chem. Ing. Tech.* **46,** 984 (1974)
[62] Herdan, G.: *Small Particle Statistics.* Butterworth, London 1960.
[63] Rose, H.: *Z. VDI,* **7,** 35 (1955); *J. Appl. Chem.,* **2,** 80 (1952); *Nature (London),* **184,** 46 (1959)
[64] Telle, O.: *Tonind. Ztg. u. Keram. Rundschau,* **76,** 369 (1952)
[65] Carman, P. C.: *J. Soc. Chem. Ind. (London),* **57,** 225 (1938); **58,** 1 (1939)
[66] Kaye, B. H.: *Powder Technol.,* **1,** 11 (1967)
[67] Rumpf, H., Gupte, A. R.: *Chem. Ing. Tech.* **43,** 367 (1971)
[68] Moleris, O., Pahl, M. M., Rumpf, H.: *Chem. Ing. Tech.* **43,** 376 (1971)
[69] (Derjagin, B. V., Talaev, M. V.) Б. В. Дерягин, М. В. Талаев: *Журнал прикладной химии,* **40,** 345 (1967)
[70] Orr, C.: Particulate Technology Seminar, Oct. 1969, Kyoto, Japan
[71] Brunauer, S., Deming, L. S., Deming, W. E., Teller, E.: *J. AM. Chem. Soc.,* **62,** 1723 (1940)
[72] Brunauer, S., Emmett, P. H., Teller, E.: *J. Am. Chem. Soc.,* **60,** 309 (1938)
[73] Feldman, R. F., Sereda, R. J.: *Matér. et constructions RILEM,* **1,** 509 (1968)
[74] Powers, T. C., Brownyard, T. L.: *Proc. Am. Concrete Inst.,* **43,** 469 (1947)
[75] Brunauer, S. Kantro, D. L., Copeland, L. E.: *J. Am. Chem. Soc.,* **80,** 761 (1958)
[76] (Hodakov, G. S., Kudrjavceva, N. L.) Г. С. Ходаков, Н. Л. Кудрявцева: *ЖФХ* **XXXVII,** 10 (1963)
[77] Opoczky, L.: *SZIKKTI Tudományos Közlemények* Budapest **84** (1985)
[78] Robens, E.: *Archiv. tech. Messen,* **1285,** 69 (1968)
[79] Haul, R., Dombgen, G.: *Chem. Ing. Tech.,* **35,** 586 (1963)
[80] Alongi, V.: *Chem. Rundschau,* **20,** 1 (1967)
[81] Leppard, C. J., Spencer, D. H. P.: *J. Sci. Instr.,* **1,** 573 (1968)
[82] Lin, I. J., Nadiv, S., Grodzian, D. J. M.: *Mineral Sci. Eng.,* **7,** 313 (1975)

Chapter 3

3. CHANGES IN THE STRUCTURE AND IN THE CHEMICAL REACTIVITY OF SOLIDS DUE TO DEFORMATION AND FRACTURE

3.1. MACROSCOPIC PHENOMENA IN SOLIDS INDUCED BY MECHANICAL LOAD

The mechanical forces affecting solids during grinding may alter the stress state and thereby the shape, the internal structure and the chemical reactivity of the particles. Since there are many forces acting upon the particles, during and as a consequence of grinding, the particles are not only of different sizes but are also in different states of stress.

The behaviour of the individual particles under mechanical load is essentially similar to that of macroscopic solids. Therefore, it is appropriate to start the discussion about the changes which are induced by grinding in the structure and chemical reactivity of solids by describing the phenomena associated with the deformation and fracture of macroscopic solids and of individual particles.

3.1.1. SOME BASIC PHENOMENA OF STRESS ANALYSIS

Stress is generated in solids under the action of mechanical forces and this results in deformation and fracture when the level of stress reaches the fracture limit. The state of stress of a solid also depends on the way the load is applied. Thus, under isostatic load the solid becomes slightly compressed, but under anisotropic stress it deforms. The degree of deformation depends on the magnitude and the direction of the force as well as on individual properties of the solid. Deformation is "elastic" when, after the release of the deforming force, the solid regains its original shape. When there is no relaxation, or only partial relaxation, then the solid suffers permanent deformation.

Static pressure may promote chemical reactions not only in gases and liquids but also in solids. Pressure-induced polymorphic transformations are also rather common. For example, the phase equilibria of quartz, of aluminium silicates, and of water, which play an important role in the behaviour of other silicates, are shown in Fig. 3.1.

In mechano-chemical activation, however, not only are the isotropic changes, which are affected by static load, important but the anisotropic stresses generated by forces acting from distinct directions are even more important. The phenomena can be studied in a macroscopic way by means of experimental "stress–deformation" curves. The common features of such curves allow solids to be classified according to the following principles (cf., Fig. 3.2):

(a) In a solid of linear elasticity (Fig. 3.2(a)), deformation is proportional to the force acting upon it. This correlation was recognised in the 18th century and was named

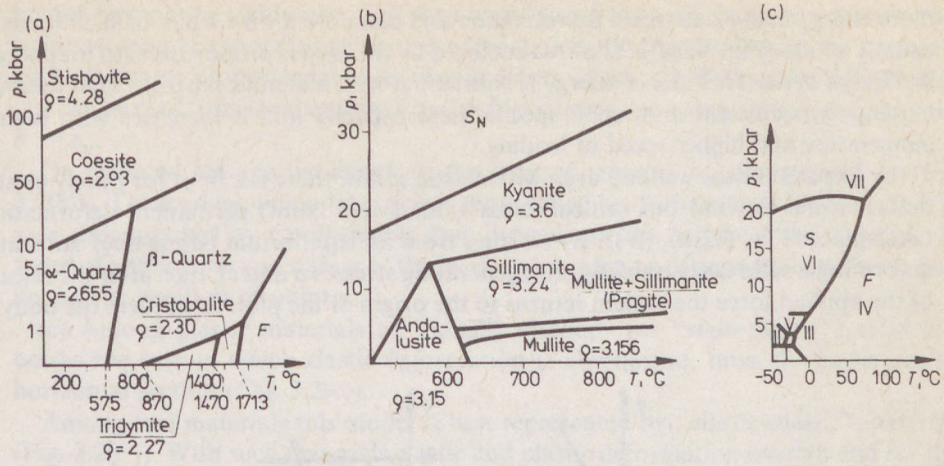

Fig. 3.1. Phase equilibria of (a) quartz, (b) aluminium silicates, and (c) water

Hooke's law after its discoverer ("ut tensio, sic vis"):

$$\sigma = E\varepsilon$$
$$\tau = G\gamma, \tag{1}$$

where σ is the perpendicular and τ the tangential stress, E the elasticity (Young) modulus, G the torsional modulus, $\varepsilon = \Delta l/l^0$ the linear relative deformation, and γ the specific torsional deformation (torsion angle).

In order to change the dimension of the body by a value of $\mathrm{d}l$

$$\mathrm{d}W = \sigma\,\mathrm{d}l \tag{2}$$

specific deformation work has to be put into it. If the elastic deformation is carried out under isothermic and reversible conditions, and if we neglect the very small change of volume, the kinetic energy associated with deformation, and other losses of heat, then the mechanical work put in during deformation is equal to the increase in free energy of the body ($\mathrm{d}f$). Therefore, according to the combined Ist and IInd laws of thermodynamics it follows that:

$$\mathrm{d}W = \mathrm{d}f = \mathrm{d}u - T\,\mathrm{d}s, \tag{3}$$

where $\mathrm{d}u$ is the change of internal energy and $\mathrm{d}s$ the change of entropy at temperature T.

Pure reversible deformation is a completely reversible process, i.e. work put in during deformation is completely released on relaxation following deformation.

The concept of an ideally elastic body is, of course, an abstraction, because it involves a fully reversible process. Deformation of real solids under stress requires

more energy than is recovered on relaxation and therefore the $\sigma - \varepsilon$ plot of such solids is usually a loop (Fig. 3.2(a)). The area enclosed by the loop is proportional to the energy lost in the cycle. This loss of energy is substantial with materials having a high thermal expansion coefficient and small specific heat capacity and it increases with higher temperature and higher speed of loading.

(b) Experience shows that, even with elastic solids, there is a limit for purely elastic deformation. Beyond this critical stress value (yield point) permanent deformation takes place (Figs 3.2(b), (b')). By starting from an equilibrium (stress-free) state and deforming a solid body only slightly (generating stresses σ and ε), then after the release of the applied force the system returns to the origin of the plot. If, in turn, the body is

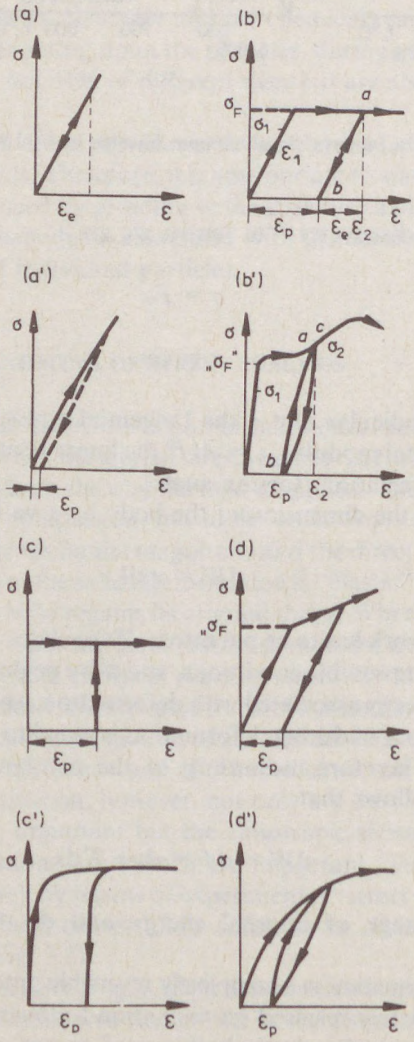

Fig. 3.2. Types of stress-deformation diagrams

loaded beyond the yield point (σ_2), then on releasing the load the system travels from point a to point b representing the stress-free state in the course of which the size of the body decreases proportional to its elastic deformation (ε_e). Permanent deformation (ε_p) can be read from the diagram. Total deformation at point a is $\varepsilon_2 = \varepsilon_e + \varepsilon_p$, at point b $\varepsilon = \varepsilon_p$.

On repeated loading we return to the stressed state σ_2, ε_2 along curve bc (Fig. 3.2(b′)). The loading–unloading cycle is represented by the hysteresis loop ab–bc. The area circumscribed by the hysteresis loop depends on the nature of the material, the speed of application and release of the load, and the degree of permanent deformation, i.e. on the position of point a.

(c) Among plastic materials an "ideally viscous" (or "rigid-plastic") solid is a borderline case in which elastic deformation is absent and, thus, the curve has no horizontal section (Fig. 3.2(c)).

Among real materials this model is best represented by "elastic-plastic" materials (Fig. 3.2(c′)). With such materials elastic and plastic deformation overlap and for this reason permanent deformation sets in at small loads.

(d) Finally, the "linearly elastic–linearly hardening" model (Fig. 3.2(d)) is approximated by the "elastic-viscous" solids, where elastic deformation is superimposed on viscous deformation.

Since specific deformation work is proportional to the area encompassed by the σ–ε plot, it can readily be seen that with plastic and viscous deformations the work put in during the deformation period cannot possibly be completely recovered during the relaxation period. The work connected with permanent deformation is transformed to other forms of energy. In such a cycle the loss of work can be approximated by the integral

$$\Delta W = \int_0^{\varepsilon} \sigma \, \mathrm{d}l - \int_{\varepsilon_p}^{\varepsilon} \sigma \, \mathrm{d}l \tag{4}$$

and is shown in isothermic processes in the form of heat dissipated to the environment and in anisothermic processes, deformation and heating of the body.

Deformation and elasticity are properties which depend also on experimental conditions, e.g. on temperature. The speed of applying the load is important from the point of view of structural changes proceeding during deformation. When, for example, two test specimens of identical dimensions, composition, and temperature are loaded (e.g. pulled) with different speed then the stress corresponding to the same specific deformation can be expressed by Prandtl's equation:

$$\sigma_a = \sigma_b + m \ln \frac{c_a}{c_b} \tag{5}$$

where σ_a is the stress corresponding to elongation velocity c_a, σ_b is the same value for c_b, and m is a material constant. Thus, an increase in the rate of load application results in an increase of stress corresponding to the same deformation. At the same time, the yield point and the specific deformation work are increased, i.e. the energy taken up by the system is increased, or in other words, the material becomes more rigid.

An opposite trend can be observed when the speed of loading is substantially lowered. This entails a reduction of the yield point, and loading the system beyond the yield point results in enhanced plastic deformation.

The change of stress in bodies under prolonged mechanical load is expressed by the Maxwell equations:

$$\sigma = \sigma_0 \exp - \left(\frac{t}{\lambda}\right)$$
$$\tau = \tau_0 \exp - \left(\frac{t}{\lambda}\right). \tag{6}$$

This phenomenon is called relaxation. In the equations, λ represents the relaxation time, i.e. the period in which the initial stress, σ_0 and τ_0, respectively, is reduced to the value $1/e$. σ and τ are stress values observed at time t.

If a solid body is pulled in a certain direction its dimensions perpendicular to that direction decrease. If, in turn, the body is compressed, a crosswise increase of its dimensions occurs. The specific changes in the two directions (ε_l, ε_c) are, however, not equal. The ratio of these values is Poisson's coefficient:

$$\nu = \frac{\varepsilon_c}{\varepsilon_l}. \tag{7}$$

The correlation between the elasticity modulus, the compressibility coefficient $\varkappa$ and Poisson's coefficient is as follows:

$$E = 3\frac{1-\nu}{\varkappa} = 2G(1+\nu). \tag{8}$$

The elasticity modulus is only meaningful with solids, since liquids lack retentivity, and have E and G values that are necessarily zero. Therefore:

$$0 = 1-2\nu \tag{9}$$

from which:

$$\nu = 0.5.$$

From the point of view of stress analysis liquids are characterised by a Poisson coefficient of 0.5 whereas, with solids, ν is always less than 0.5. The closer the Poisson coefficient of a material approaches 0.5 the more similar it is to a liquid from the point of view of stress analysis.

The distinction between liquids and solids can be defined in terms of rheology by the yield point. According to Houwink [1] the existence of a yield point is an essential feature of all solids. If a material has no yield point then it is liquid. It follows from the relaxation phenomena mentioned above that this latter definition is not completely consistent.

Mechanical strength is defined as the highest stress applicable without fracture. The strength of an individual material depends, not only on the inherent cohesion forces of the body, but also on the way the load is applied and on other experimental variables. For example, tests carried out with a very high loading speed to avoid plastic deformation, produce impact strength values which are, in general, much higher than those obtained with medium loading speeds.

Strength values also depend on the way the load is applied (tension–compression, shear, bending, torsional or combined load), as well as on the size and shape of the test specimen. "Macro" and "micro" strength may differ by several orders of magnitude. Thus, the tensile strength of a glass fibre a few μm width may be 100 to 1000 times higher than that of a glass rod a few mms thick.

The deformation of tough materials is very high before fracture, while brittle materials hardly deform at all.

Fracture is an irreversible process in which the continuity of the body is lost.

3.1.2. CHEMICAL PHENOMENA ACCOMPANYING DEFORMATION AND FRACTURE

Changes in the chemical reactivity of a material under mechanical stress can be exemplified by the following pair of model experiments [2]. The set-up of the first

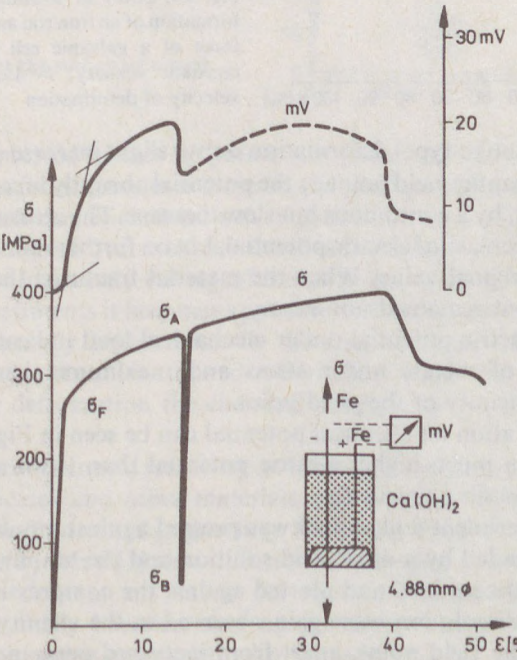

Fig. 3.3. Tensile strength diagram of a steel rod. Potential difference between a loaded and an unloaded test rod [2]

experiment is shown schematically in Fig. 3.3. A steel rod was clamped into the jaws of a tensile strength machine and surrounded by a solution of $Ca(OH)_2$. The rod was exposed to continuous tension and the electric potential difference between the rod and an unloaded specimen, submersed into the same solution, was recorded (mV). In the

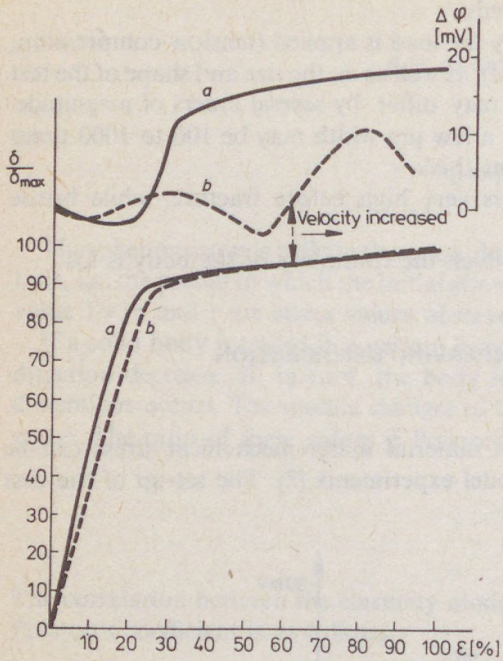

Fig. 3.4. Effect of loading velocity on the deformation of an iron rod and on the electromotive force of a galvanic cell [2]. *a*—Loading with constant velocity; *b*—Loading with constant velocity of deformation

domain of elastic (Hooke-type) deformation only a slight increase of electric potential was observed, but near the yield point σ_F the potential abruptly increased, followed, on continued stretching, by a continuous but slow increase. The return from σ_A to σ_B was accompanied by a decrease of electric potential, but on further re-loading the potential did not regain its original value. When the material fractured the electric potential dropped suddenly but remained non-zero.

This change of electric potential under mechanical load indicates a change in the chemical potential of metals under stress and maximum chemical reactivity is experienced in the vicinity of the yield point.

The effect of relaxation on chemical potential can be seen in Fig. 3.4. Fast loading (curve *a*) generates a much higher electric potential than (with an equal degree of deformation) slow loading (curve *b*).

In the second experiment a glass ball was pressed against a polished steel surface. The ball was surrounded by a nitric acid solution and the amount of iron dissolved during the test was determined and plotted against the compressive force (Fig. 3.5). The highest rate of dissolution was again observed in the vicinity of the yield point (point B). Beyond the yield point, apart from increased permanent deformation, a decrease of the rate of dissolution was observed, whereas in the domain of elastic deformation (below point A) dissolution was very slight. The electron microscope

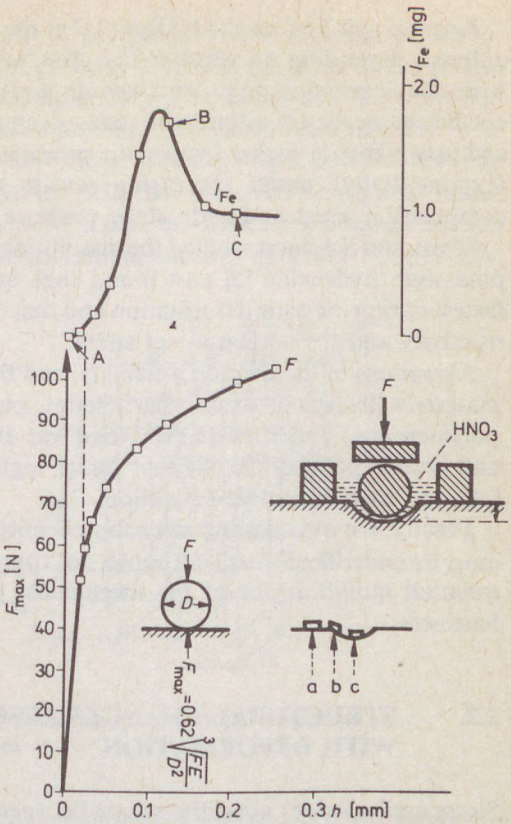

Fig. 3.5. Dissolution at the surface of a steel rod under tension [2]

image of the compressed surface (in points a, b, and c) showed the maximum number of corrosion holes for stress states close to the yield point (point b).

The rate of dissolution under load was, in general, twice as high as after the loading. For example, 1.4 mg of iron was dissolved under a load of 8.95 N whereas, after releasing the same load, only 0.6 mg of iron was dissolved around the ball.

From these experiments it becomes apparent that the increase of chemical potential under load is generally higher than in the stressed state following loading; the maximum chemical potential is attained at the critical stress near the yield point. In the domain of elastic deformation the chemical potential of a material is only slightly increased.

The dependence of chemical reactivity on the state of mechanical stress has also been observed with silicates and other materials and we shall discuss this phenomenon repeatedly in connection with fine grinding. Here we only mention, as an example, the observation made by May [3] that diffusion of nitrogen in metals is slow, or even negligible, in the domain of elastic deformation; it accelerates during plastic deformation, and finally becomes slow again before fracture. This shows that the maximum diffusion rate is associated with the same type of deformation as that for which the increase of electric potential was significant.

Nogami and Tomozowa [4] found that the diffusion rate of water in silicate glasses differed, depending on whether the glass was surrounded by water under uniform hydrostatic pressure or water taken up under unidirectional pressure. The diffusion coefficient increased with tensile stress, decreased with increasing compression stress, and was higher at higher hydrostatic pressure. Dissolution of water in glass decreased (exponentially) under increasing tensile stress and increased with increasing compression stress and hydrostatic pressure.

Senna and Schönert studied the dissolution at the surface of quartz monocrystals in potassium hydroxide [5] and found that under mechanical stress dissolution was fastest during inelastic deformation and that there was a correlation between chemical reactivity and the magnitude of stress.

Alterations of the density, wetability, and the chemical reactivity of metals and other materials (feldspars, oxides, carbonates, photographic papers, organic substances, polymers etc.) under mechanical load was discovered a long time ago [6–17]. Naeser and Scholz pointed out [8] that under high load the active state of materials was followed by chemical de-activation.

Finally, the outstanding mechano-chemical importance of such chemical reactions must be underlined which, although not triggered by mechanical loading, bring about essential modifications of the mechanical properties of solids (ductility, strength, hardness).

3.2. STRUCTURAL CHANGES ASSOCIATED WITH DEFORMATION

Stress analysis does not differentiate between materials of different internal structure. It is of no consequence for the laws of stress analysis whether the structure of the body under study is amorphous (disordered), or crystalline (ordered). According to Glockner's definition [18] the structure of an amorphous material can be adequately described by its coordination number, i.e. by the number of atoms in the environment of each individual atom, but with crystals this has also to be supported by symmetry considerations. The order of the internal structure is expressed by the symmetry laws.

However, from the standpoint of physical chemistry the solid state is restricted to materials of ordered structure, i.e. to crystals.

3.2.1. DEFORMATION OF IDEAL CRYSTALS

An ideal solid is equivalent to an ideal crystal. The ideal crystal (which is an abstraction) is characterised by a maximum of ordering at every point of that crystal [19].

Bravais (in 1848) described the internal order, or internal symmetry, of crystals by representing the individual atoms by points and considering their mutual distances and orientations [20]. This analysis is facilitated by the application of symmetry elements: translation into one, two, and three directions, rotational axes, centres of symmetry, and the combinations thereof. If, for example, an arbitrary point P_i is selected from the row of points shown in Fig. 3.6(a), it is possible to define a direction and distance (x_0)

in which we find an identical point P_{i+1} or P_{i-1}, respectively. This statement is true for each point of the row: whichever point (or atom) is shifted in the given direction and for the given distance, an identical point will invariably be overlapped. If this operation (translation) is restricted to a single direction—since in other directions there is no periodicity in the arrangement of points—then we are dealing with a linear lattice (Fig. 3.6(a)). If the latter can be shifted parallel to itself, then we arrive at a planar lattice (Fig. 3.6(b)) and finally, by parallel translation of a planar lattice in the third direction of space we obtain a model for the three-dimensional lattice (Fig. 3.6(c)). Conversely,

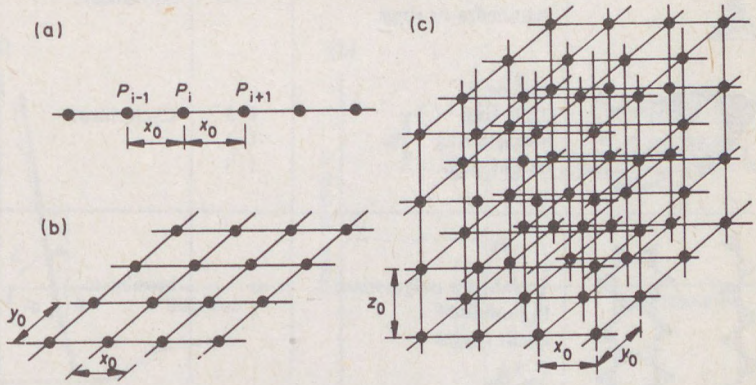

Fig. 3.6. Determination of the internal symmetry of crystals by translation into (a) one, (b) two, and (c) three dimensions

in every crystal lattice it is possible to place such parallel planes across lattice points the distances of which are x_0, y_0, and z_0 or integer multiples thereof: in this case, the minimum distance between two lattice points is called the lattice constant.

Silicates may be classified according to their internal crystalline structure, specifically by the structure of a lattice composed of SiO_4^{4-} tetrahedra.

In "inosilicates" these tetrahedra are linked by common oxygen atoms and form parallel chains. In these chains, identically positioned tetrahedra are arranged in a row as shown in Fig. 3.6(a). In "phyllosilicates" we find two-dimensional layers, whereas "tectosilicates" contain a three-dimensional network of tetrahedra. In other words, the arrangement of identically positioned tetrahedra in the crystal lattice can be described by translation in two or three directions. The ratio of oxygen and silicon atoms in the lattice depends on whether the tetrahedra are linked to each other by common oxygen atoms in one, two, or three directions.

In "nesosilicates" there are solitary tetrahedra at the translation points, in "sorosilicates" there are double tetrahedra, and finally in "cyclosilicates" there are cyclic arrays of tetrahedra. The lattice points in all of them are linked by cations.

The classification of silicates according to their crystal structure is shown in Table 3.1.

The smallest unit of a lattice which still retains the symmetry of the entire lattice is called the unit cell. Thus, by describing the unit cell we define the quality, quantity, and ratio of the atoms of the entire crystal as well as the symmetry of the whole lattice. In an

Table 3.1. The main structural types of silicates

Basic unit	Combination of tetrahedra	Si : O ratio	Name
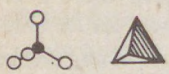 $[SiO_4]^{4-}$	Isolated tetrahedra	1 : 4	Nesosilicate
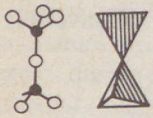 $[Si_2O_7]^{6-}$	Isolated double tetrahedra or rings:	1 : 3.5	Sorosilicate
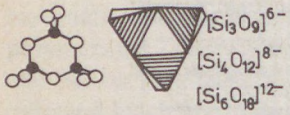 $[Si_3O_9]^{6-}$ $[Si_4O_{12}]^{8-}$ $[Si_6O_{18}]^{12-}$	triple ring fourfold ring sixfold ring	1 : 3 1 : 3 1 : 3	Cyclosilicate
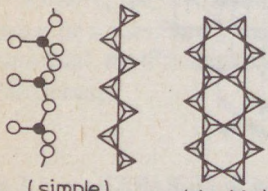 (simple) (double) $[Si_2O_6]^{4-}$ $[Si_4O_{11}]^{6-}$	Tetrahedra polymerised to "infinite" linear chains Simple chain Double chain	 1 : 3 1 : 2.75	Inosilicate
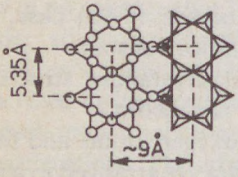 $[Si_4O_{10}]^{4-}$	Tetrahedra polymerised in two dimensions to "infinite" planes	1 : 2.5	Phyllosilicate
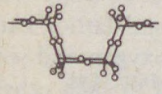 $[(Al_xSi_{n-x})O_{2n}]^{x-}$ $[Si_nO_{2n}]^0$	Tetrahedra polymerised in three dimensions to an "infinite" network	1 : 2	Tectosilicate

"ideal crystal" there is not a single region in the whole lattice which does not correspond exactly to the arrangement of atoms defined by the unit cell.

In characterising the structure of ideal crystalline solids we assumed that there were very strong binding forces between their atoms, ions, or molecules and, therefore, each structural element of the lattice was surrounded by as many neighbouring atoms as

was possible from the dimensions of these atoms and from the equilibrium of the forces of the whole system.

The magnitude of the forces between atoms depends on the type of bonding (ionic, metallic, or van der Waals), the nature of the atoms, and the type of lattice. The resultant force (composed of an attractive and a repulsive term) changes with the interatomic distance x as shown in Fig. 3.7(a). The curve intersects the x axis at distance x_0—at a point where attractive and repulsive forces compensate each other. In other words x_0 represents the equilibrium interatomic distance, and the most probable site of the centre of the vibrating atom ("lattice constant").

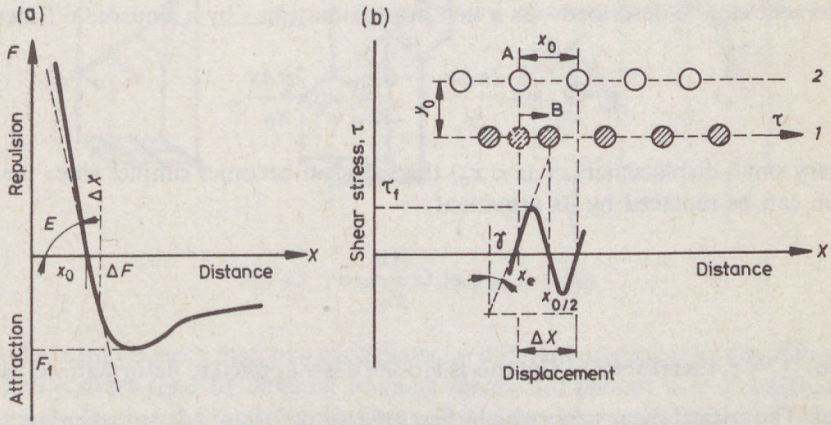

Fig. 3.7. (a) Dependence of the resultant interatomic forces on the distance between atoms [1]. (b) Shear stress in the translation of two rows of atoms [21]

If the distance between two atoms is increased, for example, by pulling the atoms apart, then a force F, corresponding to the actual distance, is generated between the two atoms. If stress is released the original distance (x_0) is restored and the force relaxes. It is clear that such an elastic deformation sets in because of the decrease of cohesion forces. F_f is thus equivalent to the "yield point" of the two atoms [1].

At a small displacement ($x_0 + \Delta x$) the curve of the resultant force shows an approximately linear section. In this case, according to de Boer [1], relative tension, as referred to a pair of atoms, may be taken as being proportional to the macroscopic elongation of a linear crystal lattice of length l_0:

$$\varepsilon = \frac{\Delta l}{l_0} = \frac{\Delta x}{x_0}. \tag{10}$$

The "elasticity modulus" for the same pair of atoms:

$$E = \frac{\Delta F x_0}{x}. \tag{11}$$

Let us now consider the shearing stress (τ) between atoms A and B associated with the translation of two lattice planes placed at a distance y_0 from each other (Fig. 3.7(b)) [21]. Starting from equilibrium (x_0) the force generated between atoms A and B increases with the distance x corresponding to the extent of translation up to one fourth of the intraplanar atomic distance x_0. From this point on the shear stress drops until $x_0/2$ is reached, where attractive and repulsive forces come to an equilibrium and thus their resultant becomes zero. Thereafter, the force acting between A and B becomes negative, attains a minimum at $3x_0/4$ and, finally, at translation by a distance of x_0 the equilibrium state is again restored. In the meantime, the first lattice plane becomes shifted relative to the second by $\Delta x = x_0$. The dependence of shear stress on displacement can be described—as a first approximation—by a sinusoidal function:

$$\tau = \tau_f \sin \frac{2\pi \Delta x}{x_0} = \frac{G x_0}{2\pi y_0} \sin \frac{2\pi \Delta x}{x_0}. \tag{12}$$

At very small displacements ($\Delta x \ll x_0$) the function becomes simpler since the sine function can be replaced by its argument:

$$\tau = G \frac{\Delta x}{y_0}. \tag{13}$$

Since $\frac{\Delta x}{y_0} = \gamma$, therefore $\tau = G\gamma$; this is Hooke's law applied to deformations caused by shear. The critical shear stress which effects plastic deformation approximates to the maximum value of τ. Therefore the "yield point":

$$\tau_{\max} = \tau_f = \frac{G x_0}{2\pi y_0}. \tag{14}$$

It also follows from our simple crystal model that the particular critical stress, at which plastic deformation sets in, depends on the ratio x_0/y_0. In such a simplified crystal there are always planes in which the atoms are arranged in closest packing (i.e. the value of x_0 is small) while, in turn, neighbouring planes are relatively distant (y_0 is large). It can be expected that plastic deformation starts along such crystal planes at relatively low shear stress. Such planes are called glide planes.

The gliding of layers can only be observed with the deformation of crystalline solids; there are no glide planes in isotropic materials, such as amorphous solids. Gliding can be defined as the translation of lattice planes along the glide plane (Figs 3.8(a) and (b)). Gliding can be achieved with minimum force when the force coincides with the direction of the glide plane. Otherwise, it depends on the angle between the glide plane and the external force whether, at a given value of force, plastic deformation or brittle fracture takes place. In the experiment depicted in Figs 3.6(c) and (d) gliding sets in when the component τ of the resultant force (σ_0) in the direction of gliding exceeds the value of the "yield limit" (τ_f); this not only depends on the load (F) but also on the angle α between the resultant force and the glide plane. If α is small, plastic deformation occurs (Fig. 3.8(c)), because at a sufficiently large value of σ_0 the shear stress acting in

the direction of the glide plane attains the critical value when its perpendicular projection is smaller than the tensile strength σ_T. When, in turn, α is large, then on continuously increasing the resultant stress its perpendicular projection matches the tensile strength of the material before the projection in the glide plane reaches the yield point. As a consequence the test piece breaks as a rigid body (Fig. 3.8(d)).

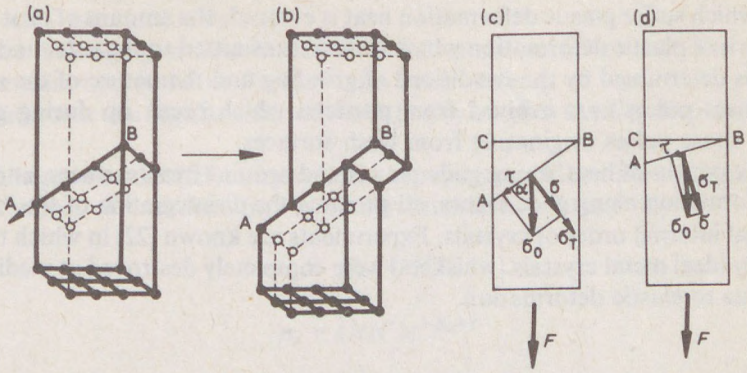

Fig. 3.8. Translation along glide planes

It follows that if more than one glide plane (at different angles to the direction of the load, and characterised by different bonding forces) are present in a crystalline body then, on increasing the load, translation sets in either along the planes of minimum bonding forces, or along those planes which are at the smallest angle to the direction of load. This gliding action is then followed by the activation of more and more glide planes, so that permanent deformation (ε_p) increases.

In silicate crystals strong polarisation of the oxygen atoms by silicon results in high stability of the Si—O bonds, which are 50% ionic and 50% covalent. Splitting such a bond requires high energy. However, there are also bonds of lower energy in the lattices of silicates. The presence of glide planes parallel to the silicate chains or layers is especially prevalent in ino- and phyllosilicates. Such materials have a tendency to break into needle-like and splintery particles or into laminar grains, especially under small load, e.g. during the initial phase of coarse grinding. Deformation and fracture perpendicular to the layers take place only when the readily moving layers have already moved away from each other (i.e. the glide planes have opened up) or when the speed of the acting force is so high that displacements along the glide planes are precluded. These events take place under impact loading, intensive grinding, or at that stage of fine grinding when the particles are very small.

In systems that consist of tiny crystals, such as in ground materials of sufficiently high dispersion grade, the particles form—at least approximately—a disordered set. If such a system is further stressed (e.g. by grinding) then the only particles to suffer further breakage are those in which stress (or a component thereof) matches the strength of the particle. Those grains in which stress is smaller than the particle strength, but is still high enough for plastic deformation, will undergo permanent deformation. It follows from the statistical character of this phenomenon that with a

sufficiently large number of loading cycles (i.e. by grinding for a long time or by using a force of high frequency) then, not only will the degree of deformation of the individual particles be different, but the magnitude and direction of plastic deformation will also vary along different glide planes within a single crystal.

Those particles which are subjected during grinding to very small forces suffer only elastic deformation and, after the release of the force, regain their original state. In particles which suffer plastic deformation heat is evolved; the amount of heat depends on the work of plastic deformation which is then transmitted to the surroundings in a way that is determined by the conditions of grinding and the nature of the particles. Finally "heat pulses" are evolved from particles which break up during grinding, especially those pulses originating from fresh surfaces.

Local evolution of heat, along glide planes and around fresh surfaces, and further plastic deformation along glide planes, all promote the disintegration of the "ideal" or nearly ideal internal order of crystals. Experiments are known [22] in which the order of virtually ideal metal crystals (whiskers) were completely destroyed at medium load entirely due to elastic deformation.

3.2.2. DEFORMATION OF REAL CRYSTALS

If the crystal structure and interatomic forces are known then the theoretical strength and yield point of ideal crystals can be calculated relatively easily [23]. However, these calculated values are several orders of magnitude higher than the experimental ones. The reason for this discrepancy is that real crystals have defective, rather than ideal, structures (Griffith [24], Smekal [25], Orowan [26], Taylor [27], and Polányi [28]). Studies by these, and other authors led to the experimentally well-supported theory which interprets the deformation and fracture of solids by the formation, flow, interaction, and elimination of dislocations.

According to our present concept the structures of real crystals necessarily differ from those of ideal crystals. It is sometimes possible to produce almost ideal crystals, such as needle shaped metal crystals (whiskers), but such structures are unstable and re-arrange, even under moderate loads, to more stable but less ordered forms. In particular, the structures of silicates are almost always defective.

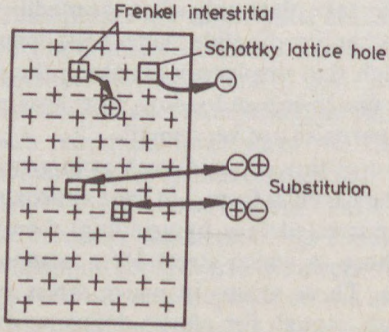

Fig. 3.9. Point defects in a lattice

According to Kittel [21] several important properties of a given solid depend more on crystal defects than on its material content, which can be regarded simply as a carrier of the defects. Lattice defects are of the following types:

Point defects (Fig. 3.9) are characterised by

—atoms missing from certain positions in the lattice (lattice hole, vacancy or Schottky-type lattice defect);
—atoms belonging to the lattice external atoms misplaced within the lattice (insertion, interstitial or Frenkel-type lattice defect);
—replacement of a regular atom of the lattice by an alien atom (substitution defect).

According to Frenkel [23] every crystal at temperature T contains, at equilibrium, a definite number of vacancies (n_v) and interstitial lattice defects (n_i):

$$n_v = Ne^{-E_v/kT}$$
$$n_i = (NN')e^{-E_i/kT} \tag{15}$$

where N is the number of lattice points, N' the number of interstitial points, k the Boltzmann constant, T the temperature, E_v and E_i the activation energy of the formation of vacancies and insertions, respectively. E_v approximates to the evaporation heat of the material concerned; therefore, the formation of vacancies is relatively easy. In contrast, since $E_i \gg E_v$, Frenkel-type lattice defects (migration of atoms from lattice points to interlattice sites) can only be generated by the application of high energy, e.g. by neutron radiation. At room temperature the number of lattice holes in relation to the number of lattice points is only a few per thousand, but this value increases exponentially with temperature and attains 1% at the melting point and 3% during melting.

Small atoms are amenable to substitution and, even in very small quantities, can alter the properties of a solid. The formation of mixed crystals [29] is interpreted as substitution and the structure of certain silicates can also be derived in this way.

Dislocations are deformations of a crystal lattice where groups of atoms are not situated exactly at the geometrical lattice points. Dislocations develop around point defects in the lattice because the equilibrium of interatomic forces, as compared with the non-defective parts of the crystal, is perturbed and this also involves a change of interatomic distances (Fig. 3.10).

A linear dislocation (an edge or a helical dislocation) develops when the deformations of the lattice are connected to each other as a row of points (Fig. 3.11). A surface-like dislocation is formed when the lattice network is deflected along an imaginary surface by an angle ϑ (Fig. 3.11(c)). Surface dislocations also demarcate those spatial elements of the crystal lattice in which the crystal structure is relatively intact. These, usually submicroscopic, elements are termed crystallites and are arranged in a more or less random fashion so that the crystal has a mosaic-like structure. Submicroscopic, or even larger, gaps having actual surfaces come into being within the lattice thus forming a three-dimensional dislocation.

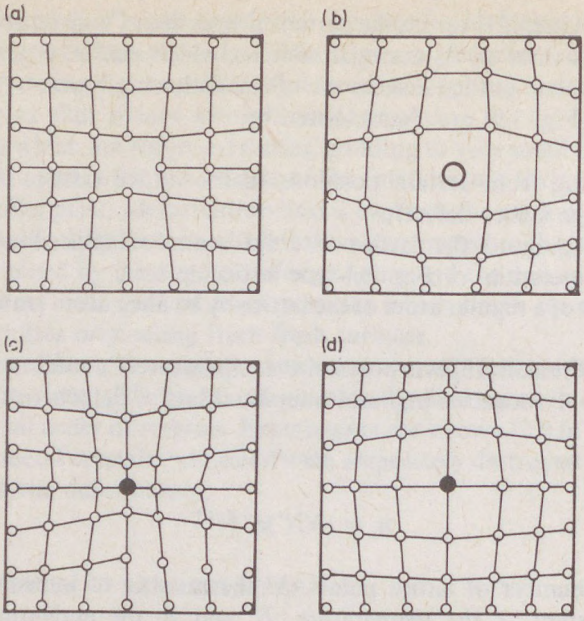

Fig. 3.10. Distortion of the crystal lattice around defects: (a) hole defect, (b) interstitial defect, (c) and (d) substitution defects [29]

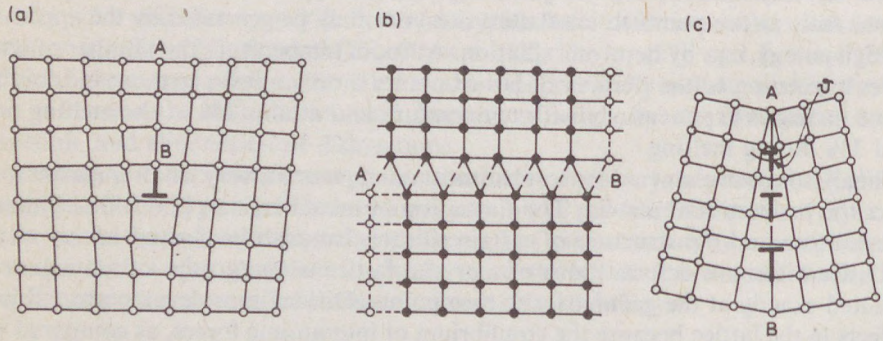

Fig. 3.11. Linear (a), torsional (b), and planar (c) dislocations

The density of dislocations in a crystal is usually high. This has been demonstrated by optical examination after etching, by X-ray diffraction [30], by calculation of plastic deformation, and by methods based on conductivity [21] that, in metals at room temperature, the number of dislocations may be as many as 10^8 or 10^9 per 100 mm^2. This number can be as much as 10^{11} to 10^{12} per 100 mm^2 in strongly deformed metals since new dislocations are generated during deformation. Dislocations can be displaced by relatively small forces so that crystals can be deformed along glide planes by forces much smaller than those calculated on theoretical grounds. Kittel [21] illustrated this phenomenon by an enlightening analogy: the movement of edge dislocations along the crystal resembles the propagation of a crease along the surface

of a carpet. The crease passes much more easily across the carpet than the whole carpet can slide on the floor, but as a consequence of the crease the whole carpet is slightly shifted on the floor.

The movement of dislocations along a given plane (AB) is shown in Fig. 3.12. Whilst, under the effect of a shear force (τ), which is much smaller than the theoretical yield point, the edge dislocation arrives at the surface and the two planes are displaced in relation to each other by a distance $\bar{b}$. The deformation $\bar{b}$ which is produced when the dislocation travels through the whole crystal is called the Burgers-vector.

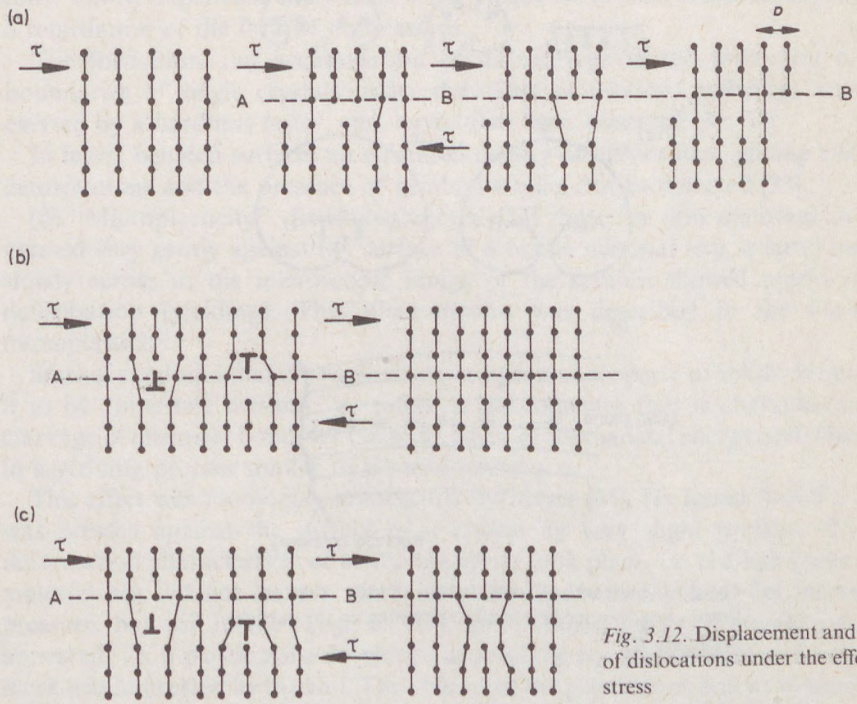

Fig. 3.12. Displacement and interaction of dislocations under the effect of shear stress

Gliding in real crystals usually proceeds in jumps, which may sometimes be accompanied by clacks which are audible in a quiet room. The magnitude of individual jumps may be a multiple of the Burgers-vector or it can exceed it by several orders of magnitude. This phenomenon also supports the view that plastic deformation is caused by a mass movement of dislocations.

Displacement of dislocations may be accompanied by secondary phenomena which result in a variation of the density of dislocations, thereby influencing the deformation process itself. Such phenomena and their effects are as follows:

(a) Interaction of dislocations. It is apparent from Fig. 3.12(a) that the shearing force acting along the glide plane AB finally results in the dislocation of an intercalated extra plane. According to convention, when this extra plane is located above the plane of the actual displacement the corresponding dislocation is called a positive one (symbol: ⊥), while when it is beneath this plane then it is negative (symbol: T). In the

course of crystal deformation all dislocations of the same sign repulse, and those of opposite sign attract each other and may even mutually cancel each other. Thus when negative and positive dislocations encounter each other along the glide plane shown in Fig. 3.12(b) and at a distance of one atom, then both are eliminated; if the distance between the dislocations is two atomic rows (Fig. 3.12(c)) their encounter gives rise to a vacancy accompanied by a distorted crystal lattice around it.

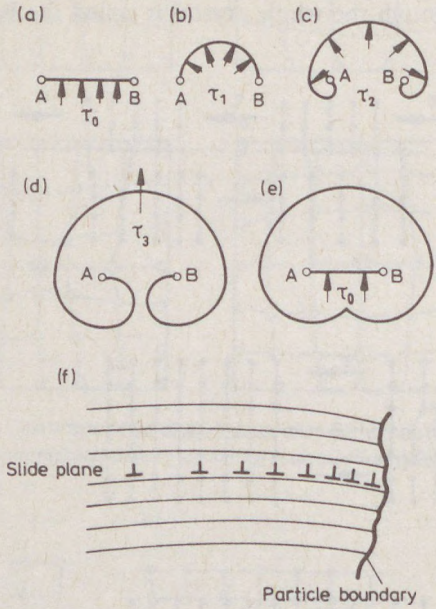

Fig. 3.13. Increase of dislocation density due to a Frank–Read source (a–e) and to jamming on the particle boundary (f)

(b) Increase of dislocation density. In general, linear dislocations go over to neighbouring glide planes and the sections of a linear dislocation associated with a single glide plane are relatively short and are "fixed" at points A and B (Fig. 3.13). In a stress-free situation dislocations are arranged linearly within this section (Fig. 3.13(a)). Under stress developing in the direction of gliding (Fig. 3.13(c), (d)) these lines take up the shape of a loop. The magnitude of bending increases with stress ($\tau_1 < \tau_2 < \tau_3$) and, finally, the loop closes completely (Fig. 3.13(e)). It then breaks away from points A and B and forms an independent dislocation, while between points A and B a new edge dislocation appears. This is capable of forming another loop. In a state of stress this phenomenon is repeated several times and new dislocations are initiated continuously—starting from points A and B. Such edge dislocations "fixed" at both ends are called Frank–Read sources (after the discoverers of the phenomenon).

(c) Accumulation of dislocations at the particle boundary. From the outset, the density of dislocations is higher on the real surfaces of crystals and on the apparent surfaces of crystallites than inside the particles. In crystals with a mosaic structure the

density of dislocations on the apparent surface of the crystallites can be assessed by the Burgers-vector and the angle of inclination of the deflected crystal lattice $\left(x_d = \frac{b}{\vartheta}\right)$: the smaller the angle of inclination, the higher the dislocation density near the "surface" of the crystallites. When, in the course of deformation, the angle of inclination is further reduced, the number of dislocations increases. Therefore (because of the interaction of dislocations), either the number of lattice defects increases, or, during deformation the dislocations eliminate each other or mutually inhibit each other's flow. Experience shows that the consequence of such interactions is most often a retardation of the flow of dislocations.

The formation and accumulation of dislocations in the proximity of particle boundaries of single crystals under the effect of friction, polishing, compression exerted by a hardness tester, etc., have often been observed [31, 32].

In layers between surfaces an enhanced density of dislocations, gliding and inelastic deformations and the presence of residual strains can be detected [33].

(d) "Microplasticity". Smekal observed [34] that if a thin diamond needle was pressed very gently against the surface of a brittle material (e.g. quartz) and drawn slowly across it, the microscopic image of the scratch showed marks of plastic deformation (yielding). This phenomenon was described in the literature as microplasticity.

Smekal supposed that microplasticity is a general property of solids. He considered it to be "athermic melting" of solids, a phenomenon that is characterised by the cleavage of chemical bonds by the absorption of mechanical energy and which results in a yielding process similar to thermal melting.

This effect was thoroughly investigated by Meyer [35]. He found that if a hard ball was pressed against the surface of a crystal by very slight pressure then elastic deformation characteristic of brittle materials took place, i.e. the ball penetrated the material but did not leave a mark after the load was released. On increasing the pressure, but still in the range of very small values, traces of plastic deformation appeared; i.e. a plastic zone developed around the point of contact and a permanent mark was impressed by the ball. The volume of the plastic zone and its shape depended on the magnitude and duration of pressure. By suitable etching the arrangement of dislocation lines around the plastic zone can be made visible. Meyer observed that by applying a weak static pressure on the 001 face of a NaCl crystal a rosette structure appeared close to the mark left by the ball. The development of the rosette pattern can be attributed to the junction of dislocations flowing along the glide planes at different orientations. Towards the inside of the crystal a zone with few dislocations occurs immediately under the compressed zone; this is caused by the mutual extinction of dislocations. Consequently, the material in this zone became harder, e.g. with sodium chloride it was 313 MPa as compared with the normal microhardness value of approximately 250 MPa. The appearance of microcracks in the hardened zone was only observed when a large force was applied for a brief period.

Starting from Smekal's concept of microplastic state, Thiessen et al. developed a theory based on another phenomenon, mainly observed during the working of metals [31]. According to this theory, if the surface of a metal is struck by some tool, then a plastic zone develops around the point of impact in which the density of dislocations

attains a level characteristic for liquids. At the same time electrons and photons are emitted from the surface and electrically charged particles leave the surface. Thus, as a consequence of mechanical action a "plasma state" zone is formed close to the surface ("magma–plasma" model).

(e) Impurities. Burgersmüller demonstrated in 1933 [36] that alien atoms incorporated into a crystal lattice may cause hardening, i.e. dislocations arising around interstitial or substitution defects impede the flow of dislocations. For example, the incorporation of as little as 0.045 mol% of $SrCl_2$ into the lattice of a rock salt crystal resulted in significant hardening. Alloying "impurities" exert a similar effect on the mechanical properties of metals.

(f) Temperature. At higher temperatures, not only does the number of lattice defects increase (see the Frenkel equations), but the rate of flow of these defects also increases. This, in turn, involves more interactions between dislocations (such as retardations of their mutual displacements). Therefore, higher temperature may both promote and impede plastic deformation.

(g) Mechanical twin-formation. Some crystals, e.g. calcite, change their crystal form when weak pressure is applied to certain edges or faces of the crystal. Under such circumstances two parts of the crystal take up symmetrical positions relative to a twin plane or a twin axis (Fig. 3.14(a)). Twin formation does not require a change in the position or distance of lattice points and, therefore, it only involves a small activation energy. Furthermore, it proceeds rapidly and without much change of volume.

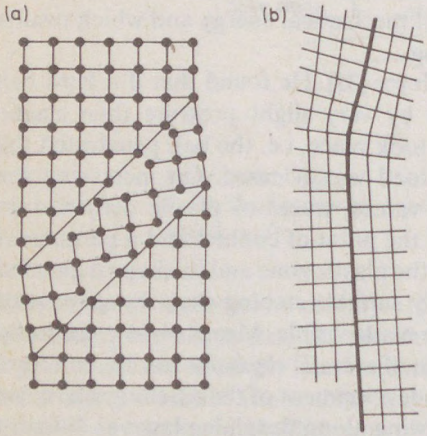

Fig. 3.14. Distorted crystal lattice due to (a) mechanical twin-formation and (b) translational gliding

Mechanical twin-formation often proceeds along glide planes and sometimes the entire deformation process is associated with twin-formation. For example, when antimony is subjected to impact-like load at low temperature the stress peak around the point of attack relaxes by "twin-formation conductance" [31]. At higher temperatures deformation of antimony takes place by "translational gliding", i.e. by flow of dislocations (Fig. 3.14(b)). It has to be noted, however, that dislocations retarding the flow of dislocations may also be generated along twin plane surface and for this reason mechanical twin-formation, though it generally promotes plastic deformation, most often inhibits "translational" deformation by the dislocation flow mechanism.

3.2.3. DEFORMATION OF POLYCRYSTALLINE MATERIALS

As pointed out above, the majority of (crystalline) bodies, including the silicates, are composed of a mosaic-like assembly of tiny, submicroscopic crystallites which may be of different chemical compositions. The development of such a structure by crystallisation from a melt [22] has been explained by assuming that crystal "germs" appear concurrently at many points of the melt. Their growth results in the formation of randomly oriented small crystals. In the course of crystallisation these crystals grow into each other but retain their original disordered orientation. The contacting surfaces, where necessary, develop a multitude of dislocations and these can be visualised by appropriate etching procedures [31].

In crystals with a regular mosaic structure the forces acting between crystallites are much smaller than the interatomic attractive forces and, therefore, the grains can be moved along each other by relatively small forces.

In polycrystalline solids the orientation of the individual crystallites is not uniform and in general, the crystallites are completely disordered. The mechanism of plastic deformation of such a structure under load is somewhat different from that of single crystals in as much that the grains mutually influence structural changes in the system.

This phenomenon will not be discussed here in detail, we only briefly refer to the following points:

(a) At very small loads each space unit of a polycrystalline solid undergoes elastic deformation.
(b) At some critical load plastic deformation of the crystallites starts along those glide planes which either coincide with the direction of force or which show a lower cohesion. Deformation is, however, retarded by the other crystallites and therefore the macroscopic phenomenon is still that of elastic deformation—accompanied, perhaps, by slight plastic deformation.
(c) On further increase of load permanent deformation sets in. Significant plastic deformation begins in the individual space elements despite the fact that the individual particles still behave in an elastic manner.
(d) At a sufficiently large stress the crystallites are re-orientated resulting in enhanced mechanical, optical, electric, etc. anisotropy. The hardening of certain metals under mechanical treatment is partly due to the re-orientation of crystallites.

3.2.4. DEFORMATION OF AMORPHOUS MATERIALS

Among silicate materials amorphous "minerals" such as glasses and gels, play an outstanding role.

The random structure of glasses can be interpreted theoretically from several points of view. Thus, according to Zachariasen [37], glass is a three-dimensional lattice without symmetry, in which SiO_4^{4-} tetrahedra and other three-dimensional elements of the structure are linked in a non-periodic, random spatial arrangement. Lebedev [38] considered glass to be a random assembly of highly dispersed (1.5 to 2.0 nm)

crystallites. Weyl and Haven [39, 40], and later Eckstein [41] proposed the concept that because of the effect of an extremely large number of defects, glass is a completely distorted silicate lattice. Since, according to the latter interpretation, the structure of glass is essentially identical with that of liquids, this concept is closest to the classical physico-chemical formulation, which states that "glass is an overcooled liquid".

The gels of silicic acid and of some silicates are also assemblages of amorphous submicroscopic particles, i.e. they are colloids [42]. Their mechanical strength is inherent in the gel skeleton, which comprises a network of fine, submicroscopic pores and capillaries. Gels are usually formed from aqueous colloidal solutions. If the particles retain their water shells they appear as jelly-like liogels (hydrogels) and are plastic solids or highly viscous liquids. On de-hydration liogels transform to xerogels.

The deformation of amorphous materials is basically different from that of crystalline materials because mechanical anisotropy is completely absent and they do not contain glide planes. Very small forces initiate plastic deformation; this starts at the weakest point of the structure and increases with increasing load. Amorphous materials should, in principle, have no yield point. In practice, however, glasses behave as brittle materials, especially at temperatures well below their softening points. This brittleness can be explained by the fact that in the course of cooling and solidification the viscosity of the melt increases to a level at which the material becomes shape-retaining. Yield point is, therefore, much dependent on temperature, in constrast to crystalline solids, for which the yield point varies only slightly with temperature.

All this does not imply that dislocation theory cannot be applied to the deformation mechanism of amorphous solids. The movement of dislocations can be observed in glasses and organic polymers under stress by illuminating them with polarised light. Such flow and diffusion under stress may cause the hardening of solids. Mechano-chemical studies have established that in amorphous bodies the generation, movement, and interaction of dislocations can entail both disordering and ordering [43].

For the sake of completeness we mention the behaviour of rubber and other amorphous polymers. The internal structure of rubber in a stress-free state is characterised by a network of long, disordered, and intertwined hydrocarbon chains. On small deformation the molecules become more-or-less stretched, while on release of stress they again become twisted like a spring. At a critical value of tension an ordered state of molecules, a so-called quasi-crystalline structure is established. In this highly stretched structure the crosslinks between hydrocarbon chains suffer gradual disruption.

With certain plastics, when under sufficiently high tension, elastic deformation is followed by permanent deformation. At even higher tension solid–elastic deformation takes place and the amorphous structure is transformed to an ordered "quasi-crystalline" structure.

The mechanical properties of the majority of amorphous gels, such as silica gel and silicate gels depend on their water content. Thus, silica gel freshly precipitated from an aqueous medium is a readily workable "jelly-like" material, but it becomes brittle when the water is evaporated. This phenomenon was first described by Bemmelen [44], who demonstrated that mechanical characteristics change abruptly and irreversibly after passing a critical value of water content. These changes confirm that water

molecules in a gel are situated at mechanically exposed sites of the skeleton structure, at contact points of the particles. Removal of the water molecules increases adhesion forces between the surfaces of neighbouring particles whereby the yield point and the elasticity modulus are increased and plastic deformation decreases.

3.3. FRACTURE

Fracture of particles is the basic aim in comminution. From the point of view of mechano-chemistry fracture is regarded as a primary process which involves an increase in the free energy of the system. In order to gain a better insight into mechano-chemical processes associated with grinding, we have to become familiar with the mechanism of fracture.

In the following passages some basic principles of the physics of fracture are summarised (Griffith [24], Smekal [25, 34], Rumpf [46–49] and Schönert [50–55]).

The physics of fracture are concerned with the effects of a single force on a single body. This process is often called "individual comminution".

A solid body subjected to mechanical force first suffers deformation (change of dimensions) and then, when the stress induced in the body reaches a limit (fracture stress), the body breaks. Stress states depend on the nature of the particle, the conditions of applying the load, and the behaviour of the particle (especially in the case of plastic deformation).

The process of fracture can be divided into two parts: initiation of a crack and the propagation of that crack.

According to theory the fracture of brittle materials takes place if stress generated by an external load reaches the molecular tensile strength at least at one point. This molecular (or theoretical) tensile strength (σ_{mol}) can be roughly estimated from the elasticity modulus using the following formula:

$$\sigma_{mol} \approx (0.1\text{–}0.2)E,$$

where E is the Youngs modulus.

In brittle materials the calculated, theoretical value of tensile strength (in the order of 10^3 to 10^4 MPa), exceeds the experimental value by two or three orders of magnitude. This difference can be rationalised by the "defect site theory" first formulated by Griffith in 1920 and further developed by many others.

Griffith took glass as an example and demonstrated, both by calculation and by experiment, that the lower experimental strength of solids, as compared with the theoretical values, is a consequence of the microcracks (defect sites) that are inherently present in them. For fracture to occur the propagation of cracks has to be promoted, and the condition that should lead to a fracture is that a certain minimum length of the microcrack should be formed. This minimum length is called the Griffith-length and is estimated to be about 1 μm.

Despite its importance, the Griffith theory provides no information about the initiation of fracture in materials such as metals in which microcracks of the length required to start fracture are absent. It was later established that for the initiation of

fractures it is not necessary that microcracks of adequate length should be present from the outset, since such cracks can also be created by the coalescence of dislocations.

The most informative model for the coalescence of dislocations and the formation of primary cracks was suggested by Cottrell [58] (Fig. 3.15). According to this model microcracks can develop and dislocations can coalesce at the interfaces of crystals,

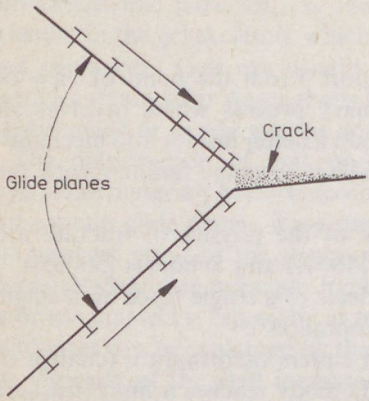

Fig. 3.15. Formation of a crack along the intersection of glide planes [58]

or at the intersection of two dislocations, or, in the case of a mosaic structure, at the boundaries of the blocks. According to Cottrell we may distinguish three partial processes in the formation of cracks: (1) displacement of dislocations, (2) coalescence of dislocations in the "empty space", and (3) expansion of the "empty space".

Meyer observed [35] that the formation of cracks depends not only on the mechanical properties of material (elasticity modulus), but also on external factors, such as temperature, the mode of loading, etc.

Fracture is a problem of energetics. The propagation of the initially-formed cracks requires that the energy of elastic deformation (E_d) should be at least as high as the interfacial energy of the system (E_γ) [24]. For unit length of crack (∂l_γ):

$$-\frac{\partial E_d}{\partial l_\gamma} \geqslant \frac{\partial E_\gamma}{\partial l_\gamma} = 2E'_{\gamma o}, \tag{16}$$

where $E'_{\gamma o}$ is the free energy of the new surface formed during the propagation of the crack (the factor of 2 is necessary because two new surfaces are produced by one elementary crack).

The energy balance used by Griffith has also been used by Orowan and further developed by Rumpf and Schönert, who have considered all possible mechanisms of fracture as well as the effect of other factors, such as plastic deformation and thermal effects.

It was pointed out by Rumpf and Schönert that fracture energy was much higher than surface free energy. Thus, the specific surface energy of solids is about 0.05 to 0.5 J m^{-2}, whereas the specific fracture energy for brittle solids is 5 J m^{-2}, for plastic solids it is 10 J m^{-2}, and for metals it is approximately 500 J m^{-2}. The energy requirement of a fracture is primarily determined by that of plastic deformation at the

crack front. The distribution of stress and its increase at the crack front is shown in Fig. 3.16.

For materials that show linear elasticity the maximum stress at the crack front (σ_{max}) can be approximately calculated by the following equation:

$$\sigma_{max}/\sigma_0 = 1+2\sqrt{l/\varrho}, \tag{17}$$

where l is the length of the crack, ϱ its radius of curvature (for an ellipse-shaped crack), and σ_0 the nominal stress. The crack can only propagate when σ_{max} exceeds the molecular tensile strength of the material.

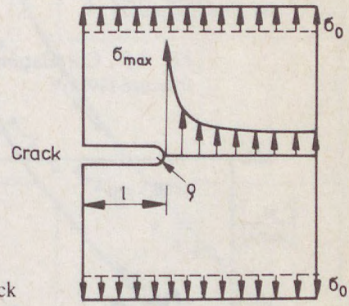

Fig. 3.16. Distribution of stress around a crack

The value of σ_{max} calculated by Eq. (17) may be extremely high if the angle of curvature of the crack (ϱ) is very small. For example, if $l = 1$ μm and $\varrho = 1$ nm, then $\sigma_{max}/\sigma_0 \approx 65$. With an applied load of $\sigma_0 = 100$ MPa the stress at the crack front (σ_{max}) is 6500 MPa. Plastic deformation has to take place at the crack front since this value is higher than the yield point [53]. Plastic deformation is also involved in apparently pure brittle fracture. This means that the energy per unit surface is three orders of magnitude higher than the surface tension. In this way (Schönert [53]), stress arising at the interface exerts little or no effect on the propagation of a crack.

Rumpf and his co-workers [49] recorded, with the aid of a specially developed instrument, the force–deformation curves of glass balls of various diameters under load and on relaxation. Three types of behaviour were distinguished. In the first (Fig. 3.17(a)) an increase in pressure resulted in the deformation of the specimen (ball) up to point P when fracture occurred. In the second type (Fig. 3.17(b)) the load was released prior to fracture, i.e. at point E. This type of behaviour is characterised by plastic deformation of materials which are brittle in the macroscopic range (e.g. quartz). The third type of load curve (Fig. 3.17(c)) resembles the second but at point P fracture took place and the particles resulting from the fracture remained in a state of plastic deformation.

The effect of plastic deformation increases with decreasing particle size. Therefore, if fine enough, particles consisting of materials usually regarded as brittle (such as quartz, calcite, cement clinker) undergo plastic deformation instead of fracture. This effect has been amply demonstrated by Schönert [55]. In Figure 3.18 the load-deformation diagrams of cement clinker particles of 16 and 2.5 μm size are shown. The larger particles are broken up on loading, while the smaller ones suffer only plastic

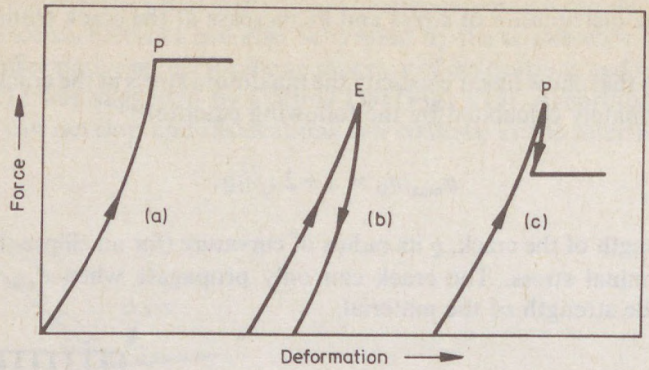

Fig. 3.17. Correlation of force and deformation in single particle fracture [49]

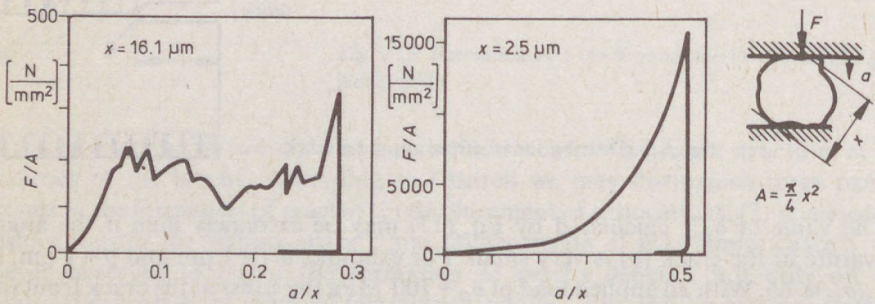

Fig. 3.18. Compression of fine particles (cement clinker) [55]

deformation. Schönert's load curves can be used to determine the particular size range in which the behaviour of the particles changes from brittle to plastic (Fig. 3.19).

With decreasing particle size both the number and the length of fissures diminish and, concurrently, the fracture strength and the resistance to crushing increase. In the size range of brittle to plastic transition the creation of cracks becomes increasingly difficult: below a certain particle size repeated mechanical stress does not result in fracture but produces plastic deformation.

The smallest particle which can still be crushed is determined by the minimum distance between two cracks. It has been calculated, using the mechanical equations of fracture, that for brittle materials ("individual comminution") the minimum theoretical particle size is around 10 nm [55].

In assessing the minimum particle size which can still be reduced ("limiting particle size"), the conditions under which the mechanical load is applied have also to be considered. With decreasing particle size, not only is the strength, and thereby the specific fracture energy greatly increased, but it becomes increasingly difficult to transfer a load to the particle. The "limiting particle size" which can be attained in a grinding operation is, therefore, in the order of 1 μm, but this value is subject to variation depending on the material and the equipment being used. For example, the

theoretical ("molecular") strength of iron whiskers was attained at 1 to 3 μm by Emrich, while with glass spheres, according to Rumpf, this value was 30 μm [49].

On grinding β-dicalcium silicate in a laboratory ball-mill for 90 hours a "limiting grain size" of 0.2 μm [59] was achieved, while after grinding for more than 250 hours in a quartz vibration mill it was 0.1 μm [60].

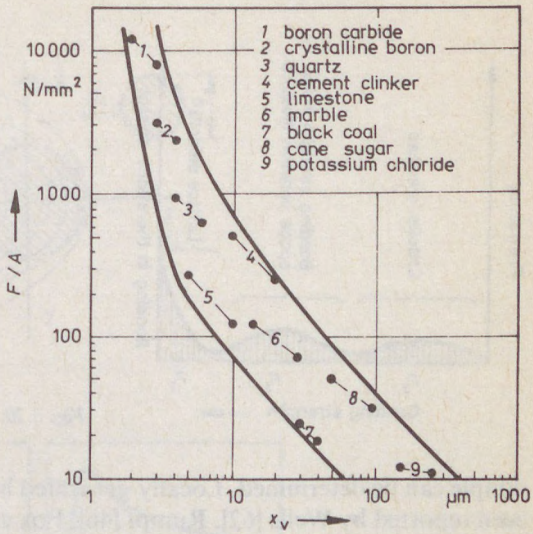

Fig. 3.19. Particle fracture strength in the brittle–plastic transition range [55]

In real crystals cracks of various sizes or areas in which the density of dislocations is higher than elsewhere in the body, are always present. The work involved in crack formation at the latter sites is less than in other ordered space elements of the same crystal. Fractures are always initiated at the weakest points, i.e. fracture first occurs on increasing the load around those cracks which are either most developed or have a favourable shape or position. When the fragments are loaded further, fracture extends to the environment of smaller cracks, then to sites of high dislocation density (e.g. to crystallite surfaces, intersections of glide planes) and it is only thereafter that the rupture of the regular crystal lattice and its parts sets in. This concept is reflected by the "bonding spectrum" of Hüttig [61] (Fig. 3.20). In this the abscissa represents the bonding forces between atoms, molecules, or ions, or forces associated with the intermediate phase, while the ordinate displays the frequency of a particular type of bonding. For example, in a sodium chloride crystal (typical for crystals with ionic bonding) the bonding force is of F_1 type and links a Na^+ ion with six neighbouring Cl^- ions. Since real crystals have a mosaic structure, i.e. they are composed of mosaics (about 10 nm in size) attached to each other directly or through an intermediate phase, the bonding spectrum has to be implemented by a second type of bonding force (F_2) which represents the interaction of mosaics. Further, since real solids contain defect sites and cracks, a third type of force (F_3) must also be included in the diagram.

Fracture always starts at the weakest bonds (F_3). When, in the course of comminution, these have disappeared, further fracture can only be initiated at the sites of stronger bonding forces (F_2), which means that fracture strength increases for the

smaller particles. Finally, when all the F_2 type bonds have also been cleaved then, since the high-energy F_1 type bonds cannot be broken up, the very small particles only suffer plastic deformation.

During comminution the energy input is absorbed by plastic deformation accompanied by a measurable temperature rise around cracks and in the fracture zone. By measuring the spectral distribution of thermal radiation the local temperature of the

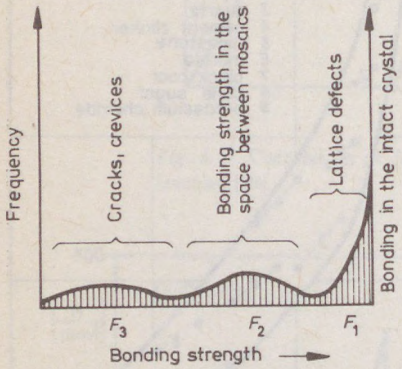

Fig. 3.20. "Bonding spectrum" according to Hüttig [61]

sample can be determined. Locally-generated high temperatures during fracture have been reported by Wells [62], Rumpf [46], Fox and Fuller [63], Schönert and Weichert [50, 64], Schönert [52, 53], Weichert [65] and others.

Wells [62] pointed out that heat waves are generated at the moment of fracture. Heating in the zone surrounding the crack front depends on the propagation velocity of the crack and the maximum fracture velocity is characteristic of a material: for example, for glass it is 1500 to 2500 m s^{-1}, for plastics 200 to 800 m s^{-1}, and for steel 800 to 1200 m s^{-1}. According to Rumpf, temperature jumps around cracks may reach, or even, exceed the melting point.

Using highly sensitive thermo-elements Schönert and Weichert [50] were able to measure the temperature in iron at a distance of about 30 μm from the fracture zone and found a jump of 150 K; while Fox and Fuller [63], using an infrared probe measured a temperature increase of 400 to 500 K.

Assuming a circular shape for the zone around the fracture front and a constant local density of energy, Weichert and Schönert [64] calculated that the temperature gradient (ΔT) should be higher than 100 K. The isothermic field obtained by Weichert and Schönert for a fracture velocity of 1000 m s^{-1} and a fracture front of 6 nm diameter is shown in Fig. 3.21. According to this figure the temperature increases at impact for the first 10 ps and then decreases during the following 100 ps.

Schönert pointed out [53] that the temperature increase induced by fracture depends on the velocity of fracture and on the hardness of the material. Thus, the following ΔT values at maximum fracture velocity were found: calcite 1300 K, orthoclase 2600 K, periclase 3200 K, and quartz 4400 K. These temperature jumps were of very short duration, about 0.1 to 10 ns, and the thickness of the layer affected was in the order of 10 nm.

Thus, in the instant of fracture, and depending on the nature of the material and the velocity of fracture, very high transient stress and temperature increases are generated. Using the terminology of thermodynamics, we may say that part of the energy stored during deformation is transformed instantaneously on fracture into heat. This heat cannot be transmitted immediately to the environment and results therefore in a temperature increase near the fresh surfaces. Energy accumulated during mechanical

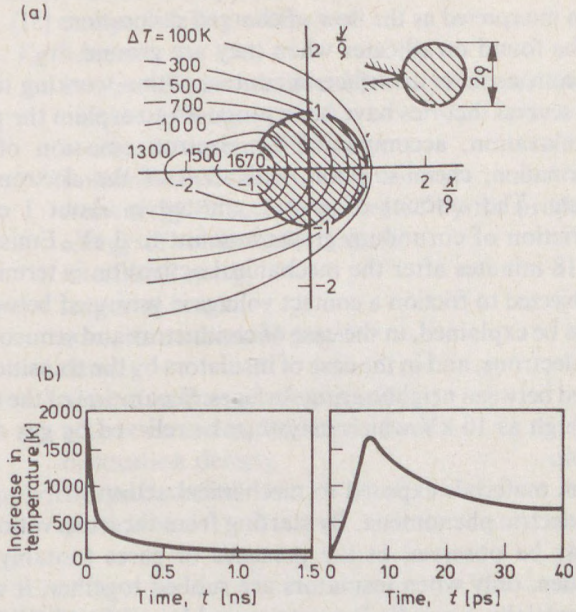

Fig. 3.21. (a) Isotherms in the fracture of glass at a velocity of 1000 m s^{-1}. Diameter of the zone around the crack front: 6 nm; (b) Temperature as a function of time in the propagation of a crack in glass [64]

loading is set free in an adiabatic process associated with the appearance of temperature peaks ("heat shocks").

The impulse-like and "vibrational" character of the phenomena associated with fracture play an important role in mechano-chemical processes, which proceed in a localised manner, first at the fronts of propagating cracks and then at contact points of particles. According to Schneider [60] these "vibrations" result in a permanent disturbance of the crystal structure and in the development of a "frozen vibrational state", i.e. amorphisation. In Schrader's terminology [66] this phenomenon may be called a "lattice fracture similar to athermic vibration".

Fracture produces fresh surfaces which differ both in their morphology and in their energetics from equilibrium state surfaces. Because of their highly active state these fresh fractures may be the sites of adsorption and chemical reactions which ultimately decrease the surface free energy.

3.4. ELECTRICAL AND LUMINOUS PHENOMENA TRIGGERED BY MECHANICAL ACTIVATION

It is well known that some solids pick up electric charge when under mechanical stress [67]. Here we will only mention piezoelectricity: when pressure is exerted on a certain face of a quartz crystal, an electric charge appears on the uncompressed faces and conversely the crystal suffers deformation, when placed in an electric field. The phenomenon has been interpreted as the flow of charged dislocations [31]. The build-up of charge can often be found on silicates when they are ground dry.

The emission of electrons from a surface in contact with a working tool is mainly seen with metals and several theories have been proposed to explain the phenomenon [31], for example, relaxation, accompanied by electron emission of the crystal de-stabilised by deformation, chemi-sorption, activation of the electron shell under mechanical action, etc. The amount of energy emitted is about 1 eV, but may sometimes, e.g. on friction of corundum grains amount to 3 eV. Emission may be observed up to 4 to 18 minutes after the mechanical activation is terminated.

When solids are subjected to friction a contact voltage is generated between particles. This phenomenon can be explained, in the case of conductors and semiconductors, by the transition of free electrons, and in the case of insulators by the transition of ions, so that dipoles are formed between neighbouring surfaces. Separation of the surfaces may generate tensions as high as 10 kV which may then be relieved by gas discharges of 10^{-7} seconds duration.

Light emission from materials exposed to mechanical action (tribo-luminescence) can also be traced to electric phenomena. By starting from the observation that tribo-luminescence can only be observed in the presence of gases (notably at medium pressure) and, even then, only when insulators are rubbed together, it was inferred, that the effect was essentially a gas discharge triggered by an electrical charge which accumulated on the surface and reached a critical surface charge density.

Tribo-luminescence has been utilised in studying the flow characteristics of air containing dust, as well as of the mechanical stress states of solid bodies. Reference [68] refers to some results by Hungarian authors.

SYMBOLS IN CHAPTER 3

σ, σ_a, σ_b, σ_F	stress, perpendicular stress
σ_{mol}	molecular tensile strength
σ_{max}	maximum stress at the crack front
σ_0	nominal stress
τ, τ_f	tangential stress, shear stress
E	elasticity (Young's) modulus
G	torsion modulus
ε, ε_e, ε_l, ε_c, ε_p	relative linear deformation
γ	specific torsion
W	specific deformation work
l	dimension of the body

u	internal energy
s	entropy
T	temperature
c, c_a, c_b	velocity of elongation
λ	relaxation time
τ_a	grinding time, activation time
ν	Poisson's coefficient
$\varkappa$	compressibility coefficient
F, F_f, F_1, F_2, F_3	force
n_v, n_i	number of point lattice defects (vacancies and interstitions, resp.)
N	number of lattice points
N'	number of intermediate sites
k	Boltzmann's constant
$E'_{\gamma o}$	free energy of surface generated by the propagation of a crack
E_d	energy of elastic deformation
E_γ	interfacial energy
l, l_γ	length of crack
ϱ	curvature radius of crack
ϱ_s	density
E_v	activation energy of vacancies
E_i	activation energy of interstitions
x_d	dislocation density
$\bar{b}$	Burger's vector
x	particle size

REFERENCES

[1] Houwink, R.: *Elastizität, Plasticität und Struktur der Materie*. Vol. I. Steinkopff, Dresden 1950.
[2] Juhász, Z.: *Acta Chim. Acad. Sci. Hung.*, **114,** 199 (1983)
[3] May, M.: *Freiberger Forschungshefte, B* **55,** 3 (1960)
[4] Nogami, M., Tomozova, M.: *J. Am. Ceram. Soc.*, **67,** 151 (1984)
[5] Senna, M., Schönert, K.: *Powder Technol.*, **32,** 217 (1982)
[6] Morgemann, H.: *Physiol. Rev.*, **33,** 1035 (1929)
[7] Sander, B.: *Jahrb. Geol. Bundesanstalt*, **73,** 209 (1923)
[8] Naeser, G., Scholz, W.: *Kolloid.-Z.*, **156,** 1 (1958)
[9] Weidenthaler, P.: *Collection Czechoslov. Chem. Communs.*, **28,** 137 (1963)
[10] Tammann, G.: *Z. Elektrochem.*, **35,** 21 (1929)
[11] Bridgman, P. W.: *Physiol. Rev.*, **48,** 825 (1935)
[12] Naeser, G., Scholz, W.: *Ber. Dtsch. Keram. Ges.*, **39,** 106 (1962)
[13] Waentig, P.: *Kolloid-Z.*, **41,** 152 (1927)
[14] Stener, E.: *Chem. Tech.*, **1,** 1 (1943)
[15] Hess, K., Stener, E.: *Z. Phys. Chem. (Wiesbaden)*, **193,** 234 (1943)
[16] Hoffmann, M., Kaufmann, W.: *Chem. Rundschau*, **9,** 13 (1956)
[17] (Barambojm, N. K.) Н. К. Барамбойм: *Механохимия высокомолекулярных соединений*. 3-е. Изд. «Химия», Мозсква 1978
[18] Glockner, R.: *Materialprüfung mit Röntgenstrahlen*. Springer, Berlin 1949
[19] Bragg, W. L.: *The Crystalline State*. G. Bell & Sons, Ltd., London 1933
[20] Náray-Szabó, I.: *Chemical Mineralogy* (in Hungarian), Akadémiai Kiadó, Budapest 1965

[21] Kittel, Ch.: *Introduction to Solid State Physics* (in Hungarian translation). Műszaki Kiadó, Budapest 1966
[22] Guy, A. G.: *Introduction to Materials Science* (in Hungarian translation). Műszaki Kiadó, Budapest 1978
[23] Frenkel, J.: *Z. Phys. A* **37,** 572 (1926)
[24] Griffith, A. A.: *Philos. Trans. R. Soc. (London)*, Ser *A*, **221,** 163 (1920)
[25] Smekal, A.: *Z. Phys.*, **103,** 495 (1936)
[26] Orowan, C.: *Z. Phys. A* **86,** 195 (1931)
[27] Taylor, G. J.: *Proc. Roy. Soc., A***145,** 362 (1934)
[28] Polányi, M.: *Z. Phys. A***84,** 660 (1934)
[29] (Budnikov, P. P., Ginstling, A. M.) П. П. Будников, А. М. Гинстлинг: *Реакции в смесях твердых веществ*. Госстройиздат, Москва 1961
[30] Krauth, A.: *Ber. Dtsch. Keram. Ges.*, **45,** 622 (1968)
[31] Thiessen, P. A., Meyer, K., Heinicke, G.: *Grundlagen der Tribochemie*. Akademie Verlag, Berlin 1967
[32] Hockey, B. J.: *J. Am. Ceram. Soc.*, **54,** 223 (1971)
[33] Lange, F. L., James, M. R., Green, D. F.: *Commun. Am. Ceram. Soc., C***16** (1983)
[34] Smekal, A.: *Anz. Akad. Wiss. Wien*, **92,** 72 (1955)
[35] Meyer, K.: *Z. Phys. Chem. (Leipzig)*, **219,** 295 (1962)
[36] Burgersmüller, W.: *Z. Phys. A***103,** 633 (1936)
[37] Zachariasen, W. H.: *J. Amer. Chem. Soc.*, **54,** 3841 (1932)
[38] (Lebedev, A. A.) А. А. Лебедев: *Труды Гос. Оптического Института*, **2,** 57 (1921)
[39] Weyl, W., Marboe, E. C.: *Glass Ind.*, **41,** 549 (1960)
[40] Haven, Y.: *Philips' tech. Rundschau*, **20,** 106 (1958–59)
[41] Eckstein, B.: *Bull. soc. franç. céram.*, **54,** 79 (1962)
[42] Hinz, W.: *Silikate*. Verlag für Bauwesen, Berlin 1963
[43] Juhász, Z.: *MTA Kémiai Közlemények*, **48,** 167 (1977)
[44] Bemmelen, J. M.: *Z. anorg. Chem.* **13,** 258 (1969)
[45] Smekal, A.: *Z. VDI.*, **81,** 1321 (1937)
[46] Rumpf, H.: *Symposium Zerkleinern*. Verlag Chemie, Weinheim, VDI Verlag, Düsseldorf 1962.
[47] Rumpf, H.: *Chem. Ing. Tech.*, **34,** 731 (1962)
[48] Rumpf, H.: *Aufbereitungs-Technik*, **7,** 422 (1966)
[49] Rumpf, H., Faulhaber, F., Schönert, K., Umhauer, H.: *Dechema Monographien*. Vol. 57, Verlag Chemie, Weinheim 1967.
[50] Schönert, K., Weichert, R.: *Chem. Ing. Tech.*, **41,** 295 (1969)
[51] Schönert, K., Steier, K.: *Chem. Ing. Tech.*, **43,** 773 (1971)
[52] Schönert, K.: *Chem. Ing. Tech.*, **46,** 711 (1974)
[53] Schönert, K.: *Grundlagen des Zerkleinerns*. Technische Hochschule, Karlsruhe 1979
[54] Schönert, K.: *Banicke Listy*. VEDA, Bratislava 1980.
[55] Schönert, K.: *Proceedings of International Symposium on Powder Technology '81*. The Soc. of Powder Technol., Kyoto 1982.
[56] (Joffe, A. J., Kirpicseva, M. V., Lebickaja, M. A.) А. Ф. Иоффе, М. В. Кирпичева, М. А. Лебицкая: *Журнал Русского Физического Общества*, **56** (1924)
[57] (Rehbinder, P. A.) П. А. Ребиндер: *Общее собрание трудов АН СССР*. Изд-во АН СССР, Москва 1947.
[58] Cottrell, A. M.: Trans. AIME **212,** 192 (1958)
[59] Opoczky, L., Wojnarovits-Hrapka, I.: *Építőanyag*, **28,** 258 (1976)
[60] Schneider, U.: *Aachner Blätter*, **18,** 1/2 (1968)
[61] Hüttig, G. F.: *Zement-Kalk-Gips*, **7,** 151 (1954)
[62] Wells, A. A.: *Welding Res.*, **7,** 348 (1953)
[63] Fox, P. G., Fuller, K. N. G.: *Nature physic. sci.*, **234,** 13 (1975)
[64] Weichert, R., Schönert, K.: *J. Mech. Phys. Solids*, **22,** 127 (1974)
[65] Weichert, R.: Dissertation. Universität (TH) Karlsruhe (1976)
[66] Schrader, R.: *Freiberger Forschungshefte, A***392** (1966)
[67] Deri, M.: *Seignette electrical ceramic materials* (in Hungarian). Akadémiai Kiadó, Budapest 1963.
[68] Kakas, J., Vigyázó, Gy.: *Automatizálás*, **10,** 34 (1977)

Chapter 4

4. THE PROCESS OF FINE GRINDING

The physics of fracture deal with the effect of a single force upon an individual body. In grinding technology, however, a multitude of forces acts upon a multitude of particles. The particles are not exposed individually to mechanical load but as a bulk ("in a material bed") and the exposure to load and its transmission takes place in a stochastic manner. In the resulting bulk (ground product) the particles may differ not only in size, shape, and surface properties but also in their compositions. In fine grinding the direct or indirect interaction of particles cannot be neglected.

In order to influence the physical and chemical changes associated with the grinding of a given material, we have to know those properties which are relevant for comminution and its behaviour during fine grinding.

4.1. MATERIAL CHARACTERISTICS RELEVANT DURING COMMINUTION

The material characteristics to be considered in comminution can be divided into three groups;

(a) Values concerning resistance to mechanical loading (shattering): strength (hardness), reaction force as related to surface area, comminution work related to volume and mass, fracture probability, reduction ratio, associated energy;

(b) values concerning the results of mechanical loading: size distribution function of the fragments, the new surface area generated, degree of unlocking, degree of agglomeration;

(c) characteristics combined from properties discussed under (a) and (b): energy efficiency, grindability, comminution resistance.

4.1.1. HARDNESS (MICROHARDNESS)

The major physico-chemical properties influencing the behaviour of crystalline materials under comminution are hardness, tensile strength, cleavage, and plastic deformation. The mechanical properties of a crystalline solid body are often anisotropic and highly dependent on temperature, the conditions of testing, and the velocity of deformation.

From a practical point of view one of the most important properties of a crystal is its hardness. This is defined as the resistance of the crystal to mechanical disintegration. Correlations between hardness, composition, and structure are highly complex, but several rules are known which can be applied with fair approximation to certain ranges of compounds.

Hardness is related to the lattice energy of the crystal and to chemical bonding and thus (for an ionic lattice), bonding, distance between ions, and the structural type affect its hardness. Crystals in which covalent bonds prevail are generally harder than those characterised mainly by ionic bonds. Hardness decreases with increasing distance between ions of opposite charge provided the structural type remains the same. If longer interionic or interatomic distances are coupled with a diminished share of covalent bonds then the drop in hardness is even more pronounced.

Hardness increases when the valency, as well as the coordination number of ions constituting the crystal, increases. A maximum of hardness and strength is encountered when covalent bonds prevail, particularly if the main cation has both a high valency and a small size: $Ca^{2+} \rightarrow Al^{3+} \rightarrow Si^{4+}$.

Compounds which are exclusively of ionic or covalent character are rare and, within a given crystal, more than one type of chemical bonding may be present simultaneously. Most of the materials used in the silicate industry comprise both ionic and covalent bonding and are of the co-ordination type [1, 2]. For example, the following types of bonding are present in such complex compounds as the aluminium hydrosilicates: ionic bonds between cations (Si^{4+}, Al^{3+}) and anions (O^{2-}); polar bonds in water molecules and SiO_4^{4-} tetrahedra; ionic-dipolar bonds between groups with polar bonds (mainly H_2O) and ions; and hydrogen bonds, depending on the state of H^+ ions.

The numerical value of hardness depends on the method of determination. The oldest, but still widely used approach is Mohs test for scratch hardness (Table 4.1).

The hardnesses (or microhardnesses) of the polycrystalline materials used in the silicate industry are determined by pressing a test cone against the material surface with a defined force (Vickers' hardness). The trace formed on the surface of the test specimen is caused by plastic deformation of the crystals. If the load exceeds the

Table 4.1. Microhardness of the standard minerals from Mohs scale [1]

Mineral	Mohs scale	Microhardness [MPa]
Talc	1	24
Gypsum	2	360
Calcite	3	1,090
Fluorite	4	1,890
Apatite	5	5,360
Orthoclase	6	7,950
Quartz	7	11,200
Topaz	8	14,270
Corundum	9	20,600
Diamond	10	100,600

limiting strength of the crystal microcracks will appear around the corner of the trace. The character of these cracks and the corresponding loads provide information about the microbrittleness of the crystal [3]. The microhardnesses of selected materials, as determined by this method, are given in Table 4.1.

4.1.2. A CONCEPT STUDY OF GRINDABILITY

Materials which are to be subjected to size reduction are characterised, in general either by their grindability, which is defined as the increase of specific surface per unit energy, or by their grinding resistance.

Several methods of assessing grindability are known; the scope and usefulness of the values produced have been covered extensively in the literature [4–23]. In the following paragraphs some methods for determining grindability in the silicate industry will be discussed.

(a) Hardgrove's method for determining relative grindability of coal has been a standard method in the United States since 1937 [5]. The procedure is based on Rittinger's law, which states that the work (energy) expended for grinding is proportional to the area of the new surface created.

In practice a defined amount of grinding work is expended on a sample and the degree of fineness attained is determined by sieve analysis. Grindability is then calculated using the empirical formula:

$$H = 13 + 6.93\, D_{74}, \tag{1}$$

where D_{74} is the portion of a 50 g sample passing a 74 μm sieve.

Higher Hardgrove numbers represent better grindability, but the numerical values are not directly proportional. For example, $H = 100$ does not mean double the efficiency of $H = 50$. Hardgrove numbers fall into the range 40 to 100 with cement clinkers, 60 to 130 with limestone, and 45 to 55 with quartz.

This method is only suitable for providing data for fracture and coarse grinding and for the purpose of comparison.

(b) In Zeisel's method [6, 7] the sample is ground to a preset fineness by gradually increasing the grinding time: the energy consumption is determined by momentum measurements. From the expended work the specific grindability (W_t) is calculated by the following formula:

$$W_t = \frac{0.275 W_z}{g}, \tag{2}$$

where W_z is grinding work, g the mass of the sample and 0.275 a conversion factor.

The results of testing are usually shown as a specific grindability—"external" specific surface plot. The change of energy with increasing fineness, i.e. the actual grindability, is determined as the ratio of corresponding values read from the abscissa and the ordinate.

Specific grindability (W_t) hardness values of some materials used in the silicate industry are shown in Fig. 4.1.

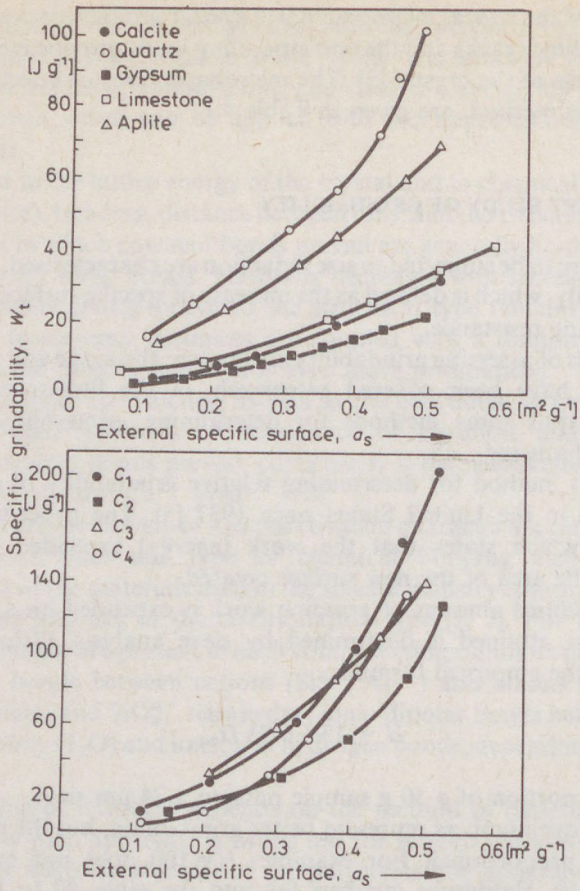

Fig. 4.1. Correlation of specific grindability (W_t) and the "external" specific surface (a_s). C_1–C_4—cement clinkers of varied composition [52]

Verdes [14] pointed out that values obtained by the Zeisel method can be closely approximated by the following correlation:

$$E = ae^{ba_s}, \tag{3}$$

where E is the energy consumption, a_s the "external" specific surface, and a and b are constants.

Constant a is characteristic for the initial specific energy consumption (E_0) (the smaller the value of a, the easier is the grinding); b is characteristic for the change of energy consumption by specific surface and also for the shape of the curve. The product of the two constants (ab) can be used for characterising the grindability of the given material.

The advantage of Zeisel's method is that it yields, over a wide range, numerical specific energy consumption values as a function of fineness and these values are

obtained directly under the given experimental conditions. At the same time a common fault of both the Hardgrove's and the Zeisel's methods is that the mode of mechanical loading (friction) is different from that actually applied in the machinery generally used by the silicate industry. Both methods are based on Rittinger's law, but it is well known that proportionality of surface area increase and energy expenditure does not hold for the entire grinding process.

(c) The methods recommended by Giprocement [8] and Mittag [9] determine grindability in laboratory mills that contain grinding bodies of various sizes. The merit of this approach is that it endeavours to model, as closely as possible, the conditions in large scale open circuit grinding: i.e. a relatively large ball mill is used; the composition of the grinding bodies can be varied (uniform or mixed); and the particle size analysis of the charge can be controlled. It is a disadvantage that the method only simulates open-circuit mills.

(d) The Bond method [10] tries to simulate closed circuit grinding. Grinding is carried out in sections until the establishment of an equilibrium. Bond's "work index" can then be calculated by the following empirical formula:

$$W_i = \frac{16}{G^{0.82}} \sqrt{\frac{r}{100}}, \tag{4}$$

This value corresponds approximately to the electrical energy required to grind a 1 Mg sample of a given particle size to give a product containing 80% of particles under 100 μm. In formula (4) r is the sieve opening in μm and G the amount of material ground during one revolution, called "ball-mill grindability".

The energy requirement for an industrial mill according to Bond's "third theory" is

$$W_z = 10W_i\left(\frac{1}{\sqrt{r_p}} - \frac{1}{\sqrt{r_f}}\right), \tag{4a}$$

where r_p and r_f are the mesh sizes in μm for passing 80% of product and feed, respectively.

Although this method simulates the processes involved in an industrial closed-circuit ball mill better than the others mentioned above, it does not reflect the effect of mill size and is informative only for relatively coarse particles, i.e. for about 70% oversize. (Industrial closed circuit cement mills, on the other hand, make a product containing only 30–40% oversize.)

In order to overcome these drawbacks, Dombrowe [15] introduced several correction factors. These allowed the results to be adapted to different fineness values (oversize values) as well as for different mill diameters and to take account of aggregation phenomena arising with fine grinding.

Table 4.2 shows the grindability values for 9 industrial clinkers of varied composition obtained by different methods. It can be seen that these methods provide different grindability values.

Several attempts have been made [13, 16–23] to establish which method reflects the best everyday milling practice. Piroczkij [16] compared the results obtained by the methods of Zeisel and Bond with results obtained on industrial mills; the Bond method

Table 4.2. Comparison of the grindability values obtained for clinker with various grinding methods [23]

Clinker of varied composition	Hardgrove-method [5]	Zeisel-method [6, 7] [J g^{-1}]	Bond-method [10] [J g^{-1}]	Mittag-method [9] [J g^{-1}]	Giprocement-method [8] $R_{0.09}=10\%$ $a_s=0.3\,m^2\,g^{-1}$ [J g^{-1}]	
C_1	58	142.56	119.52	196.92	131.04	153.00
C_2	55	96.84	126.36	136.80	109.44	127.80
C_3	75	146.16	117.72	191.16	95.76	142.92
C_4	46	108.72	111.60	143.64	69.84	109.44
C_5	75	81.72	118.80	187.56	120.96	128.88
C_6	60	131.04	124.92	—	122.40	130.32
C_7	92	129.96	108.00	162.72	106.56	148.32
C_8	110	210.24	95.76	204.84	96.48	130.32
C_9	47	108.00	123.84	156.96	124.20	128.15

provides the best approximation of industrial practice. Other authors [17–19] found deviations of 4 to 20% between the grindability values obtained by Bond's method and those observed in industrial mills. Scheibe et al. [17] pointed out that grindability studies carried out with the Zeisel apparatus did not provide exact information for the dimensioning of industrial mills. On the other hand, studies in the Cement Research Institute in Düsseldorf established a statistical correlation between the Zeisel index and the energy expenditure determined in an industrial mill [20]. In the opinion of certain authors [9, 17] processes that take place under well-defined conditions in a laboratory mill do approximate the processes that take place in an industrial mill, provided that the diameter of the mill is larger than 0.5 m. Thus, Ellerbrock [21] compared the grindability values of cement, clinker, quartz, and limestone obtained both by Zeisel's method and in a pilot plant ball mill of 0.63 × 0.63 m size, with those determined in an industrial mill.

He found that the ball mill experiment provided a better approximation of the latter than Zeisel's grindability values. This finding is further supported by data in Table 4.3 in which the parameters used in various grindability tests were compared [23].

Table 4.3. Comparison of methods for the determination of grindability [23]

Method	d_b/d_m	d_p/d_b	m_m/m_b
Hardgrove [5]	0.16	0.035	—
Zeisel [6, 7]	0.16	0.035	—
Bond [10]	0.098	0.105	0.063
Mittag [9]	0.052	0.396	0.125
Giprocement [8]	0.093	0.118	0.18
Up-to-date industrial mills	0.02–0.02	0.14–0.15	0.16–0.18

Notations: d_b—ball diameter, d_m—mill diameter, d_p—particle diameter, m_m—mass of mills, m_b—mass of ball filling

In summary it can be concluded that at present there is no laboratory method for assessing grindability which is capable of predicting adequately the energy needed to grind a given material in an industrial equipment. It is not surprising that the behaviour of a material under conditions of fine grinding cannot be characterised by a single parameter (grindability, grinding resistance), since this behaviour varies with dispersion with the individual properties of the particles being comminuted (hardness, strength, porosity, etc.), and with the so called collective properties, i.e. the interaction of particles.

Despite these difficulties, the methods discussed above, in association with a large body of experimental data and several conversion factors, are widely used both by manufacturers and users of grinding machinery.

4.1.3. PHYSICO-MECHANICAL CHARACTERISTICS AND GRINDABILITY OF CLINKER MINERALS AND CEMENT CLINKERS

The grindability values of cement clinkers of varied composition (C_1, C_2, C_3, C_4)—as determined by Zeisel's method—are shown in Fig. 4.1.

Correlations between grindability and composition of cement clinkers have been discussed in the literature [1, 2, 24–40]. In addition to their scientific value such correlations are of prime interest, since they imply that it may be possible to influence the grindability of cement clinker. The results in this field are summarised by Merić [40].

Cement clinker is a polycrystalline material composed of clinker minerals of different physico-mechanical properties.

The main components of portland cement are: tricalcium silicate ($3CaO \cdot SiO_2$, $\underline{C_3S}$, alite*) (theoretical composition CaO 73.69%, SiO_2 26.31%), β-dicalcium silicate ($2CaO \cdot SiO_2$, $\underline{C_2S}$, belite) (theoretical composition CaO 65.13%, SiO_2 34.87%), tricalcium aluminate ($3CaO \cdot Al_2O_3$, $\underline{C_3A}$) (theoretical composition CaO 62.23%, Al_2O_3 37.77%), tetracalcium aluminate ferrite ($4CaO \cdot Al_2O_3 \cdot Fe_2O_3$, $\underline{C_4AF}$, brownmillerite) (theoretical composition CaO 46.08%, Al_2O_3 21.03%, Fe_2O_3 38.81%).

Clinker minerals are brittle materials having predominantly ionic lattices, though their hardness and brittleness, i.e. the properties which decisively influence their tendency to fracture, show broad individual variations. Thus, according to our investigations, minerals constituting the "intermediate phases", i.e. C_3A and C_4AF are the hardest ($H = 9.5 \times 10^3$ and 10.19×10^3 MPa, respectively). C_3A is, however, more brittle than C_4AF as shown by the fact that during microhardness testing C_3A develops cracks at loads around 0.5 N. The hardnesses of C_3S and βC_2S are similar ($H = 8.5 \times 10^3$ and 7.85×10^3 MPa, resp.) but βC_2S is much less brittle and, therefore, crystals of βC_2S may take loads up to 1.0 N without cracking [35, 36].

* In the following passages of this book this underlined abbreviated notation system which has been adopted in cement chemistry will be used for clinker minerals:

Grindability values of clinker minerals, as determined according to Zeisel, are shown in Fig. 4.2 and it is apparent that grinding C_3S is comparatively easy and that of βC_2S is hard. Whilst C_3A and C_4AF take up a medium position; C_3A is closer to C_3S, while C_4AF resembles βC_2S.

Differences in the behaviour of clinker minerals towards mechanical effects can be explained by differences in their fine structures.

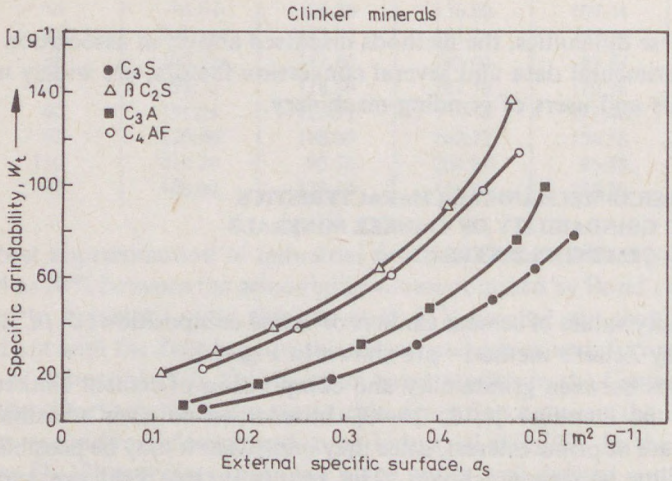

Fig. 4.2. Correlation of specific grindability and the "external" specific surface [52]

Jeffery [41] suggests that C_3S has special structure in which SiO_4^{4-} tetrahedra are linked by CaO bridges. O^{2-} ions are arranged in a disordered (lopsided) manner around the hexa-coordinate Ca^{2+} ions. This irregular coordination distorts the interionic electric field that may significantly contribute to the brittleness and instability of C_3S. Another characteristic feature of C_3S crystals is their disintegration along cleavage planes on impact or pressing.

In the structure of βC_2S [42] individual SiO_4^{4-} tetrahedra are associated with Ca^{2+} ions of rather irregular coordination. One type of Ca^{2+} ions has a co-ordination number of 6 (Ca I), another has a co-ordination number of 8 (Ca II). Out of the eight Ca^{2+} ions those of Ca I type are situated alternately under and above the SiO_4^{4-} tetrahedra, while those of type Ca II occur in the cavities between tetrahedra. This mode of co-ordination is irregular but the cavities in the structure are smaller than those in C_3S. Because of the varying co-ordination βC_2S is more closely packed and withstands mechanical action better than C_3S. βC_2S crystals become twisted during grinding and suffer extensive plastic deformation.

The physico-mechanical properties of clinker minerals (hardness, strength) can be influenced either by incorporating "alien elements" or by rapid cooling [1–2. 39, 43].

One of the important crystal–chemical properties of clinker minerals is that the principal cations in their lattices (Ca^{2+}, Al^{3+}, Si^{4+}) can be substituted by alien elements. Each of the clinker minerals may incorporate into its lattice as many as 5 to 8

alien elements [43]. This capacity for incorporation, however, shows individual variations; it is highest with aluminate and aluminate-ferrite phases (approximately 13 and 11 mass% respectively) and lowest with alite (approximately 4 mass%). Thus, Si^{4+} can be replaced by P^{5+}, S^{6+}, Cr^{6+}, Al^{3+}, and Fe^{3+}; in an aluminate-ferrite phase Al^{3+} and Fe^{3+} can be replaced by Mg^{2+}, Si^{4+}, Ti^{4+}, etc.; furthermore Ca^{2+} can be replaced by K^{+}, Na^{+} and Cr^{3+}.

It can be seen that isomorphism of clinker minerals is mainly of hetero-valent type and, therefore, the incorporation of alien atoms results in a change in the microsymmetry and in the electrostatic field of the structure.

Alien elements that replace the principial elements, or become inserted into the lattice, modify interionic bonding, co-ordination of ions, packing, and other properties such as hardness of the crystal. Hetero-valent substitutions involve significant distortion of the lattice and the formation of defect sites.

The behaviour and effect of trace elements depend basically on their electronegativity, polarisability, and ionic diameter. For example, the microhardness of alite and belite crystals can be reduced by 15 to 20% by doping them with 0.5 to 3% of Na_2O, especially if this doping is combined with fast cooling: on slow cooling the effect is smaller with belite. The introduction of BaO into alite and into belite decreases their microhardness by 10 to 30%; the effect of SO_3 is to reduce the microhardness by 10 to 25%. On the other hand, increasing the MgO content of belite and of alite crystals up to 3% enhances their microhardness: 0.5% of P_2O_5 diminishes the microhardness of belite and alite; whereas, an increase in the P_2O_5 content to 3% further increases their hardness [1, 2].

The grindability of cement clinker depends primarily on its chemical composition and the distribution of the individual minerals. Clinkers with a high alite (C_3S) content are, in general, easier to grind, while those having a high belite (βC_2S) content have poor grindability. Minerals composing the "intermediate phase" (C_3A and C_4AF) cannot be qualified so clearly. According to our own experience clinkers containing a high percentage of melt phase and C_3A+C_4AF, respectively, are hard to grind. The above statements are generally valid for clinkers of extreme composition but cannot adequately explain the differences in the grindability of clinkers that have roughly the same composition but which are prepared by different technologies. Among the parameters influencing the grindability of clinkers the importance of sintering temperature and the mode of cooling has to be emphasised, but the fineness of the raw meal, the mode of processing (dry, wet, or semiwet), the nature of fuel, etc. are also of significance. The effect of these variables is shown in the macro- and microstructure of clinkers (porosity and the distribution of pores, degree of crystallisation, size, shape, and size distribution of crystals), as well as in the physico-mechanical properties of the individual clinker minerals.

Opinions diverge about the correlation of grindability and porosity. According to Ackmann [27] there is no such correlation in the fine grinding of cement clinker and the same view was expressed by Götte [44] concerning limestone. Gille and Ruhland, however [28], established a close correlation between the porosity and grindability of cement clinkers. Deckers [29] analysed these results and pointed out that the correlation was only valid for coarse grinding, in which increasing porosity improved the grindability. Porosity becomes irrelevant for materials with a specific surface of

0.2 $m^2 g^{-1}$ (a_s). In contrast Butt et al. [30] established a clear correlation between the number of pores of specified size and the grindability of cement clinkers in coarse and in fine grinding. For example, in fine grinding (which has the highest energy demand) in the specific surface range 0.15 to 0.3 $m^2 g^{-1}$, the grindability of clinker is influenced by pores in the size range 1 μm to 4×10^{-2} μm. They also found that the pore structure of clinker is conditioned by the amount of melt phase formed during burning. In this way,

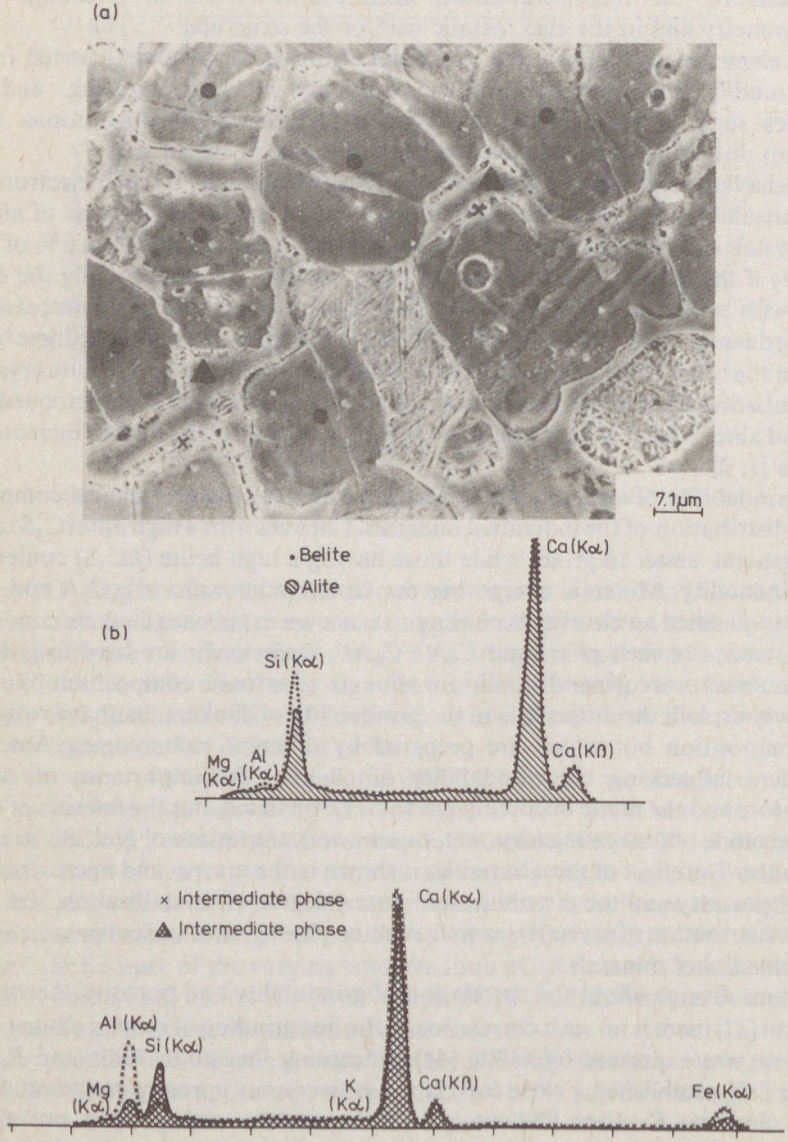

Fig. 4.3. EDAX-curves of clinker minerals [35, 45]

the structure and porosity of clinker and, thereby, its grindability can be controlled over a broad range by varying both the length of the sintering zone of the kiln and the rate of cooling.

Peterson [38] shows that an important factor affecting the grindability of cement clinker is the ratio of pores to the specific surface of the crystalline phase. This is a linear function of saturation by the melt. In his view, crystal size is the decisive factor for the magnitude of the specific surface of the pore system and, thereby, for grindability; the smaller the crystals, the better the grindability.

Fast cooling is, in general, advantageous for pore size and grindability, but in a more thorough analysis of the effect of fast cooling, it was shown that the mineral composition of the sample has also to be taken into account.

The effect of fast cooling on the grindability of aluminate and aluminate-ferrite phases crystallising from the melt (intermediate phase) is unequivocal. The brittle "glassy" material can be more readily ground than the crystalline "intermediate phase" formed during slow cooling. The grindability of clinkers with a high aluminate content can be much improved by fast cooling. In order to enhance the grindability of belite clinkers these should be cooled very quickly, by quenching. On the other hand, with clinkers having a high alite content a clear cut advantage of fast cooling only occurs during coarse grinding; fine grinding is only achieved with great difficulty. A more detailed study of this problem by Hornain and Regourd [39] demonstrated that under the effect of thermal shock two kinds of cracks generally appear in clinkers, namely macro-cracks, i.e. broad cracks which cut across particles and may lead to fracture, and micro-cracks, which are mainly characteristic for alite crystals and less so for the "intermediate phase".

Macro-cracks are more pronounced the higher the intensity of thermal shock, while micro-cracking in alite remains marginal. In order to develop a good grindability of alite clinkers they have to be cooled slowly at first and then the cooling rate should be increased. In this way macro-cracks can be suppressed and micro-cracking can be greatly increased.

Recently the fracturing and grinding of cement clinkers have been monitored in our laboratory with the aid of a scanning electron microscope equipped as a microanalyser (EDAX) [35, 36, 45]. This work allowed the determination of the particle size distribution of the ground material, and also its composition (Fig. 4.3). In this way, two basic mechanisms of fracture were observed: propagation of cracks causing fracture across the "intermediate phase" or along the boundary of the C_3A matrix on one hand, and across alite crystals on the other (Fig. 4.4).

The grindability of cement clinkers is influenced during coarse grinding by the macro-structure of the individual clinker minerals, while in fine grinding the fine structure of these minerals is decisive. In the initial period the comminution of alite and of the "intermediate phase" takes place and these minerals are broken into small particles 3 to 5 μm size. These small particles are distributed in the ground material and adhere with larger particles to form primary aggregates. Belite crystals having a round shape, and thereby a certain mobility, escape size reduction for a long time, i.e. their particle size remains practically unchanged. During fine grinding the small belite particles stick to each other or to larger belite particles and thus form closely-packed aggregates. The "intermediate phase" often forms a "smeared" adhering layer.

Because of the different grindabilities and the selective grinding of clinker minerals, fine grinding gives rise to a poly-dispersed system in which particles differ not only in size but also in composition.

The "micro-images" of the grinding process of cement clinker are demonstrated in Fig. 4.5.

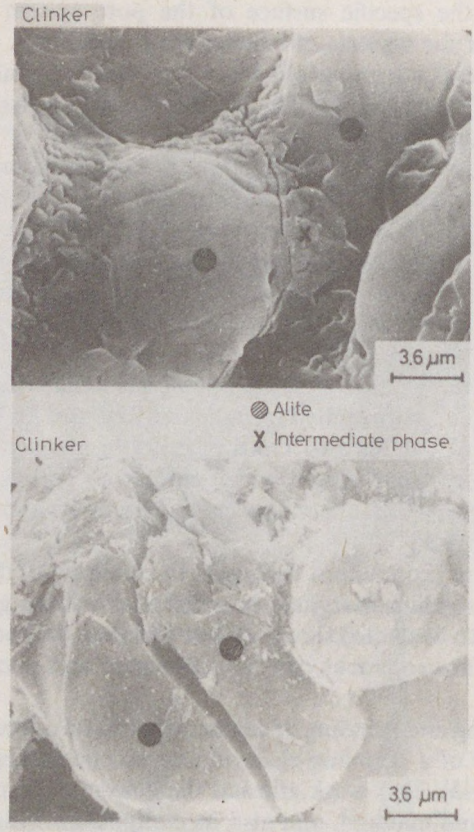

Fig. 4.4. Development of characteristic crack sites on fracture of cement clinker [35, 45]

4.2. THE PROCESS OF GRINDING AND THE INTERACTION OF PARTICLES

The object of mechanical dispersion processes is the production of a ground material having the fineness required by the technological application of the product. Experience shows that after the achievement of a certain degree of dispersion further comminution is reduced, or there may even be an increase of particle size, due to the interaction of particles.

In a typical experiment by Hüttig [46] copper was ground in a mill loaded with steel balls for 110 hours followed by separation of the ground material in a 60 μm sieve. Both the coarse and the fine fractions were ground for another 48 hours and a product of approximately the same sieve analysis was obtained because of the comminution of the coarse fraction and the aggregation of the fines. Hüttig called the particle size distribution obtained in this way an "equilibrium" distribution and he demonstrated the same phenomenon with other brittle materials, such as glass and marble. On the basis of these experiments Hüttig postulated the existence of an "equilibrium state of comminution".

Tanaka [47] suggested the following equation for characterising the kinetics of comminution equilibria:

$$a_s = a_{s_\infty}(1 - e^{-kW_z}), \tag{5}$$

where W_z is the energy input, a_{s_∞} the specific surface at equilibrium and k a constant. When agglomeration occurs the specific surface may fall below the equilibrium value.

Papadakis [31] ground some clinker in a mill loaded with balls of 20 and 30 mm diameter, respectively, and obtained a product with a specific area of 0.45 $m^2\ g^{-1}$. He continued the grinding with grinding bodies of 3 mm diameter. He found that the additional grinding—for the same period—gave a larger specific surface for the sample which was preground with 30 mm balls. He explained this result by assuming that although the apparent specific surface after pregrinding was the same for both samples, the one ground with larger balls underwent more thorough comminution, more pronounced agglomeration and then, under the effect of 3 mm balls, the less tightly aggregated particles disintegrated. Papadakis characterised agglomeration with an index A, representing the percentage of surface area lost by particle interaction related to the area calculated by Rittinger's equation:

$$A = 1 - e^{-bDd^m}, \tag{6}$$

where D is the diameter of the mill drum, d that of the grinding bodies (balls), while b and m are constants.

The kinetics and mechanism of particle interaction are very complex. The adhesion of particles to each other may result in the production of larger amounts of coarse material. On continued grinding the particles may separate again or undergo further increase of particle size. Fine grinding may be accompanied by physico-chemical changes, which may also affect the mechanism of particle interaction. According to our own experience different stages of comminution may be associated with interactions which differ quantitatively and qualitatively [48–52].

4.2.1. STAGES OF GRINDING. AGGREGATION AND AGGLOMERATION

In the silicate industry the fine stages of comminution are most often characterised by Rittinger's equation according to which the work required for comminution is

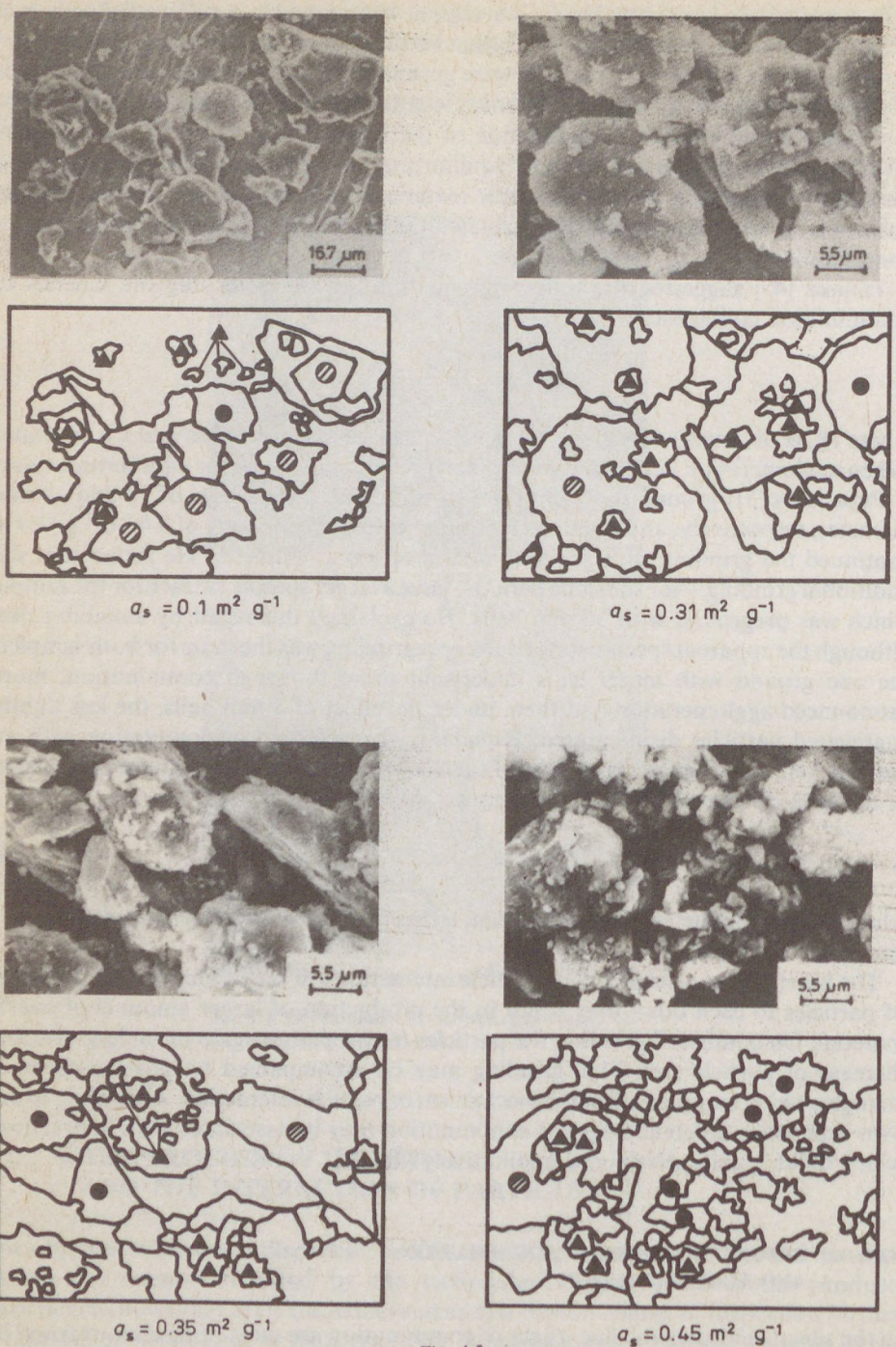
16.7 μm
5.5 μm
$a_s = 0.1\ m^2\ g^{-1}$
$a_s = 0.31\ m^2\ g^{-1}$
5.5 μm
5.5 μm
$a_s = 0.35\ m^2\ g^{-1}$
$a_s = 0.45\ m^2\ g^{-1}$

Fig. 4.5.

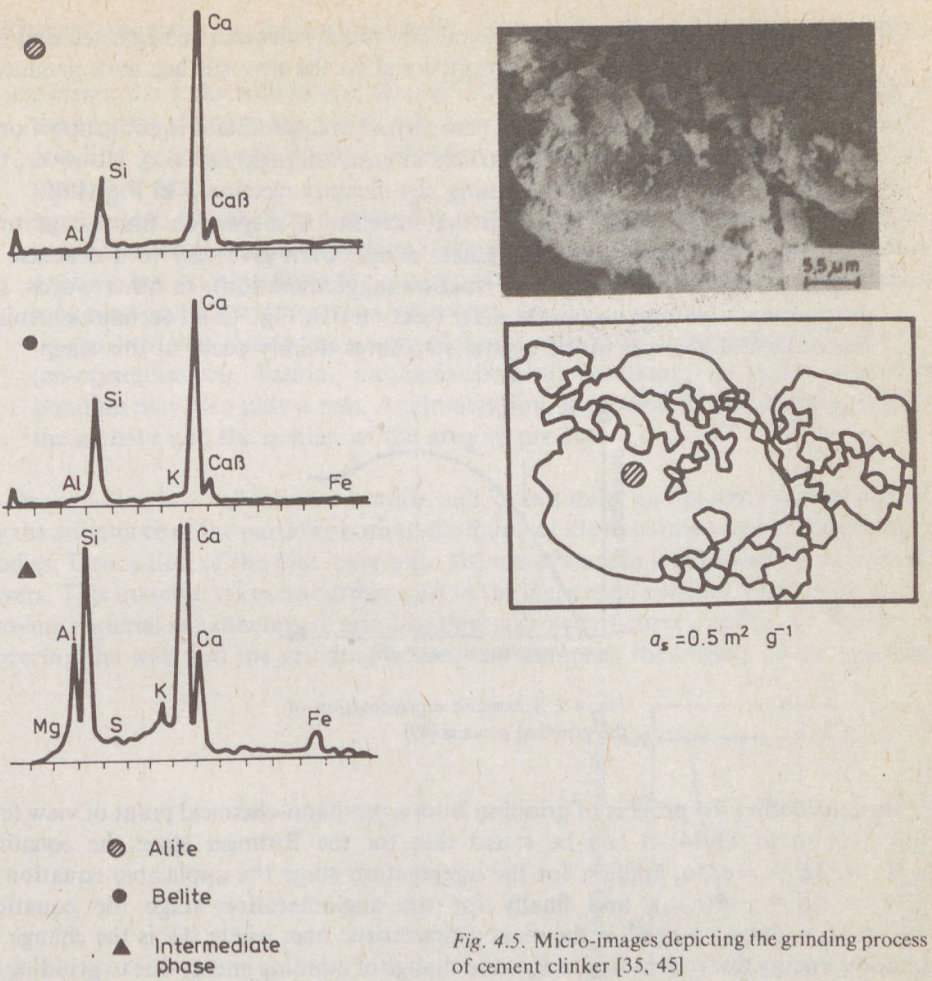

Fig. 4.5. Micro-images depicting the grinding process of cement clinker [35, 45]

proportional to the area of new surface generated. The simplified form of the equation is as follows:

$$W_Z = k\Delta a_s, \tag{7}$$

where W_Z is the work required for comminution, a_s is the increase in surface area, and k a constant.

It is clear that this linear correlation does not hold for the entire process since, with advancing comminution, the energy required for the creation of a fixed amount of new surface is continuously growing; one of the reasons for the increased energy requirement is the degree of particle interaction.

By analysing the change of the degree of dispersion with grinding time τ we can distinguish three stages of the process (Fig. 4.6):

—the *Rittinger stage,* in which the interaction of particles can be neglected and the energy input is approximately proportional to the new surface area produced (section *a* in Fig. 4.6);

—the *aggregation stage* in which the new surface area produced is not proportional to the energy input because of particle interaction (aggregation). However, the degree of dispersion is still increasing significantly (section *b* in Fig. 4.6);

—the *agglomeration stage* in which the increase of dispersion first drops to a negligible value then stops altogether; it may even give way to a decrease of dispersion because of particle interaction (agglomeration). In other words, the ground material may become coarser (section *c* in Fig. 4.6). Mechano-chemical reactions and changes in the crystal structures mainly occur at this stage.

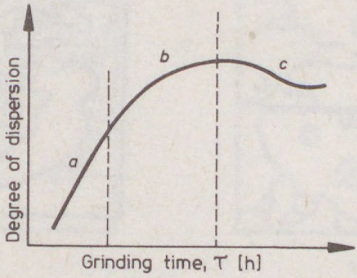

Fig. 4.6. Schematic representation of the grinding process [49]

By considering the process of grinding from a mechano-chemical point of view (cf., Eqs 1–5 on p. 13–14) it can be stated that for the Rittinger stage the equation $\eta_z W_z = \Delta E = -e_\gamma \Delta a_s$ applies, for the aggregation stage the applicable equation is $\eta_z W_z = \Delta E = -\Delta(e_\gamma a_s)$, and finally for the agglomeration stage the equation $\Delta E = \Delta E_u - \Delta(e_\gamma a_s) = \eta_z W_z$ is the most characteristic one; where ΔE is the change of bonding energy due to grinding, ΔE_u is the change of bonding energy due to grinding of the non-dispersed system, e_γ the specific surface free energy, a_s the specific surface area, W_z the work expended during grinding, and η_z the efficiency of grinding.

Verdes [53] put forward a model for the mathematical description of the process of grinding based on probability theory. The essence of this model is that the process is characterised by the moments of the particle size distribution for the ground product. Correlations are given for the change of moments with time by means of a mathematical formulation of fracture probability and a treatment using balance equations. Verdes applied this kinetic model to all three stages of grinding. He established that the value of the kinetic factor of the change of numerosity* remained constant within each stage, but the value of φ_N (the kinetic factor of the change of numerosity) pertinent to the individual stages decreased gradually. For grinding processes spanning several hours, when the effect of grinding and particle interaction alternate $-\varphi_N$ is time dependent and $\varphi_N(t)$ may even be a periodic function.

* Numerosity (number of particles in kg, and it is the first moment of particle size distribution).

Three phenomena may be distinguished in connection with particle interaction [49]:

—*adherence*, i.e. the adhesion of the particles of the disperse system to the lining of the apparatus and to the grinding bodies. Adherence (caking) interferes with the grinding process and further adhesion may also take place during storage, transport, etc.;
—*aggregation*, i.e. weak and reversible association of particles by van der Waals type adhesion (London dispersion) forces. This is a disadvantage in the grinding process, but it only affects the quality of the product very slightly. Aggregation may also occur during storage, transport, etc.;
—*agglomeration* is defined as a very compact, irreversible interaction of particles (co-crystallisation, fusion, mechano-chemical reactions) in which chemical bonding may also play a role. Agglomeration, in general, is detrimental to both the activity and the quality of the ground product.

Dry grinding in a ball mill, a vibration mill, or in similar equipment is accompanied by the adherence of the particles both to the lining of the apparatus and to the grinding bodies. Deposition of the first layer onto the metal surface is followed by additional layers. This material takes no further part in the dispersion process. The loss of freely moving material as a function of grinding time is shown by curve *a* in Fig. 4.7. The layer covering the wall and the grinding bodies also dampens the impact of the grinding

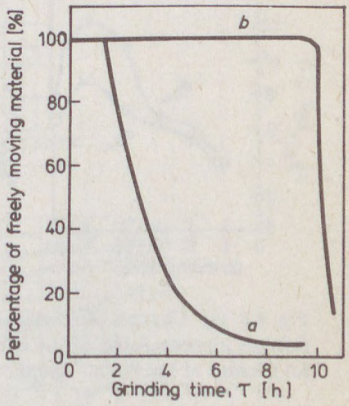

Fig. 4.7. Adhesion in a laboratory mill (curve *a*) without grinding aid and (curve *b*) with a grinding aid [32]

bodies and thus part of the energy is wasted in the deformation of the deposited layers. In closed laboratory mills which operate without ventilation adherence is generally more pronounced than in industrial mills. Adherence can be eliminated by the use of grinding aids (curve *b* in Fig. 4.7). An analysis of the degree of dispersion and the particle size distribution of the layers stuck to the walls and grinding bodies revealed that the finest particles occurred in the lowermost layer and that the degree of adherence was also influenced by the nature of the feed [32, 54, 55].

Particle interaction phenomena are exemplified by changes in the physical and physico-chemical properties of βC_2S, limestone, and quartz—all brittle materials but of different hardnesses. In Figure 4.8(a) the change of "external" specific surface (a_s)

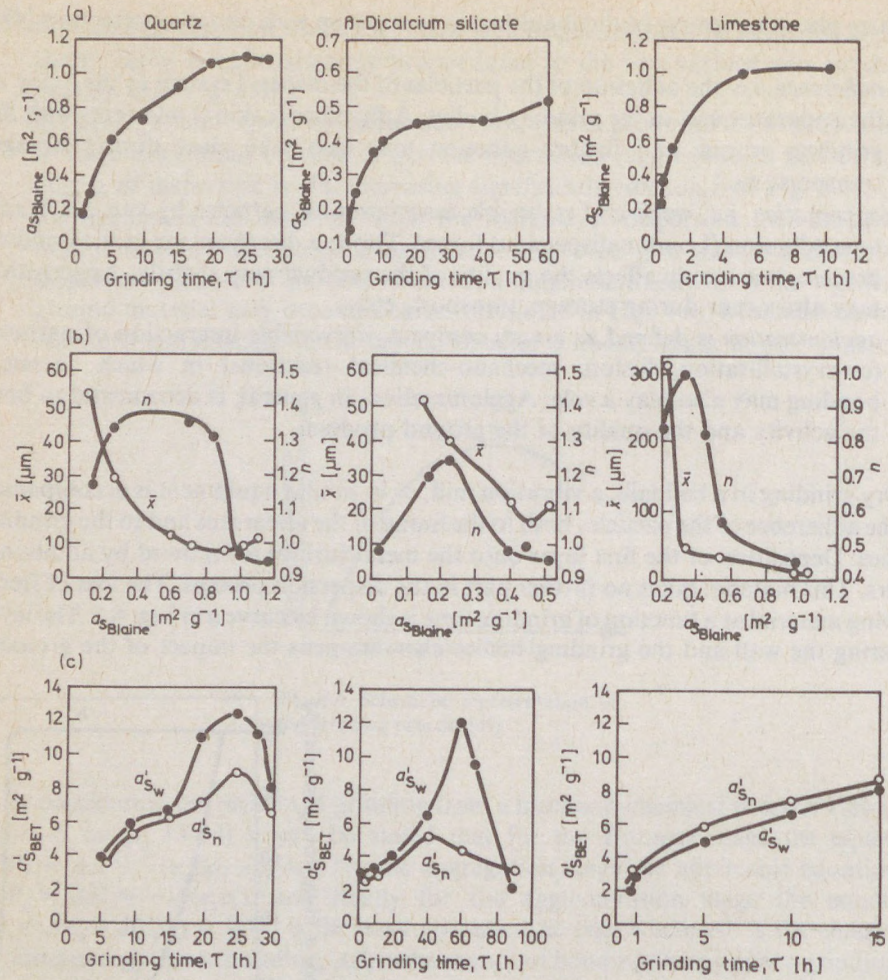

Fig. 4.8. (a) Change of "external" specific surface (a_s) with grinding time. (b) Change of fineness number $\bar{x}$ and of the uniformity coefficient (n) with the "external" specific surface (a_s). (c) Change of the "total" specific surface (a'_{s_w}) and (a'_{s_n}) with grinding time [49–51]

and the distribution of the individual grinding stages are shown as functions of time. The flattening of the curve of specific surface sets in with soft materials (limestone) after shorter—and with hard materials (quartz) after longer—grinding time. This flattening is primarily a consequence of particle interactions, i.e. aggregation.

In Figure 4.9 the change of particle size $R(x)$ with time $R(\tau)$ of some experimental samples is shown in a co-ordinate system corresponding to the RRSB equation (DIN 66145 net).

Before discussing the results in detail we must mention that by assuming the simultaneous validity of Rittinger's law and the RRSB equation, the change in time

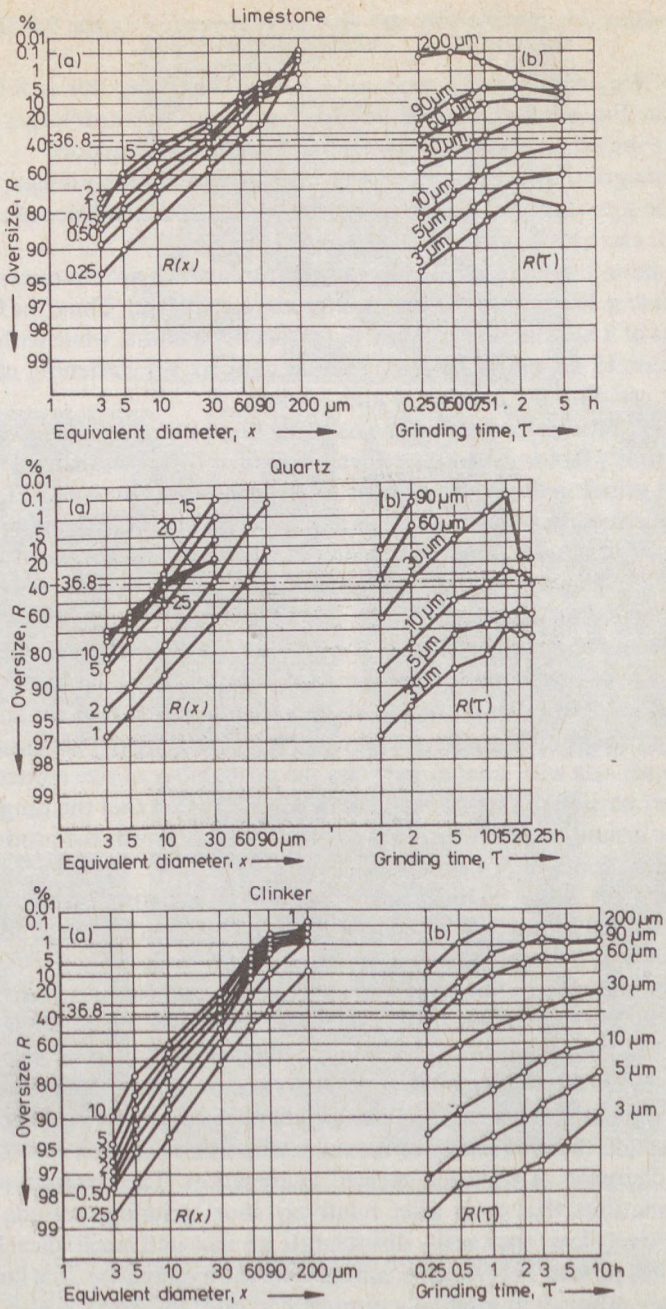

Fig. 4.9. Change of particle size distribution with grinding time: (a) $R(x)$ particle composition (numbers stand for grinding time in hours); (b) $R(\tau)$ oversize as a function of grinding time [52]

against sieve residue (i.e. particle size) can also be represented on the RRSB chart by a straight line.

Initially the $R(x)$ curves rise steeply as a function of time; this is followed by a flattened section. Further flattening of the curves and a shift towards larger particle size can also be attributed to the commencement of particle interaction.

Up to a certain grinding time, $R(\tau)$, the curves are approximately linear; beyond this time the particle sizes increase (i.e. larger sieve residues). A dependence of sieve residue on particle size can also be observed on the $R(\tau)$ curves.

$R(x)$ curves permit the recognition of some features which are characteristic for the grinding of soft (e.g. limestone) and hard materials (e.g. quartz). Thus, the flattening of the $R(x)$ curves of limestone can be observed after only 2 hours, while with quartz this only occurs after 15 hours. With most cement clinkers the flattening effect can be observed after grinding for between 4 and 5 hours.

The change of particle size distribution as a function of time can be better visualised when the uniformity factor (n) and the fineness number ($\bar{x}$) of the ground material are plotted against grinding times and degrees of dispersion, respectively (Fig. 4.8(a)). It can be seen that the curve of n has a maximum, while that of $\bar{x}$ has a minimum, but the extreme values of the curves do not coincide. The extreme value of the n curve always precedes that of $\bar{x}$. This correlation is of general application, as shown by laboratory and large scale grinding experiments.

The materials to be ground consist of particles of different sizes, since fracture under the action of mechanical load is always initiated at lattice defects then, according to lattice defect theory, first of all the larger particles that contain relatively more lattice defect sites will undergo fracture. With decreasing particle size fracture strength increases and with smaller particles the probability of size reduction is lower than with larger particles. Accordingly, it can be anticipated that the range of particle sizes within the ground product becomes smaller; in other words the product becomes more uniform (n increases, $\bar{x}$ decreases).

The development of a particle size distribution differing from the expected distribution is caused by particle interaction. This interaction begins by the adherence of small particles to the surface of bigger ones.

The fundamental recognition that a decrease of the uniformity factor (n) can be attributed to particle interaction, i.e. to agglomeration, was made by Beke [56, 57]. According to him the decrease of this factor indicates the "limit of grindability".

Our own investigations revealed that different stages of particle interaction can be distinguished, these stages become apparent in changes in the particle size distribution. A decrease of n, and the broadening of the range of particle sizes is a consequence of an initial weak adherence of particles, termed aggregation. The strength of any loose secondary formations that arise after relatively short grinding periods (at smaller fineness) is relatively low; they easily disintegrate on repeated mechanical loading and then reform. This process is reversible, and despite the aggregation, the fineness of the charge increases although at gradually diminishing rate; this effect is also shown by a decrease of the fineness number $\bar{x}$. After attaining a certain fineness, however, $\bar{x}$ values either remain practically constant, or increase, thus indicating that the curves of particle size distribution are shifted on the RRSB chart towards the coarse range. The increase of the fineness number $\bar{x}$ can be correlated with the extension of particle

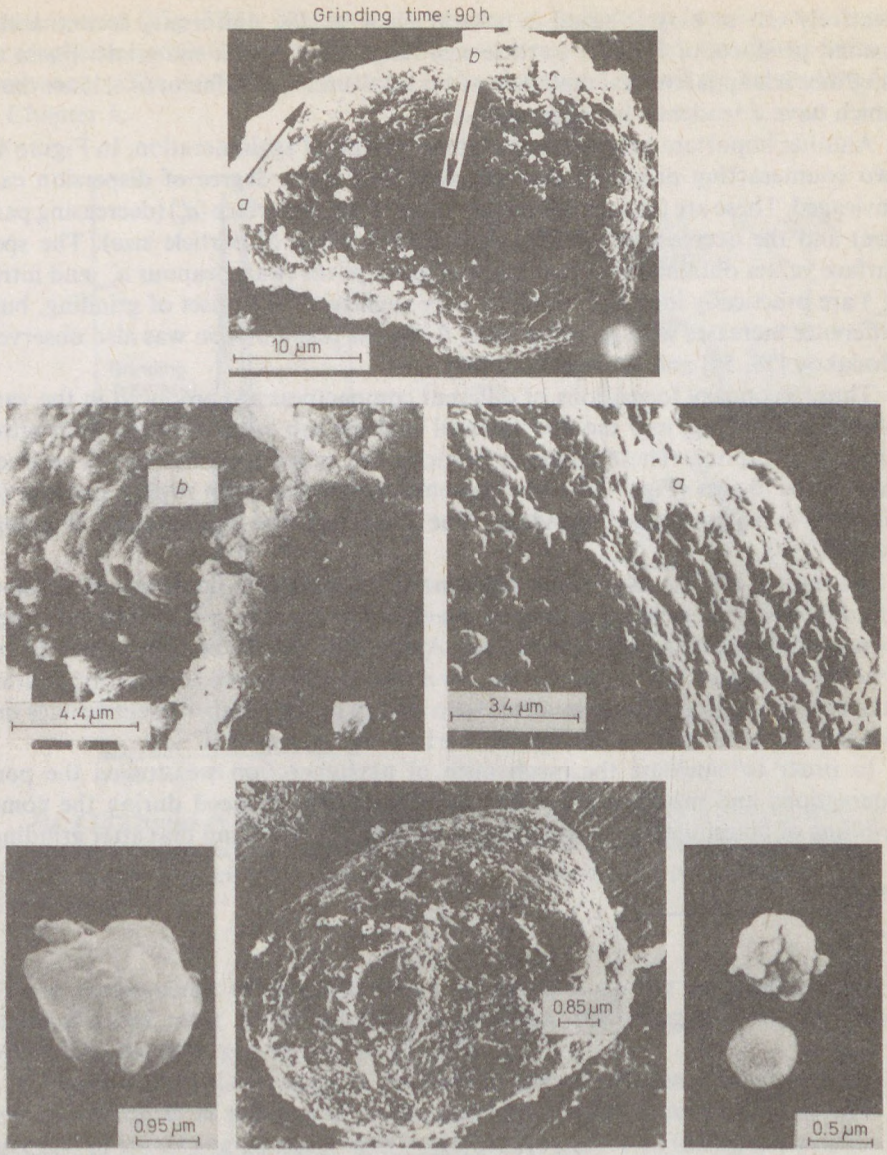

Fig. 4.10. Formation of agglomerates in the course of grinding β-dicalcium silicate [49–51]

interaction to all sizes of particles, as well as to the formation of agglomerates that have an enhanced strength and compactness.

The n diagrams shown in Fig. 4.8(b) as a function of time and degree of dispersion are suitable for distinguishing between the Rittinger stage and the aggregation stage and can be used for evaluating the aggregation tendency of materials. The uniformity factor of single-component materials is in the range of 0.4 to 1.5. Materials which are

relatively soft or easy to grind in general show smaller uniformity factors and give ground products of broader particle size range than harder materials. From the n diagrams it is apparent that materials with a small uniformity factor ($n \leqslant 1$) are the ones which have a tendency for aggregation.

Another important problem is the interpretation of agglomeration. In Figure 4.8(c) two counteracting processes that are decisive for the degree of dispersion can be envisaged. These are the increase of the "total" specific surface (a'_s) (decreasing particle size) and the decrease of specific surface (increasing of particle size). The specific surface values obtained with two kinds of adsorptives (water vapour a'_{s_w} and nitrogen a'_{s_n}) are practically identical, or differ only slightly, at the onset of grinding, but the difference increases with grinding time. A similar phenomenon was also observed by Hodakov [58, 59] and Kudrjavceva [60].

Thus, secondary formations of different compactness are produced in the various phases of grinding, and the new internal surfaces are inaccessible to both nitrogen and water vapour. These compact particles are called agglomerates. The electron microscope images (Fig. 4.10) show agglomerates formed from smaller particles (*a*) in the course of prolonged grinding. The inside of the agglomerate is compact, "caked" (*b*).

According to our experience agglomeration generally accompanies prolonged grinding when the product undergoes changes that affect its crystal structure and it is exposed to mechano-chemical reactions. Agglomeration can be detrimental to several other properties of a dispersed system; for instance, its reactivity, solubility, hydration, etc., because agglomeration involves both a drop in the number of active sites on the surface and a decrease of the specific surface free energy [61].

In order to elucidate the mechanism of agglomeration we studied the particle interactions and mechano-chemical phenomena that proceed during the common grinding of limestone and quartz (Figs 4.11 to 4.13). We found that after grinding for

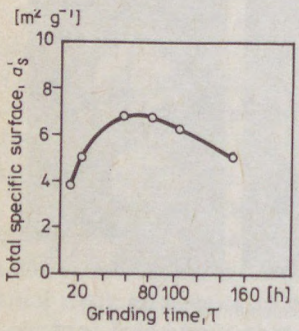

Fig. 4.11. Agglomeration during the common grinding of limestone and quartz [52]

100 hours the product underwent extensive agglomeration and mechano-chemical amorphisation (Fig. 4.11). The X-ray diffractogram (Fig. 4.12) of a product ground for 150 hours shows a reflection of low intensity at 0.298 nm: this indicates that, as a result of a mechano-chemical reaction of the components, a new compound, most probably calcium metasilicate, was formed. DTA experiments confirm that carbon dioxide is liberated during the common grinding of limestone and quartz; the endothermic peak, which is diagnostic for the decomposition of $CaCO_3$, decreases with increasing

grinding time (Fig. 4.13). The presence of quartz accelerates the mechano-chemical decomposition of $CaCO_3$, this effect indicates a metathetical reaction between the two components. The mechanism of mechano-chemical reactions will be discussed in detail in Chapter 5.

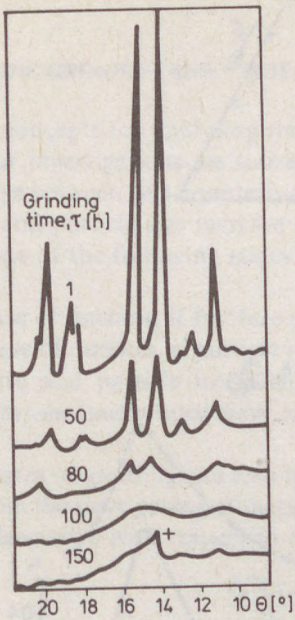

Fig. 4.12. Changes in the crystal structure and the mechano-chemical reactions that take place on common grinding quartz and limestone [52]

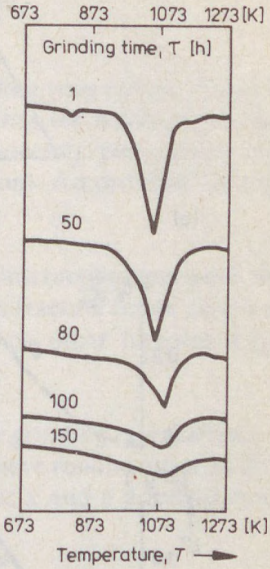

Fig. 4.13. Effect of common grinding quartz and limestone on the DTA curves of the product [52]

As a consequence of the interaction of particles during grinding the internal morphology of most of the particles is modified, this effect can be conveniently followed in the SPV system (cf., p. 17) [62].

In Figure 4.14(a) the changes in the state of samples of quartz sand and pumicite sand in the course of grinding in a vibration mill are shown in the SPV system. The direction of increasing grinding time is indicated by arrows. The quartz sand, which has compact particles (SV type), is situated along the SV side of the triangle at the start (0 hours). In the initial period of grinding a slight increase in particle porosity and in the number of interstices can be observed: because of the decreasing particle size the bulk of the product assumes a looser structure. In contrast, the pumicite sand, consisting of porous particles (SPV types), undergoes a morphological change of SPV →SV character during the initial period of grinding. This is caused by fractures along pores that lead to smaller but more compact particles. In this process pores are opened up, this leads to a more favourable distribution of particles and a bulk material with a smaller number of interstices.

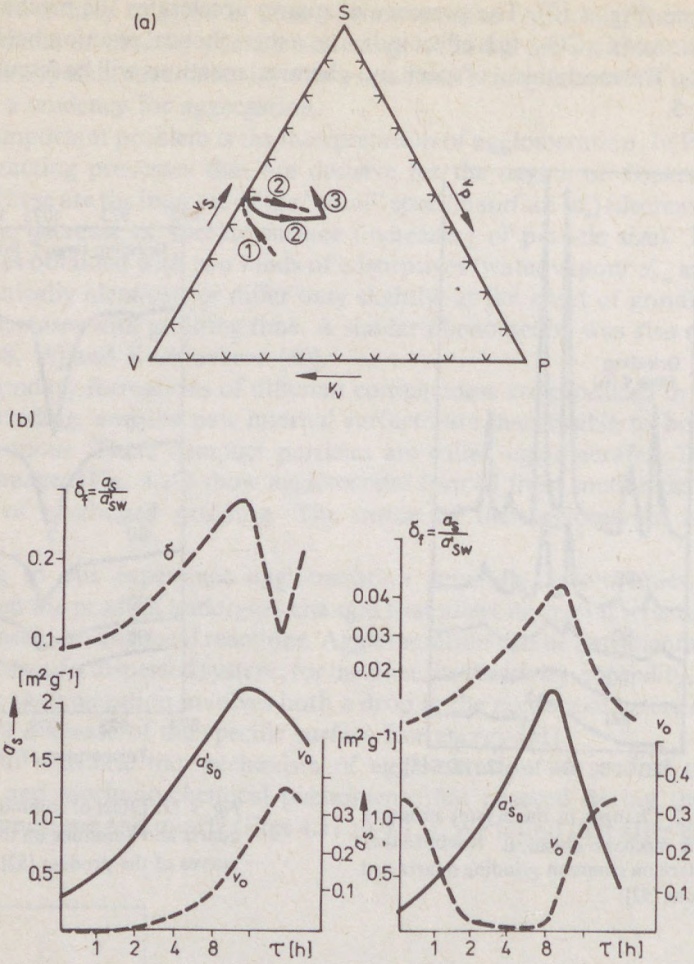

Fig. 4.14. Change in the internal morphology of quartz (Q) and pumicite (P) after mechanical activation by grinding in a vibration mill [62]

(a) Changes of state in the SPV system. Full line: quartz; broken line: pumicite. Stages of grinding are indicated by numbers in frames; increase of grinding time is shown by arrows.

(b) Changes of the "external" specific surface (a_s) and of the porosity of particles (v_0) of quartz and pumicite as a function of grinding time (τ). δ_f the "degree of unlocking" is expressed as the ratio of "external" and "total" specific surface. The "total" specific surface (a'_{sw}) was determined by the measurement of water vapour adsorption.

The second period of grinding results in an increase of porosity and a decrease in the number of interstices for both samples (transformations of V →P type).

Finally, a substantial reduction of porosity, i.e. agglomeration, is observed after prolonged grinding of quartz sand. This third period can be well demonstrated in the SPV system.

MAGYAR TUDOMÁNYOS AKADÉMIA KÖNYVTÁRA

In Figures 4.14(b) and 4.14(c) the change of a_s and v_0 as a function of time is depicted for the two samples (quartz and pumicite). The change of "external" specific surface connected with the decrease of particle size, as well as the change of porosity due to the fracture and aggregation of pumicite particles, is in good agreement with the changes of state shown in the SPV system.

4.2.2. FINE GRINDING AND EQUILIBRIUM STATES

The basic concepts for analysing the kinetics of grinding were elaborated by Hüttig [46]. In our investigations we started from the fact that the result of grinding is a compromise between two counteracting elementary processes, particle size reduction (fracture) and particle size increase (particle interaction). Accordingly, at any given moment one of the following states can be observed:

—increase of fineness, if fracture overrides particle interaction (less sieve residue);
—decrease of fineness, if particle interaction exceeds fracture (more sieve residue);
—fracture and particle interaction compensate each other forming a dynamic equilibrium (unchanged sieve residue).

These states of grinding can also be described by the grinding rate function. This is derived from the sieve passage function $D(x, \tau)$ or the sieve residue function $R(x, \tau)$ as a partial derivative with respect to time at a given size x and a grinding time τ:

$$\frac{\partial D(x, \tau)}{\partial \tau} = -\frac{\partial R(x, \tau)}{\partial \tau}. \tag{8}$$

In this formula the grinding rate means the amount of particles with sizes that pass the given size x, from any direction, during unit time at a grinding time τ.

By analysing the curves of sieve residue $R_x(\tau)$ and grinding rate $\dot{D}_x(\tau)$ at a given particle size, the state of dynamic equilibrium can be defined. This equilibrium state develops due to particle size interaction and is indicated by stagnating values of sieve residue or zero values of grinding rate.

The temporary equilibrium which is established primarily in the initial stage of grinding does not imply that the increase of fineness is terminated, but it is invariably accompanied by increased energy consumption. This equilibrium state is due to weak adhesion of the particles, i.e. aggregation. During continued grinding the particles undergo repeated fracture, i.e. the basic tendency of the process is an increase of fineness.

A state of permanent equilibrium is only established after prolonged grinding and this marks the end of the progress of fineness for a given particle size. On continuing the process grinding energy seems to be consumed for maintaining the equilibrium; in fact, it promotes superficial or mechanical activation of the particles. This second equilibrium is due to the appearance of stronger interactions. As a consequence, on further grinding the particles do not further disintegrate and the increase of particle size, i.e. agglomeration, becomes dominant (increasing sieve residue and negative grinding rate values).

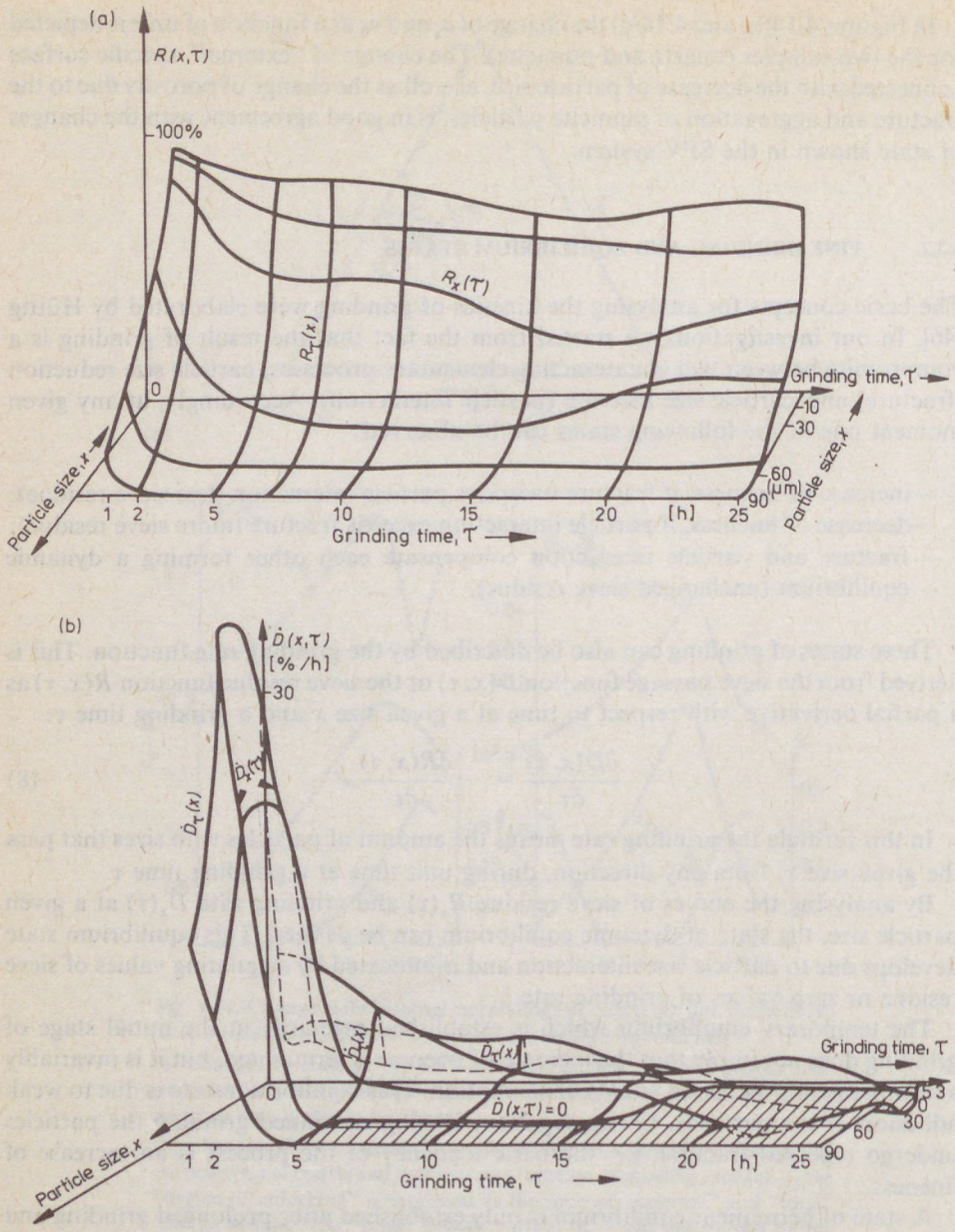

Fig. 4.15. Three-dimensional plot representing the result of applying the bivariate function to quartz: (a) $R_\tau(x)$ sieve residue versus particle size curve at constant grinding time (τ); $R_x(\tau)$ sieve residue versus grinding time curve at constant particle size x. (b) $\dot{D}_\tau(x)$ grinding rate versus particle size curve; $\dot{D}(x, \tau) = 0$, constitutional diagram of the equilibrium state of grinding [63]

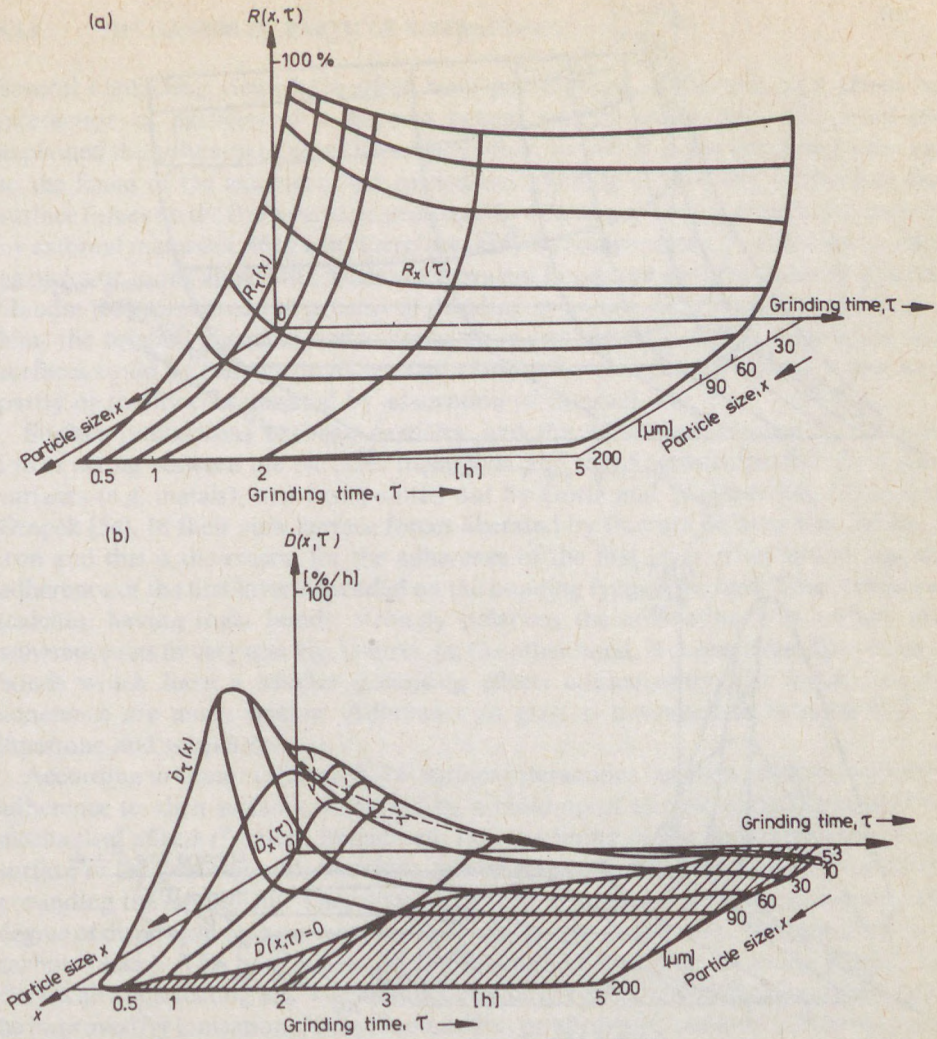

Fig. 4.16. Three-dimensional plot representing the results of applying the bivariate function to calcite. (a) $R_\tau(x)$ sieve residue versus particle size curve at constant grinding time (τ); $R_x(\tau)$ sieve residue versus grinding time curve at constant particle size x. (b) $\dot{D}_\tau(x)$ grinding rate versus particle size curve; $\dot{D}(x, \tau) = 0$, constitutional diagram of the equilibrium state of grinding [63]

The generalisation of the dynamic equilibria which are associated with individual particle size values allowed the equilibrium state curves indicating the adhesion of particles to be defined. This adhesion may be temporary or, at the end of the grinding process, they may be permanent (aggregation and agglomeration, respectively).

Based on sieve residue and grinding rate versus time curves, typical curves could also be obtained for the range of fine grinding.

Figures 4.15 to 4.17 show the surface representing sieve residues and the grinding of selected samples. The sections of the surfaces parallel to the axes contain the particle

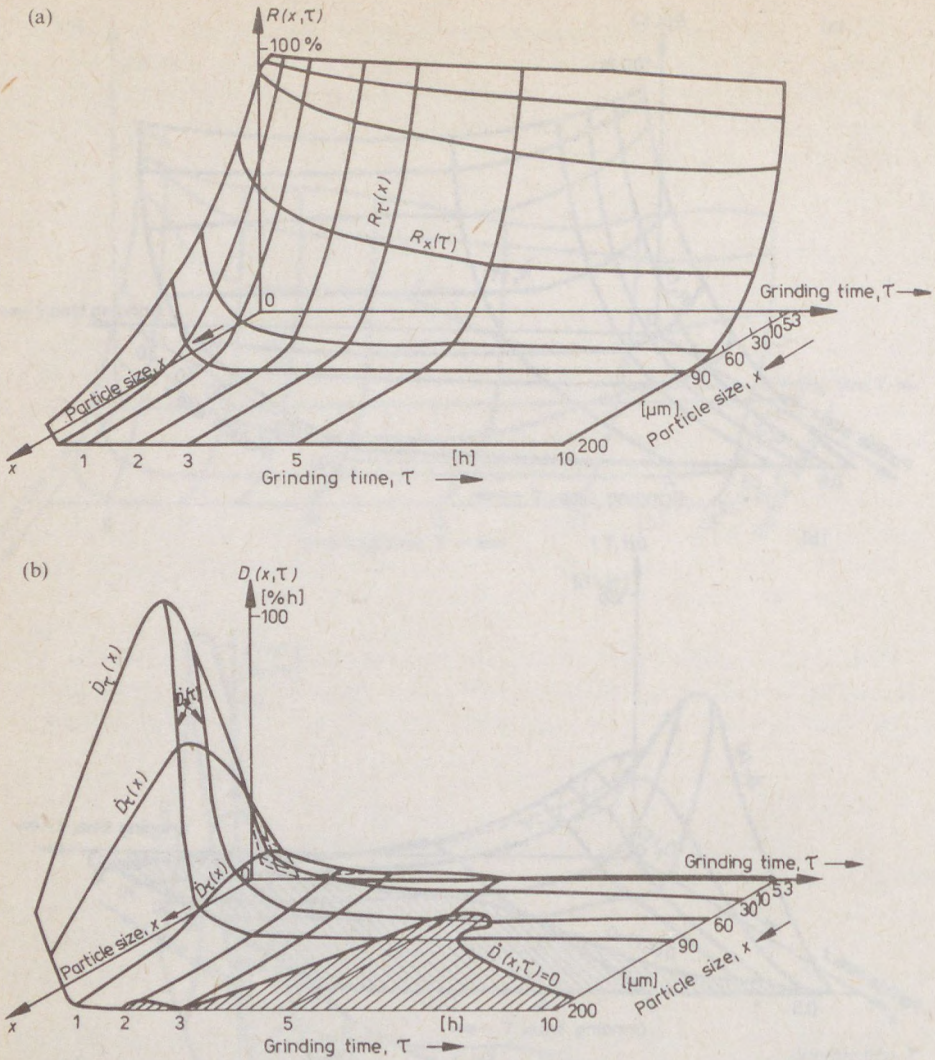

Fig. 4.17. Three-dimensional plot representing the results of applying the bivariate function to cement clinker. (a) $R_\tau(x)$ sieve residue versus particle size curve at constant grinding time (τ); $R_x(\tau)$ sieve residue versus grinding time curve at constant particle size x. (b) $\dot{D}_\tau(x)$ grinding rate versus particle size curve; $\dot{D}(x, \tau) = 0$, constitutional diagram of the equilibrium state of grinding [63]

size curves $R_\tau(x)$ and $\dot{D}_\tau(x)$ at a given grinding time τ (τ = const.) and the time curves $R_x(\tau)$ and $\dot{D}_x(\tau)$ at a given particle size x (x = constant).

An analysis of these curves proved that the fine grinding of cement clinker, although it exhibits some special features, proceeds in much the same way as that of single-component minerals [63].

4.2.3. MECHANISM OF PARTICLE INTERACTIONS

Several conflicting views have often been put forward in the literature about the interaction of particles of a disperse system and its mechanism. Obreimoff [64] explained the adhesion of particles to each other, as well as to the grinding bodies and to the lining of the equipment (he carried out grinding in vacuum), by the fact that surface forces on the fresh surfaces produced by fracture are not neutralized in vacuum by external materials: they can, therefore, only be compensated by adhering to other particles or to the apparatus. Since electrovalent bonds are separated during grinding Gaudin [65] compared the process of grinding to a chemical reaction. According to him, the original chemical bonds could be re-established if the corresponding new surfaces could be brought together again before the unbalanced valence forces were partly or totally compensated by adsorption of external ions.

Surface interactions between particles, and the differences concerning adhesion forces acting between the particles themselves and those between particles and alien surfaces (e.g. metals), was first pointed out by Götte and Wagener [66, 67] and by Ocepek [54]. In their view surface forces liberated by fracture polarise the surface of iron and this is the reason for the adherence of the first layer. They found that the adherence of the first layer depended on the bonding type of the feed. Thus, limestone (calcite), having ionic bonds, strongly polarises the contacting iron surface and adherence sets in very quickly. Quartz, on the other hand, is characterised by covalent bonds which have a smaller polarising effect; consequently, the forces causing adherence are much weaker. Adherence to glass is intermediate between that to limestone and to quartz.

According to some authors [67–74] surface interactions between particles, and their adherence to alien surfaces, is caused by a build-up of electric charge generated by mechanical effects (friction, impact, etc.) on the lining of the apparatus and on the surface of the particles and, therefore, adherence can be avoided relatively simply by grounding the equipment. They supported their concept by the observation that the degree of dispersion of the ground product can be enhanced by antistatic additives (e.g. carbon black). The best means of eliminating static charges is using humid, i.e. electrically conducting air. The conductivity of dry air in the milling equipment can be improved by ionisation (X-ray, radioactive, or ultraviolet radiation) or by spraying water and by these methods it is possible to increase significantly the fineness of ground cement.

However, Mardulier [75] and Opoczky [76] from laboratory and large scale experiments reached the conclusion that the attractive forces between particles cannot be attributed to electrostatic charges. Mardulier [75] investigated the effect of antistatics in an industrial mill and established that such additives are much less effective than conventional surfactant grinding aids which lack antistatic properties.

The forces responsible for the adhesion of cement clinker particles are explained by certain authors [77, 78] by invoking the simple molecular structure of silicon dioxide. Clinker consists of 80% calcium silicates (alite and belite) in which SiO_4^{4-} tetrahedra are dominant. Free surface forces generated during the fracture of glassy silicon dioxide can be illustrated by the well known diagram of Weyl [79] (Fig. 4.18). It can be seen that electrovalent bonding forces are liberated on the fracture surface (Fig.

4.18(b)). Because of the motion of grinding bodies in a revolving mill the fractured surfaces not only get into contact again but they are also pressed against each other: in this way, attractive forces develop between surfaces bearing opposite charges. Hansen [77] explained the adhesion of cement clinker particles to each other in the following way: $3CaO \cdot SiO_2$ contains four positive (Ca^{2+} and Si^{4+}) and five negative (O^{2-}) ions; $2CaO \cdot SiO_2$ three positive (Ca^{2+} and Si^{4+}) and four negative (O^{2-}) ions; $3CaO \cdot Al_2O_3$ five positive (Ca^{2+} and Al^{3+}) and six negative (O^{2-}) ions. Although

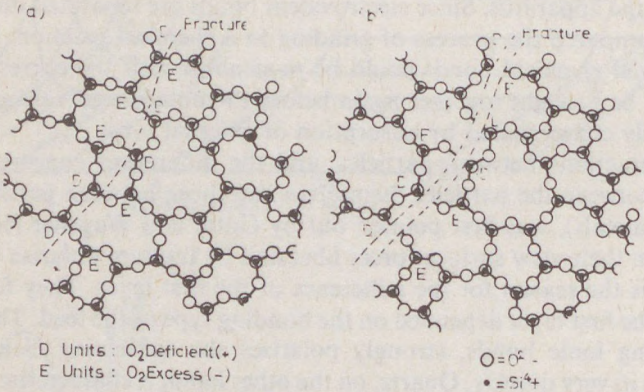

Fig. 4.18. Fracture surface of silicon dioxide [79]

positive ions are less polarisable than negative ions, they are numerous enough to provide about the same number of positive and negative charges at the fracture surfaces of clinker particles. In this way, there is no repulsion between cement particles and they can easily stick together under the effect of impact by grinding bodies. Essentially the same model was put forward by Iwabuchi [78], when he supposed that alite crystals are cleaved along the (1101) plane during fracture. It has to be noted that the cleavage planes of belite and alite crystals are not known and, therefore, the suggested models have to be accepted with caution. Studies by Weyl [79] demonstrated that there are fewer Mg^{2+} ions that expected at the surface of the particles of periclase powder and that the surface is mainly occupied by O^{2-} ions. Weyl explained this by invoking the weak polarisability of Mg^{2+} ions. The strong electric field of Mg^{2+} increases surface energy much more than the highly polarisable O^{2-} ions and, therefore, Mg^{2+} ions move away from the surface. The result is an excess of negative charges on the surface of MgO and, therefore, the particles repulse each other.

Other researchers [80, 81] correlated the interaction of particles with the coalescence of crystals and with the formation of hydrogen bridges. The forces that cause the growth of particles and, thereby coarsen disperse systems, and the possible mechanisms of particle interactions have been classified and summarised by Krupp [82] and by Rumpf and his school [83–96].

Krupp [82] elaborated his theory about the adhesion of solid particles for room temperature and for conditions not involving any change in the chemical identity of the particles. He also assumed chemical saturation of the adhering particles ("equilibrium surfaces").

Rumpf [83–89], in turn, extended the investigation of particle interaction to technological processes firstly to those such as, pelletting and granulation, aiming at producing granules with pre-defined properties (strength, porosity, etc.).

Adhesion forces between solid particles can be classified as long-distance forces (electrostatic and van der Waals forces) or as short-distance attractive forces (chemical and intermediate bonds, e.g. hydrogen bonds). Interfacial reactions (sintering effects, mutual melting and alloying on the interface) are placed into a separate group. Experiments and calculations support the view that the major role in the adhesion of solid particles is played by attractive electrostatic and van der Waals forces.

Van der Waals forces act between atoms and molecules without the transfer of electrons from one partner to the other. These forces comprise three components: attraction between opposite poles of dipolar molecules (orientation effect), attraction between dipoles induced by one molecule in neighbouring ones (induction effect), and interaction of dipoles arising from the vibration of electron shells relative to the atomic nuclei (London dispersion forces). The only forces active in an assembly consisting of non-polar molecules are dispersion forces; in polar molecules all three effects are operative, but the induction effect is always small.

Electrostatic attraction can be traced to excess charges generated by electric double layers, by mechanical action (impact, friction, etc.), and by the adsorption of ions and electrons, etc.

Calculations of the adhesion forces were carried out with the aid of three different contact-geometry models, the detailed discussion of which is outside the scope of this book. In the following discussion we only present, in a highly simplified way, the final results of these calculations. In Figure 4.19(a) a model based on the contact of a sphere and a plane is shown with the pertinent equations.

$$F_{vdW} = \frac{h\bar{\omega}}{8\pi a_0^2}\varrho \tag{9}$$

$$F_{el} = \pi\varepsilon\varepsilon_0 \frac{\Delta u^2}{a_0}\varrho \tag{10}$$

$$F_{vdW} = \frac{h\bar{\omega}}{8\pi a_0^2}\varrho\left(1+\frac{h\bar{\omega}}{8\pi^2 a_0^3 H}\right) \tag{11}$$

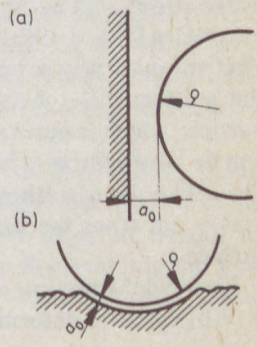

Fig. 4.19. Van der Waals forces (F_{vdW}): (a) Van der Waals forces and electrostatic forces (F_{el}) between a sphere and a plane. (b) Van der Waals forces between two contacting surfaces during plastic deformation [82, 87, 88, 95]. $h\bar{\omega}$—interaction energy, a_0—"equilibrium distance", ϱ—curvature radius, H—hardness, Δu—contact potential difference

Two geometrical factors are of prime importance from the point of view of the magnitude of the adhesion forces: distance a between particles, and the radius of curvature ϱ at contact points. The equations quoted are valid if $\varrho \geqslant a$. When the contact $a = a_0$, its value is approximately 0.4 nm. This distance (a_0) was denoted by Krupp as the "equilibrium distance" (a_0 is the distance of maximum adhesion force).

The magnitude of the adhesion force is a material characteristic and represents, along with van de Waals forces, the interaction energy $h\bar{\omega}$ [94], and with electrostatic attraction it represents the potential difference Δu.

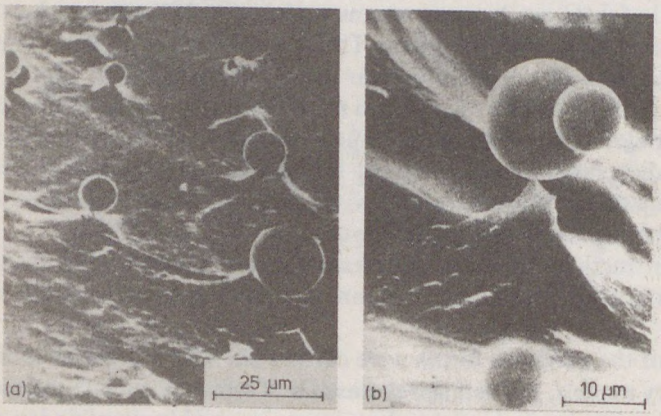

Fig. 4.20. Adhesion of gold particles to the surface of anthracene [96]

The approximate value of $h\bar{\omega}$ has been determined for some materials. It was found to be 1.7 eV with plastics, 2.0 eV with ionic crystals (e.g. KBr), 7.0 eV with hard minerals and semiconductors (e.g. Si), and 9.0 eV with metals (e.g. Ag). It can be seen that the value of $h\bar{\omega}$ is especially high with metals and rather low with crystals, such as KBr, which have ionic lattices.

The maximum value of the potential difference Δu was set to about 0.5 V. However, this value has not been determined accurately for several important materials. Note that the Eq. (10) shown in Fig. 4.19 is only valid for metals. The attractive forces are generally smaller when non-metals come into contact.

According to Rumpf and Krupp adhesion forces at distances of atomic magnitude are so strong that at the contact points of the particles elastic and plastic deformations take place (Fig. 4.19(b)). Deformations first affect the protrusions. In Figure 4.20 an electron-microscopic image of an anthracene-gold system is shown at the instant when the gold particles become severed from the anthracene surface. The anthracene particle, which is normally solid and crystalline, becomes deformed under the effect of van de Waals forces. The forces required to sever the gold particle are much higher than the yield point of anthracene and, therefore, before separation, a cone of anthracene is drawn out from the surface. After separation the cones remain and form a "hilly" surface.

Plastic deformation of the contact zone greatly increases the adhesion forces (Fig. 4.19(b)). Plastic deformation first affects the adhesion due to van der Waals forces,

especially when the interaction energy ($h\bar{\omega}$) is high and hardness (H) is low, Eq. (11). This latter condition is realised when materials of different quality adhere to each other, i.e. adhesion of soft and hard materials.

On comparing electrostatic and van der Waals forces Rumpf established that the magnitude of electrostatic attraction is much smaller than that of van der Waals forces but, at the same time, the former acts at longer range. Consequently, where the distances between particles are "large" the excess charges may play an important role in the interaction of particles. Electrostatic attraction promotes the approach of particles, their collision, and the establishment of weak primary interactions. However, as soon as the particles have made contact, the van der Waals forces override the electrostatic interactions. According to Rumpf, attraction due to excess charge can be neglected with particle sizes under 100 μm as compared with van der Waals forces.

Based on studies by Krupp and Rumpf, and by our own investigations, the formation, rupture, and severance of surface bonds that are characteristic for particle interactions in fine grinding can be summarised as follows.

After a relatively short period of grinding and at relatively low fineness the adherence of particles sets in as a consequence of van der Waals adhesion forces (primarily London dispersion forces)—this is called aggregation.

The distance between particles and the number of contacts plays an important role in the appearance of adhesion. The number of contacts depends on the fineness, the shape of the particles and the particle size distribution.

In real poly-disperse systems the presence of very fine particles along with relatively coarse particles will greatly promote the formation of aggregates, and this accounts for the marked tendency for aggregation in ground products that have a broad range of particle sizes.

With increasing dispersion and decreasing distance between particles the effect of van der Waals forces gains in importance and the strength of secondary formations increases. Particles are initially joined by protrusions; thereafter, contact surfaces are formed by rearrangement. Plastic deformation at contact points greatly increases both the area of the adhesion surfaces, and the magnitude of the adhesion forces and, thereby, increases the strength, compactness, and resistance to mechanical effects of particle agglomerates. The magnitude of contact surfaces and the strength of the linkages (i.e. the strength and compactness of secondary formations) thus depends on the plastic–elastic properties of the contacting particles.

In the course of the adhesion of particles in a mechano-chemically activated ground product the chemical interactions may also proceed at the contacting surfaces. These interactions result in a very compact, irreversible adhesion of the particles due to welding, co-crystallisation, and mechano-chemical reactions. This phenomenon is called agglomeration.

Agglomerates can be formed by welding or coalescence of crystals, by direct initiation at the contacting surfaces, or by means of "melt-bridges" that appear at the surfaces of particles—initially at protrusions, edges, etc. Such bridges are similar to those formed during high temperature sintering, except that in fine grinding the heat required for melting is provided by mechanical effects, friction, and plastic deformation.

In mills operating on the basis of combined friction and impact (primarily ball mills) conditions favouring the formation of agglomerates are provided since the grinding bodies promote the interpenetration of particles and the formation of melt-bridges.

4.3. ENERGY REQUIREMENTS DURING GRINDING

Energy consumption during grinding is very high; about 3% of the total electric energy produced in the world is used for grinding. The main consumers of this energy are the cement industry (0.77%), wood milling (0.62%), ore processing, and power plants (0.21%) [97, 98]. Therefore, any activity that can reduce the energy demand of grinding is highly relevant.

One of the important objectives of comminution theory is to establish correlations between the degree of dispersion of the ground product and the amount of energy used during its production but, because of the complexity of the processes involved in comminution, this objective has not been completely attained. The literature on the problem is quite extensive and the theories of Rittinger [99], Kirpichov [100], and Bond [102, 103] deserve to be mentioned. A summary and a critical appraisal of these theories have been presented in a monograph by Beke [56].

(1) According to the "surface" theory of Rittinger [99] the energy consumption of comminution is proportional to the new surface produced by the process. The common form of Rittinger's law is:

$$W_z = c_1\left(\frac{1}{x_2} - \frac{1}{x_1}\right) = c_1\left(\frac{\nu - 1}{x_1}\right), \tag{12}$$

where c_1 is a constant, the values $1/x_1$ and $1/x_2$ characterise the specific surface per unit volume of the bulk which consists of particles of hypothetically uniform size; x_1 is the starting and x_2 the final particle size, while $\nu = x_1/x_2$ is the reduction ratio.

Rittinger's law is based on the effective work required for overcoming cohesion, but it ignores the energy absorbed by elastic deformation, which is several times greater. At the same time, it correctly reflects the increase of energy required with progressive comminution.

(2) The "volume" theory suggested by Kirpichov [100] and Kick [101] postulates the equivalence of the work of fracture and the work associated with elastic stretching. Accordingly, the energy demand for a cube of 1 cm edge length is:

$$W_z = \int_0^{\lambda} \sigma \, d\lambda \quad \text{and since} \quad \lambda = \frac{\sigma}{E} \tag{13}$$

$$W_z = \frac{1}{E}\int_0^{\sigma} \sigma \, d\sigma = \frac{\sigma^2}{2E}, \tag{14}$$

where E is the elasticity modulus, σ the fracture strength, and λ the specific elongation.

For a cube of edge length x the fracture force is $P = \sigma x^2$, the total elongation $l = \lambda x$, i.e.

$$W_z = x^3 \frac{\sigma^2}{2E} = V \frac{\sigma^2}{2E}, \tag{15}$$

where V is the volume of the body to be comminuted.

The "volume" theory of comminution accounts for the work of triggering fracture, but it assumes that the energy demand is independent of the particle size attained. This is a simplification which cannot be accepted, especially in fine grinding.

(3) According to the "third" theory put forward by Bond [102, 103], the total energy that is specific to any size is inversely proportional to the square root of the particle size. If comminution proceeds from particle size x_1 to x_2, then the comminution energy is equal to the difference between the total energy required for the two particle sizes:

$$W_z = c_3 \frac{1}{\sqrt{x_2}} - \frac{1}{\sqrt{x_1}} = c_3 \frac{\sqrt{v} - 1}{\sqrt{x_1}}, \tag{16}$$

where c_3 is constant.

It is a common fault of all three theories that they do not take account of the particle size distributions of the feed and the product, nor do they take account of particle interactions and the energy consumed by plastic deformation.

(4) Some progress is made by the "fourth" theory. This was elaborated initially by Charles [105] and Holmes [106], and further developed by Svenson and Murkes [107]. This theory gives the following basic equation for calculating comminution energy:

$$W_z = c_4 \left(\frac{1}{x_2^{n_2}} - \frac{1}{x_1^{n_1}} \right), \tag{17}$$

where x_1 is the average particle size of the feed, x_2 average particle size of the end product, n_1 and n_2 are uniformity factors, and c_4 is a constant.

This formula takes particle size distribution into consideration and, in accordance with general experience, a higher free energy is attributed to a bulk material of wider scatter, i.e. to a material with a larger specific surface. Beke [108], took into account the experimental fact that energy demand is a monotonous non-linear function of specific surface and that the scatter of distribution has a similar correlation to specific surface. He attempted to formulate the energy demand by the inclusion of this scatter of distribution:

$$W_z = c \left(\frac{v_2}{x_2} - \frac{v_1}{x_1} \right), \tag{18}$$

where v is the variation factor of distribution, i.e. the relationship between scatter and the reference size:

$$v = \sqrt{\frac{2}{n}! - 2\left(\frac{1}{n}!\right) + 1}, \tag{19}$$

where n is the uniformity coefficient of RRSB distribution.

The above formula is suitable for the empirical description of the energy demand of grinding, but as with the other formulations, it is based on arbitrary assumptions.

(5) In deducing his grinding energy equation Hodakov [58] had already brought into consideration the effect of the grinding medium and the energy spent for plastic deformation and particle interaction. In his equation the effect of the medium was represented by the depth of plastic deformation (l_{plast}), the characteristics of the mill by the maximum specific surface which can be realised in the given equipment ($a_{s\max}$) and, finally, particle interaction by a factor (r) which also depends on the effect of the medium. Hodakov's deduction yielded the following formula

$$W_z = \eta\left[\frac{9be}{a}\left(\ln\frac{a_s}{a_{s0}} + \ln\frac{a_{s\max}-a_{s0}}{a_{s\max}-a_s}\right) + \right.$$

$$+\frac{(3b\beta l_{plast}+1.1el_r+r+aE_\gamma)a_{s\max}}{a}\ln\frac{a_{s\max}-a_{s0}}{a_{s\max}-a_s} +$$

$$\left.+\frac{b\beta l_{plast}^2-a_{s\max}^2}{4a}\left(\frac{a_s-a_{s0}}{a_{s\max}}-\ln\frac{a_{s\max}-a_{s0}}{a_{s\max}-a_s}\right)\right], \tag{20}$$

where W_z is the energy density required for grinding the solid body from a specific surface of a_{s0} to a_s, β the energy density of plastic deformation, e the energy density of elastic deformation, b is a shape factor of the particles ($b \approx 1$), a is the ratio of the gain in surface area due to the fracture of a single particle and the square of particle size, η the efficiency of the mill, l_r the critical crack length of the given material, and E_γ the surface free energy.

The first member of the equation stands for elastic deformation work, the second member accounts for plastic deformation work, as well as the excess work consumed by particle interaction and comminution of particles. The third member takes into consideration plastic deformation connected with the volume change of particles.

(6) For formulating a mathematical model of grinding Tkačova and Krupa [104] adapted the second order differential equation developed for describing an electric circuit consisting of a resistance, a capacitor, and an inductance. This model permitted the study of the distribution of mechanical energy for forming new surface, for particle interaction, and for internal structural and enthalpy changes. However, its main field of application is in batch grinding.

(7) Interpreting the efficiency of grinding is an intriguing problem. The Rittinger principle, which states that the only result of the process of grinding is the formation of new surface, has been criticised in several passages of this book. In Smekal's view [109] the result of comminution is the production of new surface energy and, thereby, he introduced the concept of efficiency of grinding. If the surface energy of quartz is about 1 J m^{-2} and if an industrial mill is producing from a feed of 1 Mg a product of about 0.7 m^2 g^{-1} specific BET surface by the investment of 108 J g^{-1} of energy, then the efficiency is 0.7%. A criticism of this concept was published by Beke [110]. According to him the efficiency of any energy transforming machinery is given by a fraction, the numerator of which is the utilized energy (w) and its denominator the total energy

input (W_z): $\eta' = w/W_z$. The unused energy transforms to heat (Q) and, therefore, the efficiency is:

$$\eta = \frac{W_z - Q}{W_z}. \tag{21}$$

If, as stated by Smekal, efficiency is in the order of a few tenth of a percent, then practically all the energy input should appear as heat. Studies conducted in industrial mills, however, indicate a deficit of about 10 to 20% in the energy balance [110, 111].

Schellinger [113] placed a laboratory ball mill inside a calorimeter and when the mill contained only the grinding bodies, the total energy was recovered as heat. In the presence of a feed material a deficit of about 10 to 20% was observed. He obtained the same results in large scale experiments [114]. Bessonov [115] used a calorimeter to study the energetics of polishing and established about 30% deficiency as related to the energy input. Rose [116] gave the following energy balance for grinding quartz in a vibration mill:

mechanical losses	37.2%
losses in the lining	46.8%
heating up of the feed	12.0%
phase transformations	3.7%
surface energy and experimental error	0.3%

A similar report by Hiorns [117] gives:

idle running	25–30%
generation of new surface	5–10%
friction	40–50%
other processes	15–20%

(8) A series of experiments carried out by several authors on mills placed in calorimeters indicated that approximately 25 to 30% of the energy input is "accumulated" in the feed [118–126]. The energy accumulated in the feed depends on the nature of the feed, grinding time, the intensity of energy transfer, etc. However, the results obtained in laboratory mills in batchwise operation cannot be directly transferred to continuously-operated industrial mills.

The following values of "accumulated energy" for solids and ground products have been compiled for comparison purposes.

The results are relatively consistent, considering the variety of materials investigated and the different modes of applying mechanical load, but the problem is far from being solved. We have demonstrated by an analysis of the grinding process from a mechano-chemical point of view that, under the action of mechanical energy, there is an increase of surface energy, as well as other processes, which either increase or decrease the free energy of the disperse system. It is especially important to acquire information about the energy distribution of mechano-chemical processes under various forms of

Type of process	Author	Energy (J/g)
Single particle fracture	Rumpf, Patat, Schönert, Steier [129–131, 133, 134]	8– 83
Slow grinding in a mill	Bown [112]	12– 16
Grinding in a ball mill	Schellinger (113, 114]	25–175
Polishing	Bessonov [115]	8– 12
Drilling	Sekula, Tkačova, Krupa [118–121]	250–335
Grinding in a disintegrator or in a vibration mill	Heegn, Bernhardt et al. [122–126]	21–335

mechanical load, since this is the theoretical foundation for the design and development of new efficient mechano-chemical reactors and activators.

The theoretical basis for determining the efficiency of individual milling equipment, as well as for the design of new, more efficient mills is provided by the series of experiments carried out from 1957 by the school of Rumpf and Schönert [97, 98, 127–139]. These experiments defined the minimum energy demand of grinding, independently of the actual equipment, on the basis of the principle of individual fracture ("individual comminution").

4.4. THE ROLE OF THE MEDIUM IN FINE GRINDING

The fluid medium has an important role in fine grinding and in mechanical activation. It has been proved for example, that, by adding a surfactant to the feed, the whole grinding process and thus the fineness of the product and the energy spent for grinding can be significantly influenced. The extensive literature dealing with the effects of the medium on the mechanical properties of the ground product, as well as with the mechanism of this effect, also comprises practical aspects of the problem. Here we will attempt to summarise the available information and will include results of our own.

4.4.1. THE EFFECT OF THE MEDIUM ON THE MECHANICAL PROPERTIES OF SOLID BODIES

The basic fact that the mechanical properties of a solid body are significantly influenced by the physical and chemical effects of the surrounding medium was recognised by Rehbinder [140]. The application of surfactants in the drilling of hard rocks, in the comminution of ores prior to flotation, in coal crushing, and in the fine grinding of cement clinker and other materials of the silicate industry etc. owe much to this pioneering discovery.

According to Rehbinder the adsorption of alien molecules results in a decrease of the surface energy of solid bodies whereby their strength and resistance to mechanical

effects decrease. This phenomenon was discovered by him in 1928 and was later introduced into the literature as the Rehbinder effect or as "adsorptive decrease of strength".

If there is fracture without macroscopic deformation then the strength of the body (σ) is, according to Griffith, approximately proportional to the square root of the work spent for the formation of new surface: $\sigma \approx W_z^{1/2}$. With brittle materials the factor W_z is determined by the value of surface free energy and, therefore, it is approximately $\sigma \simeq E_\gamma^{1/2}$. If significant plastic deformation occurs during fracture then the work expended in the formation of new surface is not proportional to the change of surface free energy, but there is still a correlation between the two values. Therefore, if the surface energy (E_γ) is changed this is associated with a change of W_z in the same direction. The role of the medium is important because, due to adsorption from the medium, E_γ is changed and, thereby, the correlation of W_z and E_γ is subject to the individual properties of both the adsorbent and the adsorbed medium. With positive adsorption, the value of E_γ always decreases and the strength and surface-forming work also decreases when fracture is connected with adsorption.

According to Rehbinder the fracture of a material is preceded by the appearance of wedge shaped cracks, which, being unstable, may close again under the effect of external forces ("self-healing"). Additional cracks are formed at certain points of the body under the action of mechanical forces that exceed the internal stress and a "prefracture zone" comes into being extending from the surface to a certain depth. Molecules and ions of the surfactant intrude into the microcracks and become adsorbed into their surface whereby they decrease surface tension and inhibit the "self-healing" of microcracks. The extremely thin liquid films at the surfaces of microcracks become spontaneously thicker, depending on the decrease of surface free energy and, in this way exert a "wedging pressure" which promotes the propagation of cracks and reduces the resistance to fracture.

The concept of the Rehbinder effect comprises the whole complex of phenomena promoting deformation and fracture. The essential feature of the Rehbinder effect is that, because of the reversible interaction of the solid body with the medium, less work is required for the generation of new surface.

The effects of the medium on the mechanical properties of solids were studied by Rehbinder, Shchukin and others [140–151]. They established that for any type of material (amorphous or crystalline, porous or compact, having metallic, ionic, covalent or molecular bonds) there is a medium which significantly decreases its surface free energy in the course of fracture and, thereby, reduces the strength of the solid body. By using a developed version of Rehbinder's theory it was substantiated in a quantitative way, that the medium also influences the limiting deformation preceding fracture. Furthermore, the medium promotes the formation, migration and coalescence of dislocations, and the formation of cracks [150, 151]. These workers pointed out that the hardness of several materials depended on the medium in which the test was carried out. Thus, no change of hardness could be observed with any material in dry air or in hydrocarbons but the hardness of minerals dropped by 20 to 30%, as compared with the value measured in air, when they were moistened with water. The effect of aqueous solutions of electrolytes is even more pronounced and they are most effective at low concentration (up to 0.25%). The strength of quartzite,

for example, may be reduced by 50 to 60% when treated with the solution of salts of multivalent cations ($TiCl_4$, $FeCl_3$, $AlCl_3$) or of sodium silicate. The strength of calcite is most affected by sodium silicate, sodium fluoride and sodium hydroxide; the strength of pyrite by $FeCl_3$. The strength of brittle materials can be highly influenced by organic surfactants such as long chain fatty acids and alcohols, as well as by ionic surfactants (soaps). The hardness of quartz or calcite can be reduced by 40 to 60% by adding organic surfactants.

Obreimoff [152] studied the effect of the medium on the cleavage of mica plates and he was the first to measure directly the surface energy of a solid body. He placed a wedge into a crack in the plate and cleaved the plate gradually by moving the wedge. The force required for the penetration of the wedge was determined by measuring the inflection of the plate. By knowing the work expended during cleavage the surface energy of mica was calculated by dividing the former with the surface area. He established that the cleavage of mica in vacuum was a reversible process, i.e. after removing the wedge the crack closed and repeated cleavage required the same amount of work as the first operation. In contrast, cleavage in air is easier than in vacuum and becomes irreversible, probably due to adsorption of air and water vapour on the fresh surface. Studies by Rehbinder and his co-workers revealed that the force necessary to cleave mica was reduced in water by 18%, in solutions containing aniline, sodium oleate, or isoamyl alcohol by 30 to 40%. A similar effect was experienced when thin plates of mica were subjected to tension in a direction perpendicular to the cleavage planes. In toluene and in solutions in toluene there were no changes in the tensile strength, while in aqueous solutions of surfactants the tensile strength decreased dramatically.

The decrease of surface energy caused by physical adsorption can be calculated using Gibbs' adsorption equation. These calculations were performed for the adsorption of organic vapours and water vapour on quartz and on barite [153]; for the adsorption of water vapour on α- and γ-Al_2O_3 [154]; and for the adsorption of cyclohexane on cement clinker [155]. Values in excess of 0.25 J/m^2 were obtained and a loss of strength of 15 to 20% could be calculated [156]. The calculated values closely approximated the bending strength of glass in vapours of various liquids [157] and that of α- and γ-Al_2O_3 in water vapour [154].

At the same time it was found that the loss of strength (hardness) caused by the medium also depended on the kind of mechanical action, its intensity, and its velocity. Thus, for short loading times (1 to 2 s) the results were not reproducible, and at even shorter loading times the effect of the medium on the microhardness of solids could not be detected [158–160]. However, Westwood [161, 162] later demonstrated that even at very short loading times (< 100 μs) there was a measurable effect of the medium on the microhardness of solids.

In the early 1950's a great controversy took place concerning not only the mechanism of the Rehbinder effect but also about its very existence [163–165]. Some authors questioned its significance in comminution techniques, pointing out that loading times in industrial mills were quite short (<0.1 s) and that there was a significant difference between the propagation velocity of fracture cracks and the spreading velocity of surfactants [155, 166–171]. According to some authors all liquids propagate along the surface of solid bodies with approximately the same velocity,

partly by pure surface migration and partly indirectly through the vapour space. The upper limit of propagation velocity is 10^2 m s^{-1}. At the same time, fracture triggered by impact or collision in brittle bodies propagates with a velocity corresponding to the transverse propagation velocity of sound, e.g. more than 10^3 m s^{-1} for quartz. Under such conditions the surfactant solution is unable to follow the crack front and, therefore, cannot affect the process of cracking [170, 172, 173].

The controversy about the Rehbinder effect, and studies in his own laboratory, were summarised in a review by Westwood et al. in 1981 [162]. In this review he confirmed the existence and the technological importance of the Rehbinder effect and showed that the properties of a solid can be modified by the application of surfactants. At the same time he revised concepts put forward earlier about its mechanism and, by adapting the dislocation theory, he proposed an advanced explanation of the effect.

Rehbinder's concept about the reduction of surface energy of a solid body and the consequent decrease of fracture energy is now untenable, since we know that fracture energy is primarily determined by plastic deformation at the crack front and that stresses arising on fracture surfaces can only marginally, if at all, influence the propagation of cracks.

The "chemo-mechanical effects" proposed by Westwood can be summed up as follows [162]:

—the medium (surfactant) may, in certain types of crystals, influence the mobility of dislocations in layers near the surface and, therefore, may modify hardness;
—the medium (surfactant) can influence the mechanical behaviour of the solid body by interacting with electric charges on the surface; this can be followed by changes in the zeta potential.

Experiments carried out by Gilman and Johnston [174, 175] indicated that adsorbed surfactants affect the behaviour and mobility of dislocations near the surface. Experiments with crystals of MgO and CaF_2 by Westwood [176, 177] demonstrated unambiguously that the mobility of individual dislocations depends on adsorption. He also noted that cracks, which he made visible by etching, propagated faster in moist air and water than in dry toluene; furthermore the velocity of crack propagation increased further as a consequence of adsorption of surfactant from an aqueous solution.

The existence of a potential barrier associated with the formation and growth of a new surface has been proved repeatedly. This barrier influences plastic deformation and, under certain circumstances, retards the migration of dislocations in layers near the surface [144, 178–180]. A direct study of dislocations shows that the medium promotes the migration of dislocations near the surface [181–183].

Jushchenko et al. [150, 151] studied the medium-dependent mechanical behaviour of materials at atomic dimensions by simulating the deformation and fracture of crystals by the methods of molecular dynamics (MD). According to this model, at a defined initial temperature the atoms are arranged within a "box" in a regular hexagonal lattice (Fig. 4.21(a)). Opposite walls of the "box" can be pulled apart resulting in a deformation of a certain velocity. The computer program for the treatment of this model contains coordinates and moments for the atoms at different moments of time.

It also involves the sum of the potential and kinetic energies of the system and the forces exerted by the "walls". The results of the calculations indicated that atoms regarded as active—from the point of view of adsorption—often produce brittle cracking. Atoms in the environment, apart from interacting with the walls of the cracks, may also produce such forces; these forces are compatible with interatomic bonding forces and promote the further propagation of cracks.

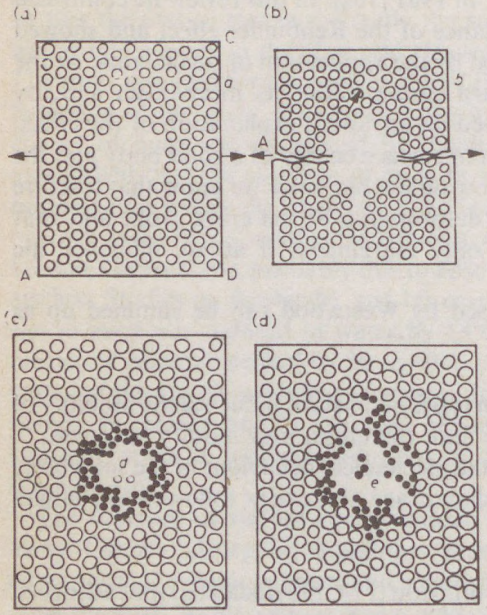

Fig. 4.21. (a) Initial state of the model *(a)*. (b) Propagation of a brittle crack *(b)* with deformation at low temperature; formation of a dislocation *(c)* with deformation at high temperature [150]. (c) Adsorption of an alien atom (medium) at the wall of the "cavity" (*d*—initial state). (d) Formation of a crack during the penetration of alien atoms (medium) into the stressed (deformed) system *(e)* [151]

Recently El-Shall and Somasundaran [184] reviewed the physico-chemical aspects of grinding and the effect of chemical additives in grinding, especially wet grinding. In their view, additives affect grinding in a complex way and they stated that the "influence on the strength of the material is due to: (1) the effect on crack initiation and crack extension energy, and (2) the retardation of the rejoining or the sealing of freshly created cracks". According to Westwood: "Indeed the potential economic and energy-conserving benefits of utilizing Rehbinder-chemo-mechanical effects in the machining, drilling, comminuting, and surface finishing of hard solids would appear to justify a substantially greater level of research and development effort in this than now exists" [162].

4.4.2. EFFECT OF MEDIUM ON GRINDING

The effect that the medium exerts on the mechanical properties of solids can be exploited in practical comminution, dispersion, cutting and finishing processes. Materials used to promote grinding are called grinding aids.

Surfactants are the reagents most often used as grinding aids, i.e. those materials which, by being adsorbed onto the surface of the solid to be ground, modify its surface energy. Other materials such as carbon powder, graphite, etc. were previously used to promote grinding. These materials are no longer used and the term grinding aid is nowadays used as an equivalent for surfactant.

Lubman [185] studied the effect of sodium oleate, alizarin red and other additives on the grinding of ores in a ball mill and he recognised, as early as 1936, that in the presence of some additives the yield of the fine fraction increased by 15 to 18%. Mechanical dispersion of corundum is 15 to 20% more efficient in the presence of a surfactant [186]. A similar increase of grindability was observed when quartz, magnesite, or dolomite was ground in a ball mill in the presence of a surfactant [187, 188].

Rehbinder et al. [142] added 0.01 to 0.1% of different electrolytes to the flushing water used for deep drilling of hard rocks (quartzite, granite, limestone) and they increased the drilling velocity by between 20 and 60%. In studying the basic problems of wet grinding Szánthó [189] also established that certain additives (e.g. "Flotigan") substantially decreased the energy demand of grinding.

When a soap solution or sodium oleate was added in the grinding of an apatite–nepheline rock the yield of the fraction finer than 0.11 mm increased by 4 to 10% compared with grinding in pure water [190].

Without giving numerical values Alberti [191] patented the use of dispersion aids in the grinding of ores.

Shepherd [192] corroborated the findings of Rehbinder and studied the effect of conditioning time on the strength of rocks.

In order to reproduce the results of Rehbinder, Frangiskos and Smith [193] ground limestone in a laboratory drop mill in solutions of NaOH and Na_2CO_3, in the same way, ground quartz in aqueous solutions of $AlCl_3$ and $CuSO_4$ and in the presence of silicones and methanol. Water, by itself, was already effective, and when surfactants were applied at optimum concentrations the specific surface of limestone was increased by 40% and that of quartz by 20%. With methanol and silicones the increase amounted to 50%.

Siebel and Zeisel [194] obtained a patent for the application of additives to facilitate the size reduction of ores and coal. Thus, the addition of 0.01 to 0.04% of Calgon enhanced the efficiency of comminution by 30%.

Shosh et al. found [195] that the addition of NaOH and Na_2CO_3 increased the grinding rate and the specific surface during the wet grinding of limestone.

On the other hand, Gilbert and Hughes [196] failed to record a positive effect with silicones as additives in the wet grinding of quartz and calcite in a Hardgrove mill. Moreover, the addition of some surfactants when wet-grinding quartz and limestone in a ball or rod mill has a negative effect. On this basis the authors stated that, in ball and roller mills used in industrial practice, the addition of surfactants either reduced the efficiency of grinding or had no effect on the process.

At the same time several reports stated that grinding in the presence of organic and inorganic additives was more efficient than dry grinding or grinding with water alone [184, 197–200].

Engelhardt [197, 198] established that grinding quartz in alcohol required less

energy for the production of the same specific surface than grinding in water. In another study Lin and Metzmayer [199] ground quartz in various media and found that grinding rate could be increased by as much as 25% in carbon tetrachloride and in methylcyclohexane, as compared with the values obtained in nitrogen. Malati et al. [200], and El-Shall and Somsundaran [184] independently found that a finer product was obtained by wet grinding hematite when oleic acid was added. Recently El-Shall and his co-workers reported that grinding quartz in a ball mill made of stainless steel gave a finer product in neutral or alkaline media when dodecyl ammonium chloride was added. The authors correlated their result with the effect of amine on the surface properties of quartz (zeta potential, flocculation characteristics) under simulated chemical conditions. Since wet grinding is not a subject of this book we restrict ourselves to some observations concerning the effect of chemical additives in wet grinding.

Smekal pointed out in 1937 that the surface energy of solids could also be reduced by the adsorption of gases [201]. Dry grinding in the presence of gases and vapours was studied in detail by Götte and his co-workers [202–206].

Ziegler was the first [202] to experiment with dry grinding in the presence of vapour phase additives. Cement clinker, two kinds of glass, marble, and quartz were used as feed, while benzene, carbon tetrachloride, hexane, and petroleum ether were used as apolar additives, and nitromethane, acetone, and ethyl formate as polar additives. It was found that, compared with dry air, the grindability of cement clinker was improved by the vapours of polar liquids, while the beneficial effect of apolar additives was less marked. The change in the grindability of marble was identical to that of clinker; quartz behaved similarly, but the effect was smaller. Apolar additives improved the grindability of glass, while polar additives had the opposite effect. It is an important feature, in practice, that the grindability of cement clinker is enhanced by saturated water vapour.

With similar materials Eichborn obtained similar results [207].

Götte and Ziegler [202, 203, 205, 206] explained the improvement of grindability in the vapours of polar liquids by the Rehbinder effect.

According to Eichborn [207, 208], and Engelhardt and Haussühl [209], adsorption of surfactant molecules onto the surfaces of rigid solids may reduce their resistance towards comminution.

Götte and Scherrer [204] observed that some of the additives used by Ziegler not only improved grindability but also inhibited particle interactions.

Wagener [67] studied the effect of vapour phase additives and radioactive radiation on the grinding of glass, quartz, and limestone in a laboratory vibration mill. Polar liquids such as water, acetone, 1,2-dichloroethane, and apolar liquids, such as carbon tetrachloride and benzene, were used as additives. By examining the particle structure of the material sticking to the lining and to the grinding bodies and that material which freely moved in the mill, they found that additives improved grindability and also diminished adhesion and aggregation of particles.

The application of grinding aids with surface active properties is especially extensive in the cement industry. The first patent on this subject was filed in England in 1930 [210] and covered the use of a solid resin. The first liquid additive to be used as a grinding aid was TDA, a mixture of triethanol amine and water-soluble calcium salts

of lignine sulphonic acids. This was patented in 1935 in the United States [211]. The output of an industrial cement mill is enhanced by 30 to 50% [211–213] by adding TDA; this simultaneously increases the strength and the storage time.

A small amount of water, lignine solution, and colloidal carbon added to a cement mill partly suppresses the tendency of the product to stick to the grinding bodies and thereby improves the specific surface of the grind [214]. Also by adding colloidal carbon the time required to reach the same fineness was reduced by 30% in a laboratory mill [215]. Higerovits and his co-workers improved the output of a cement mill by 15% by adding 0.3 to 0.5% of naphthene soap [216]. Other authors obtained similar effects by applying sulphite waste liquor [217], a by-product of sunflower oil manufacturing [218, 219], and lignin [220].

Mardulier [221–223] reported a positive effect from the use of some types of lignine. In addition, HEA–2, an aqueous solution of acetylated ethanolamine improved the grinding of cement clinker. The author explained the effect by the improvement in the flow characteristics of the ground product giving a shorter residence time of the product in the mill. Mardulier pointed out that grinding aids can be successfully applied in open mills and also in closed circuit mills. In the latter instance the additive improves the functioning of the classifier and the product recycled from the classifier contains less fines.

Rojak and Pirockij [224–226] reported that triethanolamine and a 1 : 1 mixture with sulphite waste liquor was a most effective additive in the grinding of cement clinker. By spraying an aqueous solution of triethanolamine into the first chamber of an industrial cement mill the output of that mill was raised by 17 to 20%.

Grachian and Doviborova [227, 228] found that the adsorption ability of aliphatic fatty acids on the surface of cement clinker and clinker minerals increased with decreasing chain length and that their effectiveness as grinding aids increased concurrently. A by-product obtained during the manufacture of sunflower oil is an effective grinding aid in the comminution of white cement clinker. Industrial studies revealed that mill output was increased by 30% and the whiteness of the product was improved by 6% when this surfactant was used.

Grzymek et al. [229, 230] report a significant improvement in the grinding of cement clinker when oleic acid, triethanolamine, naphthene-sulphonic acid, sulphite waste liquor, and water were used as grinding aids.

Ghigi and Rabbottino [231] reported the positive effect of sodium stearate on the grinding of cement clinker in a laboratory rod mill and attributed this to less resistance to comminution of the feed and to reduced adhesion of the particles of the ground product. The effect depended on the rotational speed of the mill and the diameter of the rods. Thus on increasing rotational speed the effect first increased and then decreased. Smaller diameter rods always produced a smaller effect.

When investigating the mechanism of action of grinding aids Ghigi found [232] that a correctly selected additive reduced the resistance of clinker fracture and their effect was rather of a physical than of a chemical nature.

Iwabuchi and his group [233–240] studied in detail the effect of various additives on the grindability of cement clinker, limestone, blast furnace slag, etc. Among other effects they found that the use of diethylene glycol increased mill output by about 20% when portland cement was ground to produce a fineness (a_s) of 0.32 to 0.35 $m^2\ g^{-1}$.

An improvement of 10% was obtained for a mixture of blast furnace slag and portland cement containing 40% granulated slag and having a fineness of about 0.4 $m^2 g^{-1}$. Interesting results were obtained in grinding experiments with mixtures of clinker and various modifications of gypsum (dihydrate, α- and β-hemihydrate): in addition as blast furnace slag was ground after rapid or slow cooling. In Iwabuchi's view, grinding aids inhibit, or at least retard, the formation of crusts both on the grinding bodies and on the lining of the mill; furthermore, they retard the development of aggregation. He assumed that certain grinding aids (e.g. low melting point organic compounds) inhibit the self-sealing of cracks by the adsorption of the aids onto the surfaces of particles and by penetration into microcracks.

According to data published by Schneider [168] in the Federal Republic of Germany in 1969, 10% of cement was manufactured using grinding aids, especially ethanolamines and glycols.

The best results were achieved by spraying the grinding aid directly into the fine-grinding chamber of the mill. With portland cement, of grade 375, the mill output increased by 10 to 30% and, for grade 475 portland cement, the gain was as high as 25 to 50%. At the same time, fluidity increased and the residence time in the mill dropped. The sharpness of classification improved under the effect of surfactants and pneumatic conveying, and the emptying of silos and containers became easier.

Seebach [155] compared the grinding of defined fractions of cement clinker (1.25 to 1.41 mm and 0.125 to 0.16 mm) in a laboratory ball mill in an atmosphere saturated with the vapours of cyclohexane, ethylene glycol, and butylamine. He also compared the results obtained by grinding in air and in vacuum at temperatures between 293 K and 393 K. He concluded that the vapours of organic compounds exerted no significant effect on the energy demand of fracture and grinding. This conclusion implies that the nature of the medium and kind of surfactants have no effect on the strength and fracture of cement clinker in a ball mill.

Schneider [168] and Seebach [155] explained the positive effect of grinding aids in the grinding of cement clinker by their effect in diminishing the adhesion forces between particles and the increasing fluidity of the ground product. On the other hand, Edelyman and Sominskij [241] pointed out that the effect of surfactants in the grinding of cement clinker in a vibration mill cannot be restricted to the above features since it also involves a "decrease of strength by adsorption" and an increase of brittleness.

According to Blanks and Kennedy [242] surfactants facilitate the operation of a mill even in that period in which adherence is not yet a problem but, in this case, the effect is small.

Scheibe and his co-workers [243, 244] concluded that the effect of grinding aids can first be traced to the counteraction of adherence and aggregation. The control of adhesion forces is invariably connected with increased fluidity which, among other things, cuts down residence time in the mill and may result in modifying the movement of the charge in the mill.

Hodakov and Kudrjavceva observed that significant assistance was provided during grinding of cement clinker and other materials in a vibration mill by the use of acetone, oleic acid, alcohol, and triethylamine. The authors attributed this to the dual effect of the additive (Rehbinder effect and inhibited aggregation). They also surveyed the applicability of various methods for determining the degree of dispersion, sieve

analysis, sedimentation and the measurement of specific surface for grinding containing surfactants. It was found that specific surface values obtained by sorption methods provided the best approximation to the theoretical values [58, 245].

Zadák et al. [246, 247] found that the addition of 0.01 to 0.05% of liquid silicones improved the grindability of clinker by 10 to 20%. Melnik and his co-workers [248] also reported that silicone-based additives could be used to improve the grinding process.

The application of a grinding aid (HEA–2) in a mill of large diameter (∅ 3.71 m) has been discussed by Quella et al. [249].

Tanaka [250] studied the role of additives in the fine grinding of limestone in a laboratory mill. A positive effect was only recorded for calcium stearate and Vinsol. These results, and some calculations, prompted Tanaka to say that one of the conditions for an effective grinding aid was that it should have a relatively low melting point since liquids can readily form a monomolecular adsorption layer on the surface of particles.

Krichtin and Nudely [251, 252] investigated the effect of surfactants in the dry grinding of the raw materials of the cement industry and found a 15 to 25% increase of mill output and, because of the higher fluidity of the raw feed, it could be more easily homogenised. If added in a proper way, surfactants can also be applied at higher temperatures (573–973 K) (drying–grinding).

Similar surfactants (glycols and amines) have been tested in the grinding of limestone [253–256]. Limestone is softer and more easy to grind than cement and the main effect was a reduction of particle interaction and aggregation.

The effect of a small amount of water in the grinding of silicates, especially of cement clinker, deserves to be mentioned. The effect of water is important partly because surfactants are usually added as aqueous solutions, and partly because the feed is rarely completely dry. It has been observed repeatedly that up to 1% of water has a beneficial effect on grinding. It improves the grindability of brittle materials and, therefore, acts as a grinding aid [202, 203, 229, 231, 257–259]. In addition, if a surfactant is added in the form of an aqueous solution of appropriate concentration, its effect is much enhanced, especially in the coarse range of grinding. A small amount of water acts as a surfactant also in the grinding of asbestos in an edge mill [267].

Water is used as a coolant and to improve the efficiency of electrostatic filters. In such cases water is sprayed directly into the fine-grinding chamber of the mill.

Recently a number of publications have reported positive results achieved by the addition of various chemicals both in dry and wet grinding. For example, in this respect the grinding of gypsum [268], magnesite and chromite [269], additives used in glass industry [270], feldspar [271] Si_3N_4 [272], mullite and corundum [273], quartz, obsidian, andesite, and granite [274], aluminium powder [275], sericite powder [276], quartz, calcite, talc, and wollastonite [277], α-Fe_2O_3 [278].

The review by El-Shall and Somasundaran [184] published in 1985 is important both from the theoretical and the practical points of view.

The important role of chemical additives in grinding is also supported by several patent applications [191, 192, 194, 210, 211, 260–266].

4.4.3. MECHANISM OF ACTION OF GRINDING AIDS

Despite some contradictions in the literature (which may be attributed to differences in the reagents used, their mode of application, the quantity added, the fineness of the product, etc.) the preceeding sections have revealed, unambiguously, that the process of grinding and its efficiency can be much influenced by the use of grinding aids.

The application of grinding aids may offer the following advantages:

—increased output of the mill for a specified energy input;
—preparation of a finer product with unchanged output and the same energy consumption of the mill;
—in closed circuit mills—apart from the above mentioned advantages—an improvement of classification and selectivity [279–282].

Examples from the laboratories of the authors will be presented below showing the application of grinding aids in various types of mills. Triethanolamine (TEA) and MAVEKLIN [270] were used as grinding aids with approximately the same results.

In Table 4.4 data for industrial cement mills (experiments 1–7), and those for grinding limestone (experiment 8) and burnt lime (experiment 9) in pilot plant mills were compiled in order to exemplify the above effects. Thus in experiment 1 a significant increase of fineness was achieved at a constant mill output, while in experiment 2 fineness was kept constant and output was increased by 25%. In experiment 3 both fineness and output increased. Experiments 4–7 refer to grinding of cement in closed circuit mills: an improvement of classification was attained—as expressed by a smaller recycling factor (τ_0). A smaller amount of recycled material permitted a significant saving in electric energy consumption. By applying surfactants it was also possible to increase the fineness of the product in closed circuit grinding (experiments 4 and 6). With the grinding of limestone (experiment 8) the addition of a surfactant resulted in a significantly increased output of the classifier, a decrease of recycling factor (τ_0) and, to a lesser extent, an increase of fineness. When grinding burnt lime the aim was to produce much increased fineness and an improvement in classification.

The optimum dosage of grinding aid is of prime importance and this has to be adjusted to match the required fineness, the molecular dimensions of the surfactant, and its surface requirement. Overdosage of the surfactant may lead to dust formation, and a cancellation of the effect or even to the production of a negative effect.

Surfactants interfere with the process of grinding in a complex way as the following examples illustrate.

The grinding of cement clinker in a ball mill is usually accompanied by adhesion of particles to the lining and to the grinding bodies and this effect can be eliminated by the addition of a surfactant (Fig. 4.22).

Figures 4.23 and 4.24 illustrate the correlation of grinding time with "external" and "total" specific surface area, respectively, in the grinding of cement clinker of varied composition (C_1, C_2) and β-dicalcium silicate in a laboratory ball mill—both in the presence and in the absence of a surfactant. It is apparent that when a surfactant is added both "external" and "total" specific surfaces are increased (at identical grinding

Table 4.4. Effects of the application of grinding aid in large-scale grinding [282]

No. of experiment	Machinery	Feed	Grinding fineness				Output [Mg h^{-1}]		Result
			$R_{0.09}$ [%]		a_s [m^2 g^{-1}]				
			Without grinding aid	With grinding aid	Without grinding aid	With grinding aid	Without grinding aid	With grinding aid	
1	Open-circuit ind. mill (∅ 1.5 × 11 m)	Cement	9.4	4.8	0.23	0.25	7.5	7.6	Increased fineness
2	Open-circuit ind. mill (∅ 2.0 × 13 m)	Cement	12.0	12.2	0.18	0.19	14.8	19.6	~25% increase of output
3	Open-circuit ind. mill (∅ 2.0 × 13 m)	Cement	12.0	5.5	0.18	0.24	14.8	17.2	Increased fineness and ~16% increase of output
4	Closed-circuit ind. mill (∅ 3.0 × 12 m)	Cement	0.5	0.45	0.40	0.47	22.0	22.0	Increased fineness
5	Closed-circuit ind. mill (∅ 3.0 × 12 m)	Cement	0.5	0.60	0.40	0.40	22.0	27.0	~23% increase of output
6	Closed-circuit ind. mill (∅ 3.0 × 12 m)	Cement	2.7	1.00	0.27	0.32	40.0	40.0	Increased fineness
7	Closed-circuit ind. mill (∅ 3.0 × 12 m)	Cement	2.7	2.40	0.27	0.27	40.0	47.0	~17% increase of output
8	Closed-circuit air-swept pilot plant mill (∅ 1.2 × 2.2 m)	Limestone	19.2	16.1	0.38	0.39	66%	83%	~17% increase of output
9	Closed-circuit pilot plant mill (∅ 0.86 × 1.54 m)	Lime	29.6	5.9	0.46	0.52	0.3	0.3	Increased fineness

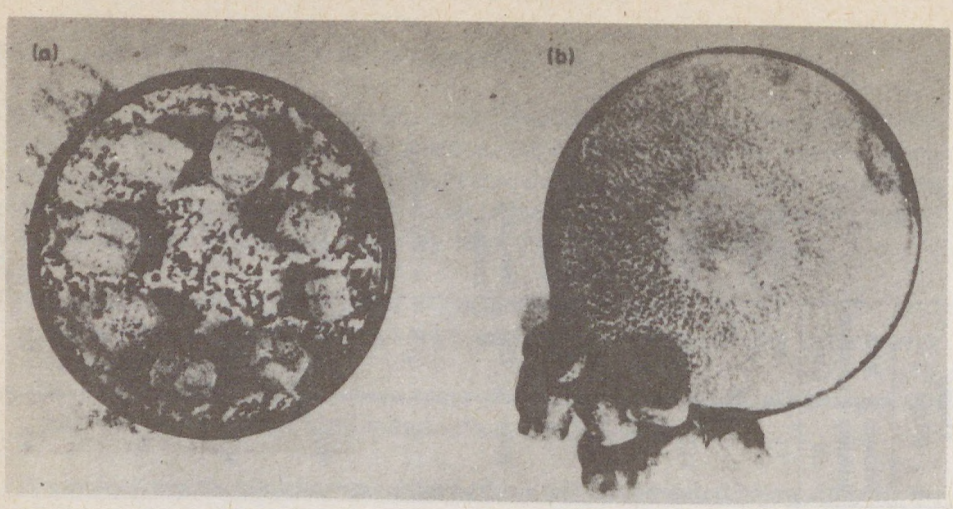

Fig. 4.22. Adhesion in a laboratory mill (a) in the absence and (b) in the presence of a surfactant [282]

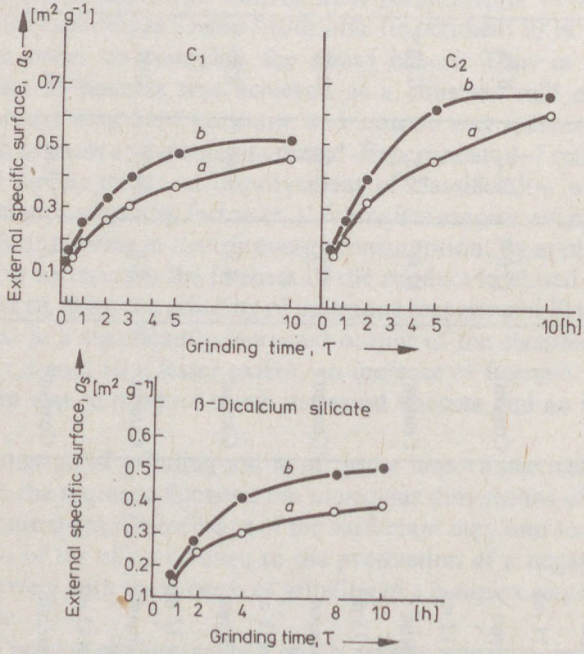

Fig. 4.23. Change of the "external" specific surface (a_s) as a function of grinding time: *a*—in the absence and *b*—in the presence of a surfactant [282]

time) and—in the fineness range covered—the "total" specific surface increased continuously with grinding time.

The $R(x)$ and $R(\tau)$ curves, and the change of fineness number ($\bar{x}$) and uniformity factor (n) with time, shown in Figs 4.25–4.27 indicate that surfactants retard aggregation and, in this way, a finer and more uniform product could be attained under identical conditions of grinding.

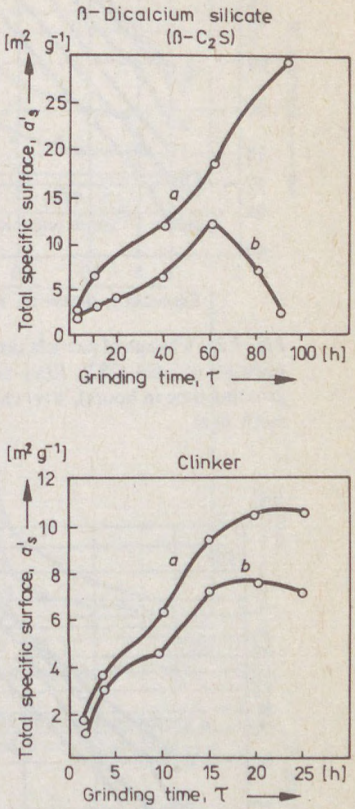

Fig. 4.24. Change of the "total" specific surface (a'_s) as a function of grinding time: *a*—in the absence and *b*—in the presence of a surfactant [282]

The advantageous effect of surfactants is also shown by an increase of grinding rate $\dot{D}_\tau(x)$ (Fig. 4.28). It is remarkable that this increase is already quite significant after short grinding times (0.5 to 1.0 hours) and with relatively coarse particles.

We extended our studies on the effect of surfactants to the range of mechano-chemical changes.

Quantitative evaluation of X-ray diffractograms of β-dicalcium silicate ground in the presence of a surfactant are presented in Fig. 4.29 and reveal unambiguously that amorphisation of β-dicalcium silicate was promoted by the surfactant.

Before explaining the effect of surfactants it has to be mentioned that there are some processes associated with fine-grinding which result in a decrease in the free energy of the system. The simplest process is the spontaneous re-ordering, after the termination

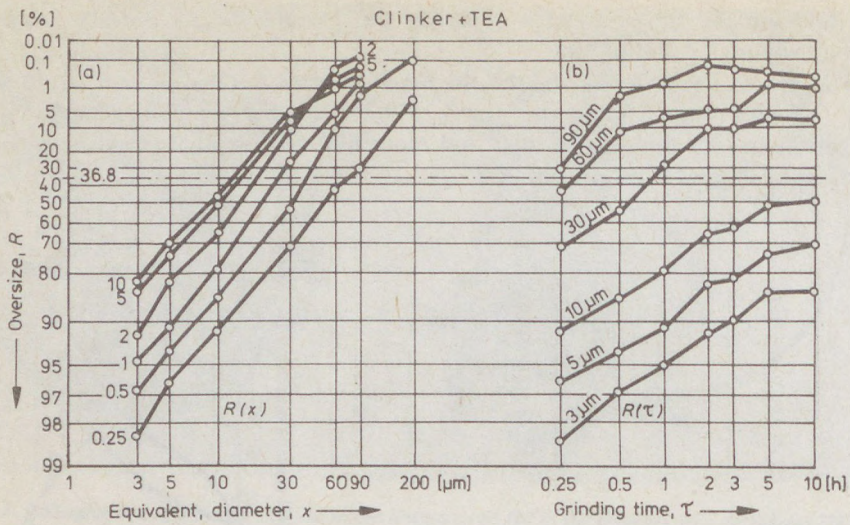

Fig. 4.25. Change of particle size distribution as a function of grinding time for clinker in the presence of TEA [282]. $R(x)$ change of oversize as a function of particle size (parameter: grinding time in hours), $R(\tau)$ change of oversize as a function of grinding time (parameter: mesh size)

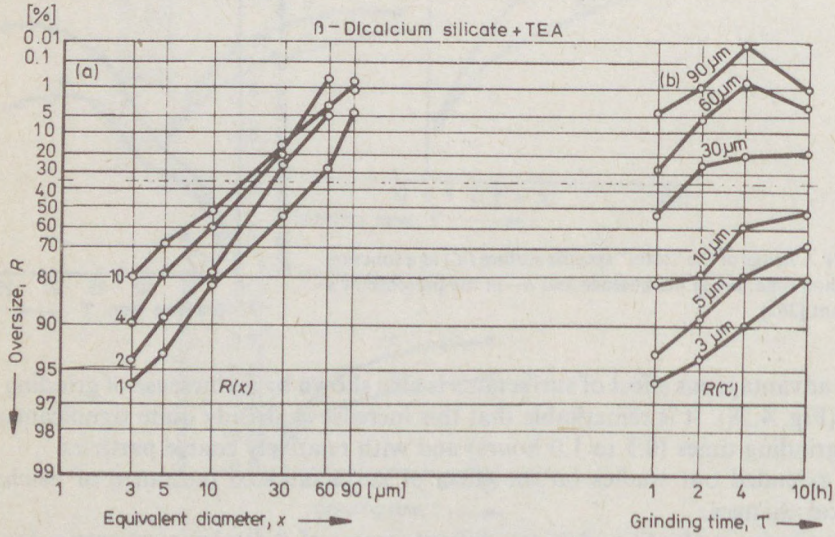

Fig. 4.26. Change of particle size distribution as a function of grinding time for β-dicalcium silicate in the presence of TEA (notations as for Fig. 4.25) [282]

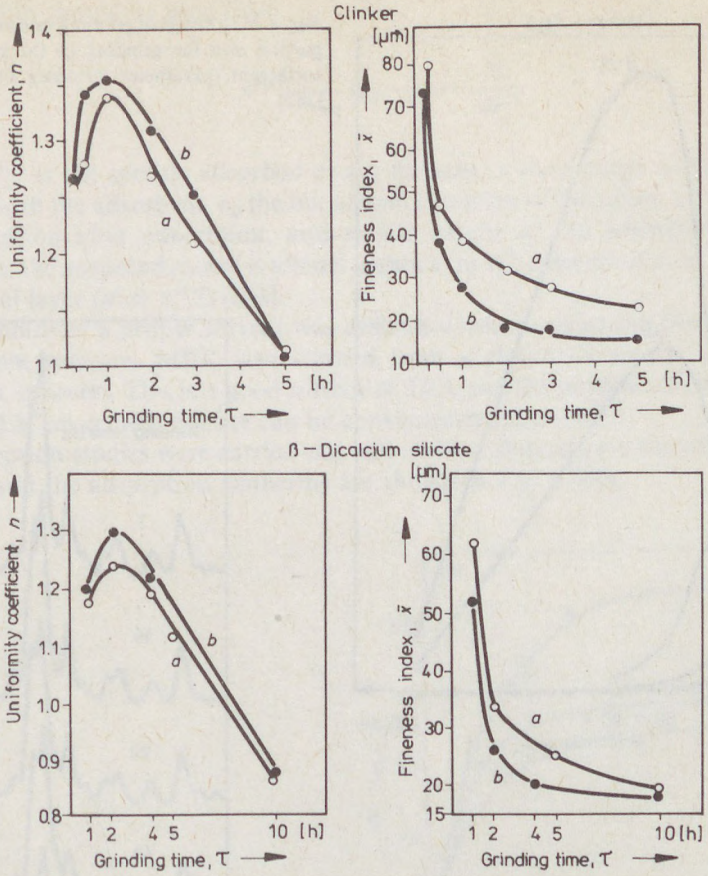

Fig. 4.27. Change in the uniformity coefficient (n) and the fineness number ($\bar{x}$) as a function of grinding time [282]: *a*—in the presence, and *b*—in the absence of a surfactant

of mechanical action, of crystal structures that have been perturbed by fine grinding. This re-ordering (which takes place mainly after the appearance of agglomeration) is often observed with the grinding of silicates. Re-ordering is, however, never complete and, therefore, disorders that remain after each cycle accumulate and the crystal structure of the solid undergoes gradual amorphisation. Re-ordering, in other words, retards amorphisation.

Triethanolamine is often used as a grinding aid in the cement industry. In order to rationalise the beneficial effect of the triethanolamine it is necessary to study the interfacial interaction of cement clinker with the reagent. The enthalpy of adsorption was determined with a microcalorimeter applying flow techniques; comparative studies were also undertaken with β-dicalcium silicate and calcite [283].

The Gibbs surface excess should be given in order to characterise adsorption taking place at the solid/liquid interface. For adsorption from solution the following

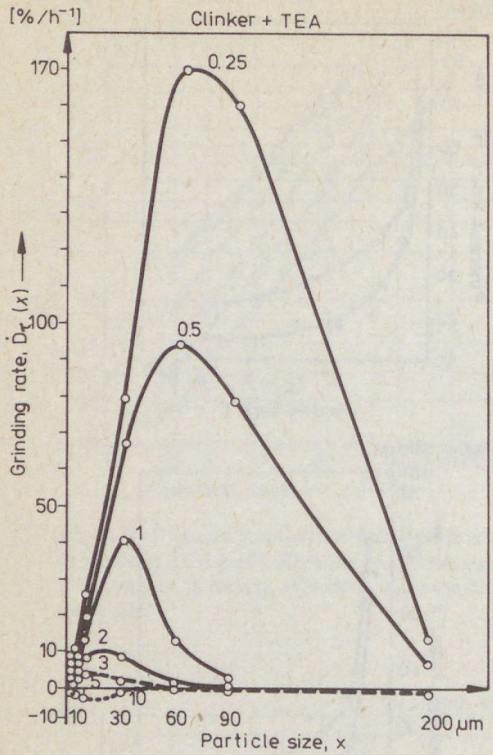

Fig. 4.28. Change of grinding rate as a function of particle size for grinding in the presence of a surfactant (parameter: grinding time in hours) [282]

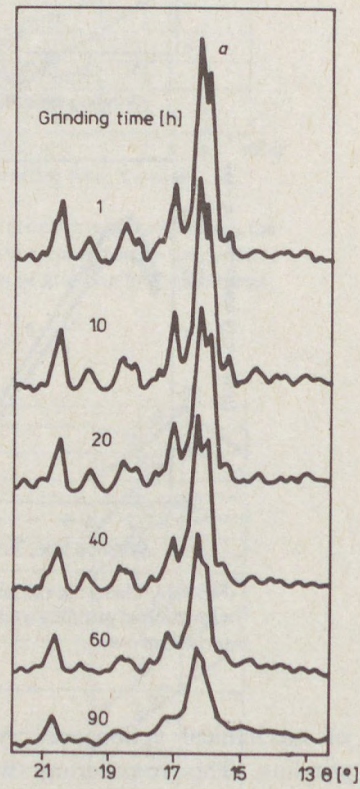

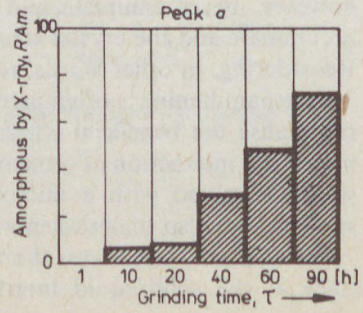

Fig. 4.29. Change of crystal structure of βC_2S during grinding in the presence of a surfactant (TEA) [282]

relationship should be used [284]

$$n^{\sigma(v)} = \frac{v}{m}(c_0 - c) = \frac{v\Delta c}{m}, \tag{22}$$

where $n^{\sigma(v)}$ is the specific adsorbed excess amount, v the volume of the solution in contact with the adsorbent, c_0 the initial concentration of the solute, c its equilibrium concentration after adsorption, and m the weight of the adsorbent. For dilute solutions, the adsorbed excess is almost identical to the amount of material (n^s) in the interfacial layer ($n^s \simeq n^{\sigma(v)}$) [284].

The choice of a proper solvent was difficult when investigating the adsorption of TEA from solution. MEK was selected from a choice of several polar solvents (alcohols, ketones). This is a good solvent of TEA and the positive adsorption of TEA from MEK on cement clinker can be conveniently measured.

Adsorption studies were carried out with calcite, β-dicalcium silicate, and cement clinker and the adsorption isotherms are shown in Fig. 4.30(a).

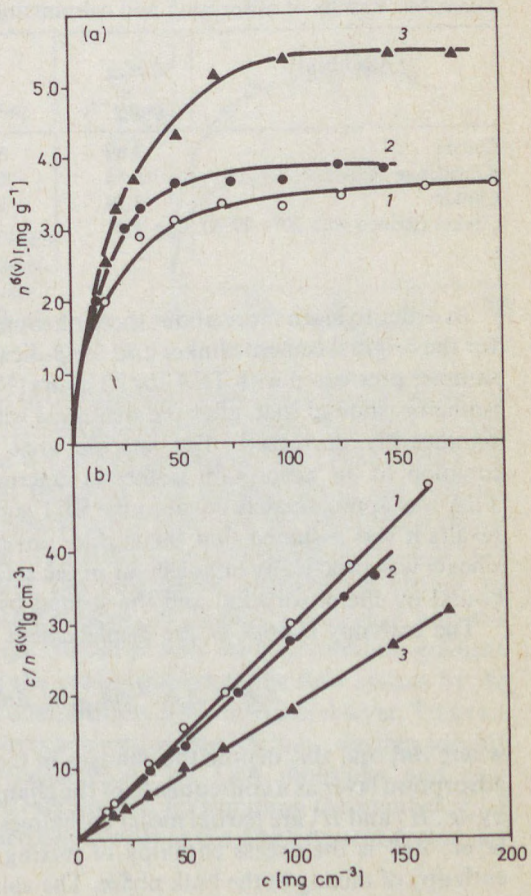

Fig. 4.30. (a) Adsorption excess isotherms of TEA in MEK solution, and (b) reciprocal Langmuir representation for adsorption on *1*—calcite, *2*—cement clinker, and *3*—β-dicalcium silicate [283]

These adsorption isotherms can be classified as being of Langmuir-type and can be described by the Langmuir isothermal equations, since in the representation:

$$\frac{c}{n^{\sigma(v)}} = \frac{1}{n^s_{max}}\left[\frac{1}{K-1} + c\right] \tag{23}$$

the experimental data show a linear function (Fig. 4.30(b)). In the above equation n^s_{max} is the maximum adsorption capacity and K the equilibrium constant of the adsorption.

By knowing n^s_{max}, determined according to Eq. (23), the specific surface areas of the samples could also be calculated (a^s_L). The cross-sectional area of TEA, as calculated from its molar volume, is 0.40 nm² per molecule.

The calculated surface area of a calcite sample agreed well with the BET surface area, i.e. TEA molecules form a practically unimolecular adsorption layer on the surface of calcite. The surface area of β-dicalcium silicate powders, calculated from the Langmuir equations is, however, three times as large, and cement clinkers is twice as large, as the BET surface area (Table 4.5).

Table 4.5. Results of adsorption and calorimetric measurements [283]

Adsorbent	n^s_{max} [mg g^{-1}]	a^s_L [m^2 g^{-1}]	a'_s (BET) [m^2 g^{-1}]	$-\left(\frac{\Sigma\Delta_d h}{n^s}\right)_{max}$ [kJ mol^{-1}]
Calcite	3.69	5.90	5.85	—
β-dicalcium silicate	5.54	8.86	2.88	—
Clinker	3.39	5.42	2.71	628
Clinker (treated with 20% TEA)	1.95	3.12	2.95	113

In order to learn more about these phenomena adsorption isotherms were recorded for the original cement clinker and for β-dicalcium silicate samples, and also for those samples pretreated with TEA for 72 hours (Fig. 4.31). A comparison of the two sets of isotherms showed that, after pre-treatment with TEA, the amount of adsorbed material significantly decreased. The specific area calculated by applying the Langmuir equation to the adsorption isotherms determined on cement clinker pre-treated with TEA was approximately equal to the BET surface area (a^s_L = 3.12 m² g^{-1}). From these results it was assumed that the surface coverage on cement clinker and β-dicalcium silicate was practically bimolecular in the saturation range and that the first layer was bound by chemi-sorption and the second by physical adsorption.

The enthalpy change of the displacement reaction on the solid surface is:

$$\Delta_d h = \Delta_d h' - \Delta h_{mix} = \Delta n^s_1 H^s_1 + \Delta n^s_2 H^s_2 + \Delta h^{se}, \tag{24}$$

where Δn^s_1 and Δn^s_2 denote the changes in the quantity of components 1 and 2 in the adsorption layer as a consequence of the change in composition of the flowing solution by Δc; H^s_1 and H^s_2 are partial molar enthalpies of components 1 and 2 in the adsorption layer; Δh^{se} is the excess enthalpy of mixing in the adsorption layer, and Δh_{mix} the enthalpy of mixing in the bulk phase. The value of Δh_{mix} can be determined by micro-

calorimetry in a separate experiment in which the same value of Δc and flow rate is realised. The sorption cell in the micro-calorimeter is filled with an "inert" substance (Teflon) of the same volume as the adsorbent.

If the $\Delta_d h$ values are summated from $c=0$ to $c \rightarrow c_n (c < c_n)$ the integral enthalpy of the displacement isotherm is obtained: $\Sigma \Delta_d h = f(c)$.

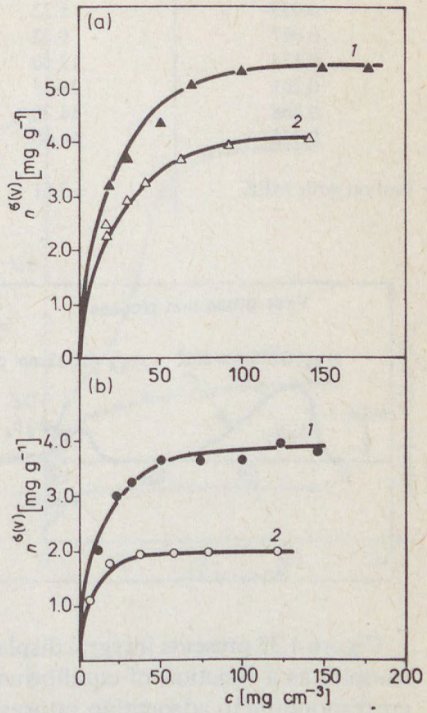

Fig. 4.31. Adsorption excess isotherms of TEA in MEK solution. (a) β-Dicalcium silicate: *1*—original sample, *2*—sample treated with 20% TEA. (b) Cement clinker: *1*—original sample, *2*—sample treated with 20% of TEA [283]

The aim of micro-calorimetric studies is to obtain quantitative data for the change of enthalpy following the interfacial interaction between cement clinker and TEA. At the beginning of the measurement the liquid which has penetrated the clinker sample is suspended in MEK until the instrument indicates that heat-exchange has reached equilibrium. Therefore, at constant temperature and flow rate the micro-calorimeter does not show any heat change. If, instead of pure MEK, a TEA/MEK solution of very low concentration penetrates the sample, the instrument registers the change of enthalpy accompanying adsorption. Concentration is gradually increased and the change in the enthalpy of displacement $\Delta_d h$ associated with the concentration gradient Δc is measured (Fig. 4.32). A change in the concentration of the flow system by Δc results, due to adsorption, in a change of composition in the interfacial layer. This can only take place if—compared to the previous adsorption equilibrium—further solvent molecules are displaced from the interfacial phase by TEA molecules and new conditions of adsorption equilibrium are established. By summing the number, i, of heat effects until concentration n is reached one arrives at the displacement enthalpies shown in Table 4.6.

Table 4.6. Data of enthalpy of displacement experiment [283]

C_{TEA} [mol dm^{-3}]	$-\Sigma\Delta_d h$ [J g^{-1}]		
	First adsorption	Second adsorption	Clinker treated with 20% TEA
0.016	3.92	2.48	0.44
0.033	5.22	4.05	0.75
0.067	6.22	4.50	1.05
0.134	12.10	5.20	1.35
0.201	14.15	5.01	1.55
0.268	14.20	5.32	1.48
0.335	14.40	5.71	1.50
Elution with MEK	−2.61	−2.17	−1.48

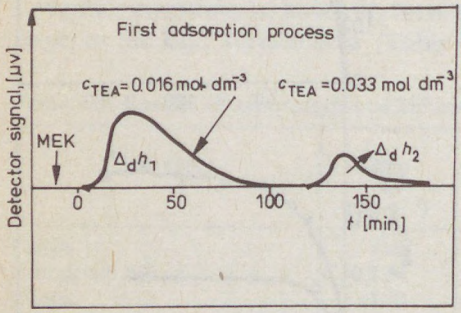

Fig. 4.32. The heat effects of first adsorption of TEA on cement clinker in MEK solution [283]

Figure 4.33 presents integral displacement enthalpies determined on original clinker samples as a function of equilibrium TEA concentration. In a concentration range corresponding to adsorption saturation the binding of TEA molecules on the surface results in a high heat effect. The linear representation of the displacement enthalpy isotherm is given by:

$$\frac{c}{\Sigma\Delta_d h} = \frac{1}{(\Sigma\Delta_d h)_{max}}\left[\frac{1}{K-1} + c\right]. \tag{25}$$

This is analogous to Eq. (23). If the parameters of the functions presented in Fig. 4.34 are given, the integral displacement enthalpy ($\Sigma\Delta_d h$) corresponding to the maximum amount of material adsorbed can be calculated; knowing the amount of adsorbed material and the enthalpy data, the molar integral displacement enthalpies $(\Sigma\Delta_d h/n^s)_{max}$ can also be calculated (Table 4.5).

When, after saturation, pure MEK has again penetrated the clinker sample some of the TEA molecules are desorbed from the surface by elution. The change of enthalpy (endothermic heat effect) associated with desorption is much lower than that measured during adsorption; this effect indicates that the first layer was irreversibly adsorbed onto the surface. On repeated adsorption (Fig. 4.35) significantly lower changes of enthalpy were observed than in the first phase. This result also indicated

that, on first adsorption, most of TEA molecules were irreversibly bound (chemisorbed) on the surface and this layer could not be removed by elution. On repeated elution the endothermic change connected with desorption agreed well with that of the first elution, indicating that almost the same amount of TEA was removed from the surface in each case. In other words, this mode of measurement implies that during the first series of adsorption measurements the surface was pre-treated with TEA, then the

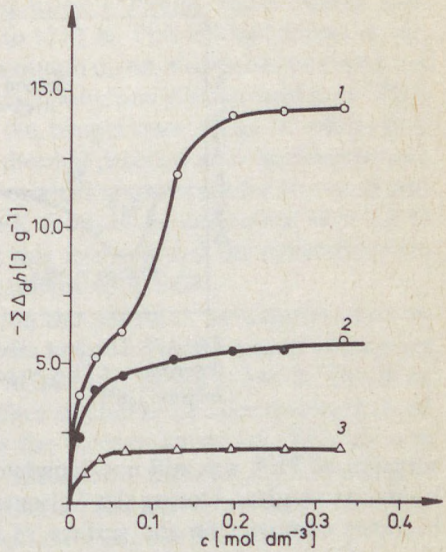

Fig. 4.33. Enthalpy of displacement isotherms for adsorption on cement clinker surface. *1*—First adsorption, *2*—second adsorption, *3*—cement clinker treated with 20% of TEA [283]

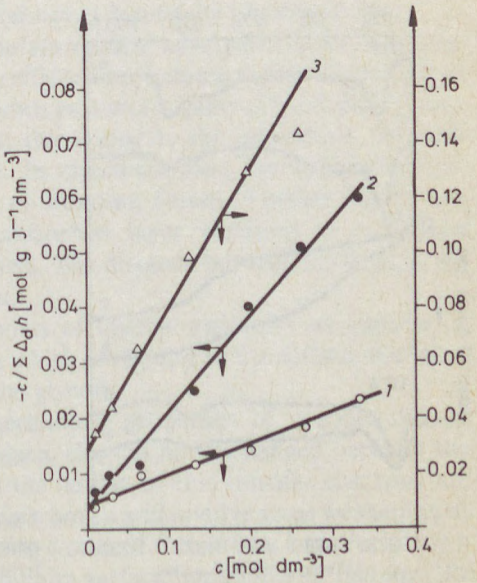

Fig. 4.34. Reciprocal Langmuir representation of flow calorimetric data. *1*—First adsorption, *2*—second adsorption, *3*—cement clinker treated with 20% of TEA [283]

reversibly adsorbed layer was removed and the second series was performed on the pre-treated sample.

The results obtained for a sample pre-treated with a 20% solution of TEA in MEK for 72 hours are presented in Fig. 4.33. Data in Table 4.6 show that in this instance the displacement enthalpies decreased even more than earlier. The values are lower than those obtained for the original sample in the second adsorption cycle; this is because in the first one, which can be considered as a pre-treatment with TEA, the chemi-

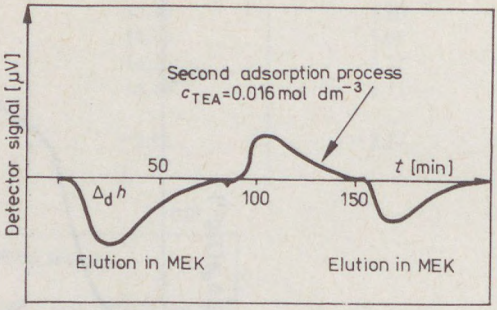

Fig. 4.35. The heat effects of second adsorption and desorption of TEA on cement clinker surface in MEK solution [283]

sorption of TEA was still not complete. A series of measurements requires 10 to 12 hours to complete. During the 72 hours of pre-treatment the chemi-sorption of TEA becomes complete on the surface of the clinker and the displacement enthalpies characteristic of physical adsorption are obtained. This statement is clearly supported

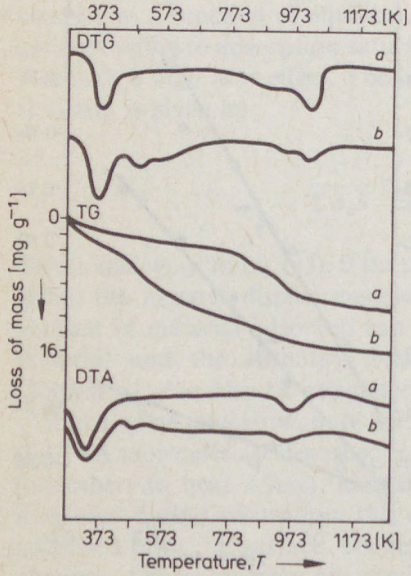

Fig. 4.36. Thermal desorption of TEA from the surface of cement clinker surface. *a*—original sample, *b*—sample treated with 20% of TEA [283]

by data in Table 4.2 where a difference of almost one order of magnitude between the molar integral displacement enthalpies on the original and pre-treated samples is assignable to the maximum of adsorbed material. This clearly shows that the sorption of TEA on the surface of clinker is followed by a rather large change of enthalpy caused, primarily, by chemi-sorption. Changes of enthalpy that are smaller by almost one order of magnitude can be observed if TEA has previously been adsorbed on the surface of clinker.

Thermal desorption studies were performed using a Paulik–Paulik–Erdey type derivatograph in the temperature range of 298 to 1273 K. This method allows one to analyse clinker powder treated with TEA and to obtain direct information on whether TEA actually remains on the surface during adsorption and elution studies. If TEA does remain it is also possible to determine the temperature range in which it is removed from the surface as a consequence of thermal desorption or decomposition.

Figure 4.36 shows the thermal curves of the original clinker powder (curve *a*) and that pre-treated with a solution of TEA in MEK followed by extraction with MEK (curve *b*). On the basis of adsorption studies it was assumed that the molecules were chemisorbed on the surface during the pre-treatment with TEA.

Curve *a* exhibits endothermic peaks indicating the release of adsorption water at 363 K and the decomposition of $CaCO_3$ at 973 K. In curve *b* the release of adsorption water is followed by another endothermic peak in the range of 503 to 543 K. This peak indicates that TEA was removed from the surface of clinker powder due to thermal desorption. The loss of weight calculated from the thermo-gravimetry (TG) curve is 4.01 mg g^{-1}; this is close to the value of adsorption saturation, 3.39 mg g^{-1}, determined indirectly from the adsorption isotherm. The difference arises from the inaccuracy of the thermal desorption determination using the TG curve.

It can be concluded that, in the saturation range, TEA molecules form almost a bimolecular adsorption layer on the surface of cement clinker and βC_2S, the first one, is bound by chemi-sorption, while the second one is bound by physi-sorption.

Chemi-sorption and the formation of a polymolecular adsorption layer has to be regarded as a positive factor in evaluating the effect of surfactants as grinding aids. It is well known that the degree of adhesion between particles is generally reduced by any medium situated between the two surfaces; this is due to the interaction between molecules of the medium and the surface. In chemi-sorption the binding of the adsorbed material takes place by means of bonding forces. Further layers are superimposed onto the unimolecular chemisorbed layer resulting in a thicker adsorption layer on the surface of the particle. The distance between particles is the decisive factor for the adhesion of particles.

According to Seebach [155] only the vapours of organic molecules are capable of inhibiting adhesion forces between particles which are bound to the surface of clinker by chemi-sorption (e.g. butylamine, ethylene glycol).

Chemi-sorption may also effect the mechanical properties of a solid and its grindability. When chemi-sorption takes place, charges are exchanged between the surface of the solid and the adsorbate; in the course of this transfer electrons are transferred from the energy levels of the surface bonds and involve some weakening of bonds between atoms on the surface. In other words, if the surface acquires either a negative or a positive charge this charge impairs surface bonding and, thereby, the

development of dislocation loops is facilitated to a depth of a few nanometers. The result is a reduction of surface hardness [162].

On the basis of our experimental results we may summarise the effects of surfactants on grinding as follows;

—decrease of fracture strength of the solid and improvement of its grindability;
—reduction of particles interaction (adherence, aggregation, and agglomeration) and a weakening of interparticle bonds;
—improvement of the flow characteristics of the grind;
—promotion of changes in the crystal structure in the phase of mechanical activation.

These effects also depend on the fineness and on the nature of the feed material.

SYMBOLS IN CHAPTER 4

A	Papadakis coefficient
a_s	"external" specific surface
a'_s	"total" specific surface
a'_{sw}	"total" specific surface based on water vapour adsorption
a'_{sn}	"total" specific surface based on nitrogen adsorption
a^s_L	"total" specific surface calculated by the Langmuir equation
a_{s_∞}	specific surface at equilibrium
a	distance between particles
a_0	"equilibrium" distance between particles (according to Krupp)
b	shape factor of particles
c_0	initial concentration of solute
c	equilibrium concentration of solute
D, d_m	diameter of mill
D	undersize
$\dot{D}_x(\tau)$, $\dot{D}_\tau(x)$	grinding rate
d, d_b	diameter of grinding bodies (balls)
d_p	particle diameter
E	elasticity modulus
E	bonding energy
E_u	bonding energy of non-disperse system (lattice energy of ideal crystal)
E_γ	surface free energy
E_0	energy consumption
e_γ	specific surface free energy
e	energy of elastic deformation
F_{vdW}	van der Waals adhesion
F_{el}	electrostatic attraction forces
g, G	amount of material, mass

H	Hardgrove number
H	hardness, microhardness
H_1^s, H_2^s	partial molar enthalpy of components
Δh^{se}	excess enthalpy of mixing
Δh_{mix}	enthalpy of mixing
$h\bar{\omega}$	interaction energy
$\Delta_d h$	enthalpy of exclusion
K	equilibrium constant of adsorption
l	total elongation
l_{plast}	depth of plastic deformation
l_r	critical crack length
m	mass of adsorbent
m_m	mass of mill
m_b	mass of ball filling
n	uniformity coefficient, uniformity factor
$n^{\sigma(v)}$	specific adsorbed excess mass
n_{max}^s	maximum capacity of adsorption
P	force of fracture
R, $R_{0.09}$	oversize
r, r_p, r_f	mesh size
T	temperature
Δu	contact potential difference
V	volume of body to be comminuted
v	variation coefficient of distribution
v_0	porosity of particles
v	volume of solution in contact with the adsorbent
W_t	specific grindability
W_i	"work index" according to Bond
W_z	grinding work, grinding energy
x	particle size (mesh size)
$\bar{x}$	fineness number
ε	dielectric constant, relative permeability
ϱ	curvature radius at contact points
Q	heat
σ	fracture stress, strength
η, η_z	efficiency of grinding
φ_N	kinetic factor of the change of numerosity
τ	grinding time
t	time
C	clinker
τ_0	recycling factor
δ	degree of comminution
δ_f	"degree of unlock"
w	utilized energy
β	energy of plastic deformation
a, b, k, m, c_1, c_2, c_3, c_4	constants
λ	specific elongation

REFERENCES

[1] (Butt, J. M., Timasev, V. V.) Ю. М. Бутт, В. В. Тимашев: *Портландцементный клинкер*. Изд-во литературы по строительству, Москва 1967

[2] (Butt, J. M., Timasev, V. V.) Ю. М. Бутт, В. В. Тимашев: *Портландцемент*. Стройиздат, Москва 1974

[3] Lawn, B., Marshall, D.: *J. Am. Ceram. Soc.*, **62,** 347 (1978)

[4] Reményi, K.: *The Theory of Grindability and the Comminution of Binary Mixtures*. Akadémiai Kiadó, Budapest 1974

[5] *ASTM Standard D 409–51:* Publ. by the American Society for Testing Materials (Philadelphia), **49** (1951)

[6] Zeisel, H.: *Schriftenreihe der Zementindustrie*. **14,** Verein. Deutscher Zementwerke e. V., Düsseldorf (1953)

[7] Lehmann, H., Haese, U.: *Tonind. Ztg. u. Keram. Rundschau*, **79,** 91 (1955)

[8] (Andreev, S. E., Tovarov, V. V., Perov, V. A.) С. Е. Андреев, В. В. Товаров, В. А. Перов: *Закономерности измельчения и исчисления гранулометрического состава*. Металлургиздат, Москва 1959

[9] Mittag: *Prüfverfahren zur Ermittlung von Hochleistungen in Kugel- und Rohrmühlen*. Springer, Berlin 1954.

[10] Bond, F.: *Brit. Chem. Eng.*, **6,** 378 (1961); *Aufbereitungs-Technik*, **5,** 211 (1964)

[11] Proks, M., Horoscak, T.: *Stavivo*, **10,** 316 (1975)

[12] Haese, U.: *Zement-Kalk-Gips*, **31,** 439 (1978); *Zement-Kalk-Gips*, **32,** 10 (1979)

[13] Zisselmar, R.: *Zement-Kalk-Gips*, **34,** 187 (1980)

[14] Verdes, S.: *Építőanyag*, **33,** 30 (1981)

[15] Dombrowe, H.: *Építőanyag*, **38,** 300 (1986)

[16] (Piroczkij, V. Z., Borjakov, V. F.) В. З. Пироцкий, В. Ф. Борьяков: *Труды НИИ Цемента (Москва)* **36** (1976)

[17] Scheibe, W., Bernhardt, C., Winkler, E.: *Aufbereitungs-Technik*, **9,** 574 (1968)

[18] Wasmuth, H. D.: *Aufbereitungs-Technik*, **10,** 284 (1968)

[19] Rowland, C. A.: *10. Intern. Kongr. Mineralaufbereitung*. London 1973

[20] *Tätigkeitsbericht 1969–1971*. Verein Deutscher Zementwerke e. V., Düsseldorf 1972

[21] Ellerbrock, H.: *Verfahrenstechnik der Zementherstellung*. BAUVerlag, Düsseldorf–Wiesbaden–Berlin 1979

[22] Opoczky, L., Mrákovics-Török, K., Dombrowe, H.: in Untersuchungsmethoden zur Charakterisierung mechanisch aktivierter Festkörper (ed. Juhász, Z.), *BME Tud. Közlemények*, **13,** KÖZDOK, Budapest 1978

[23] Mrákovics-Török, K.: Methods for testing grindability (in Hungarian). *SZIKKTI Tud. Közlemények*, Budapest, **76,** 1983

[24] (Rojak, S. M., Piroczkij, V. Z.) С. М. Рояк, В. З. Пироцкий: *Труды НИИЦемента (Москва)* **14** (1960)

[25] (Rojak, S. M., Piroczkij, V. Z.) С. М. Рояк, В. З. Пироцкий: *Научные сообщения НИИЦемента (Москва)*, **6** (1958)

[26] Schmid, A.: *Schriftenreihe der Zementindustrie*. Verein Deutscher Zementwerke e. V., Düsseldorf, **14,** 7 (1953)

[27] Ackmann, G.: *Schriftenreihe der Zementindustrie*. Verein Deutscher Zementwerke e. V. Düsseldorf, **20,** 7 (1955)

[28] Gille, F., Ruhland, W.: *Zement-Kalk-Gips*, **16,** 170 (1963)

[29] Deckers, M.: *Zement-Kalk-Gips*, **25,** 445 (1972)

[30] Butt, Jn. M., Kolbazov, V. M., Melnickij, G. A.: *Zement-Kalk-Gips*, **27,** 27 (1974)

[31] Papadakis, M.: *Rev. matériaux construction*, **519,** 321 (1958), **542,** 295 (1960)

[32] Opoczky, L.: Investigation of grinding process of the cement clinker and intensifying them by grinding aids (in Hungarian). Ph. D. thesis, Budapest 1968.

[33] Opoczky, L., Mrákovics-Török, K.: *Freiberger Forschungshefte*, *A***533,** 71 (1976)

[34] Opoczky, L., Mrákovics-Török, K.: *World Cement Technology (London)*, **11,** 245 (1980)

[35] Opoczky, L.: *Banicke Listy*. VEDA, Bratislava 1984

[36] Opoczky, L.: Fine grinding processes of brittle materials in silicate industry (in Hungarian). *SZIKKTI Tud. Közlemények*, Budapest, **84**, 1985.
[37] Gouda, G.: *Cement Concrete Res.* (USA), **9**, 209 (1979)
[38] Peterson, I.: *7e Congres Intern. de la Chimie des Ciments.* Vol. *II*, Editions Septima-14, Paris 1980
[39] Hornain, M., Regourd, M.: *7e Congres Intern. de la Chimie des Ciments.* Vol. *II*, Editions Septima-14, Paris 1980
[40] Merič, I.: *7e Congres Intern. de la Chimie des Ciments*, Vol. *I*, Editions Septima-14, Paris 1980
[41] Jeffery, J.: *Third International Symposium on the Chemistry of Cement.* Cement and Concrete Assoc., London 1952
[42] Nurse, R.: *Third International Symposium on the Chemistry of Cement.* Cement and Concrete Assoc., London 1952
[43] Bojkova, A.: *Cement*, **2**, 7 (1982)
[44] Götte, A.: *Zement-Kalk-Gips*, **5**, 383 (1952)
[45] Opoczky, L., Wojnarovits-Hrapka, I.: *Proceedings of the XIII. Siliconf.*, Sect. C, OMIKK, Budapest 1981
[46] Hüttig, G.: *Dechema Monographien. Vol. 21*, Verlag Chemie, Weinheim 1952
[47] Tanaka, T.: *Staub*, **18**, 157 (1958)
[48] Beke, B., Opoczky, L.: *Dechema Monographien, Vol. 57*, Verlag Chemie, Weinheim 1967
[49] Opoczky, L.: *Powder Technol.* **17**, 1 (1977)
[50] Opoczky, L.: *MTA Kémiai Közlemények*, **48**, 235 (1977)
[51] Opoczky, L.: *European Symposium on Particle Technology.* Preprints, *Vol. A*, Dechema, Frankfurt am Main 1980
[52] Opoczky, L.: Fine grinding processes of brittle materials in silicate industry (in Hungarian). DSc thesis, Budapest 1982
[53] Verdes, S.: Kinetic model of grinding in a ball mill (in Hungarian). Ph.D. thesis, Budapest 1982
[54] Ocepek, D., Eberl, E.: *Rudarsko-Metalurski Zbornik*, **4**, 385 (1963)
[55] Ocepek, D.: *Dechema Monographien. Vol. 57*, Verlag Chemie, Weinheim 1967
[56] Beke, B.: *Principles of Comminution.* Akadémiai Kiadó, Budapest 1964
[57] Beke, B.: The process of fine grinding. KÖZDOK, Budapest 1977
[58] (Hodakov, G. S.) Г. С. Ходаков: *Тонкое измельчение строительных материалов.* Изд-во литературы по строительству, Москва 1972
[59] (Hodakov, G. S., Kudrjavceva, N. L.) Г. С. Ходаков, Н. Л. Кудрявцева: *ЖФХ*, **XXVII**, 10 (1963)
[60] (Kudrjavceva, N. L.) Н. Л. Кудрвяцева: Исследования изменения физико-химических свойств портландцемента при измельчении. Кандидатская диссертация, Москва 1967
[61] Opoczky, L., Juhász, Z.: *The VI. International Congress on the Chemistry of Cement. Vol. II*, Moscow, Strojizdat 1976
[62] Juhász, Z.: Mechanical activation of raw materials in industry of building materials (in Hungarian). DSc. thesis, Budapest 1979
[63] Opoczky, L., Farnady, F.: *Powder Technol.*, **39**, 107 (1984)
[64] Obreimoff, I. V.: *Proc. Roy. Soc. (London)*, Ser. *A* **127**, 290 (1930)
[65] Gaudin, A. M.: *Mining Eng.*, **7**, 531 (1955)
[66] Götte, A., Wagener, W.: *Aachener Blätter*, **11**, 53 (1961)
[67] Wagener, W.: Untersuchungen über das Ansetzen fester Stoffe beim Zerkleinern und seine Beeinflussung durch dampfförmige Zusatzmittel und radioaktive Bestrahlung. Thesis TH, Aachen 1960
[68] Rockwood, N. C.: *Rock Products*, **42**, 38 (1939)
[69] (Drinberg, A. Ja.) А. Я. Дринберг: *Технология пленкообразующих веществ.* Ленинград–Москва 1948
[70] (Derjagin, B. V., Krotova, N. A.) Б. В. Дерягин, Н. А. Кротова: *Адгезия.* Изд-во АН СССР, Москва 1949
[71] (Derjagin, B. V., Smilga, V. P.) Б. В. Дерягин, В. П. Шмилга: *Доклады АН СССР*, **121, 877 (1958)**
[72] Rearson, V. N.: *Rock Products*, **55**, 105 (1952)
[73] (Lurje, Ju, S.) Ю. С. Лурье: *Портландцемент.* Москва–Ленинград 1963
[74] Derjagin, B. V., Aleinikova, I. N., Toprov, Y. P.: *Powder Technol.*, **2**, 154 (1968)
[75] Mardulier, F. J.: *Am. Soc. Testing Mat. Proc.*, **61**, 1078 (1961)
[76] Opocky, L.: *Keram. Z.*, **31**, 390 (1979)

[77] Hansen, W.: *Am. Soc. Testing Mat. Proc.*, **60**, 3 (1960)
[78] Iwabuchi, T.: *CAJ Review of the 22nd General Meeting*, Technical Session (1968)
[79] Weyl, W. A.: *A New Approach to Surface Chemistry and Heterogeneous Catalysis*. Bulletin *57*, Mineral Ind. Exp. Station, Pennsylvania, 1959
[80] Bikerman, I.: *Surface Chemistry, Theory and Application*, Academic Press, New York 1958
[81] Bischoff, E.: *Deut. Farben-Z.*, **13**, 275 (1959)
[82] Krupp, H.: *J. Colloid Interface Sci.*, **1**, 111 (1967)
[83] Rumpf, H.: *Chem. Ing. Tech.*, **25**, 144 (1953)
[84] Rumpf, H.: *Chem. Ing. Tech.*, **30**, 329 (1958)
[85] Rumpf, H.: *Chem. Ing. Tech.*, **42**, 538 (1970)
[86] Rumpf, H., Hermann, W.: *Aufbereitungs-Technik*, **11**, 117 (1970)
[87] Rumpf, H.: *Pharm. Ind.*, **34**, 270 (1972)
[88] Rumpf, H.: *Powder Technol. (Japan)*, **9**, 3 (1972)
[89] Rumpf, H.: *Chem. Ing. Tech.*, **46**, 1 (1974)
[90] Pietsch, W.: *Aufbereitungs-Technik*, **8**, 297 (1967)
[91] Pietsch, W., Rumpf, H.: *Chem. Ing. Tech.*, **39**, 885 (1967)
[92] Turba, E., Rumpf, H.: *Chem. Ing. Tech.*, **36**, 230 (1964)
[93] Pietsch, W.: *Staub*, **27**, 20 (1967)
[94] (Lifsitz, E. M.) Е. М. Лифшитц: *Журнал экспериментальной физики*, **2**, 73 (1956)
[95] Dahneke, B. J.: *J. Colloid Interface Sci.*, **40**, 1 (1972)
[96] Borho, K.: Zur Agglomeration von Stäuben in Rohrströmungen. Thesis University Karlsruhe (TH) 1972
[97] Rumpf, H.: *Dechema Monographien. Vol. 79*, Verlag Chemie, Weinheim 1976
[98] Schönert, K.: *Zement-Kalk-Gips*, **32**, 1 (1979)
[99] Rittinger, P. R.: *Lehrbuch der Aufbereitungskunde*. Ernst u. Korn, Berlin 1867.
[100] (Kirpichov, V. L.) В. Л. Кирпичев: *Журнал русского физико-химического общества*, **VI, 1**, Часть физическая, *IX*, 152 (1874)
[101] Kick, F.: *Dinglers Polytech. J.*, **247**, 1 (1883)
[102] Bond, F. C., Wang, J. T.: *Min. Eng. Trans. AIME*, **187**, (1950)
[103] Bond, F. C.: *Chem. Eng.*, **59**, 242 (1952)
[104] Tkačova, K., Krupa, V.: *Banicke Listy*. VEDA, Bratislava 1980
[105] Charles, R. J.: *Min. Eng. Trans. AIME*, **208**, 80 (1957)
[106] Holmes, J. A.: *Trans. Inst. Chem. Eng. (London)*, **35**, 125 (1957)
[107] Svensson, J., Murkes, J.: *International Mineral Dressing Congress*. Stockholm 1957
[108] Beke, B.: *Építőanyag*, **13**, 241 (1961)
[109] Smekal, A.: *Z. VDI*, **81**, 1321 (1937)
[110] Beke, B.: *Építőanyag*, **25**, 47 (1973)
[111] Stairmand, C.: *Dechema Monographien. Vol. 79*, Verlag Chemie, Weinheim 1976
[112] Bown, R. W.: *Bull. Trans. Inst. Min. Metall. Sect. C. (London)*, **75**, 163 (1966)
[113] Schellinger, W.: *Mining Eng.*, **4**, 369 (1952)
[114] Schellinger, W., Lakala, R. D.: *Mining Eng.*, **3**, 523 (1951)
[115] (Bessonov, N. A.) Н. А. Бессонов: Работа, тепло и поверхностная энергия при шлифовании. Канд. диссерт. Томск 1941
[116] Rose, H. E.: *Dechema Monographien. Vol. 57*, Verlag Chemie, Weinheim 1967
[117] Hiorns, F. I.: *Dechema Monographien. VOl(. 57*, Verlag Chemie, Weinheim 1967
[118] Sekula, F., Krupa, V., Merva, M., Hocmanova, I.: *Banicke Listy*, VEDA, Bratislava 1973
[119] Merva, M., Krupa, V.: *VI. Symposium für Mechanoemission und Mechanochemie, Summary*. Kammer der Technik, Berlin 1977
[120] Tkačova, K., Sekula, F., Krupa, V., Bejda, I., Kavecanska, V.: *VI. Symposium für Mechanoemission und Mechanochemie, Summary*. Kammer der Technik, Berlin 1977
[121] Krupa, V., Sekula, F., Merva, M., Miklusova, V., Krajecova, O.: *Banicke Listy*, VEDA, Bratislava 1980
[122] Bernhardt, C., Gottschalk, J., Heegn, M., Husemann, K.: *Silikattechnik*, **25**, 183 (1974)
[123] Husemann, K., Bernhardt, C., Gottschalk, J., Heegn, M.: *Silikattechnik*, **25**, 238 (1974)
[124] Heegn, M., Bernhardt, C., Gottschalk, J., Husemann, K.: *Chem. Tech.*, **26**, 696 (1974)
[125] Heegn, M., Bernhardt, C.: *Freiberger Forschungshefte, A* **553**, 57 (1976)

[126] Bernhardt, C., Heegn, H., Ilgen, S., Reinsch, E.: *Banicke Listy*, VEDA, Bratislava 1980
[127] Rumpf, H.: *Symposium Zerkleinern*. Verlag Chemie, Weinheim, VDI Verlag, Düsseldorf 1962
[128] Rumpf, H.: *Chem. Ing. Tech.*, **34,** 731 (1962)
[129] Rumpf, H.: *Aufbereitungs-Technik* **7,** 422 (1966)
[130] Rumpf, H.: *Chem. Ing. Tech.*, **37,** N3, 187 (1965)
[131] Rumpf, H., Faulhaber, F., Schönert, K., Umhauer, H.: *Dechema Monographien. Vol. 57*, Verlag Chemie, Weinheim 1967
[132] Rumpf, H.: *Aufbereitungs-Technik*, **40,** 59 (1973)
[133] Patat, F.: *Dechema Monographien. Vol. 57*, Verlag Chemie, Weinheim 1967
[134] Steier, K., Schönert, K.: *Dechema Monographien. Vol. 69*, Verlag Chemie, Weinheim 1972
[135] Schönert, K., Weichert, R.: *Chem. Ing. Tech.*, **41,** 295 (1969)
[136] Schönert, K., Steier, K.: *Chem. Ing. Tech.*, **43,** 773 (1971)
[137] Schönert, K.: *Chem. Ing. Tech.*, **46,** 711 (1974)
[138] Schönert, K.: *Banicke Listy*, VEDA, Bratislava 1980
[139] Schönert, K.: *Proceedings of International Symposium on Powder Technology '81*. The Soc. of Powder Techn., Kyoto 1982
[140] (Rehbinder, P. A.) П. А. Ребиндер: Сб. *Доклады на VI. съезде физиков*. Госиздат, Москва 1928; *Физико-химическая механика дисперсных структур*. Изд-во АН СССР, Москва 1966
[141] (Rehbinder, P. A., Vestrem, E. K.) П. А. Ребиндер, Е. К. Вестрем: *Известия ОМЕН АН СССР*, сер. физ. *4/5* (1937)
[142] (Rehbinder, P. A., Shreiner, L. A., Zhigach, K. F.) П. А. Ребиндер, Л. А. Шрейнер, К. Ф. Жигач: *Понизители твердости в бурении*. Изд-во АП СССР, Москва 1944
[143] (Lihtman, V. I., Rehbinder, P. A., Karpenko, G. V.) В. И. Лихтман, П. А. Ребиндер, Г. В. Карпенко: *Влияние поверхностно-активной среды на процессы деформации металлов*. Изд-во АН СССР, Москва 1954
[144] (Shchukin, E. D., Rehbinder, P. A.) Е. Д. Шукин, П. А. Ребиндер: *Коллоидный журнал*, **20,** 645 (1958)
[145] (Rehbinder, P. A., Lihtman, V. I., Kochanova, L. A.) А. П. Ребиндер, В. И. Лихтман, Д. А. Кочанова: *ДАН СССР*, **111,** 1 (1956)
[146] (Gorjunov, Ju. V., Percov, N. V., Summ, B. D.) Ю. В. Горюнов, Н. В. Перцов, В. Д. Сумм: *Эффект Ребиндера*. Изд-во Наука, Москва 1966
[147] (Shchukin, E. D.) Е. Д. Шукин: *Адсорбционное влияние сред на механические свойства материалов*. Изд-во АН СССР, Москва 1976
[148] (Shchukin, E. D.) Е. Д. Шукин: Эффект Ребиндера. Межд. ежегодник. *Наука и человечество*. Москва 1970
[149] (Shchukin, E. D., Brjuhanova, L. S., Polukerova, Z. M., Percov, N. V.) Е. Д. Шукин, Л. С. Брюханова, З. М. Полукерова, Н. В. Перцов: *Адсорбционное влияние сред на механические свойства материалов*. Изд-во АН СССР, Москва 1976
[150] (Jushchenko, V. S., Grivtsov, A. G., Shchukin, E. D.) В. С. Юшенко, А. Г. Гривцов, Е. Д. Шукин: *ДАН СССР*, **215,** 148 (1974)
[151] (Jushchenko, V. S. Grivtsov, A. G., Shchukin, E. D.) В. С. Юшенко, А. Г. Гривцов, Е. Д. Шукин: *ДАН СССР*, **219,** 162 (1974)
[152] Obreimoff, I. V.: *Proc. Roy. Soc. (London)*, Ser. *A* **127,** 290 (1930)
[153] Boyd, G., Livingston, H.: *J. Amer. Chem. Soc.*, **64,** 2383 (1942)
[154] Hardie, D., Petch, N.: *Proc. Br. Ceram. Soc.*, **5,** 85 (1965)
[155] Seebach, N.: *Zement-Kalk-Gips*, **22,** 202 (1969)
[156] Rumpf, H.: *Materialprüf.*, **3,** 253 (1961)
[157] Hammond, M., Ravitz, S.: *J. Amer. Ceram. Soc.*, **46,** 329 (1963)
[158] Westbrook, J. H., Jorgensen, P.: *Trans. AIME*, **233,** 425 (1965)
[159] Westbrook, J. H.: *Metallurgical Society Conferences. Vol. 35*, Gordon and Breach, New York 1966
[160] Westwood, A. R. C.: *Metallurgical Society Conferences. Vol. 35*, Gordon and Breach, New York 1966
[161] Ahearn, J. S., Mills, J. J., Westwood, A. R. C.: *Phil. Mag.*, **34,** 391 (1976)
[162] Westwood, A. R. C., Ahearn, J. S., Mills, J. J.: *Colloids & Surf.*, **2,** 1 (1981)
[163] Kemsley, O. S.: *Nature (London)*, **164,** 381 (1949)
[164] da C. Andrade, E. N., Randall, R. F. Y.: *Proc. Phys. Soc. (London)*, Sect. *B* **63,** 198 (1950)
[165] Harper, S., Cottrell, A. M.: *Proc. Phys. Soc. (London)*, Sect. *B* **63,** 116 (1950)

[166] Hildinger, P.: Einzelkornzerkleinerung durch Fallkörper Untersuchungen an Glaskugeln sowie Quarz-, Zementklinker und Kalksteinteilchen im Korngrößenbereich zwischen 1 und 12 mm. Thesis University Karlsruhe (TH) 1972
[167] Schönert, K., Umhauer, H., Klemm, W.: The influence of temperature and environment on the slow crack propagation in glass. Paper presented at the *2nd Conference on Fracture*, Brighton, 16–18, 4, 1969
[168] Schneider, H.: *Zement-Kalk-Gips*, **22**, 193 (1969)
[169] Graichen, K., Müller, H., Schubert, H.: *Silikattechnik*, **25**, 169 (1974)
[170] Kiesskalt, S., Dahlhoff, B.: *Chem. Ing. Tech.*, **37**, 277 (1965)
[171] Ocepek, D., Eberl, E.: *4. Europ. Symp. Zerkleinern*. Preprints. Schön & Wetzel GmbH, Frankfurt am Main 1975
[172] Wolf, K.: *Physik und Chemie der Grenzflächen. Vol. I*, Springer, Berlin 1957
[173] Schardin, H.: *Symposium Zerkleinern*. Verlag Chemie, Weinheim, VDI Verlag, Düsseldorf 1962
[174] Gilman, J. J., Johnston, W. G.: *Dislocation and the Mechanical Properties of Crystals*. Wiley, New York 1957
[175] Gilman, J. J.: *Phil. Mag.*, **6**, 159 (1961)
[176] Westwood, A. R. C.: *Phil. Mag.*, **7**, 633 (1962)
[177] Westwood, A. R. C., Goldheim, D. L., Opperhauser, H.: *Phil. Mag.*, **6**, 1475 (1961)
[178] (Lihtmann, V. I., Shchukin, E. D., Rehbinder, P. A.) В. И. Лихтман, Е. Д. Шукин, П. А. Ребиндер: *Физико-химическая механика металлов*. Изд-во АН СССР, москва 1962
[179] (Juschenko, V. S., Dikarevich, M. N., Chuvaev, V. F., Shchukin, E. D.) В. С. Ющенко, М. Н. Дикаревич, В. Ф. Чуваев, Е. Д. Шукин: *ЖФХ*, **43**, 1556 (1969)
[180] (Maksimovich, G. G.) Г. Г. Максымович: *Микромеханические исследования свойств металлов и сплавов*. Наукова думка 1974
[181] Shchukin, E. D., Justsenko, V. S.: *J. Materials Sci.*, **16**, 313 (1981)
[182] (Shchukin, E. D., Savchenko, V. I., Kochanova, L. A., Rehbinder, P. A.) Е. Д. Шукин, В. И. Савченко, Л. А. Кочанова, П. А. Ребиндер: *ДАН СССР*, **200**, 406 (1971)
[183] (Shchukin, E. D., Savchenko, V. I., Kochanova, L. A., Rehbinder, P. A.) Е. Д. Шукин, В. И. Савченко, Л. А. Кочанова, П. А. Ребиндер: *ДАН СССР*, **200**, 1329 (1971)
[184] El-Shall, H., Somasundaran, P.: *Powder Technol.*, **38**, 275 (1984)
[185] (Lubman, N. M.) Н. М. Лубман: *Исследования в области поверхностных явлений*. ОНТИ, Москва 1936
[186] (Bjalkovskij, V. I., Kudinov, I. A.) В. И. Бялковский, И. А. Кудинов: *Керамический сборник*, **10** (1940)
[187] (Kukolev, G. V., Melnichenko, L. G.) Г. В. Куколев, Л. Г. Мельниченко: *Огнеупоры*, **13** (1948)
[188] (Popova, E. J.) Э. И. Попова: Кандидатская диссертация. ВНИИ Стекло, Москва 1932
[189] Szántho, E.: *Z. für Erzbergbau und Metallhüttenwesen*. **2**, 353 (1949)
[190] (Chernij, L. M.) Л. М. Черный: *Труды Института Горнохимического сырья*, **1** (1950)
[191] Alberti, R.: FRG Pat. No. 904, 019, 1954
[192] Shepherd, R.: *Mine & Quarry Eng.*, **21**, 329 (1955)
[193] Frangiskos, A. Z., Smith, H. G.: in *Progress in Mineral Dressing*. Almquist and Wirksell, Stockholm 1958
[194] Siebel, I., Zeisel, H.: FRG Pat. No. 1, 071, 455, 1959
[195] Shosh, S., Harris, C., Jowett, A.: *Nature (London)*, **188**, 1182 (1960)
[196] Gilbert, L. A., Hughes, T. H.: *Symposium Zerkleinern*. Verlag Chemie, Weinheim, VDI Verlag, Düsseldorf 1962
[197] Engelhardt, W. V.: *Nachrichten Akad. Wiss. Göttingen, Math. Phys.*, **2** (1942)
[198] Engelhardt, W. V.: *Naturwissenschaften*, **33**, 195 (1946)
[199] Lin, I. J., Metzmager, A.: *Trans. AIME*, **241**, 412 (1968)
[200] Malati, M. A., Orphy, M. K., Yousef, A. A.: *Powder Technol.* **2**, 21 (1968)
[201] Smekal, A.: *Verfahrenstechnik, Beih. Z. VDI*, **1**, 1 (1937)
[202] Ziegler, E.: *Schriftenreihe der Zementindustrie, 19*, Verein Deutscher Zementwerke e. V., Düsseldorf 1956
[203] Götte, A., Ziegler, E.: *Z. VDI*, **98**, 373 (1956)
[204] Götte, A., Scherrer, E.: *Aachener Blätter*. **8**, 3 (1958)
[205] Götte, A.: *Freiberger Forschungshefte A 2810* (1963)

[206] Götte, A., Ziegler, E.: *Z. VDI.*, **98,** 373 (1956)
[207] Eichborn, J. L.: *Kolloid, Zh.*, **1,** 149 (1956)
[208] Eichborn, J. L.: *Chemiker-Ztg./Chem. Apparatur*, **92,** 803 (1968)
[209] Engelhardt, W., Haussühl, S.: *Fortschr. Mineral.*, **42,** 5 (1965)
[210] *Brit. Pat. No. 350538*, 12 March 1930
[211] *US. Pat. No. 2141571*, 9 November 1935
[212] Kennedy, H. L.: *Ind. Eng. Chem.*, **28,** 936 (1936)
[213] Dawley, E. R.: *Pit and Quarry*, **32(7),** 44, 63 (1939); *Pit and Quarry*, **36(7),** 57 (1943), *Cement and Lime Manf.*, **17(1),** 1 (1944)
[214] Bond, F. G., Agthe, F. T.: *Mining Technol.*, **4** (1960)
[215] Sweitzer, G. W., Craig, A. E.: *Ind. Eng. Chem.*, **32,** 751 (1940)
[216] (Higerovits, M. I., Leibovits, H. M., Muhamedzjanov, M. M.) М. И. Хигерович, Х. М. Лейбович, М. М. Мухамедзянов: *Информационные Сообщения НИИцемента (Москва*, **10** (1951)
[217] (Skramtaev, B. G., Rojak, S. M., Malinin, Ju. S.) Б. Г. Скрамтаев, С. М. Ряк, Ю. С. Малинин: *Производство и применения пластифицированного цемента.* Промстройиздат, Москва 1953
[218] (Salidzhanov, S. B.) С. Б. Салиджанов: *Применение соапстока в качестве интенсификатора помола сырья и клинкера и гидрофобизация цемента на цементных заводах.* Стьроиздат, Ташкент 1965
[219] (Ginzburg, Ju. N.) Ю. Н. Гинзбург: *Новое в науке и технике о цементе*, **75,** Гипроцемент, Ленинград 1958
[220] (Muchin, N. B.) Н. Б. Мухин: *Новое в науке и технике о цементе*, **7–8,** Гипроцемент, Ленинград 1950
[221] Mardulier, F. J.: *Rock Products*, May (1967)
[222] Mardulier, F. J.: *Rock Products* (4th annual industry operations seminar). Chicago, III. **12,** 1 (1968)
[223] Mardulier, F. J.: *Cemento-Hormigón (Barcelona)*, **49,** 1363 (1978)
[224] (Rojak, S. M., Pirockij, V. Z.) С. М. Рояк, В. З. Пироцкий: *Строительные материалы*, **7,** 33 (1961)
[225] (Rojak, S. M., Pirockij, V. Z., Macuev, N. S.) С. М. Рояк, В. З. Пироцкий, Н. П. Мацуев: *Цемент*, **30,** 5 (1964)
[226] (Pirockij, V. Z.) В. З. Пироцкий: Исследование сопротивляемости измельчению цементных клинкеров и физико-химических способов интенсификации процесса помола в трубных мельницах. Кандидатская диссертация, Москва 1966
[227] (Grachian, A. N., Doviborova, L. E.) А. Н. Грачьян, Л. Е. Довиборова: *Исследования в области химии силикатов и окислов.* Изд-во Наука, Москва–Ленинград 1965
[228] Gratschjan, A. N.: *Silikattechnik*, **22,** 405 (1971)
[229] Grzymek, J., Gustaw, K., Ostap, K.: *Cement-Wapno-Gips*, **52,** 1 (1965)
[230] Grzymek, J., Gustaw, K., Ostap, K.: *Cement-Wapno-Gips*, **54,** 297 (1967)
[231] Ghigi, G., Rabbottino, L.: *Dechema Monographien. Vol. 57*, Verlag Chemie, Weinheim 1967
[232] Ghigi, G.: *Cement Technol.*, **3,** 97 (1972); *Cemento*, **3,** 107 (1972)
[233] Iwabuchi, T., Saito, Ch.: *CAJ Review of the 22nd General Meeting.* Technical Session 84 (1966)
[234] Iwabuchi, T., Fujits, Yu., Suzuki, M.: *CAJ Review of the 21th General Meeting.* Technical Session 115 (1967)
[235] Iwabuchi, T., Shimobayashi, S., Suzuki, M.: *CAJ Review of the 23th General Meeting.* Technical Session 121 (1969)
[236] Iwabuchi, T., Okane, H., Sanami, T.: *CAJ Review of the 23th General Meeting.* Technical Session 191 (1969)
[237] Iwabuchi, T.: *CAJ Review of the 24th General Meeting.* Technical Session 75 (1970)
[238] Tanemura, T., Iwabuchi, T., Okane, H., Nahano, S.: *CAJ Review of the 24th General Meeting.* Technical Session 74 (1970)
[239] Iwabuchi, T., Takeuchi, Sh.: *CAJ Review of the 27th General Meeting.* Technical Session 58 (1972)
[240] Iwabuchi, T.: *CAJ Review of the 26th General Meeting.* Technical Session 70 (1972)
[241] (Edelyman, L. I., Sominskij, D. S.) Л. И. Эдельман, Д. С. Соминский: *ДАН СССР*, **114** (1957)
[242] Blanks, R. F., Kennedy, H. L.: *The Technology of Cement and Concrete.* Wiley, New York 1955
[243] Scheibe, W., Dallmann, W., Rosenbaum, A.: *Silikattechnik*, **21,** 11 (1970)
[244] Scheibe, W., Dombrowe, H., Hermann, R.: *Építőanyag*, **27,** 290 (1975)
[245] (Kudrjavceva, N. L., Hodakov, G. S.) Н. Л. Кудрявцева, Г. С. Ходаков: *Коллоидный журнал*, **33,** 11 (1971)

[246] Zadák, Z., Kurka, F.: *Silikaty*, **13,** 241 (1969)
[247] Zadák, Z., Zezulka, I.: *Silikaty*, **14,** 49 (1970)
[248] (Melnik, M. T., Piven, J. A.) М. Т., Мельник, И. А. Пивень: *Цемент*, **42,** 6 (1969)
[249] Quelle, M. S., Rochietta, C., Rosignioli, D., Cussino, L.: *Zement-Kalk-Gips*, **25,** 234 (1972)
[250] Tanaka, T.: *Zement-Kalk-Gips*, **15,** 28 (1962)
[251] (Krichtin, G. S., Nudely, M. E.) Г. С. Крыхтин, М. Э. Нудель: *Труды НИИЦемента, (Москва)*, **26,** 1972
[252] (Nudely, M. E., Krichtin, G. S.) М. Э. Нудель, Г. С. Крыхтин: *Труды Всесоюзного Научно-исследовательского Института цем. пром. (Москва)*, **26,** 1976
[253] Börner, H.: *Zement-Kalk-Gips*, **21,** 148 (1968)
[254] Weinhold, H.: *Zement-Kalk-Gips*, **23,** 479 (1970)
[255] Péntek, L.: *Építőanyag*, **28,** 453 (1976)
[256] Péntek, L.: *Építőanyag*, **38,** 305 (1986)
[257] (Tovarov, V. V.) В. В. Товаров: *Труды ГИПРОЦемента (Ленинград)*, **1,** 1940
[258] (Butt, Ju. M., Berkovich, T. M.) Ю. М. Бутт, Т. М. Беркович: *Вяжсущие вещества с поверхностноактивными добавками*. Стройиздат, Москва 1953
[259] (Krichtin, G. S., Pirockij, V. Z., Rojak, S. M.) Г. С. Крыхтин, В. З. Пироцкий, С. М. Рояк: *Цемент*, **34,** 31 (1961)
[260] *FRG Pat. No. 924965*, 19 July 1952
[261] *Brit. Pat. No. 788 155*, 21 April 1954
[262] *Öster. Pat. No. 190 022*, 15 July 1956
[263] *FRG Pat. No. 1158 348*, 21 April 1960
[264] *FRG Pat. No. 1220 775*, 21 April 1965
[265] *Canad. Pat. No. 778 814*, 4 May 1967
[266] *Hung. Pat. No. 155 524*, 1968
[267] Opoczky, L.: *Forschungen im Zusammenhang mit Asbesten neuer Lagerstätten*. Verlag BAUFA, Leipzig 1975
[268] Fietsch, I., Ramdohr, H.: *Baustoffindustrie (Berlin)*, **26,** 172 (1983)
[269] (Jalanskij, S. T., Shcherbina, R. O., Belokrus, C. A.) С. Т. Яланский, Р. О. Щербина, Г. А. Белокрус: *Огнеупоры*, **7,** 30 (1983)
[270] (Kovzin, T. G., Kop, Ju. I., Procenko, I. P.) Т. Г. Ковзин, Ю. И. Коп, И. П. Проценко: *Стекло и керамика*, **8,** 19 (1983)
[271] Maksudchodmaeva, M. S., Ismailov, A. H., Vidrik, G. A.: *Silikattechnik*, **31,** 261 (1980)
[272] Suzuki, K., Kuwahara, Y.: *Kona*, **2,** 2 (1984)
[273] (Ustichenko, V. A., Shapovalov, V. S.) В. А. Устиченко, В. С. Шаповалов: *Огнеупоры*, **6,** 17 (1981)
[274] Carta, M., Giuliani, S., Rossi, G.: *European Symposium on Particle Technology*, Preprints, *Vol. A*, Dechema, Frankfurt am Main 1980
[275] Sureshan, M. K., Vederaman, R., Ramanujam, M.: *Particulate Sci. and Technology (Washington)*, **1,** 55 (1983)
[276] Suzuki, K., Tomura, S., Kuwahara, Y.: *Kona*, **20,** 122 (1983)
[277] Laapas, H., Lahtinen, U. R. Luhkarinen, T.: in *Reagents in the Minerals Industry*. The Institution of Mining and Metallurgy, London 1984
[278] Huhn, H. I., Heegn, H.: *Chem. Tech.*, **36,** 510 (1984)
[279] Opoczky, L.: *Építőanyag*, **21,** 188 (1969); *Építőanyag*, **27,** 284 (1975)
[280] Beke, B., Opoczky, L.: *Freiberger Forschungshefte, A* **408,** 67 (1970)
[281] (Nudely, M. E., Krichtin, G. S., Ivanov, M., Opoczky, L., Mrákovics-Török, K.) М. Э. Нудель, Г. С. Крыхтин, М. И. Иванов, Л. Опоцки, К. Т. Мраковичне: *Цемент*, **2,** 15 (1978)
[282] Opoczky, L.: Possibilities for the application of surfactants in grinding technology (in Hungarian). *SZIKKTI Tud. Közlemények*, Budapest, **77,** 1983
[283] Opoczky, L., Dékány, I.: *Colloids & Surf.*, **20,** 121 (1986)
[284] Kipling, J. J.: *Adsorption from Solutions of Non-Electrolytes*. Academic Press, London 1965. IUPAC Manual Appendix II, Part I, *Pure Appl. Chem.*, **31,** 579 (1973)
[285] Gregg, S. J., Sing, K. S. W.: *Adsorption, Surface Area and Porosity*. Academic Press, London 1967

Chapter 5

5. STRUCTURAL CHANGES AND MECHANO-CHEMICAL REACTIONS INDUCED BY FINE GRINDING

The primary mechano-chemical processes that take place during grinding, and which are characterised by an increase of free energy, are essentially induced by three different effects: (1) destabilisation of the internal structure due to lattice deformation, (2) increase of the degree of dispersion and the rupture of chemical bonds resulting in the formation of unstable surface structures of the particles, (3) plastic deformation and heat evolution due to fracture and friction.

Unstable crystal structures may persist even after secondary processes associated with a reduction of free energy (recrystallisation, agglomeration, etc.) have been completed. Also, because of activation, the chemical reactions that lower the chemical potential may already start during grinding, and the ground material gradually acquires a tendency for surface and chemical interactions. In summary, the characteristics of the material may substantially change during, and as a consequence of, fine grinding.

The general features of these phenomena will be presented and will be followed by a specific discussion of mechano-chemical activation and mechano-chemical reactions of a number of silicate systems.

(a) The deformation of the crystal lattice and some of the related general structural problems have already been discussed in Chapter 3. Here we emphasize, once more, that for materials and modes of loading for which a yield point exists, then the maximum chemical reactivity occurs around the yield point because it is at this point that the dislocation density is at its maximum. If this limit is exceeded, due to relaxation phenomena, then the dislocation density and, therefore, the chemical reactivity, may diminish.

For real crystals the free energy and the number of lattice defects show the following relationship [1]:

$$f = u - Ts = nE_u - kT \ln \frac{N!}{(N-n)!\,n!}, \qquad (1)$$

where n is the number of lattice defects, N the total number of lattice atoms, E_u the lattice energy, and k the Boltzmann constant. This function has a minimum at the critical value of n_c which represents the most probable number of lattice defects. It then follows that any external effect that increases the free energy of the system may either increase or decrease the number of lattice defects. This explains the observation that

chemical reactivity often changes periodically on increasing the mechanical load ("mechanical activation" and "passivation" in the terminology of Naeser and Scholz [2]).

(b) Several authors show [3–6] that fracture may be connected with the rupture of chemical bonds by the application of mechanical energy. According to Smekal [3, 4] chemical bonds are ruptured, when, for example, during tension, the distance between particles (ions, molecules or atoms) amounts to twice the equilibrium distance.

The possibility of bond cleavage in a vibration mill has been supported by Schrader and Tetzner [7]. First, they calculated the force (F_g) acting upon the particles of the ground material by the balls of the vibration mill using Liebold's equation:

$$F_g = 1.5c(k\sqrt{E_\rho 2v_a})^{1/3}, \tag{2}$$

where F_g is the compression force of one grinding ball, c is a material constant depending on the Poisson constant, k is a constant, E is the elasticity modulus of the balls, ϱ their density, and v_a their elevation velocity. It was established that the experimental value of F_b in mills is 6660 MPa with steel balls, and 2280 MPa with porcelain balls.

Thereafter, they determined the force required to crush the crystals (e.g. LiF) in the ground material. For this they used Born's formula for the lattice energy (E_u) of ideal crystals of ionic lattice type based on Eucken's theory:

$$E_u = \alpha' V_0^{-1/3}\left(1 - \frac{1}{m}\right), \tag{3}$$

where α' is the modified Madelung constant depending on the lattice type, V_0 the molar volume, and m the attraction constant.

If a sphere having a volume of V_0 in an unloaded state is extended to volume V, work, equal to the difference of lattice energy in the unloaded and extended state, has to be supplied:

$$W = \alpha' V_0^{-1/3}\left(1 - \frac{1}{m}\right) - \alpha' V^{-1/3}\left[1 - \frac{1}{m}\left(\frac{V_0}{V}\right)^{\frac{m-1}{3}}\right]. \tag{4}$$

The plot corresponding to Eq. 4 is shown in Fig. 5.1(a) (curve W). Its value at V_0 is 0; from this point to the right W increases steeply to a critical value of V_z; beyond this point its increase is less steep. In other words, specific extension between V_0 and V requires the input of more work than that beyond V_z and this is due to weaker attraction between ions in this latter section. V_z represents the volume of the crystal in the instant of fracture; its exact value was determined by two additional differentiations:

$$\frac{dW}{dV} = P, \tag{5}$$

where P is the force generated on tension of the lattice. This varies with V according to the curve for P shown in Fig. 5.1(a). Subsequently, the function $P = f(V)$ was

differentiated according to V, in order to find the maximum of the function. These calculations indicated that the volume of a hypothetical spherical LiF crystal of 1 mol mass changes at 293 K temperature from the equilibrium volume of 11.3 cm^3 to 17.1 cm^3 on being elongated to the point of fracture. The corresponding energy input is 54.85 kJ/mol and the limiting tension 13,370 MPa.

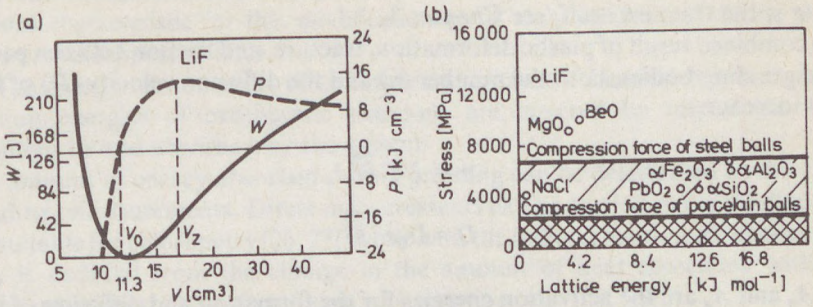

Fig. 5.1. Results of calculations concerning the possibility of cleaving chemical bonds by comminution [7]

The force exerted by the balls in the vibration mill is 6660 MPa and, therefore, the bonds of the lithium fluoride crystal cannot be cleaved in this way. Similar calculations were carried out by the same authors for other crystals. It becomes apparent from Fig. 5.1(b) that crystals of NaCl, PbO_2, SiO_2 and Fe_2O_3 can only be crushed by using steel balls: they cannot be crushed with porcelain balls. Even the force calculated for steel balls was insufficient to rupture the bonds in LiF, BeO, and MgO. Experience shows, however, that MgO crystals do disintegrate in a vibration mill [8]. In an attempt to explain this finding Schrader and Tetzner [7] supposed that, even when grinding with porcelain balls, stress peaks exceeding the theoretical values are generated in certain space elements of the crystals which are sufficient to cleave chemical bonds. Anyway, strong electron emission and tribo-luminescence is often observed with solids, such as mica, gypsum, quartz, calcite, K_2SO_4, alkali halides, in the instance of fracture and indicate that mechanical forces generated in the course of grinding are capable of disrupting chemical bonds [9–14].

The possibility of chemical bond cleavage during mechanical activation is supported by more data. Thus, Boldirev and his co-workers [6] used EPR spectroscopy to demonstrate the formation of paramagnetic centers in certain ionic-covalent bonded salts under the action of mechanical load. The presence of such centres indicates that, in the course of mechanical treatment first of all at fracture fronts and then at contact points of the particles, the electrons at certain sites of the lattice are excited to such high levels that covalent bonds undergo cleavage and this produces free atoms or radicals. Due to the impulse character of mechanical loading these radicals remain in the matrix and, in the period of local heating that accompanies fracture, they initiate the formation of new paramagnetic centres. They disappear if the local temperature reaches their decomposition temperature.

(c) As a consequence of mechanical loading—by impact, friction, or fine grinding—a substantial increase of temperature occurs. Bowden and Teabor [15] coupled two

rods made of different metals to a thermo-element, subjected them to friction between rotating discs and found that they heated up by 1273 K. The increase of temperature depended on the nature of the sample as well as on the mode of applying the load (e.g. speed of rotation of the discs). According to their calculations, hot spots due to fast deformation appeared in the material and these spots had a lifetime of about 10^{-4} s.

One source of increase in temperature during mechanical dispersion and fine grinding is the fracture itself, see Chapter 3.

As a combined result of plastic deformation, fracture, and friction between particles and the grinding bodies, both the number (n) and the diffusion velocity (D) of lattice defects increase:

$$n = Ne^{-\frac{A_n}{kT}} \tag{6}$$

$$D = D_0 e^{-\frac{A_d}{RT}}, \tag{7}$$

where A_n and A_d are the activation energies for the formation and diffusion of lattice defects, and D_0 is a material constant.

The increase of lattice defects in the course of grinding promotes auto- and hetero-diffusion processes, as well as interaction of the reaction partners.

As already pointed out in the discussion on the mechanism of agglomeration (Chapter 4), the particles are compressed and rubbed against each other during the process of fine grinding. In this way they approach closer to each other, their contacting surface increases and, at the same time, their mutual penetration is promoted. All this is a pre-condition for chemical reaction to take place.

Although heating during grinding facilitates the modification of the crystal structure and the mechano-chemical interactions, heating is not the sole cause of these phenomena. The mechanisms and products of the chemical reactions induced by fine grinding and by mechanical activation differ from those produced by thermal energy alone [16–23]. From the point of view of mechano-chemical reactions the decisive effects are the combined effects of stress, heat, and pressure, and their impulse-like character.

Mechano-chemical effects are highly dependent on the propagation velocity of cracks and of the nature of the material. The usual products are formed with slowly propagating cracks while fast propagation produces novel products.

(d) The extremely high local pressures which are generated at contact points of the particles play an important role in mechano-chemical reactions (for example, formation of polymorphic modifications stable at high pressure, amorphisation, etc.).

Structural changes that proceed during grinding and under high pressures have been the subject of several studies. For example, experiments by Carey Lea [24] deal with mechano-chemical reactions and amorphisation, and those by Krauth [25] compare the deformation of the crystal structures of ground vanadium carbide, tantalum carbide and zirconium nitride with active products of the same materials produced in a vibration mill. He established that the structural effect of grinding in a vibration mill for 300 hours was equivalent to a pressure of 5000 MPa applied in their experimental device. The density of dislocations increased from the static value of 10^6 cm^{-2} to 10^{10}

or 10^{11} cm^{-2}. The experiments showed that the degree of amorphisation depended on the nature of the material.

By making measurements with a diffractometer of very high resolution Boldirev and his co-workers [20] established that during the deformation of metallic tin cut by a tool, pressures in the order of 10^{10} Pa were induced locally in areas of about 0.1 mm^2 and the tin was transformed into another modification (Sn II), but the 110, 101, and 100 reflections characteristic for this modification could only be detected during the first 900 ms and disappeared later.

(e) The energy requirements of endothermic mechano-chemical reactions and the activation energies of exothermic reactions are covered by mechanical energy transmitted to and absorbed by the system.

The amount of energy absorbed during grinding can be determined both by direct and indirect measurements. Direct measurements can be carried out in modified mills made suitable for calorimetry [26, 27], while with the indirect method the change in free energy is deduced from the change in the amount of heat associated with some chemical reaction such as dissolution, dehydration, etc. [28, 29].

(f) The rate of a mechano-chemical reaction is influenced by the nature of the reaction partner; by the mode of mechanical loading (compression, impact, shear, friction, etc.); by the type of mill; by the medium; and by secondary effects and processes. All these factors make the description of the kinetics of a mechano-chemical process rather complex and, despite repeated attempts in recent years [30–34], no general correlations can be put forward.

5.1. CHANGES IN THE CRYSTAL STRUCTURE

According to Budnikov and Ginstling [35] two kinds of thermally induced transformations can be distinguished in solids and these leave the chemical composition unchanged: shrinking and polymorphic transformations. With mechano-chemical reactions these effects have to be complemented by a special type of transformation, amorphisation. Amorphisation is preceded by the distortion of the crystal lattices.

(a) Shrinking is the co-crystallisation of neighbouring particles resulting in diminished specific surface and surface free energy, i.e. in the stabilisation of the system. In general, the higher the degree of dispersion of a material the greater its tendency to shrinking. The process is coupled with the gradual disappearance of pores; the smaller pores are eliminated before the larger ones.

Frenkel [46] distinguished two phases of the shrinking process:

—co-alescence of particles: closed pores appear, open ones disappear;
—the volume of closed pores become smaller due to surface tension (compacting).

Shrinking is caused both by the interpenetration of individual particles (fritting), and by the appearance of a liquid film (melt) on the surface of the particles: these initiate the co-crystallisation of particles (sintering).

The process that corresponds to shrinking (fritting and sintering) in mechano-

chemical processes connected with comminution is agglomeration, which was discussed earlier in this book.

(b) Polymorphic transformations are structural changes which do not involve an alteration of chemical composition. One of its forms is enantiotropic transformation which is usually reversible and endothermic. An other form is monotropic transformation which is mostly irreversible and exothermic.

Two kinds of polymorphic transformations can be distinguished. In the first, an increase of temperature changes the crystal structure abruptly at well defined temperatures and show a significant thermal effect. At the transformation temperature the vapour pressure curves of the two phases intersect (e.g. inter-conversion of α- and β-quartz). In the other case, transformation takes place in the form of small jumps and, thus, it appears to be continuous: the two inter-converting crystal structures are not very different and no measurable thermal effect appears (e.g. inter-conversion of α- and β-cristobalite).

Mechano-chemically induced polymorphic transformations have often been observed and they may produce either the more stable or the less stable modification.

The transformation of a modification that is unstable at room temperature to the stable form is rather common; the activation energy of such a process is provided by the absorbed mechanical energy. The flow of dislocations during plastic deformation permits the displacement of atoms to such a degree that the more stable crystal structure may develop spontaneously. An example of such a transformation is the transformation of wurtzite (β-ZnS, $\varrho = 3.98$ g/ml) to sphalerite (α-ZnS, $\varrho = 4.1$ g/ml) which is stable at room temperature: this effect takes place by grinding wurtzite in air or in cyclohexane [36, 37]. Imamura and Senna explained this phenomenon [38] by the changing of the loose hexagonal lattice of wurtzite to the more compact cubical sphalerite structure by the movement of dislocations. The same change can also be induced by heating wurtzite to 1123 K. Similar transformations can be observed when dry grinding many other materials, e.g. Ag, Co, Fe_2O_3, $CaCO_3$ (vaterite), AgZn, CdS and CdSe [36, 39–43]. Examples from the silicate field include modifications of Ca_2SiO_3 [44], and the transformation of proto-enstatite to clino-enstatite [45].

In mechano-chemical processes characterised by the transformation of a stable modification to an unstable one, the energy requirement of the process is covered by the absorbed mechanical energy. Modifications which are stable at higher pressure or temperature, and are formed by instantaneous local jumps of temperature or pressure generated by mechanical load, persist after unloading because their state is "frozen in". Two explanations are offered for the formation of unstable modifications: internal stresses induced by deformation may induce a one-step transformation of the stable modification; alternatively, a transient amorphous structure which comes into being under the gradual re-ordering effect of deformation, fracture, and heat, and according to Ostwald's rule, via already ordered but metastable intermediate structures. If any of the transformation rates of the intermediate phases are very low then the unstable modification may survive for a long time. Both processes probably occur among mechano-chemically induced changes.

An example for such a polymorphic transformation is the conversion of massicot (orthorhombic PbO, $\varrho = 9.64$ g/ml) to the unstable lithargite (tetragonal, $\varrho = 9.35$ g/ml) at room temperature [38]. According to Senna and Iguchi [60] during the

grinding of massicot, the nucleation of lithargite is initiated by the flow of dislocations. Increases of pressure and temperature result in a reversal of the above transformation [47], and this may occur also during the grinding of lithargite. But, Senna says that this process is slow and is often further retarded by the formation of $PbCO_3$ due to the uptake of CO_2 from the atmosphere. Other examples are the transformation by grinding of hexagonal graphite to the unstable rhombic modification (Naeser and Scholz [48]) and of rhombic graphite to the hexagonal form (Boehm and Hofmann [49]). The latter transformation normally requires a pressure of 14,700 MPa [50]. The formation during grinding of modifications which are stable at high pressure has been observed with PbO, PbO_2, MnF_2, and Sb_2O_3 [51, 52], as well as the formation of complex salts [48]. Bridgman [53] reported the transformation, on grinding, of red HgO to the black modification and the transformation of red phosphorus to black phosphorus. This latter modification is normally formed at 473 K and at static pressures of several thousands MPa [54].

The transformation of trigonal calcite during grinding to rhombic aragonite, which is unstable at room temperature and atmospheric pressure, has been reported by several authors [55–59]. According to Schrader and Hoffmann [55] the calcite $\rightleftarrows$ aragonite transformation is reversible. This result was supported by the fact that after grinding either calcite or aragonite for a sufficiently long time the product ratio was the same. In other words, the process leads to a mechano-chemical equilibrium. The position of the equilibrium depends, of course, on the conditions of grinding and can be influenced by impurities in the calcite [60].

The transformation of calcite to aragonite is influenced by the magnitude of the mechanical forces which are acting upon the particles of the grind. As it becomes apparent from Fig. 5.2, aragonite appears at a critical value of the grinding force and its proportion increases on increasing this force. The formation of aragonite is preceded by distortions of the calcite lattice. Mechano-chemically induced polymorphic interconversions have been observed with many other compounds (PbO_2, ZrO_2, ZnS) [61, 62].

It is remarkable that, despite the fact that it can exist in several polymorphic modifications, no mechano-chemical polymorphic transformations of SiO_2 have been described in the literature or observed in our own experiments.

(c) Distortions of crystal lattices are disorders which do not involve fundamental qualitative alterations of the crystal structure. This concept covers the formation of lattice defects, the increase of their density, the rearrangement of atoms within the lattice (stepping out of atoms from lattice points), the alteration of the distance of lattice planes due to the appearance of dislocations, etc.

(d) Mechano-chemical amorphisation of the crystal lattice means the total disintegration of the ordered structure of a crystal as a consequence of mechanical forces. The internal structural disordering of solids which is generated by mechanical load is associated with the formation, flow, and interaction of dislocations, and it may persist after "unloading". If the decay of internal atomic order in a material after the release of the deforming mechanical force attains a degree which is more characteristic of an amorphous material than for a crystalline one, then the phenomenon is called mechano-chemical amorphisation.

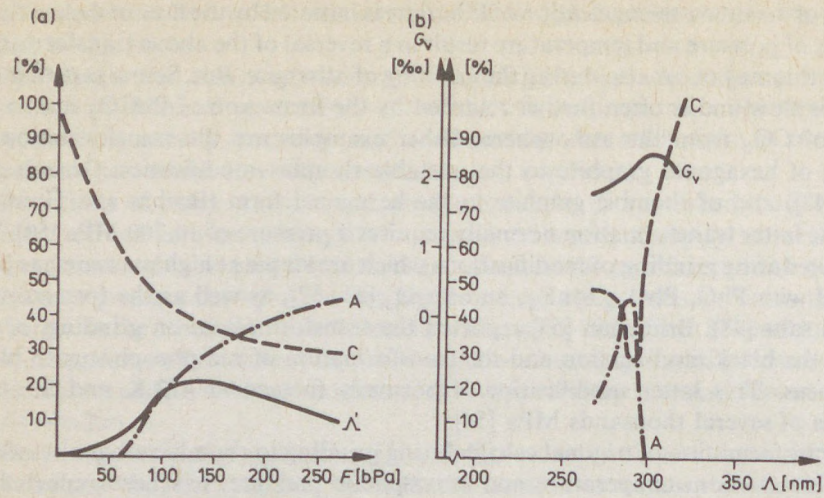

Fig. 5.2. (a) Transformation of calcite (C) into aragonite (A) and the relative change of crystallite size (Λ') as a function of mechanical grinding force (F). (b) The change in percentage of calcite (C) and aragonite (A), and lattice distortion (G_v) as functions of crystallite size [59]

Amorphisation that proceeds during fine grinding can be attributed to plastic deformation of sufficiently small particles in the grind.

The kinetics of the amorphisation of minerals have been thoroughly studied by Schrader and his school [7, 8, 55 etc.]. A diminution in the size of crystallites, distortion of the lattice, and amorphisation, are processes which can be more or less separated in time.

The degree of amorphisation increases steadily as a function of grinding time until it reaches a final equilibrium value. The position of the equilibrium depends both on the nature of the material and on the mode of grinding. The role of recrystallisation processes is also important.

(e) Structural changes and amorphisation during grinding can be detected by X-ray crystallography [63–69].

The dimensions of the individual, mostly submicroscopic, crystallites can be inferred from the width of X-ray peaks. However, line broadening is not only the consequence of a reduction of crystallite size; it can also show a change in crystal structure. Both effects have to be considered in fine grinding. Kochendörfer [64] pointed out that the two effects may be distinguished by an analysis of line broadening as a function of the angle of inclination.

It has been known for many decades that X-ray peaks broaden on plastic deformation of the specimen. This phenomenon has been observed mainly in the cold-working of metals and alloys. Thus, an alteration of the X-ray pattern of tungsten on cold-working was observed by Arkel [70] and Goucher [71] as early as 1926 and it was interpreted by them as being a manifestation of the disintegration of crystalline order. Burgers [72] and Wassermann [73] observed a similar change after cold-drawing of Ni—Fe rods, and Paudert and his co-workers observed the same effect with zinc [74].

Dehlinger [75] pointed out in 1927 that the diffraction pattern of aluminium can be correlated with its processing history.

Amorphisation was not only observed with metals but also with many other types of materials, such as inorganic compounds (e.g. the salts of iron, nickel, and titanium, phosphates, ores), organic compounds (e.g. cellulose [76, 77]), and certain crystalline polymers [78]. Amorphisation was triggered both by simple macroscopic deformation and by fine grinding.

Since changes in the fine structure of a material, as indicated by a broadening of its X-ray lines and the energy stored in the crystal lattice are closely correlated, the study of these phenomena is important in the fine grinding of minerals. However, the structure of minerals is usually more complex than metals. Structural alterations due to mechanical action are, therefore, less pronounced and they are less easy to detect than with metals which can also be subjected to plastic deformation. In addition, the majority of materials used in the silicate industry are mixtures of several minerals, e.g. cement clinker and, therefore, their X-ray diffraction patterns appear as complexes of superimposed lines which can only be evaluated with much difficulty.

In the fine grinding of materials used in the silicate industry the structural changes and amorphisation is often coupled with agglomeration, and this renders the evaluation even more complex.

In recent years the methodology of mechano-chemical studies has been enriched by a number of modern physical methods, such as EPR, and IR spectroscopy, electron diffraction, radio-spectroscopy, photoelectron spectroscopy, Mössbauer spectroscopy etc. [20, 79–84, 100].

5.2. MECHANO-CHEMICAL REACTIONS

Among secondary processes that take place in systems activated by mechanical energy and which are characterized by a drop in free energy, only those chemical reactions and structural changes which proceed in solids directly during the application of mechanical load will be summarised in this section. According to Peters [16] only such processes can be called mechano-chemical reactions.

By following the usual classification of physical chemistry, mechano-chemical reactions can also be characterised as being homogeneous or heterogeneous [85]. However, for any specific reaction it is often difficult to make such a clear-cut distinction when the whole sequence of processes is considered. Therefore, the above classification is only meaningful for the starting materials and the products of the reaction.

5.2.1. HOMOGENEOUS MECHANO-CHEMICAL REACTIONS

The simplest process involving a decrease of free energy is the spontaneous re-ordering of a crystal structure which has been disarrayed by mechanical activation. However, this re-ordering is never complete and, therefore, on repeated loading (e.g. during

grinding or repeated mechanical treatment) the residual disordering after each cycle accumulates and the solid undergoes gradual amorphisation.

Re-ordering can often be observed when grinding silicates, especially following agglomeration. One example is provided by the polymorphic transformations of unstable phases into stable variations.

Mechano-chemical re-crystallisation of crystalline materials, which can be observed, for example, with materials containing water of crystallisation is somewhat different from the above process. For example [86]: if pure $CuSO_4 \cdot 5H_2O$ is ground for a few hours in a closed vibration mill, no change in its chemical composition or in its X-ray diffractogram can be observed. Grinding in an open mill or in vacuum reduced the crystal water content (H_2O_{cryst}). This effect is typical of mechano-chemical processes, the first stage of which is the release of crystal water in the deformation phase, followed by capillary condensation of this water in the pores of the particle during the unloading period:

$$H_2O_{cryst} \rightarrow H_2O_{cond}.$$

This process requires the surmounting of a potential barrier and the necessary energy is provided by mechanical activation. Energy absorbed in the elimination of crystal water is partly recovered during condensation. The magnitude of the activation energy depends both on the bonding energy of crystal water and on the morphology of the pore system.

The second stage of the process is, for water soluble solids, the dissolution of the walls of the capillaries in the condensed water. Minute crystals precipitate when this solution becomes oversaturated, for example, $CuSO_4 \cdot 5H_2O$ (re-crystallisation).

Similar behaviour has been observed with other materials containing crystal water [87, 88]. For example, mechanical activation of gypsum hemihydrate ($CaSO_4 \cdot 0.5H_2O$) results in a gradual increase of setting time. In fact, after very long grinding in a closed mill, the start of the setting process cannot be determined exactly. This can be

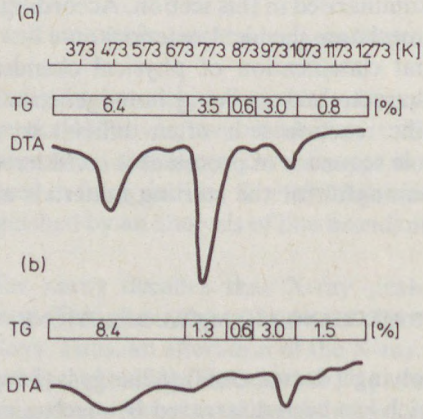

Fig. 5.3. DTA curves and loss of mass of set cement (a) before, and (b) after grinding [98]

explained by the fact that the water released from the hemihydrate and which condenses in the capillaries forms a solution of calcium sulphate from which crystals of the dihydrate precipitate. In this way, the readily setting hemihydrate is gradually transformed to a mixture of non-setting dihydrate and slowly setting anhydrite ($CaSO_4$).

When grinding hydroxides or hydroxy-containing silicates the transformation of structural water with a high bonding energy to one with less bonding energy or to gel-water has often been observed. For example, the transformation of kaolinite into fire clay and the formation of tobermorite gel from portlandite during the grinding of cements that are not fully hydrated. Such reactions, which can be represented by the scheme,

$$2(R—OH) \rightarrow R_2O(H_2O)_{gel},$$

where R is the rest of the silicate structure, can be conveniently followed by thermal analysis (cf., Fig. 5.3).

In a prolonged grinding procedure gel water is transformed to the gas phase or retained as adsorption water of smaller bonding energy.

5.2.2. MECHANO-CHEMICAL DISSOCIATION

The dissociation of carbonates under mechanical load has often been reported in the literature. Fischer et al. observed [89] the evolution of carbon dioxide on grinding calcite, magnesite, ankerite, aragonite, and iron spar in a vacuum mill. Other authors have described the dissociation of the carbonates of sodium [90], the alkaline earths, and of Ni, Cd, Mn, and Zn [91–93]. The evolution of carbon dioxide and a decrease of the original carbonate content by 40% were found on grinding limestone in an air-jet mill [94]. No change in the CO_2 content was observed when the mill was run in an atmosphere of carbon dioxide, but in this case most of the calcite suffered amorphisation.

It should be noted, however, that the details of the mechano-chemical amorphisation of carbonates are still not clear. Pure alkaline earth carbonates resisted mechano-chemical decomposition and amorphisation. This effect may be explained by analogy with the example of copper sulphate described above, i.e. by assuming that decomposition of carbonates takes place in the instant of deformation, and that after relaxation of deformation the released carbon dioxide is immediately reabsorbed by the remaining oxides, resulting in no net loss of carbonates. The reversible nature of the reaction was experimentally verified by Peters [16] for the decomposition of $ZnCO_3$. When zinc oxide was ground under carbon dioxide, the formation of zinc carbonate was observed, i.e. the reaction

$$ZnCO_3 \rightleftarrows ZnO + CO_2$$

is reversible leading to a mechano-chemical equilibrium, the position of which depends on the mode of grinding. With materials such as alkaline earth carbonates, for which

the equilibrium constant of dissociation is small at room temperature, unloading may involve almost complete re-formation of the carbonates.

The role of the other materials which are present in the mill during the decomposition of carbonates is still obscure. Smekal [95] observed the formation of CO_2, CaO, and $Ca(OH)_2$ during the grinding of calcite in, most probably, humid air. Heinicke et al. [96] assumed that the dissociation of $NiCO_3$ was promoted by the H_2S content of air; the H_2S immediately reacted with the NiO to give NiS. Decomposition of Na_2CO_3 is promoted by a sufficiently high partial pressure of water in the air space of the mill and, in this case, a few percent of $NaHCO_3$ can be detected in the ground material [97]. It seems that decomposition of carbonates is promoted by some extraneous molecules; these either bind the liberated carbon dioxide or diffuse into the deformed structure of the solid partially converted to the oxide.

Evacuation of the mill may also promote the decomposition of certain carbonates (Fig. 5.4).

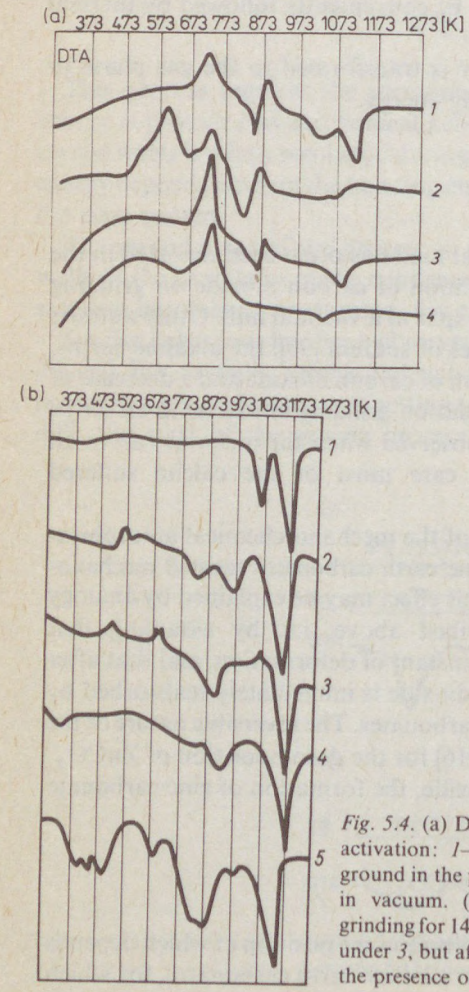

Fig. 5.4. (a) DTA curves of carbonates before and after mechanical activation: *1*—$MgCO_3$, *2*—$MgCO_3$ ground in vacuum, *3*—$MgCO_3$ ground in the presence of water vapour, *4*—$CaCO_3$, *5*—$CaCO_3$ ground in vacuum. (b) DTA curves of dolomite: *1*—Untreated, *2*—after grinding for 14 hours, *3*—after grinding for 32 hours (vacuum mill), *4*—as under *3*, but after washing with water and drying, *5*—after activation in the presence of water [59]

New phases, compounds of changed stability and, occasionally, new complex compounds may be formed from materials in which the individual components modify the dissociation equilibria of each other under the action of mechanical load. This effect is shown by thermo-analytical curves and the change in acid-solubility of the individual components after comminution (in a vibration mill) of a complex carbonaceous iron ore from Rudabánya which consists of a mixture of siderite, dolomite, magnesite and calcite (Fig. 5.5). It was mainly the solubilities of the iron and the magnesium carbonates which were enhanced—probably due to the formation of less stable carbonates, oxides, and complex compounds.

The formation of dolomite was observed during the fine grinding of magnesite and calcite [99].

In contrast to the behaviour of simple alkaline earth carbonates, it was shown that double carbonates decompose relatively readily under the action of mechanical energy [87]. According to DTA studies by Bartha and Bruthans [101], the grinding of dolomite results in a decrease of the decomposition temperature and a decrease of the endothermic peak height of $MgCO_3$. If the experiment is carried out in a closed mill from which water vapours have been carefully removed then exothermic peaks appear in the DTA curves and can be attributed to the crystallisation of MgO arising from the decomposition of $MgCO_3$. This MgO probably contains a large number of lattice defects and is thus, unstable or it may even completely be amorphous [59] (Fig. 5.4). Washing this ground material with water eluted a considerable amount of MgO and the dry residue of the eluted solution did not exhibit the exothermic peaks in the DTA curves. Amorphous magnesium oxide can thus be eluted from the system by water.

The mechanism of the above reaction is not clear, but it is assumed that the CO_2, liberated by the load-induced deformation of the crystal structure, diffuses to the surface and the residual structure undergoes transformations (e.g. formation of interstitial lattice defects). These transformations retard or totally inhibit the re-adsorption of CO_2 after unloading and render the process irreversible.

In the mechano-chemical dissociation of certain carbonates the evolution of CO_2 is associated with oxidation. For example, siderite and rhodochrosite decompc with the uptake of oxygen [52]:

$$2FeCO_3 + O \rightarrow Fe_2O_3 + 2CO_2$$

$$3MnCO_3 + O \rightarrow Mn_3O_4 + 3CO_2$$

The positions of the equilibria of these reactions also depend on the partial pressure of oxygen in the mill, while simple dissociation processes only depend on the partial pressure of CO_2.

Mechano-chemical dissociation can be encountered with materials other than carbonates. Examples include the dissociation of barium peroxide giving rise to BaO and O_2 [102]; the liberation of methane from brown coal; and the dissociation of NaCl.

Some hydroxides [217] and silicates [88] containing structural water (OH groups) may dissociate directly in the course of grinding as follows;

$$2(R—OH) \rightarrow R_2O + (H_2O)_{vapour}.$$

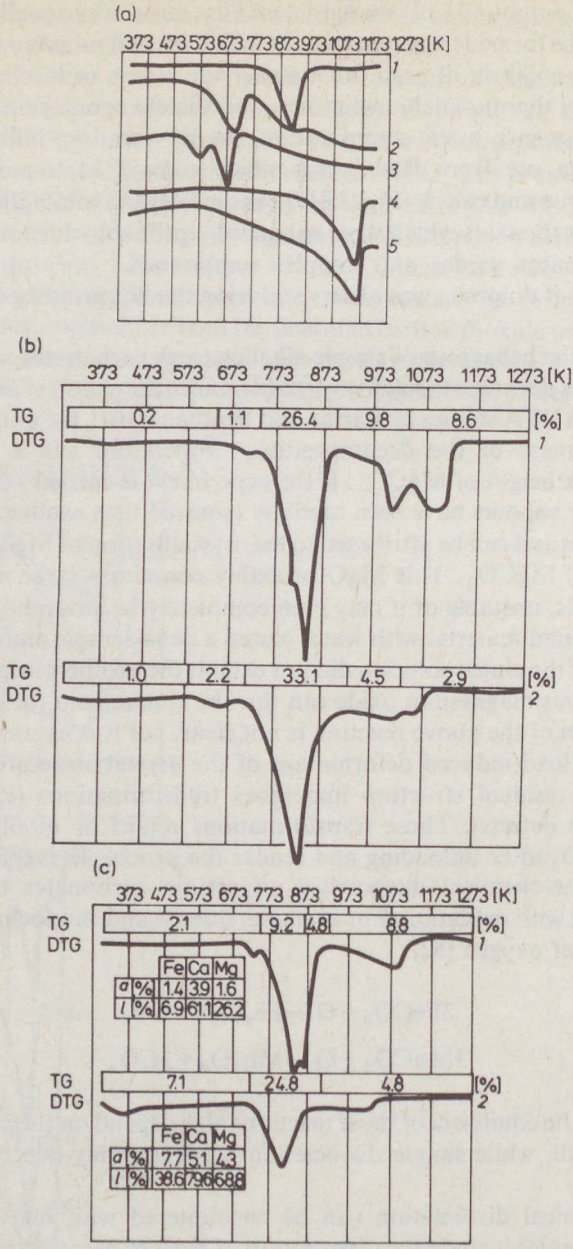

Fig. 5.5. (a) DTA and (b) DTG curves of a complex carbonate ore from Rudabánya (Hungary): *1*—Untreated, *2*—after mechanical activation, *3*—acid dissolution residue from untreated material and *4*—from the activated material. (c) Solubility in diluted hydrochloric acid and DTG curves (after treatment) of a complex carbonate ore from Rudabánya. *1*—Untreated, *2*—after mechanical activation. The quantities of dissolved cations are related to the mass of the sample (*a*) and to the original cation content (*l*) of the sample [59].

On prolonged grinding the silicate gels that are produced during a homogeneous phase reaction will also decompose;

$$(R_2O)\cdot(H_2O)_{gel} \rightarrow R_2O + (H_2O)_{vapour}.$$

5.2.3. MECHANO-CHEMICAL DECOMPOSITION OF ORGANIC AND SILICATE POLYMERS. SURFACE ACTIVATION

Primary mechano-chemical processes induced by deformation can be demonstrated with organic high polymers and plastics. Materials of this kind (e.g. cellulose, polystyrene and other organopolymers) under mechanical load undergo amorphisation or transition to a less ordered structure, and also suffer a significant decrease in the degree of polymerisation and may change their chemical reactivity [103–107].

Barambojm [78] pointed out that during the deformation of plastics (which is often coupled with amorphisation), either the fragmentation of chain molecules takes place (mainly in the "glassy" state) or secondary linkages between chains are cleaved. In the latter, plastic yielding can also be observed. In crystalline polymers amorphisation usually precedes the decrease in the degree of polymerisation.

Chain fragmentation generates free radicals, the lifetimes of which are temperature dependent. In this initial phase chain degradation may be followed by isomerisation.

In the growth period free radicals may induce reactions involving an increase of the degree of polymerisation, either by direct reaction with the polymer itself or with the incorporation of intermediates, solvent molecules, monomers, oxygen, etc. Finally, in the termination phase the free radicals gradually disappear, either as a consequence of the above mentioned reactions or, after the termination of mechanical action, by diffusion or other processes.

The above mechano-chemical processes modify the chemical reactivity of polymers. In general, the solubility increases, changes occur in strength (positive or negative), and plasticity may occur. The acid and ester number and the thermal properties of alkyde resins are altered. Deformation without chain fragmentation may also bring about differences in chemical behaviour. For example, degradation of rubber by ozone is accelerated by stretching.

In the case of crystalline silicates, which can be regarded as polymers (crystal compounds), in the instant of fracture chemical bonds are ruptured and "free valencies" appear on the fresh surface. In such cases comminution involves both a size reduction of crystallites and an enrichment in active surface centres (i.e. of surface elements having a charge surplus). As a consequence, secondary processes are activated and these more or less eliminate this highly unstable state of the surface. Such processes are structural changes due to internal or surface diffusion and to binding of molecules from the environment or from adjacent particles by adsorption, chemisorption, agglomeration. The cleavage of chemical bonds and their exposure at the surface increases the tendency of the grind to trigger off chemical reactions on the surface.

A consideration of the net increase of the chemical potential of the system by increased surface energy allows one to regard fine grinding as surface activation.

Surface activation has important practical implications such as:

"Loosening" of the surface layer and the increased abundance of lattice defects in these regions can be inferred from the change of activity of some metals or contact catalysts during, or as a consequence of, grinding [108]. Thus, the activity of ZnO in the catalysis of hydrogen peroxide decomposition [109], of Si—Cu alloys in the conversion of methyl chloride to chlorosilanes [110], and the efficiency of Ni contact catalysts in a variety of synthetic processes, can be improved by mechanical treatment [111, 112]. These phenomena can only be partly explained by the increase in surface area. At least as important (and sometimes more important) are defective structures on the fresh surfaces, i.e. surface elements with high dislocation density which persist for some time after fracture; these may all function as active centres during contact catalysis. It follows, therefore, that ordering processes or re-crystallisation during storage, or during the use of the catalyst may diminish its activity. If a contact catalyst is also subjected to grinding during a reaction, then the above effects are complemented by the effects of mixing, and the elimination of products accumulated on the surface which inhibit further reaction. Additional effects include accelerated diffusion, thermal effects, and the continuous formation of fresh surfaces rich in lattice defects. Important developments can be anticipated in the application of contact catalysts activated by mechanical energy.

A good example of the surface activation of metal powders is the process developed by Paudert and his co-workers [74] for the recovery of metallic copper and cadmium using mechanically activated zinc powder (cementation). The equilibrium

$$Zn + Cd^{2+} \rightleftarrows Cd + Zn^{2+}$$

can be shifted to the right by increasing the dissolution tension of zinc (which is the less noble partner). It has been found that this task can be solved by intensively grinding the zinc, since the electrode potential of zinc increases as a function of the degree of deformation whilst the yield of cadmium or copper is improved.

It has been known for a long time that the reactivity and hydraulic activity of silicates (which are, essentially, polymers) can be increased by fine grinding. The often very substantial increase in the reactivity of silicate systems cannot be fully explained by smaller particle size and higher degree of dispersion. A wealth of experimental data shows that fine grinding and mechanical activation result in a modification of the atomic structure on the surface. Adamtschik [113] and, Rasch [114] who relied on Adamtschik's concepts and experimental results, rationalised the mechanical activation of silicates by the theory of "separated valencies". "Surface ions" generated by fracture are very active and are capable of forming stable compounds, e.g. with calcium hydroxide. Adamtschik established that minerals that are inert to hydraulic activation, such as basalt, or andesite, may be activated by fine grinding: silicon and aluminium oxide groups on the fracture surface react vigorously with compounds liberated in the course of cement hydration (e.g. $Ca(OH)_2$). Rasch added that $(SiO_3)^{2-}$ ions generated in the instant of fracture are unstable and oxidise rapidly in an exothermic reaction to SiO_4^{4-} by taking up oxygen, water, or other substances from the environment.

The majority of the chemical reactions discussed later, which concern various

crystalline materials, are connected with the surface activation of silicates. (In presenting these reactions there is no need to discuss silicates separately or to distinguish them in any way from other substances.)

5.2.4. MECHANO-CHEMICAL REACTIONS BETWEEN GASES AND SOLIDS

The accelerated oxidation of metals [115], and the oxidation of passive metals under the effect of mechanical load (or as a consequence thereof) has been observed earlier. The rate of tribo-chemical (frictional) oxidation is comparable, even at the temperature of liquid air, to that measured at room temperature. Heinicke et al. [91, 96] observed increased "oxidisability" of a series of metals (Ni, Al, Sb, Cr, Fe, Sn, Zn, Co, Pb, Cu, Hg, and Ag) when grinding them under oxygen and they found that curves of the oxidation rate versus grinding time exhibited a maximum. On the rising branch the rate of oxidation changed in a similar manner to Hüttig's comminution rate [116].

The formal parallelism of oxidation and comminution rates suggested to the authors that high oxidation rates during grinding can be explained by the fact that the oxide layer at the surface is continuously eroded and, therefore, this is always a fresh surface exposed to oxidation. Progressive reduction of oxidation rate after prolonged grinding can, in turn, be rationalised by the depletion of non-oxidised metal and the accumulation of oxides.

Oxidation during grinding or deformation in an atmosphere of oxygen can also be observed with other elements and with non-metallic compounds. Thus, mechano-chemical oxidation of Si, Bi, C, As, Pb, FeS and of other sulphides, as well as FeO and Fe_2O_3, has been reported [2, 91, 117]. Galena gives $PbSO_4$, while FeS gives iron oxides and SO_2.

Metals and inorganic substances may also react with gases other than oxygen under mechanical load.

Heinicke and Harenz [91] studied the formation of $Ni(CO)_4$ from the metal when ground in a CO atmosphere. He established that, in addition to mechanical treatment, the reaction could also be promoted by using a mixture of H_2S and CO. The same phenomenon was encountered when the starting material was $NiCO_3$ and has been explained by the authors by the formation, as an intermediate, of NiS which has a highly disordered lattice and is, therefore, more reactive towards CO than either Ni or $NiCO_3$. The stages of this "sensitised" mechano-chemical reaction are;

$$NiCO_3 \rightleftarrows NiO + CO_2$$
$$NiO + H_2S \rightleftarrows NiS + H_2O$$
$$NiS + 4CO + H_2O = Ni(CO)_4 + H_2S$$

H_2S liberated in the third reaction is used in the second.

On grinding PbO Menyhárt and Domsa [94] observed the formation of yellow lead carbonate according to the following equation:

$$2PbO + CO_2 + H_2O = 2PbCO_3 \cdot Pb(OH)_2.$$

The present authors prepared ZnS, with a yield of 95%, by grinding ZnO in an atmosphere of H_2S. The grinding of polyvinyl chloride in a jet mill under CO_2 resulted in chain fragmentation and in the incorporation of CO_2 at the cleavage sites [118].

The grinding of iron carbide in the presence of hydrogen gave rise to metallic iron and methane [119]. The reduction of iron silicates by hydrogen can be significantly accelerated by mechanical deformation [120]. The same effect can be observed with the reduction of Fe_2O_3 [2].

Elementary silicon can be directly chlorinated by mechanical treatment [121].

$$2Si + 4Cl_2 \rightarrow 2SiCl_4.$$

Beke and Opoczky [122] found that cement clinker takes up CO_2 during grinding. Silanol groups appear on the surface of quartz when it is ground in very humid air. Such interactions between silicate surfaces and water are rather common in connection with grinding and mechanical activation of silicates [123], especially when the humidity of the air in the mill exceeds a certain minimum value, which depends on the particular material, during the whole grinding period.

5.2.5. MECHANO-CHEMICAL REACTIONS BETWEEN LIQUIDS AND SOLIDS

Reactions that proceed at the liquid/solid interface under the effect of intensive stirring are well known: for example, the methylation of a suspension of cellulose in aqueous alkali is promoted by vigorous stirring and shaking to give cellulose methyl ethers [124]. The faster reaction rates cannot always be ascribed to good mixing or to the increase of specific surface: the role of mechano-chemical phenomena discussed earlier may also be important in the activation of such solids.

Alexander and Byers [125] in 1932 observed the evolution of hydrogen in a vibration mill used for grinding wet sand. Mechanical effects which modify the electric and thermal conductivities of metals, or, in general, modify their chemical activity, also affect electrochemical processes. They affect the electric potential and the corrosion behaviour of metals [88]. Their reactivity, and thereby their interaction with liquids, is also changed. For example, $AlCl_3$ is formed when aluminium is strained under CCl_4 whereas $AlCl_3$, HCl and elementary carbon are formed under $CHCl_3$. In the presence of ether and halogen-containing compounds Grignard reactions proceed faster when carried out with deformed than with untreated magnesium [126].

The grinding of silicon under CCl_4 in a vibration mill gave rise to the following reactions (Grohn et al. [127]):

$$Si + CCl_4 \rightarrow SiCl_4 + C_2Cl_6$$

$$CCl_4 + 2H_2O \rightarrow CO_2 + 4HCl$$

$$CCl_4 + H_2O \rightarrow CO + Cl_2 + 2HCl.$$

Reaction products could be detected by electron microscopy [128] at certain points of

the fresh surfaces after splitting calcite and rock salt crystals in styrene. The formation of SiO—C bonds and the hydrophobisation of the grind was observed [129–131] on grinding quartz in the presence of various organic compounds (alcohols, amines). Similar reactions probably take place with various silicates.

5.2.6. MECHANO-CHEMICAL REACTIONS BETWEEN SOLIDS

According to Budnikov and Ginstling [35] reactions between solid phases are feasible at room temperature if the atoms or molecules of the interacting solids are able to penetrate into each other and when the products formed during the reaction do not inhibit further interaction. Diffusion within solids is, in general, extremely slow and, therefore, even such spontaneous reactions are soon halted.

The rate of diffusion within solids is controlled by the number and mobility of dislocations and can usually be increased by heating. As shown in Chapter 3 the number of dislocations can also be increased by lattice deformation, and plastic deformation is closely coupled with the flow of dislocations. It follows that mechanical effects may increase the rate of auto- and hetero-diffusion directly, and by the concomitant elevation of temperature indirectly. In addition, compression, co-grinding, friction, and wear promote the aggregation of reaction partners, reduce the distance apart of these partners, and bring about a continuous removal of the reaction products from the surface. Therefore, mechano-chemically induced reactions between solids at room temperature are not uncommon. It has to be stressed again, however, that the products of mechano-chemical reactions are usually different from those obtained from thermal reactions.

Isakov [132] developed colour tests for most of the elements for the purpose of analysing minerals. The essence of his method is to grind a very small sample with the appropriate reagent and infer, from the colour change, which element is present in the sample. Certain reactions were made more visible by masking. For example, when both Co and Fe(III) salts were present, the sample (e.g. a mixture of $Fe_2(SO_4)_3$ and $CoSO_4$) was ground with NH_4SCN, and gave a red powder due to the $Fe(SCN)_3$ that was formed. Thereafter, this powder was ground with a few crystals of sodium thiosulphate, which reduced Fe(III) to Fe(II) whereby the red colour disappeared and the blue colour of the cobalt complex became apparent. Other reactions were promoted by grinding the minerals in the presence of water vapour. Isakov described a great number of mechano-cheamical reactions.

Lin and Somasundaran [133] ground Ag_2SO_4 with ZnS and CdS under nitrogen and observed chemical reactions that produced colour changes.

Hristo [134] studied the rates and products of reactions in metal–halogen mixtures.

An example of a mechano-chemical reaction between solid silicates has been reported by Tamman [115]. He found that by grinding quartz and calcite together he produced calcium silicate and CO_2. Recently, the formation of Na, Ca, and Mg silicates has been described when quartz has been ground with the corresponding carbonates [16, 94, 135].

According to Peters [16] common grinding of limestone and quartz produced CO_2: a small amount of calcium metasilicate was also formed, as shown by the following

equation:

$$CaCO_3 + SiO_2 = CaO \cdot SiO_2 + CO_2.$$

Mechano-chemical reactions of similar type were observed by Mehta [136] in non-thermal cement manufacturing, in which a mixture of kaolinite, quartz and $Ca(OH)_2$ is subjected to mechanical treatment, i.e. grinding. Co-grinding of clay and lime produced calcium silicates and calcium aluminates.

Mechanical activation combined with heating may perhaps open up new possibilities in the manufacture of silicates. Coney [137] subjected a mixture of CaO, clay, sand, aluminium oxide, and siliceous earth to grinding in a ball mill at 427 K. He obtained a grind showing hydraulic properties and a capacity for setting. Schrader and Köhnke [138] ground cement raw meal in a vibration mill heated to 850 K. The reaction time was controlled by recycling the product. With an input of 2 kg/h the residence time of the material was about 30 min, of which 10 min was at 850 K. After seven-fold recycling about two thirds of the calcium oxide became bound; the intensity of X-ray lines characteristic for calcite, clay minerals, and quartz diminished considerably and, at the same time, new unidentified silicate lines appeared. The strength of the grind, which was supplemented with gypsum in order to adjust setting time, was very low.

By continuing this line of research Philipp and Schrader [139] succeeded in reducing the content of free CaO in cement raw meal to 2% by using a combination of thermal, mechanical, and chemical activation.

Menyhárt and Domsa [94] observed the formation of $MgSiO_3$ after common grinding of MgO and SiO_2; they also observed the formation of sodium aluminate from Na_2CO_3 and Al_2O_3.

5.2.7. MECHANO-CHEMICAL REACTIONS COMBINED WITH CAPILLARY CONDENSATION

Many of the mechano-chemical reactions which appear to take place directly between solid phases, take place, in fact, in a liquid phase that has condensed inside the pores of the ground material. This liquid originates either from the environment or it is the product of an intermediate process. Thus when $CuSO_4 \cdot 5H_2O$ is ground together with alkali or alkaline earth oxides, carbonates, chlorides, or sulphides, chemical reaction between grains of different composition becomes apparent from discolouration, gas evolution, or a muddy appearance [86]. On examining the reaction products one often encounters new materials (e.g. amorphous $CuO \cdot 2H_2O$) which can only be prepared in this way (Fig. 5.6). When anhydrous copper sulphate is ground with the exclusion of moisture no macroscopic signs of a chemical reaction can be noticed. If, however, the grind is exposed later to humid air then, depending on storage time and relative humidity, changes of mass and discolourations can be observed (Fig. 5.7). The composition of the reaction products varies with the relative humidity (Fig. 5.8).

Such experiments suggest that the reactions observed when grinding salts containing water of crystallisation do not take place between solid phases but occur in an aqueous

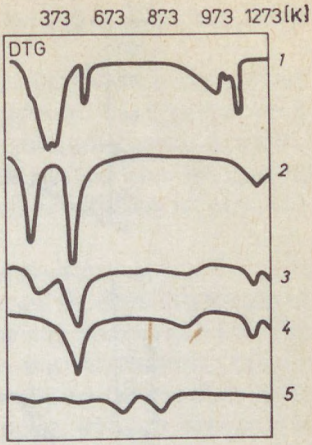

Fig. 5.6. Common milling of $CuSO_4 \cdot 5H_2O$ and $BaCO_3$. Thermoanalytical curves: *1*—Pure $CuSO_4 \cdot 5H_2O$, *2*—mixture of $CuSO_4 \cdot 5H_2O$ and $BaCO_3$ ground for 0.5 hours, *3* and *4*—the same as under *2* but ground for 14 and 23 hours, respectively, *5*—the latter product after storage in air for 8 years [86]

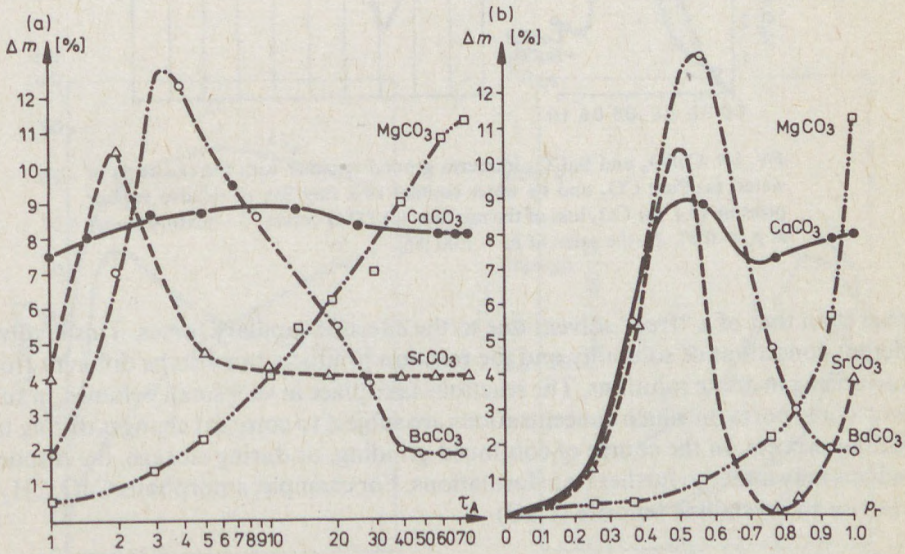

Fig. 5.7. Increase of mass (Δm) of $CuSO_4$ and alkali earth carbonate mixtures ground with the exclusion of water when stored in vapour as a function (a) of time and (b) of the relative vapour pressure (p_r) [86]

medium, i.e. in pores of appropriate size. If the above experiment is carried out with $CuSO_4 \cdot 5H_2O$, the aqueous phase comes from water of crystallisation which is then retained by capillary condensation in the pores. This water, as shown earlier, is then reincorporated into the lattice or, if no proper reaction partner is present results in recrystallisation. In our case, however, water condensed at the contact points of particles of different composition is the location of the chemical reactions.

The examples shown are regarded as special mechano-chemical reactions, since they were exclusively the result of mechanically-induced crystal deformations. It has to be emphasized that these reactions proceed in a solvent the internal pressure of which is

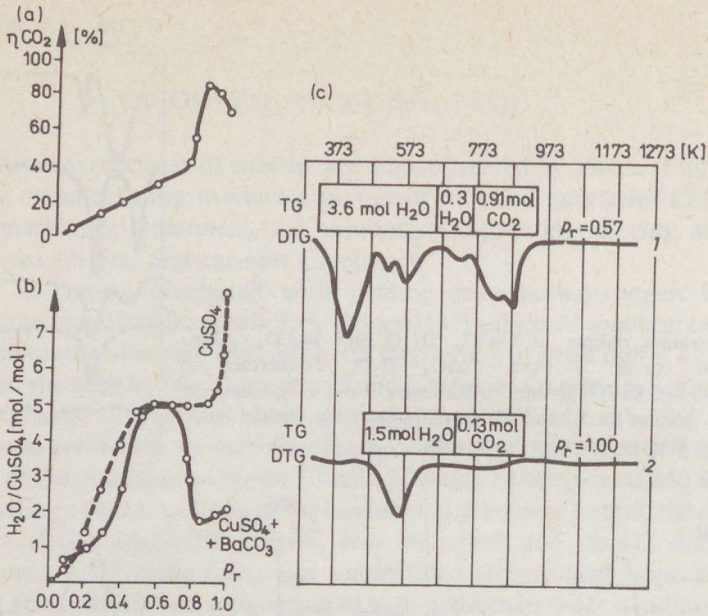

Fig. 5.8. $CuSO_4$ and $BaCO_3$ mixtures ground together with the exclusion of water. (a) Pure CO_2 and its water content as a function of relative vapour pressure (p_r). (b) CO_2 loss of the mixture. (c) DTG curves: *1*—mixture stored at $p_r = 0.57$, *2*—the same at $p_r = 1.00$ [86]

higher than that of a "free" solvent due to the effect of capillary forces. This involves different conditions of solubility and the reaction products can also be different from those arising in dilute solutions. The reactions take place in very small volumes, in sub-microscopic pores, in which concentrations are subject to constant changes during the grinding process. In the course of continued grinding, or during storage, the reaction products may undergo further transformations. For example, amorphous $CuO \cdot 2H_2O$ gives rise to crystalline tenorite (CuO).

5.2.8. CHEMI-HESION AND THE OVERLAPPING EFFECT

Dispersed systems may undergo particle size increases and mechano-chemical reaction may be an important factor in this change. For example, agglomeration can be caused by mechano-chemical processes which are localised at the contact points of particles and which result in particle size increases, as discussed already in the section dealing with agglomeration. This phenomenon is attributed to chemi-hesion [88]. Chemi-hesion is the interaction of qualitatively different contacting phases associated with the exchange of electrons. In contrast to adhesion, chemi-hesion is only effective if the distance between contacting surface elements is in the range of atomic interactions.

It is convenient to introduce the concept of "overlapping effect" for characterising mechano-chemical processes. This secondary mechano-chemical phenomenon is

characterised by surface changes caused by mechanical forces that result in a sharp decrease of reactivity.

The overlapping effect can be triggered by (1) a decrease of the specific surface and of the number of active surface sites due to particle interactions, i.e. agglomeration [135, 140]; (2) overlapping of active surface elements by neighbouring surfaces to such a degree that the loss in reactivity exceeds that of the specific surface; (3) a decrease in the energy of reactive surface centres due to internal or surface diffusion, as well as to chemi-sorption and adsorption.

The overlapping effect is specific for different chemical reactions.

In Figure 5.9 the change of the cation-exchange capacity and the solubility in acid of a kaolin sample is shown as a function of activation time and specific surface. The overlapping effect has little or no influence on solubility, but the reduction of ion-exchange capacity was more pronounced than that of the specific surface after attaining a critical activation time (fineness). After this point, which is similar to a hystersis loop, the curve of T-values returns.

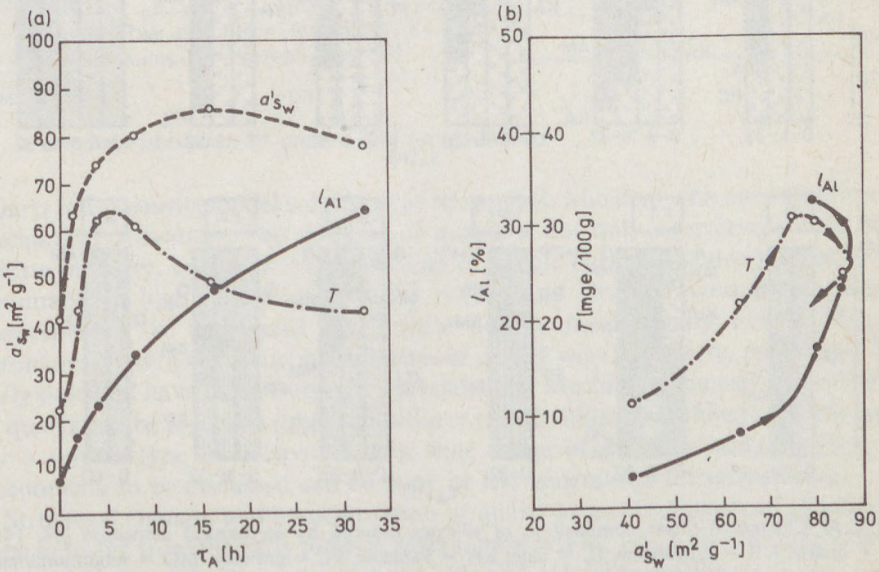

Fig. 5.9. Demonstration of the "overlapping effect" for the grinding of kaolin. Change of specific surface (a'_{s_w}), solubility (l_{Al}) and cation-exchange capacity (T) as a function of (a) activation (τ_A) and (b) specific surface (a'_{s_w}) [88]

5.3. EFFECT OF MECHANO-CHEMICAL ACTIVATION ON THE PHYSICO-CHEMICAL AND TECHNOLOGICAL PROPERTIES OF SILICATES AND OTHER MATERIALS USED IN THE SILICATE INDUSTRY

5.3.1. EXAMPLES OF CHANGES IN CRYSTAL STRUCTURE

Substantial lattice distortion and amorphisation of silicates and other materials used in the silicate industry are often encountered after fine grinding. Some examples are shown in Fig. 5.10 [141]. The rate of amorphisation depends on the type of mill, the conditions of grinding, and the nature of the feed.

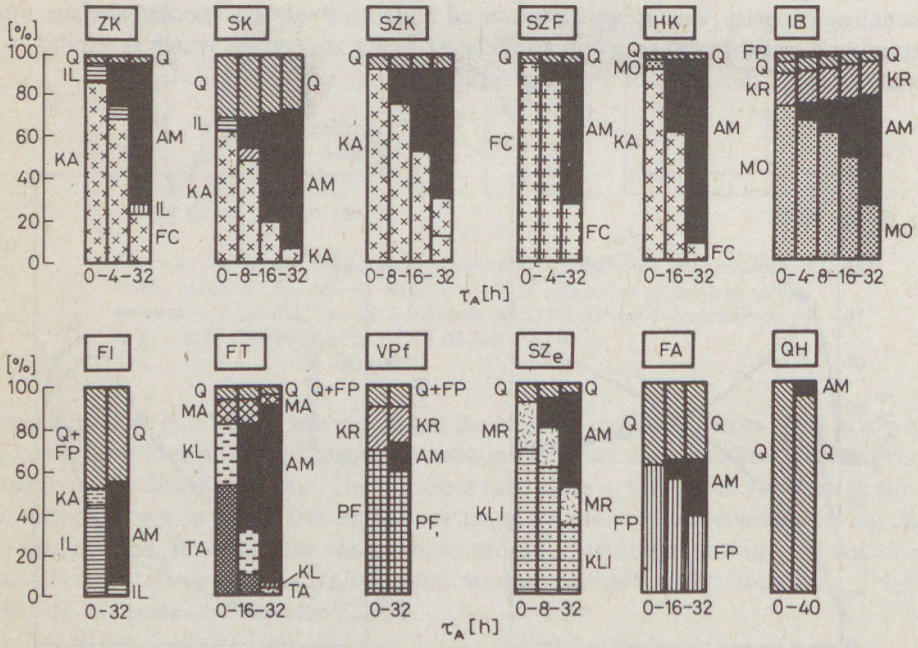

Fig. 5.10. Change of phase composition of silicates induced by mechanical activation [88, 141]. Q = quartz, KR = cristobalite, IL = illite, KA = kaolinite, FC = fire-clay, MO = montmorillonite, KL = chlorite, TA = tale, MA = magnesite, FP = feldspars, PF = pyrophyllite, KLI = clinoptiolite, MR = mordenite, AM = amorphous, ZK = kaolin from Sedlecz (Zettlitz), SK = kaolin from Sárisáp, SZK = kaolin from Szegi, SZF = fire-clay from Szegi, HK = kaolin from Hercegköves, IB = bentonite from Istenmezeje, FI = illite from Füzérradvány, FT = talc from Felsőcsatár, VPf = pyrophyllite from Velence, SZe = zeolite from Mád-Suba, FA = aplite from Fehérvár, QH = quartz sand

A remarkable, although yet not fully explained, phenomenon is the change of "oxygen compactness" during activation in a vibration mill. Oxygen compactness (ξ_0) is defined as the relative space filling of oxygen atoms in the silicate skeleton; this can be determined from the chemical composition and the density of the sample [249]. It has been found that the oxygen compactness of crystalline materials decreases, while that of silicates with an initially amorphous structure (such as silicate glass, silica gel and

volcanic glasses) increases by mechanical activation. Both changes have a tendency to approximate the oxygen compactness value of cristobalite, which seems to represent some sort of equilibrium to which mechano-chemically induced structural changes converge (Fig. 5.11).

The structural changes of some representative minerals are discussed in detail in the following passages.

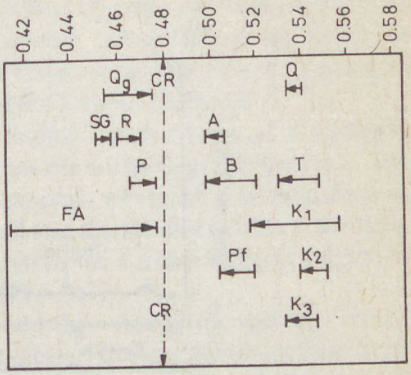

Fig. 5.11. "Oxygen compactness" (ξ_0) of various silicates before and after grinding. Arrows start from the initial state and point towards the final state. Q = quartz, CR = cristobalite, Qg = quartz glass, SG = silica gel, R = technical glass, A = aplite, P = perlite, B = bentonite, T = talc, FA = fly-ash, K_1, K_2, and K_3 = various kaolins, Pf = pyrophyllite [249]

Amorphisation of quartz and tectosilicates

Quartz is a favourite model substance of researchers who deal with comminution and mechanical activation. The grinding of quartz is not only an everyday task in the silicate industry, but quartz is a material of simple chemical and crystal structure, obtainable in high purity, crystallising readily and having favourable mechanical properties. It is very hard and brittle and is mechanically nearly isotropic. Mechanically-induced structural changes of quartz were, therefore, recognised at an early date and have been thoroughly investigated. Mechano-chemical amorphisation of quartz can be regarded (although subject to individual variations) as being typical for a certain type of behaviour of a wide range of minerals and, therefore, the phenomena to be discussed can be more or less generalised for tectosilicates.

Structural changes and amorphisation of quartz as a consequence of grinding has been reported from the early fifties in several papers [117, 142, 147]. The methods used included X-ray diffraction, thermal analysis and solubility studies.

The changes in the X-ray diffractogram of quartz as a result of grinding in a vibration mill is exemplified by measurements published by Szánthó and Lindner [142]. Figure 5.12 shows changes in crystallite size and lattice distortion as a function of time based on the measurements of Schneider [148]. By applying a differential equation to the curve representing the change of crystallite size as a function of time Schneider demonstrated, by calculation, that size reduction was dominant in the initial phase of grinding, but after prolonged grinding (i.e. in the domain of small particle size) the main process was amorphisation accompanied by agglomeration and re-crystallisation.

Comparative studies with rock salt by Schneider revealed that, on grinding, some of the dislocations present in rock salt prior to grinding disappeared, i.e. lattice defects

were partially healed under the effect of mechanical energy and the dislocation density began to increase only after prolonged grinding. There was also a difference between the average line density of quartz and rock salt. With rock salt the line density remained practically unchanged during grinding but, with quartz, after 40 hours of grinding, a decrease of about 85% was observed. The author explained differences in the amorphisation of the two materials by their different tendency for re-crystallisation.

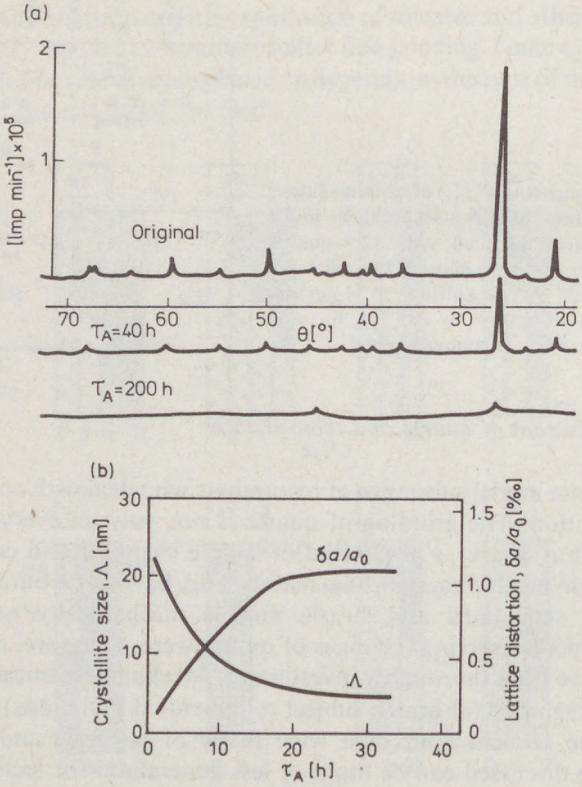

Fig. 5.12. Change in (a) the diffractogram [142] and (b) crystallite size and lattice distortion [148] of quartz (both as functions of grinding time)

The activation energy of the latter is much higher with covalent bonds than with ionic bonds and, therefore, re-crystallisation of quartz, which contains 50% covalent bonds, is inhibited in contrast to the ionically bonded rock salt, in which re-crystallisation only requires a small energy of activation and is, therefore, fast. As a consequence, the quartz retains its amorphous structure after the termination of mechanical activation while rock salt regains its crystalline structure immediately after deformation has stopped.

The marked tendency of quartz to amorphisation was explained by Steier et al. [149] by the fact that, after cleavage, the mainly covalent bonds of quartz can only be re-

established with difficulty. In addition, in quartz there is no definite glide plane system which would enable the defectless translation of plates: it also has an amorphous modification.

Amorphisation has also been demonstrated by the change of DTA peaks associated with the transformations $\alpha \rightarrow \beta$-quartz and quartz $\rightarrow$cristobalite [101, 150], although it was assumed by Flörke [151] that thermal effects disappear more rapidly than the crystal structure disintegrates. Hoffmann and Roth [152] observed that amorphous silicon dioxide and quartz with a degraded crystal lattice transform faster to cristobalite than non-activated quartz. Szánthó found differences in the degree of amorphisation when steel or corundum grinding balls were employed [117].

It has been established by several authors, mainly on the basis of dissolution experiments, that the amorphous layer develops on the surfaces of the particles. The presence of an amorphous layer can be demonstrated, when, as a consequence of grinding, the particle size becomes sufficiently small and the specific surface sufficiently large so that the proportion of amorphous material in the surface layer, as related to the total mass of material, becomes significant [153–161].

Based on the amount of amorphous material and the value of the specific surface, Rehbinder and Hodakov [161] calculated the thickness of the amorphous surface layer and they found that, for coarsely ground quartz, it was only 2 nm. However, it increased in the course of dry grinding to several tens of nm and finally, after prolonged grinding, the entire particle became amorphous. They also compared wet and dry grinding of quartz and found that in wet grinding (grinding time being equal) the specific surface of the system was much larger than it was with dry grinding. However, with wet grinding there was no change in the thickness of the amorphous surface layer. In other words, the thickness of the amorphous layer only increased during dry grinding. In the opinion of Lin et al. [17] this observation cannot be interpreted in such a way that amorphisation of quartz does not take place during grinding in water. On the contrary, amorphisation must be even more pronounced, but it is accompanied by the dissolution of the material in the water. Henderson and his co-workers observed [17] that the amount of silicon dioxide dissolved in a buffer of pH 7 decreased by 20% when the sample had been washed five times in water. The pre-treatment probably removed the amorphous layer. If water is present during the development of the amorphous layer and the particles are continuously rinsed by water (as it is the case with wet grinding) it is reasonable to assume that the amorphous layer totally dissolves in water [17].

In the present authors' view, dissolution of the amorphous layer is also promoted by continuous mechanical abrasion.

Takamura et al. [159] have also made the observation that water may promote the amorphisation of quartz if it can form an adequate adsorption layer on the fresh fracture surfaces.

Rehbinder and Hodakov [161] expressed the view that amorphisation of quartz during grinding should not be attributed primarily to the process of fracture, but to plastic deformation of the small particles. They added that such a deformation is only feasible in a thin surface layer, where "stresses are concentrated", i.e. where the dislocation density increases. According to Hoffmann and Schönert [162], however, it

is impossible to discern whether fracture itself or pure plastic deformation is responsible for the amorphisation of quartz.

Plastic deformation at the surface of particles was directly demonstrated by Heegn and Bernhardt [163] by electron microscopy.

The best proof that the amorphous portion is indeed localised on the surface layer is the change of solubility of ground quartz as a function of the degree of dispersion. By studying solubility in pure water and in 20% aqueous sodium hydroxide solution Rehbinder and Hodakov [161] established that the solubility of the amorphous surface layer was about 15 times higher than the expected value calculated using Kelvin's formula. They found that the equilibrium concentration in the solution (120 to 140 mg/l in pure water) was independent of the degree of dispersion of quartz. If the solution is in contact with the ground quartz it deposits silicic acid, but if the finely dispersed fraction is removed, e.g. by centrifuging, then over-saturation can be kept for a long time. The equilibrium concentration of a solution, in the case of a quartz ground dry for 8 hours and with a specific surface of 19 $m^2 g^{-1}$, was higher than that of a sample obtained by wet grinding for 11 hours. Although the wet ground material had a specific surface of 74 $m^2 g^{-1}$, the particles were covered with only a thin amorphous layer.

The amorphous layer is readily soluble in sodium hydroxide solutions: at room temperature 5 to 15 mass% was leached out over a period of two months. The rate of dissolution is, in general, constant up to the point where the entire amorphous layer becomes dissolved, i.e. the activity is constant throughout its whole depth. Solubility in sodium hydroxide solutions depends only on the amount of the amorphous fraction and is independent of the degree of dispersion.

Sakabe and his co-workers [164] investigated a series of quartz samples originating from five different sources and ground for different lengths of time in a vibration mill. They reached similar conclusions and reported that solubility increased substantially in 10% sodium hydroxide and in hot concentrated phosphoric acid: they explained this phenomenon by reference to the amorphisation of the samples. They employed X-ray techniques and infrared spectroscopy for detecting amorphisation. If, prior to measurement, the samples with an amorphous surface layer were treated either with sodium hydroxide or heated at 973 K, the line density increased in the X-ray diagrams of those samples that had been deprived of their amorphous layer or re-crystallised by heat treatment, respectively. A band at 1100 cm^{-1}, which is diagnostic for the Si →O bond, was conspicuous in the infrared spectra of the ground samples. From these observations they concluded that distortion only affected part of the lattice and that this part was confined to the surface of the particles resulting in an amorphous layer in that particular area.

Recently, the effect of a gaseous atmosphere (H_2, O_2, air, acetylene, ethene, Ar, CO_2) on the structural changes of quartz induced by grinding was investigated by ESR spectroscopy [84, 165–169]. It was found that Ar, H_2, and air did not intensify the primary structural changes, but the amount of radicals (paramagnetic centres) generated was highly dependent on the nature of the adsorbate. Lattice defects of different type and density are formed under different gases. Adsorbed gas is mainly present in the amorphous surface layer of quartz and the quantity adsorbed increases with the proportion of the amorphous phase.

Feldspars may undergo amorphisation similar to that of quartz and a proportion of the alkali metal ions becomes water soluble [141]. As yet, the present authors have not detected any amorphisation in zeolites.

Amorphisation of phyllosilicates

Phyllosilicates comprising two-dimensional atomic clusters lose their ordered crystalline structure under mechanical activation and become amorphous from the point of view of X-ray crystallography. Such structural changes can also be followed by thermal analysis, since amorphisation is generally connected with a loss of structural OH groups and a decrease of their bonding energy which results in a distortion of DTA, TG and DTG curves or may even result in a profound change in the shape of the entire curve (Fig. 5.13).

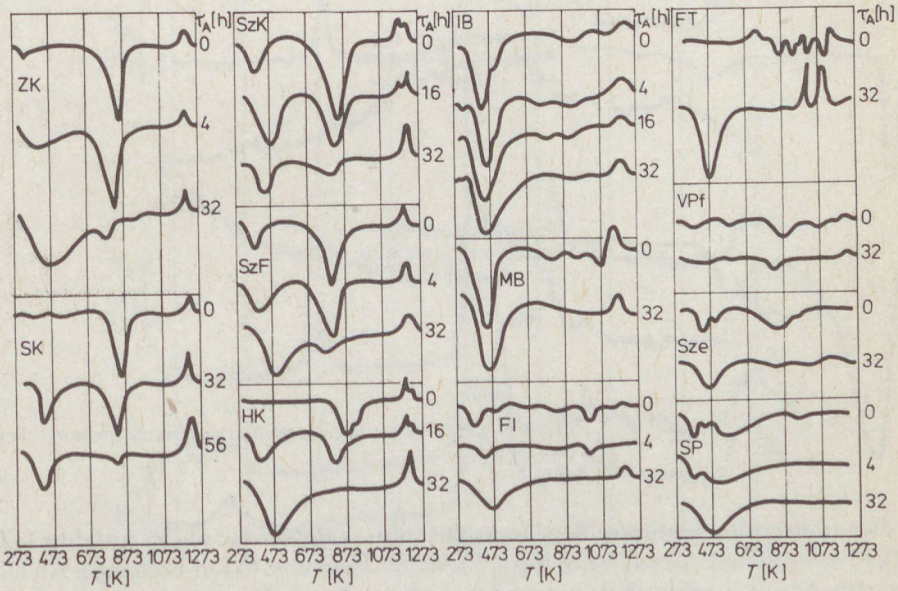

Fig. 5.13. Changes of the DTA curves of silicate minerals in the course of mechanical activation [88]. ZK = kaolin from Sedlecz (Zettlitz), SK = elutriated kaolin from Sárisáp, SzK = kaolin from Szegi, SzF = fire-clay from Szegi, HK = dickite with kaolin from Hercegköves, IB = bentonite from Istenmezeje, MB = bentonite from Mád, FI = illite from Füzérradvány, FT = talc with chlorite from Felsőcsatár, VPf = pyrophyllite from Velence, Sze = zeolite from Mád-Subaoldal, SP = pumicite from Szurdokpüspöki

Kelley and Jenney were the first [170] to study the grinding-induced amorphisation of muscovite, biotite, kaolinite, and montmorillonite in detail. These studies were later followed by many others who agree that amorphisation is a characteristic of dry grinding. If the same materials are ground wet in the same equipment for the same, or even longer, periods of time, amorphisation is reduced and may even be absent, but the degree of dispersion of the product increases.

Amorphisation of talc and chlorite sets in after relatively brief periods of grinding and some of the Mg^{2+} ions become exchangeable.

On grinding pyrophyllite in a vibration mill it undergoes partial amorphisation and this can be made complete if the feed is treated with a solution of magnesium chloride prior to grinding; it is then dried, and thereafter it is provided for the retention of adsorption water throughout the grinding process (Fig. 5.14).

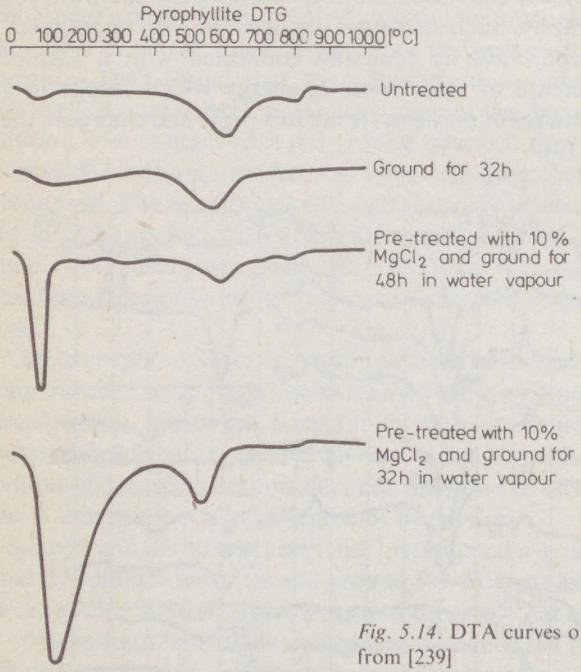

Fig. 5.14. DTA curves of pyrophyllite and grinds prepared therefrom [239]

Mica (muscovite, biotite) suffers amorphisation in the course of dry grinding [170, 171]. In amorphised mica some of the K^+ ions are amenable to ion-exchange. An illite type structure is attributed to the amorphised product [172], based on the way the water is bound.

Amorphisation of clay minerals during dry grinding has been reported repeatedly. Degradation of crystallinity and the appearance of amorphous material can be readily followed on X-ray diffractograms (Fig. 5.15).

Amorphisation of kaolin has also been thoroughly studied by X-ray crystallography, thermal analysis, infrared spectroscopy, and by the measurement of solubility and ion-exchange capacity [88, 98, 141, 170–193].

The change of crystallite size and the amorphisation of kaolin, based on the results of Schrader et al. [188], are shown in Fig. 5.16 along with DTA curves recorded by the same authors. These DTA curves clearly demonstrate changes in the bonding energy of the OH groups. At medium grinding times the DTA curves of kaolin were identical with those of "fire-clay" ("kaolin-d") which possesses a disordered structure. This phenomenon had been reported previously by several authors who interpreted the

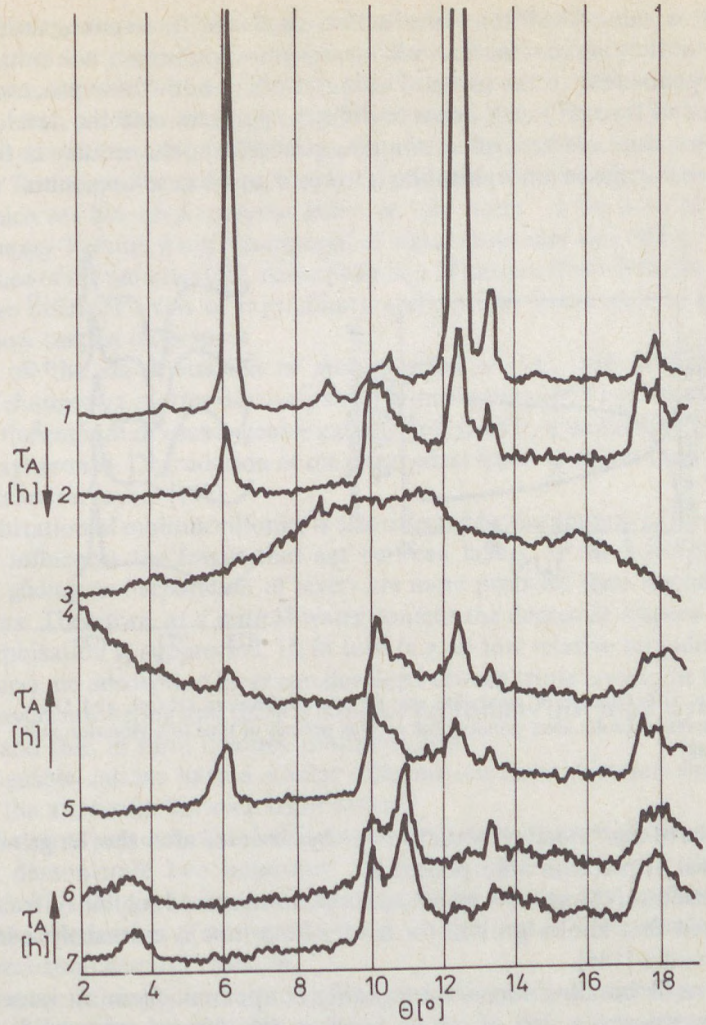

Fig. 5.15. X-ray diffractograms of some clay minerals before and after activation [97]. *1*—kaolin from Sedlecz (Zettlitz), untreated; *2*—kaolin from Sedlecz, τ_A = 4 h; *3*—kaolin from Sedlecz and Szegi, τ_A = 32 h; *4*—kaolin from Szegi, τ_A = 4 h; *5*—kaolin from Szegi, untreated, *6*—bentonite from Istenmezeje, τ_A = 4 h; *7*—bentonite from Istenmezeje, untreated

mechano-chemical amorphisation of kaolin as a stepwise process of this kind, in the course of which "fire-clay" was formed as an intermediate phase.

The appearance of "fire-clay" can be explained by deformation of the original crystal structure. It was observed in the course of grinding that the distance between double layers increases and, within the layers, those which were formed from SiO_4^{4-} tetrahedra and from AlOOH octahedra glide along translation planes in the direction of the *b* axis [97, 190], i.e. kaolin suffers plastic deformation. Schrader and his co-

workers [188] explained the formation of a "fire-clay" state by assuming the permanent deformation of the crystal structure, while amorphisation proper was traced back to fractures perpendicular to the layers. During grinding both these processes (plastic deformation and fracture) may occur in different particles, and the development of "fire-clay" structure and amorphisation may proceed simultaneously in the ground product. Since the rate of amorphisation is lower than the development of "fire-clay",

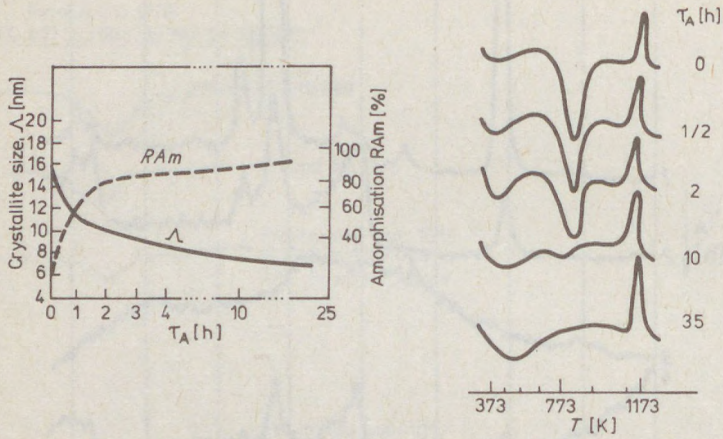

Fig. 5.16. Change of crystallite size (*Λ*), amorphisation (*RAm*), and DTA curves of kaolin after grinding for various periods of time in a vibration mill [188]

the appearance of the "fire-clay" structure can be observed after shorter grinding times and, in general, it precedes amorphisation.

Internal structural changes are also manifested in enhanced solubility, from which it can be inferred that kaolin ground for a very long time is essentially a mixture of amorphous oxides [186].

The rupture of bonding forces by grinding is apparent from an increased ion-exchange capacity, and a shift of certain bands in the infrared spectra [18, 183, 193–195]. A decrease of the integrals of peaks at 540 and 760 cm^{-1} (characteristic for Si—O—Al bonds) and finally their disappearance indicate the complete elimination of bonds between tetrahedral and octahedral layers. The disintegration of the crystal structure of kaolin under mechanical effects should not be regarded as an apparent amorphisation due to size reduction and the disordered secondary arrangement of small particles. Instead it should be seen as real amorphisation of the structure characterised by the cleavage of bonding forces between clusters of atoms, and the irreversible displacement of atomic groups which do not revert on release of the external load [19, 88]. The product of such an activation is a water-containing xerogel of random structure, which develops in several stages via "fire-clay"-like intermediates [18].

It should be pointed out that structural OH groups play an important role in the amorphisation of kaolin. The DTA curves demonstrate that, in the amorphous

structure, these groups and the water molecules derived from them by a condensation reaction within the phase (homogeneous mechano-chemical reaction) are still bound to the deformed kaolin lattice. However, their bonding energy is much less than in the crystalline state. In other words, in the deformation period during grinding the OH groups that constitute the active building elements of the crystal structure are displaced from their lattice points and are unable to return in the period of unloading. OH groups which are liberated reappear either as "gel water" in the amorphous ground product, or as "hydrate water" composed of water molecules and OH groups located at the surface of the particles [88]. Amorphisation of kaolins from different sources and which have different levels of crystallinity and contain lattice defects to a varying degree, show certain differences.

Studies on the amorphisation of montmorillonite [141, 196–199] revealed that structural changes set in after relatively short grinding periods. They were first seen in a change in the amount of exchangeable cations, followed by a weakening of bonding of the hydroxyl groups. Degradation of the tetrahedral layers is slower than degradation of the octahedral layers [197].

Amorphisation of montmorillonite is also affected by the amount of adsorbed water since this influences the forces that act between layers. If the adsorption layer is saturated, gliding and separation of layers are more probable than fracture across the triple layers. Therefore, at a critical water content the degree of dispersion increases and amorphisation is suppressed. If, in turn (e.g. at low relative humidity or at high temperature), no adsorption layer can develop between triple layers, the forces acting between layers are strong and there is a higher probability that triple layers will suffer fracture, and this, in turn, favours amorphisation.

Exchangeable cations have a similar influence on amorphisation since they also influence the attraction between triple layers.

DTA curves of bentonite that has been ground for varying periods are shown in Fig. 5.17 and demonstrate two important changes: a decrease in the thermal effect associated with dehydration, and the broadening of the first endothermic peak showing the elimination of adsorption water and gel water. This transformation is a typical mechano-chemical reaction.

The structural changes that occur in illite after fine grinding can be seen in Fig. 5.18. A characteristic feature of illite is that some of the potassium ions become exchangeable after mechanical activation.

The effect of mechanical activation on the structure and properties of chrysotile asbestos was studied in detail by the present authors [200–202]. The main components of fibrous chrysotile asbestos in $Mg_3Si_2O_5(OH)_4$ are the clino- and ortho-chrysotile form. The sample investigated also contained lizardite, brucite, and hydrotalcite. The effect of prolonged mechanical treatment was examined using a laboratory edge mill and a vibration mill [202]. Mechanical treatment of chrysotile asbestos resulted in fibre shortening as well as in changes of the short-distance internal order of the elementary fibrilles. The character and the degree of this effect depended on the type of equipment used.

Figure 5.19 shows that the "total" specific surface and adsorption capacity of asbestos are increased more by edge milling than by treatment in a vibration mill. This may be explained as follows: edge milling produces a superficial activation of asbestos,

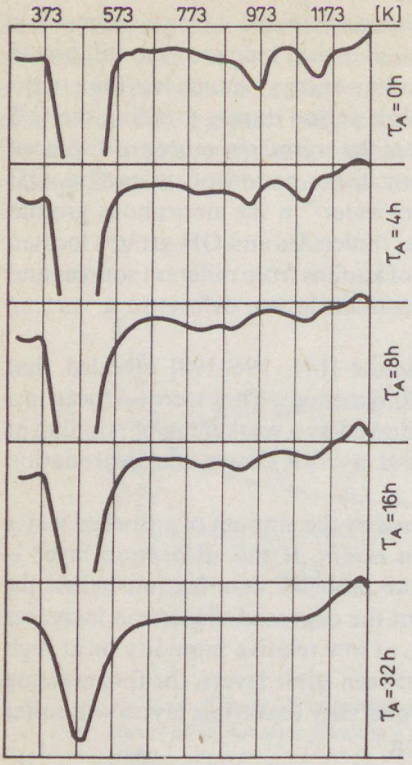

Fig. 5.17. DTA curves of bentonite after mechanical activation [141]

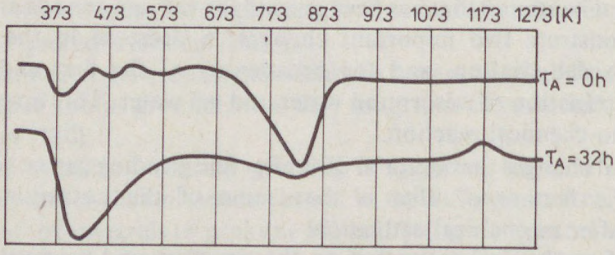

Fig. 5.18. DTA curves of illite before and after activation [88]

while rupture of the fibres is predominant in a vibration mill. According to the literature [203], the peak at approximately $2\theta \simeq 32'$ in the small-angle X-ray diffractogram can be assigned to the short distance internal order of elementary fibres (fibrilles). The change and, ultimately, the disappearance of this peak under mechanical treatment indicates a change in the internal order of the fibrilles. Degradation of the internal structure is extensive during edge milling. The adsorption capacity of asbestos increases due to mechanical treatment and its thermal properties are also altered.

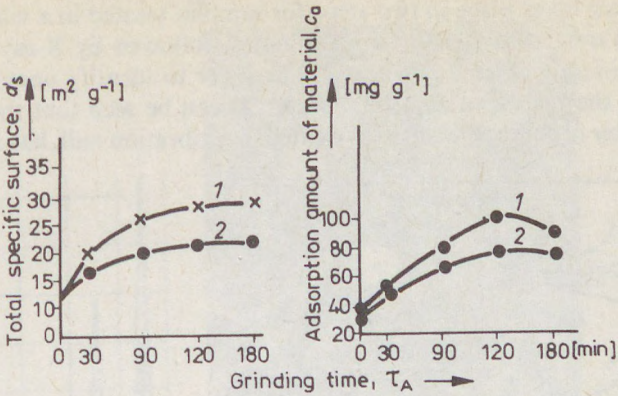

Fig. 5.19. Effect of mechanical treatment on the properties of asbestos. *1*—Edge mill, *2*—vibration mill [202]

When chrysotile is heated to 1273 K its crystal lattice disintegrates and the mineral decomposes to give forsterite:

$$2Mg_3Si_2O_5(OH)_4 \rightarrow 3Mg_2SiO_4 + 4H_2O + SiO_2.$$

Figure 5.20 shows that in a mechanically untreated asbestos sample the endothermic peak characteristic of the release of structural water is at 953 K and a very small exothermic peak at 1073 K indicates forsterite formation. After mechanical treatment the first peak is shifted by 50 K to lower temperatures. Moreover, the release of

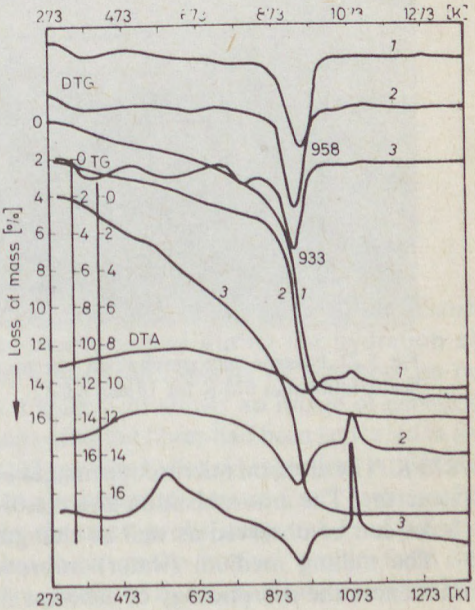

Fig. 5.20. Derivatograms of asbestos samples: *1*—Untreated, *2*—ground in an edge mill, *3*—ground in a vibration mill [202]

structural water takes place in two steps for samples treated in a vibration mill. The samples were treated at 873 K for 15 minutes, followed by X-ray diffraction and electron microscopy (Figs 5.21 and 5.22) in order to identify unambiguously these changes with the release of structural water. It can be seen that the elimination of structural water in chrysotile asbestos treated in a vibration mill, has already begun at

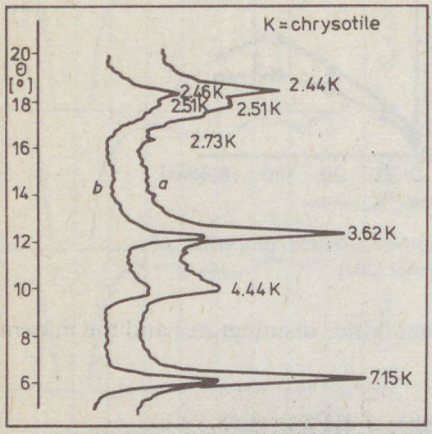

Fig. 5.21. X-ray diffractograms of untreated and heat-treated asbestos samples: *a*—milling in a vibration mill for 6 h; *b*—as for *a* followed by heating at 873 K for 15 min [202]

Fig. 5.22. Electron micrograph of an asbestos sample ground in a vibration mill for 4 h followed by heat treatment at 873 K for 15 min [202]

873 K. The electron microscope images also show partial decomposition of the crystal structure. The amorphisation and dissolution of layers on the walls of the interfibre holes can be observed as well as changes in the outer silicate layers.

The milling medium (water) improves the efficiency of milling and positively influences the morphology of asbestos fibres.

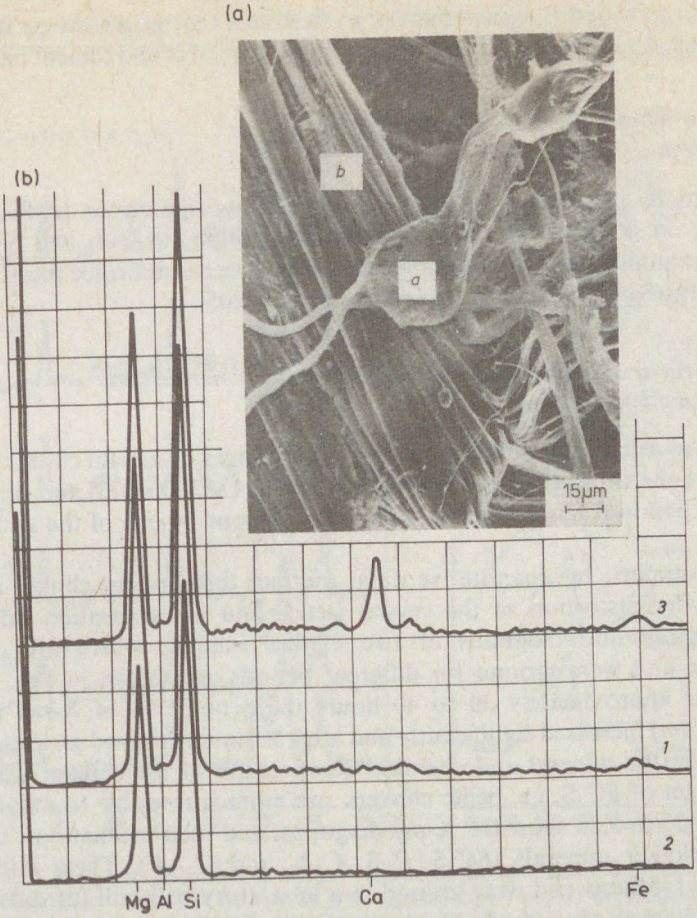

Fig. 5.23. Mechanical activation of chrysotile asbestos after storage in a solution of calcium hydroxide [202]. (a) Image taken by a scanning electron microscope. (b) EDAX-curves: *1*—spectrum of untreated chrysotile asbestos (only peaks for Mg and Si are visible); *2*—spectrum taken from point *b* (only peaks for Mg and Si are visible); *3*—spectrum taken from point *a* (a peak for Ca has emerged)

One of the important properties of chrysotile asbestos is its capacity to adsorb calcium hydroxide and other hydration products formed during the hydration of cement clinker. Figure 5.19 shows that the adsorption capacity of asbestos can be much enhanced by mechanical activation. Figure 5.23 shows an image of asbestos fibres taken by a scanning electron microscope after the fibres had been activated in an edge mill, and after being stored in a saturated calcium hydroxide solution. At certain points of the surface (Fig. 5.23(a), point *a*) the accumulation of Ca^{2+} ions can be observed and this was further supported by the microprobe image taken of point *a* (Fig. 5.23(b) curve *3*). It can be assumed that these are the "active" centres from the point of view of adsorption and that they were generated by mechanical treatment. It is

likely that in set asbestos cement there is, at these very centres, a stronger bonding than simple physical adhesion at the interfaces of asbestos fibres and cement particles [200].

Structural changes in neso- and inosilicates during grinding

Experiments by Motoi [204] on size reduction show that zircon ($ZrSiO_4$) becomes amorphous on grinding. Moreover, partial dissociation to ZrO_2 and SiO_2 can also occur and solubility in HF increases substantially. The polymorphic transformation of enstatite $Mg_2(Si_2O_6)$ has been referred to earlier [205].

Structural changes and amorphisation of cement clinker and clinker minerals

In contrast to calcite and quartz, the structural changes of cement clinker and clinker minerals are the subject of only a few papers [122, 135, 206–213] and, therefore, the present discussion is based primarily on investigations by one of the authors of this book.

We can support, by quantitative data, the fact that cement clinker and clinker minerals suffer distortion of the crystal lattice and amorphisation on prolonged grinding. X-ray diffractograms of two clinker samples which are of different composition and were ground for different periods are shown in Fig. 5.24. After grinding for approximately 30 to 40 hours the proportion of X-ray amorphous material (*RAm*) increased significantly and after 50 hours attained an average of 40% depending on the mineral and chemical composition of the clinker. Clinkers with higher content of βC_2S, i.e. belite clinkers, are more susceptible to amorphisation.

Figures 5.25 to 5.28 show the X-ray diagrams, and their evaluations, of the more important clinker minerals (βC_2S, C_3S, C_3A, and C_4AF). These minerals were obtained by synthesis and were ground in a laboratory ball mill for different times. Important changes can already be observed with βC_2S after grinding for about 20 hours (Fig. 5.25). After 90 hours the *RAm* value amounted to about 50%, the density of the sample dropped by 10%, and its heat of dissolution was reduced by 15%. Mechano-chemical amorphisation of βC_2S was also proved by electron microscopy.

The thermal analysis of ground βC_2S samples was characterised by the weakening, and later by the complete disappearance, of the endothermic peak on the DTA curve at 943 K (this is probably connected with the polymorphic change $\beta C_2S \rightarrow \alpha' C_2S$). The two endothermic peaks have been assigned to the dehydration of $Ca(OH)_2$ (at 753 K) and the de-carbonisation of $CaCO_3$ (at 1023 K). These peaks gradually diminish on continued grinding and later disappear completely. Their emergence indicates that, during grinding, the feed material takes up from the grinding environment both water vapour and carbon dioxide and this leads to the formation of $Ca(OH)_2$ and then $CaCO_3$ on the surface of the particles. From the amount of $Ca(OH)_2$ and $CaCO_3$ that is formed (these amounts can be determined from the TG curves and from the specific surface of the ground product) it was established that the thickness of these surface layers could not exceed 3 nm [212].

In order to identify the reasons for the change that occurred at the 943 K peak on the

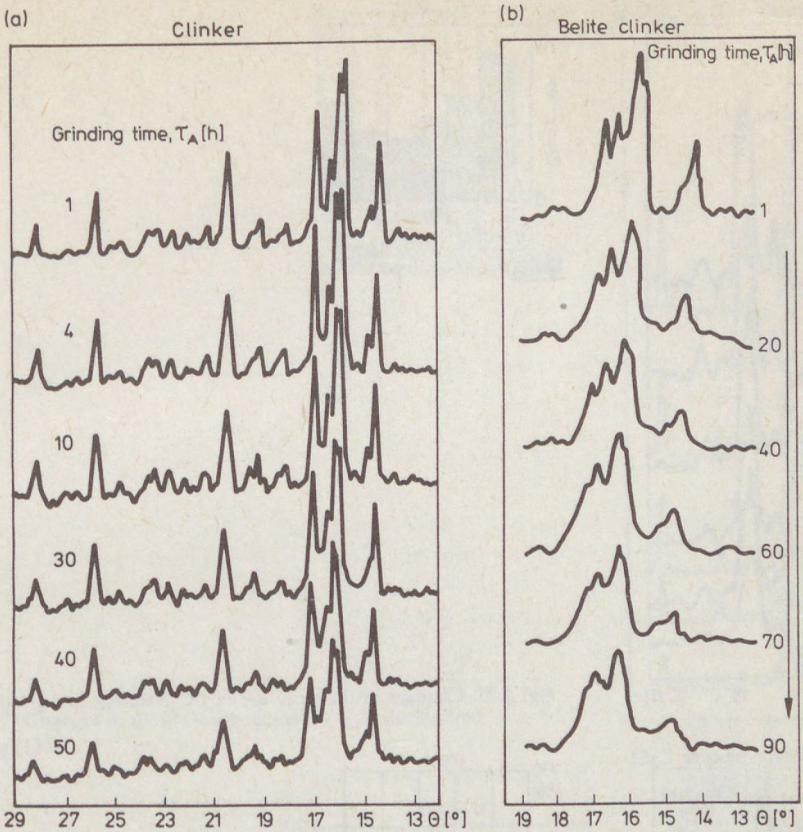

Fig. 5.24. X-ray diffractograms of cement clinker samples ground for various times: (a) composition: C_3S 49.81%, C_2S 24.31%, C_4AF+C_3A 20.62%; (b) composition: C_3S 30.27%, C_2S 43.58%, C_4AF+C_3A 16.39% [206]

DTA curve X-ray diffractograms were produced from βC_2S samples ground with heating for 60 min, 20 hours and 90 hours. It turned out that the lines characteristic of the modification are much less intense with the sample ground for 20 hours than with the sample ground for 60 min, and they are absent in the specimen ground for 90 hours. From this result it can be inferred that prolonged grinding affect the polymorphic changes of βC_2S but the exact nature of this effect is still unknown. Polymorphism of C_2S is in itself a rather complex problem. In βC_2S which had been stabilised with P_2O_5 and ground in a vibration mill for 4 to 6 minutes, Kudrjavceva and Hodakov [211, 212] observed polymorphic transformation of βC_2S to γC_2S. At the same time when βC_2S which had been stabilised by rapid cooling was ground in a ball mill, the appearance of γC_2S was not detected by X-ray crystallography.

The transformation of βC_2S to the more stable γ form under the effect of mechanical treatment is thermodynamically feasible. Proof for this is provided by the experiments of Jannaquis and Guinnier [214] who induced the $\beta \rightarrow \gamma$-transformation by compressing βC_2S in a hydraulic press at room temperature. The degree of

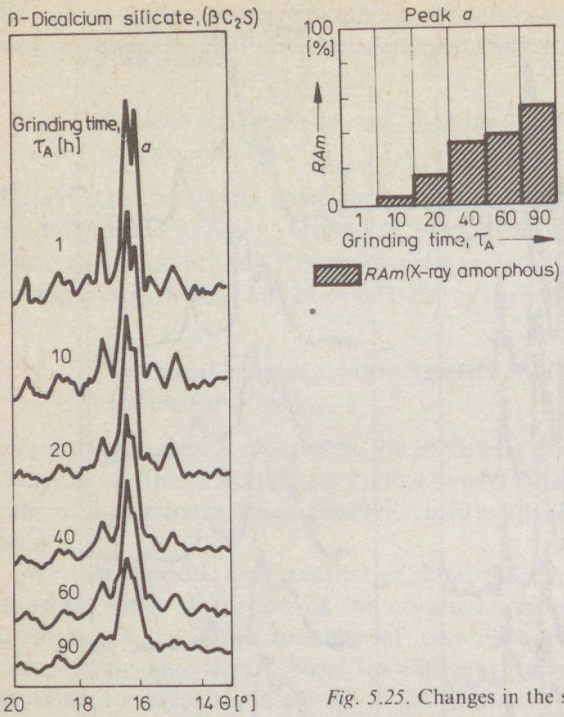

Fig. 5.25. Changes in the structure of βC_2S during fine grinding [135]

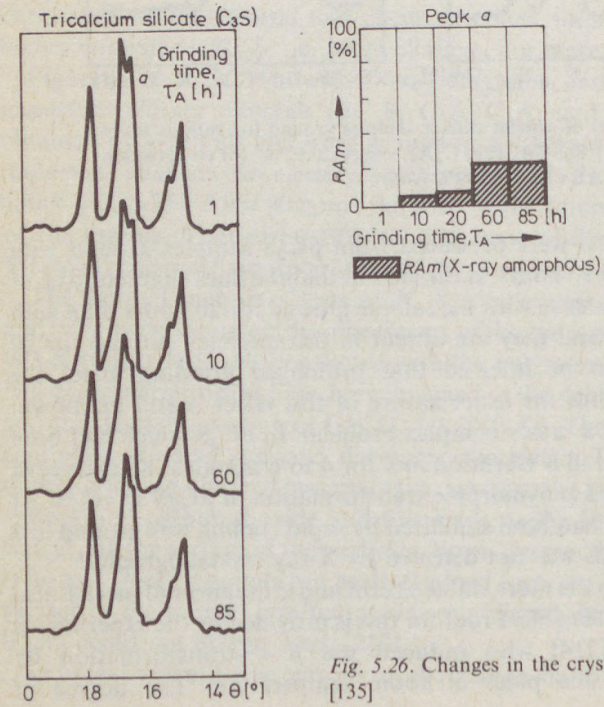

Fig. 5.26. Changes in the crystal structure of C_3S during fine grinding [135]

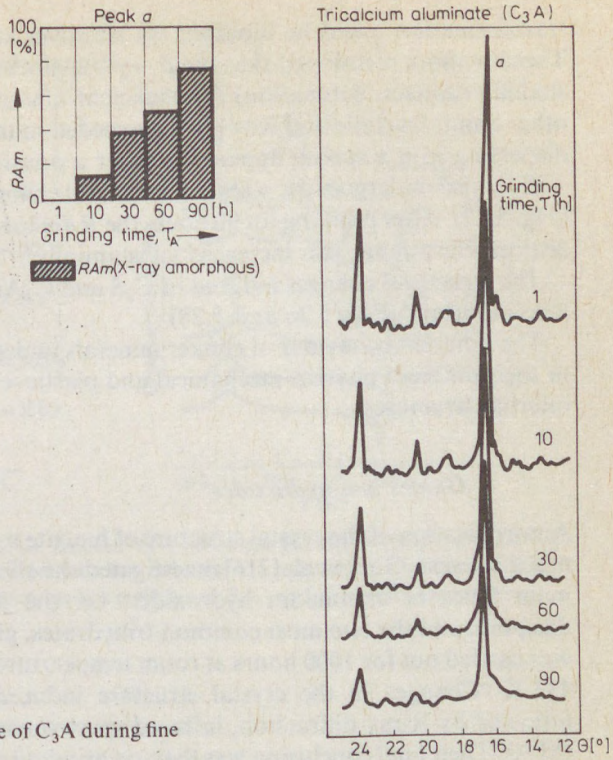

Fig. 5.27. Changes in the crystal structure of C_3A during fine grinding [135]

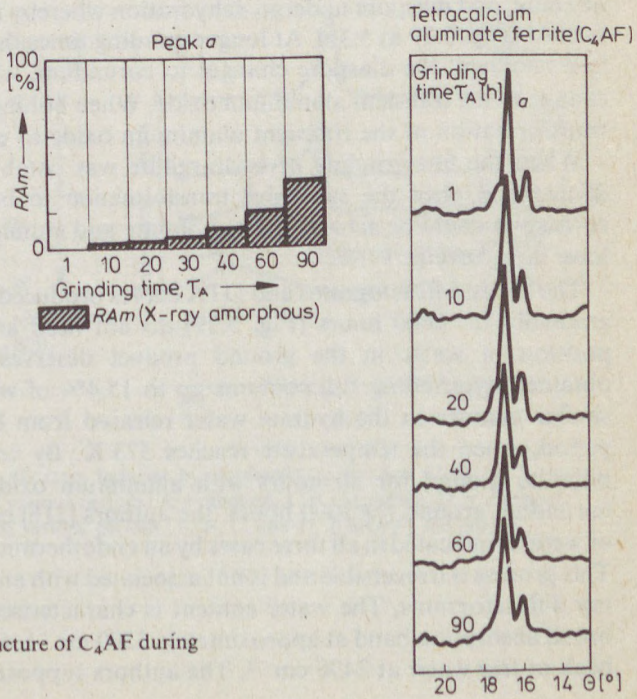

Fig. 5.28. Changes in the crystal structure of C_4AF during fine grinding [135]

transformation could be modified by additives such as Na_2O, K_2O, B_2O_3, P_2O_5. These authors mentioned that the $\beta \rightarrow \gamma$-transformation may also occur on repeated shaking (impact, detonation) if a sufficient amount of work was expended. On the other hand, Dachille and Roy [215] succeeded in transforming γC_2S to the β form by dispersing it in a special apparatus under a quasi-static pressure of 2943 MPa.

C_3A also undergoes deep-seated structural changes and amorphisation on grinding (Fig. 5.27). After grinding for 90 hours the *RAm* value amounted to about 80% and the lattice defect value also increased substantially.

The structural changes induced in C_3S and C_4AF by prolonged grinding are much less important (Figs 5.26 and 5.28).

The different behaviour of clinker minerals under mechanical load is a consequence of their different physico-mechanical and plastic–elastic properties as well as of their internal structures.

Oxides and hydroxides

Amorphisation of the crystal structure of bauxite minerals is a field which has aroused much interest. Gout et al. [216] investigated the effect of mechanical activation on the main types of aluminium hydroxides, i.e. the two monohydrates, böhmite and diaspore, and the two most common trihydrates, gibbsite and hydrargillite. Grinding was carried out for 1000 hours at room temperature and at 353 K, 393 K, 413 K, and 433 K. Changes in the crystal structure induced by mechanical activation were followed by X-ray diffraction, infrared spectroscopy, and thermal analysis (TG and DTA). Their final conclusion was that, on grinding at room temperature, hydrargillite, böhmite, and diaspore undergo dehydration whereby amorphous aluminium oxide is formed (Figs 5.29 to 5.31). At longer grinding times the amorphous aluminium oxide re-crystallises: the diaspore changes to corundum, while böhmite and hydrargillite change to the transient aluminium oxide. When böhmite was ground even longer, the transformation of the transient aluminium oxide to corundum was detected.

When the fine-grinding of hydrargillite was combined with heating, it was first de-hydrated, then the successive transformation to böhmite, aluminium oxide, and corundum could be achieved. The böhmite and aluminium oxide formed in this way have large specific surfaces.

The X-ray diffractograms and DTA curves produced from böhmite samples ground gradually for 1000 hours (Fig. 5.29) do not need any further discussion, but the position of water in the ground product deserves some comment. Corundum obtained by grinding still contains up to 15.4% of water, and this is released, in a similar manner to the hydrate water released from böhmite ground for a shorter period, when the temperature reaches 573 K. By comparing the DTA curves of böhmite ground for 80 hours with aluminium oxide ground for 200 hours and corundum ground for 1000 hours, the authors [216] established that the elimination of water is indicated in all three cases by an endothermic peak at approximately 573 K. This process is irreversible and is not associated with any perceptible changes in the X-ray diffractograms. The water content is characterised in the infrared spectra by a broad absorption band at approximately 3500 cm^{-1}, which almost coincides with the peak of free water at 3490 cm^{-1}. The authors supposed that hydroxyl groups of the

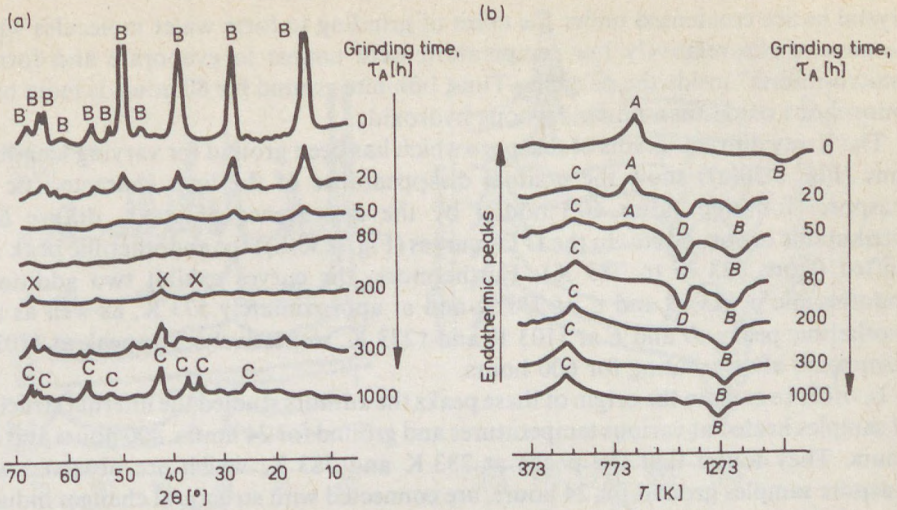

Fig. 5.29. Structural changes in böhmite induced by mechanical activation [216]. (a) X-ray diffractograms after grinding for various periods: B = böhmite, C = corundum, X = aluminium oxide; (b) DTA curves after grinding for various periods (*A*, *B*, *C*, and *D* identify the peaks)

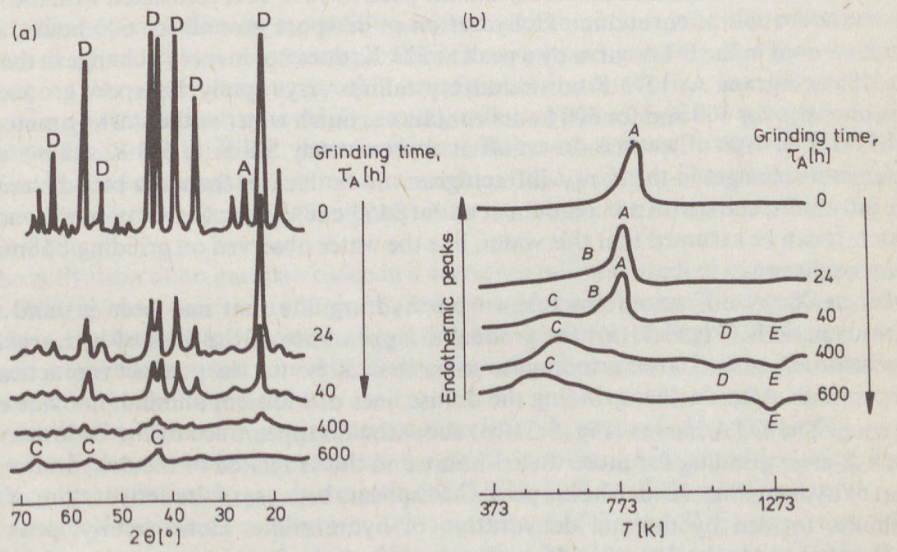

Fig. 5.30. Structural changes in diaspore induced by mechanical activation [216]. (a) X-ray diffractograms after grinding for various periods: A = anatase, C = corundum, D = diaspore; (b) DTA curves after grinding for various periods (*A*, *B*, *C*, and *D*, *E* identify the peaks)

crystal lattice condensed under the effect of grinding to form water molecules which because of the relatively low temperature were unable to evaporate and formed "micro-inserts" inside the particles. Thus, böhmite ground for 80 hours is more of an amorphous oxide than an amorphous hydroxide.

The X-ray diffractograms of diaspore which has been ground for varying lengths of time (Fig. 5.30(a)) show the gradual disappearance of the lines characteristic for diaspore, followed (after 600 hours) by the appearance of weak, diffuse lines attributable to corundum. In the DTA curves (Fig. 5.30(b)) the endothermic peak *A* is shifted (from 823 K to 783 K): Furthermore, the curves exhibit two additional endothermic peaks, *B* and *C* at 733 K and at approximately 573 K, as well as two exothermic peaks, *D* and *E* at 1103 K and 1273 K, respectively. The peak at 1103 K disappears after grinding for 600 hours.

In order to explain the origin of these peaks the authors studied the internal structure of samples heated at various temperatures and ground for 24 hours, 400 hours and 600 hours. They found that the peaks at 733 K and 783 K, which are observed with diaspore samples ground for 24 hours, are connected with structural changes induced by grinding and are characterised by a decrease of dehydration temperature. Dehydration of diaspore ground for 400 hours at 573 K did not result in any alteration of the X-ray diffractograms; at 773 K the remaining diaspore was dehydrated to corundum. The exothermic peak at 1073 K is connected with the re-crystallisation of transiently formed aluminium oxide, and the peak at 1273 K is connected with the fast re-crystallisation of corundum. Dehydration of diaspore ground for 600 hours, and characterised in the DTA curve by a peak at 523 K, does not involve a change in the X-ray diffractogram. At 1273 K corundum crystallises very rapidly. Diaspore ground at low intensity for 400 and for 600 hours contains as much water as the starting material (14.4%). This type of water is driven off at approximately 523 K to 573 K without any observable changes in the X-ray diffractogram. In both cases there is a broad band in the infrared spectra with a maximum at about 3450 cm^{-1}, near to that of non-bonded water. It can be assumed that this water, like the water observed on grinding böhmite, is an occlusion.

In the X-ray diffractograms taken from hydrargillite that had been ground for various periods (Fig. 5.31(a)) the gradual disappearance of the lines of hydrargillite can be observed and, after grinding for more than 50 hours, the product is practically amorphous. After further grinding the diffuse lines of transient aluminium oxide can be seen. The DTA curves (Fig. 5.31(b)) show the disappearance of the endothermic peak *A* after grinding for more than 3 hours and this is related to the dehydration of part of hydrargillite. After 8 hours peak *C* disappears because of the dehydration of the böhmite formed by thermal dehydration of hydrargillite. Concurrently, peak *B*, showing the dehydration of hydrargillite, is shifted to a lower temperature of 623 K with the untreated sample and 573 K with hydrargillite ground for 15 hours. According to the TG analysis, ground hydrargillite contains a significant amount of water and this is only eliminated at about 473 K. The water content (30 and 26%) depends on grinding time (50 and 400 hours, respectively). In the infrared spectra this water is indicated by a broad absorption band at 3500 cm^{-1} and it is probably present as occlusions.

Studies by Kachalova [217] show that intensive grinding of bayerite is accompanied

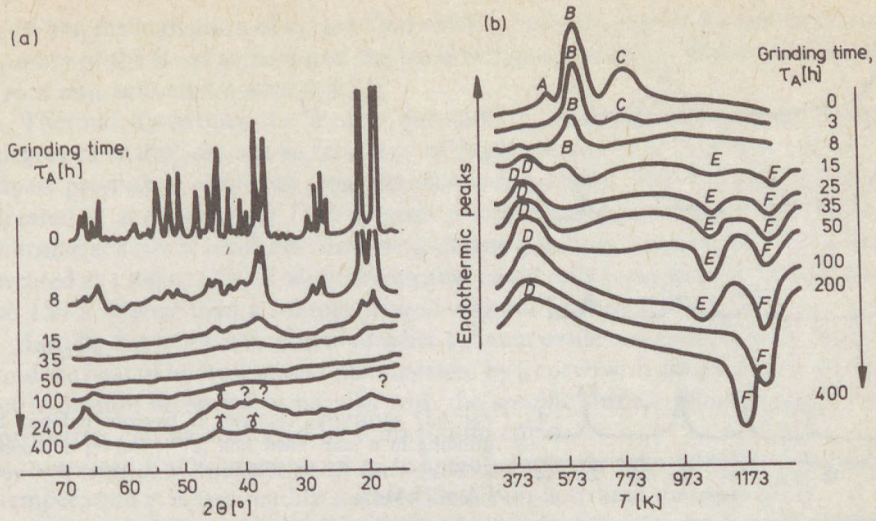

Fig. 5.31. Structural changes in hydrargillite induced by mechanical activation [216]. (a) X-ray diffractograms after grinding for various periods. γ = aluminium oxide. (b) DTA curves after grinding for various periods (*A*, *B*, *C*, *D*, *E*, *F* identify the peaks)

by dehydration, as well as by morphological and structural changes which result in the formation of amorphous aluminium oxide. On continued grinding (for periods that depend on the equipment and other conditions) it transforms into amorphous aluminium oxide, directly to α-Al_2O_3, or crystallises by binding OH^- groups to form böhmite. If, during grinding, the sample becomes contaminated with iron then the product is either amorphous aluminium oxide, or as a result of a mechano-chemical reaction between amorphous aluminium oxide and iron, the compound $FeAl_2O_4$ is formed (Fig. 5.32).

The activation of magnesium oxide in a vibration mill was studied by Schrader and Kneschke [8] who observed a continuous decrease of crystallite size with grinding time and an increase of lattice distortion (Fig. 5.33). Lattice distortion sets in, however, only beyond a critical crystallite size and, during the initial period of grinding, particle size reduction is the dominant effect.

Recently, the effect of a gaseous atmosphere (Ar, O_2 or air, C_2H_4, C_2H_2, H_2, and CO_2) on the structural changes and on the reactivity of magnesium oxide during fine grinding has been investigated in much detail [218–220] by EPR spectroscopy.

Mechanical activation is shown by the appearance of F- and SDE-type centres. F centres are associated with the formation of anion holes at lattice points, while the structure of SDE (electron defect oxygen) centres (O^-, O_3^-, O_3^{3-}) has not been clarified.

It was found that if the MgO was activated with the exclusion of oxygen then predominantly SDE centres were formed; however, in the presence of oxygen, F centres prevailed. The presence of SDE centres indicates a more stable state.

Degradation of the primary structure of MgO is independent of the surrounding atmosphere. At the same time, the concentration of paramagnetic ions (F and SDE

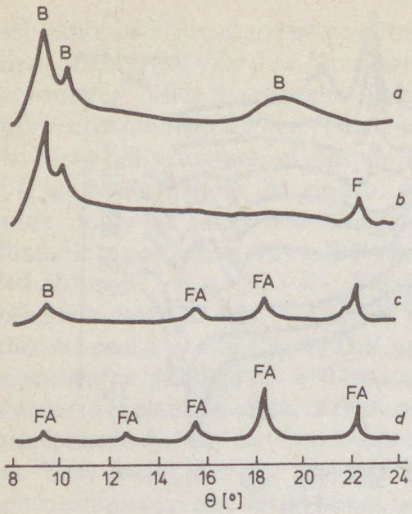

Fig. 5.32. Structural changes in bayerite induced by grinding in a steel lined mill [217]. Curves *a*–*d* mean grinding times 45 to 90 min; B = bayerite, F = iron, FA = $FeAl_2O_4$

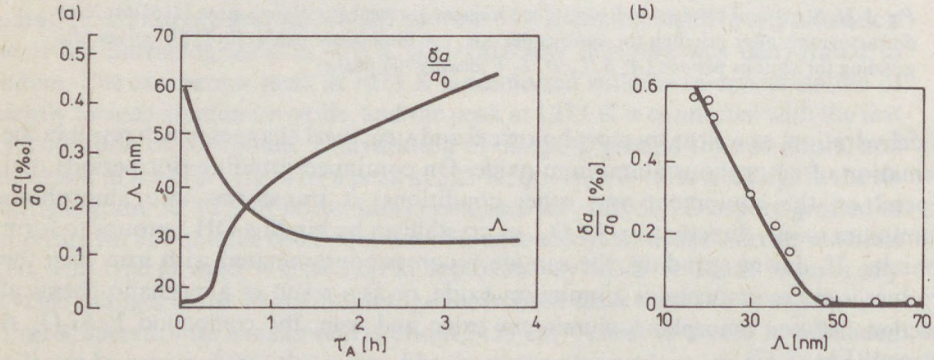

Fig. 5.33. Grinding of MgO [8]. (a) Change of crystallite size (Λ) and lattice distortion ($\delta a/a_0$) as functions of grinding time (τ_A); (b) Correlation of crystallite size and lattice distortion

centres) may differ even by an order of magnitude, depending on the atmosphere in which grinding was performed. Structural changes and the appearance of paramagnetic centres are not confined to the surface layers of MgO but, under certain conditions of activation and grinding, they may encompass the whole volume of the particles. The adsorption characteristics of ground MgO may vary as much as two orders of magnitude according to the nature of the adsorbed gas (with Ar and H_2 as one extreme and C_2H_4 the other).

Activation considerably improved the sintering characteristics of MgO at high temperatures.

Schlagel and Morgner reported [221] that mechanical activation only improved the sintering up to 1610 K; beyond that temperature it did not result in any improvement (the density of test specimens prepared by pressing decreased). They assumed that isolated pores are formed by coalescence of lattice defects in activated systems. The diffusion of the pores to the surface is slow.

When the activation of magnesium oxide is carried out at optimised conditions the quality of the Sorel cement and the basic refractory bricks is higher than those made from non-activated material [222].

Thermal pre-treatment affects the grindability and degree of dispersion as well as the degree of hydration and sinterability of MgO ground in a vibration mill [223]. The finest product is produced from periclase pre-burnt at 1800 K, while periclase pre-treated at approximately 1600 K gives a medium degree of dispersion; finally, pre-burning at 1300 K results in coarsening during grinding. A sample which had been pre-treated at 1300 to 1600 K and then ground could only be sintered at temperatures 100 to 150 K higher than a sample ground without heat treatment.

Lattice distortion was observed when calcium oxide was ground in a vibration mill, and the heat of hydration was characterised by a curve with a maximum [224]. The rate of hydration increased in parallel with the specific surface. The change of technical properties can be described by a maximum curve.

Activated CaO sinters better at temperatures lower than 1340 K, but beyond this temperature it is less readily sintered than non-activated material [221].

Activated CaO can be produced either by grinding $CaCO_3$ in a heated vibration mill or by grinding crystalline CaO [224]. In both cases the hydration characteristics change along a curve with a maximum.

5.3.2. EXAMPLES OF SOLUBILITY CHANGES

Increased solubility and increased rates of dissolution of solids can often be observed after mechanical treatment. The first reports about this phenomenon are quite old [225–227] and refer to the dissolution of metals in acids. Data have also been published concerning enhanced solubility and rate of dissolution due to mechanical activation of organic compounds in organic solvents [228], as well as of calcite [229], cassiterite [230], corundum [231], bauxite [232], chromic iron ore [233], böhmite [234], magnetite, galena, titano-magnetite [235], pumicite [236], etc. in inorganic acids.

Mechanical dispersion involving an increase of specific surface is, in itself, a process that accelerates dissolution and this is expressed also by the Nernst equation. If, in addition, the particle size and the size of protrusions on the surface are very small, the solubility of the material also increases (Kelvin's equation). In surface activation and mechanical activation the solubility may further increase, since amorphous materials are always more soluble than their crystalline counterparts. Thus, the solubility of quartz in hydrofluoric acid, phosphoric acid, and sodium hydroxide is much enhanced by mechanical activation; even the solubility of quartz in pure water becomes detectable [146, 153, 154, 161, 164, 237].

Figure 5.34 plots the "free silicic acid content" of quartz activated in a vibration mill, as determined by the Schmidt method [238]. (This is also the chosen method for assaying the silicosis provoking effect of ground quartz products.) It can be seen that after grinding for 56 hours 70% of the sample dissolved [141].

Bartholomä and Schwiete found [186] that after sufficiently long activation Al_2O_3, MgO, and K_2O can be almost entirely leached with hydrochloric acid from a kaolin sample from Zettlitz. The residue consisted of a mixture of SiO_2, TiO_2, and Fe_2O_3.

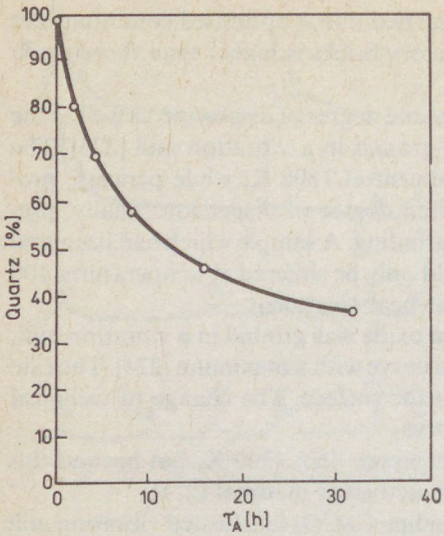

Fig. 5.34. Change in the quantity of "free quartz" induced in quartz sand by mechanical activation [97]

After acidic dissolution of a bentonite from Mainburg the residue was mainly SiO_2 with small amounts of TiO_2 and CaO. Selective enhancement of the solubility of some of the constituents was attributed to the amorphisation of the crystal structures [191]. With chlorite the acid solubility of each of the oxide components, including SiO_2, increased [186].

In Figure 5.35 the relative solubilities of individual components of silicate minerals activated in a vibration mill are depicted as functions of specific surface.

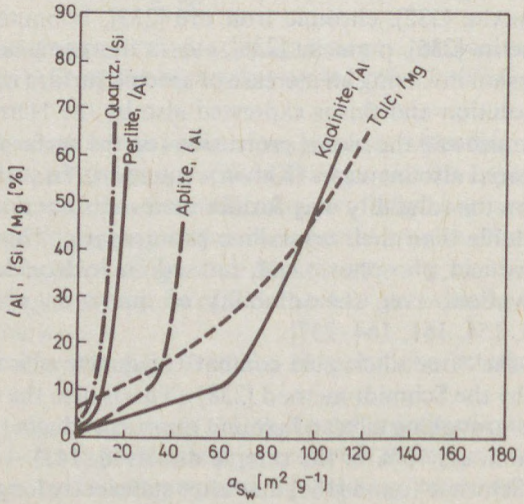

Fig. 5.35. Solubility of some silicate minerals as a function of specific surface [236]

In Figure 5.36(a) correlation is made of the relative solubilities of Al and Fe in hydrochloric acid of various concentrations for samples of kaolin from Szegi (Hungary). These samples contained relatively large numbers of substitution lattice defects of Fe →Al type and were activated in a vibration mill. In a non-activated sample iron-containing components are more readily leached than those containing aluminium; this order is reversed by mechanical activation of the sample because the

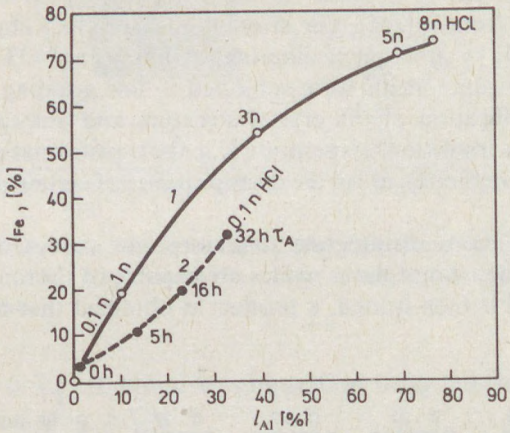

Fig. 5.36. Correlation between the relative solubility of Al and Fe in a kaolin sample from Szegi. l_{Al} = percentage of Al dissolved, l_{Fe} = percentage of Fe dissolved [239]. *1*—Dissolution of untreated kaolin in hot hydrochloric acid of various concentrations, *2*—solubility of kaolin ground for various periods in 0.1 *n* hydrochloric acid

kaolin lattice is disintegrated and stable, sparingly-soluble "enclaves" are formed around the iron atoms in the amorphous xerogel structure. This is an occasion when mechanical activation reduces the number of those lattice defects which de-activate the system to certain reactions [239].

5.3.3. EXAMPLES OF CHANGES IN HIGH TEMPERATURE REACTIONS

The influence of fine grinding and mechanical activation on the behaviour of silicates and other materials during heating has often been observed. Such changes can be deduced from thermo-analytical curves, phase analysis of systems under heating, and technological studies.

The changes induced in thermal processes by mechanical activation can be classified according to causes and types as follows:

(a) The system becomes liable to solid phase reactions due to increased dispersion. Thus, the sintering of MgO can be carried out at temperatures that are lower than the unchanged material by 373 to 446 K [240]; activated aluminium oxide can be more

readily sintered than material that has not been activated [241]; and the compaction of some kaolins by heating proceeds more thoroughly, etc.

When dolomite is finely ground in a vibration mill the sintering temperature in the manufacturing of refractories is lowered by 373 to 573 K and there is also an improvement of the mechanical properties of the product [242–244, 247]. The sintering time of enamels can be shortened when the quartz and feldspar are subjected to fine grinding [246]. Fine grinding of porcelain mass (paste) improves the strength of earthenware prepared from it [245]. The strength of a product obtained from fine-ground Fe_2O_3 and SiO_2 by subsequent sintering for 4 hours at 1423 K increased by a factor of 10, when the components were subjected to fine grinding [2].

(b) Sometimes modification of the crystal structure and amorphisation are the reasons for a shift in the transition temperature (e.g. the transformations $\alpha \rightarrow \beta$-quartz, cristobalite, calcite $\rightarrow$aragonite), or for the disappearance of certain peaks in the DTA curves.

(c) Most silicate minerals disintegrate to amorphous oxides during mechano-chemical activation. These amorphous oxides are capable of thorough mixing in the xerogel. If this xerogel is then heated, a product is obtained that differs both in its

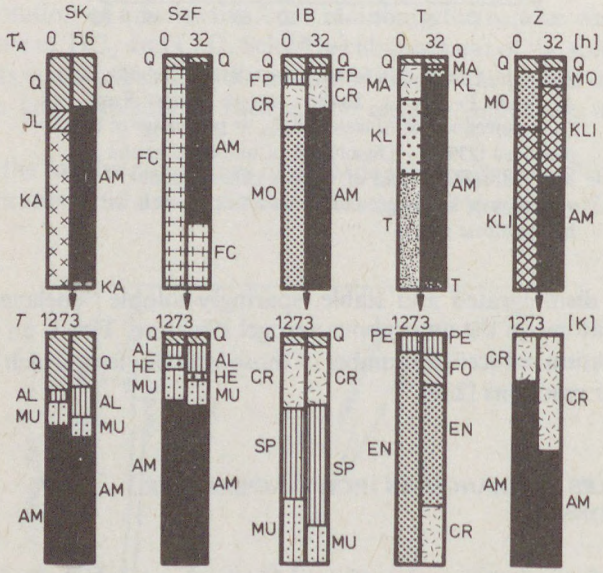

Fig. 5.37. Phase composition of various silicate minerals before and after activation (left and right half of columns) as well as with or without calcination [141]. Phases: AL = γ-Al_2O_3, AM = amorphous, CR = cristobalite, EN = enstatite, FC = fire-clay, FO = forsterite, FP = feldspar, HE = hematite, IL = illite, KA = kaolin, KL = chlorite, KLI = clinoptiolite, MA = magnesite, MO = montmorillonite, MU = mullite, PE = periclase, Q = quartz, SP = spinel, T = talc; Samples: SK = kaolin from Sárisáp, SzF = fire-clay from Szegi, IB = bentonite from Istenmezeje, T = talc from Felsőcsatár, Z = zeolite from Mád

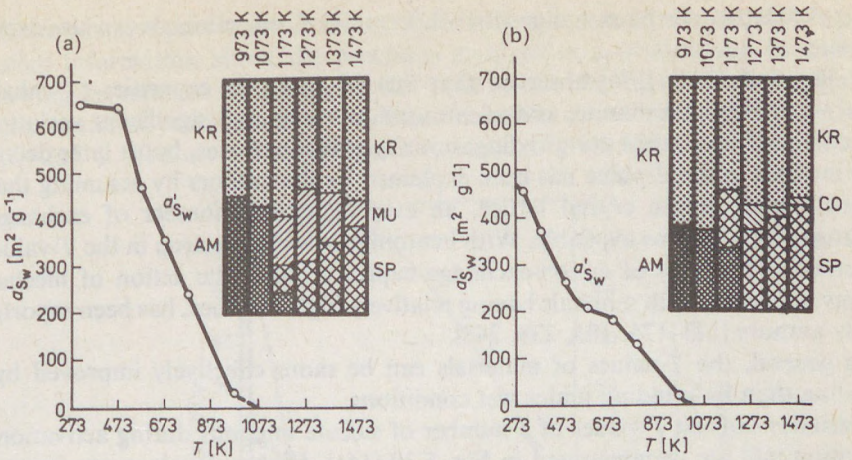

Fig. 5.38. Behaviour of bentonite during heating [249]. (a) Untreated sample, (b) after mechanical activation for 32 h. KR = cristobalite, CO = cordierite, SP = spinel, MU = mullite, AM = amorphous

qualitative and in its quantitative composition from that obtained by heating the untreated material (Fig. 5.37).

This phenomenon is well demonstrated by the behaviour of bentonite (montmorillonite) and of the xerogel obtained from it by fine grinding under heat treatment (Fig. 5.38) [249]. When untreated montmorillonite is heated at gradually increasing temperatures there is initially a shrinking of the internal specific surface because of the linking of triple layers. This is followed by the release of structural water, and later by the formation of aluminium silicate (mullite) by mutual reaction of the SiO_4^{4-} and Al(Mg, Fe)OOH units of montmorillonite. In contrast, after mechanical activation, the xerogel of montmorillonite sinters at low temperature. On raising the temperature the SiO_4^{4-} units unite to form a cristobalite structure. In this way the silicon oxide component becomes de-activated for further reactions, e.g. for mullite formation. Thus, the interaction of the oxides of aluminium, magnesium, and iron becomes dominant and, in the heated sample, the amount of mullite diminishes, or it becomes absent altogether and gives way to spinel or to cordierite that have lower silicon contents.

The thermal reactions of mechano-chemically activated systems can also be influenced by cation-exchange or adsorption of water vapour [239]. Lőcsei [247] promoted the formation of mullite from kaolinite by co-grinding raw kaolin with fluorides. With activated kaolin the mullite appeared at 923 K.

5.3.4. EXAMPLES OF THE MODIFICATION OF CATION-EXCHANGE CAPACITY

A characteristic of one group of silicate minerals is their high cation-exchange capacity, i.e. the property that cations which neutralise the excess negative charges of

the crystal lattice can be exchanged for other cations. Some minerals can also exchange anions.

Kelley and Jeney [170] observed that the ion-exchange capacities (T-values) of muscovite, biotite, kaolinite, and montmorillonite undergo significant variations in the course of prolonged dry grinding: initially value increases, but it later decreases. The increase in the T-value has been explained by the authors by assuming that, on fragmentation of the crystal lattice, an ever increasing number of exchangeable hydrogen ions become available. With bentonite, however, a drop in the T-value was observed. Variations of cation-exchange capacity under the action of mechanical energy, especially with minerals having relatively high T-values, has been reported by many authors [173–175, 185, 239, 248].

In general, the T-values of materials can be more effectively improved by dry grinding than by grinding under wet conditions.

Variations of the T-values of a number of silicate minerals during activation in a vibration mill are demonstrated in Fig. 5.39 [141]. Higher T-values are, in general, interpreted as being due to ion-exchange, i.e. they are caused by the generation of new active sites. On the fresh fracture surfaces a multitude of areas with uncompensated charges emerge and these act as surface centres for polar adsorption. With some minerals, e.g. talc, some of the Mg^{2+} ions brought to the surface by mechanical activation are amenable to ion-exchange. The fact that after prolonged grinding the T-value declines is due to the agglomeration of particles.

The effect of mechanical activation on the ion-exchange reaction of bentonite is shown in Fig. 5.40 [141]. A rise of the T-value and its decrease after prolonged grinding is also, in this case, the result of two counteracting processes: fracture of the particles involving an increase in the number of exchangeable sites and agglomeration of the

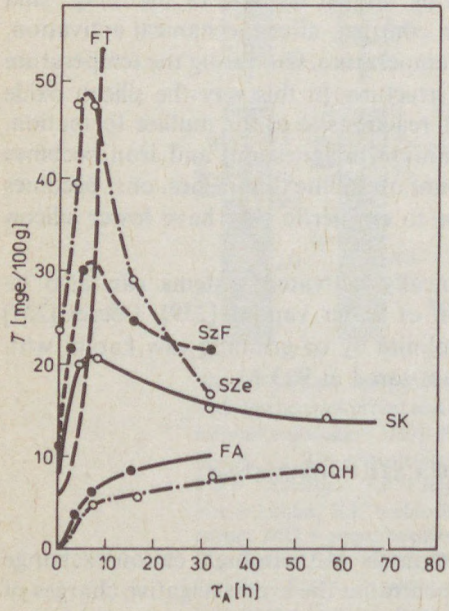

Fig. 5.39. Cation-exchange capacity (T) of some silicate minerals after activation in a vibration mill [141]. FT = talc from Felsőcsatár, SzF = fire-clay from Szegi, SZe = zeolite from Mád-Suba, SK = kaolin from Sárisáp, FA = aplite from Fehérvár, QH = quartz sand

particles which results in the covering of active sites by neighbouring particles. More detailed information about the processes involved in activation can be gained by following the amount of exchanged Ca^{2+} (Ca_T), the electric conductivity ($\varkappa$) of the ground material, and the number of water molecules co-ordinated around Ca^{2+} ions (H_2O/Ca^{2+}). Because of agglomeration, some of the Ca^{2+} ions get into non-

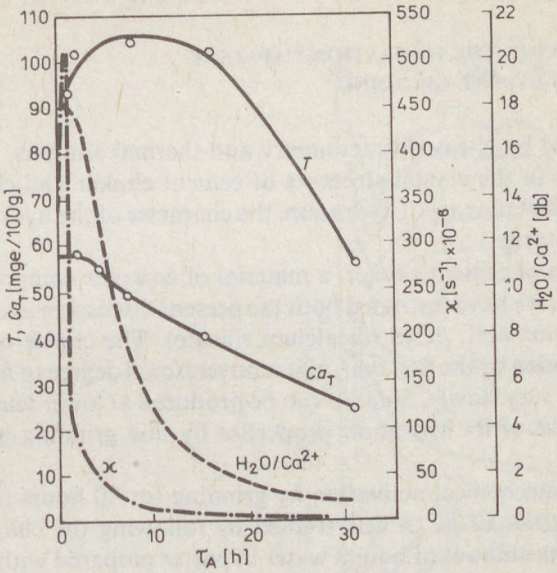

Fig. 5.40. Cation-exchange capacity of bentonite (T) and ion-exchange capacity of Ca^{2+} ions (Ca_T) as a function of grinding time. The number of water molecules which can be co-ordinated around the Ca^{2+} ions (H_2O/Ca^{2+}) as well as the electric conductivity of the ground product ($\varkappa$) are shown [141]

exchangeable positions (inside the agglomerates). Thus both the maximum number of water molecules which can be co-ordinated around the remaining exchangeable cations, and the mobility of the hydrated Ca^{2+} ions (determining the conductivity of the air-dry ground material) decrease significantly. This phenomenon cannot be fully rationalised by assuming that the Ca^{2+} ions which are situated between the triple layer of montmorillonite, and on the outside surfaces of the layers, are withdrawn into the silicate lattice which is being extensively damaged and loaded by lattice errors due to activation. It is much more important that, on agglomeration, neighbouring particles will shield exchangeable cations and make them inaccessible to external ions. Therefore, the cation-exchange capacity is reduced more than the specific surface.

Investigations of the cation-exchange reactions of kaolinite, montmorillonite, and chlorite by Bartholomä [185] established the changes that occur during the course of activation. Thus, the quantity of exchangeable Ca^{2+} increases, and the quantity of Mg^{2+} decreases as a function of grinding time, while the amount of exchangeable Na^+ remains essentially constant.

These variations of ion-exchange capacity with the history of the sample show how important it is to prepare the sample carefully before determining T-values. Mechanical activation may not only change the cation-exchange capacity of silicates, but it may also significantly modify the whole exchange process and, thereby, the results of the determinations.

5.3.5. IMPROVING THE HYDRATION CAPACITY OF βC_2S BY FINE GRINDING

As demonstrated by X-ray diffractometry and thermal analysis, prolonged grinding induces changes in the crystal structure of cement clinker and clinker minerals and these changes affect the rate of hydration, the character of the hydration products, and the course of setting.

The hydration of cement clinker, a material of complex composition, is a separate topic. Therefore, we have restricted both the present discussion and our own studies to a single clinker mineral, βC_2S (dicalcium silicate). The choice of βC_2S as a model substance is justified by the fact that, at its conventional degree of fineness, this mineral is hydrated only very slowly. Since, it can be produced at lower temperature than C_3S, any improvement of its hydration properties by fine grinding is of great practical interest.

The effect of mechanical activation by grinding for 90 hours in a ball mill on the hydration properties of βC_2S was studied by following the changes in the heat of hydration and the amount of bound water in pastes prepared with a water/solid ratio of 0.4 [140].

A significant increase of heat of hydration (for both 7-day and 28-day values) occurs after 20 hours of grinding and, up to 90 hours, it continues to increase with grinding time (Fig. 5.41). At the same time, between 20 hours and 90 hours of grinding there is

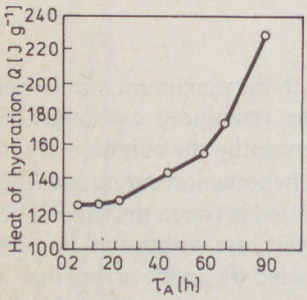

Fig. 5.41. Hydration heat of βC_2S as a function of grinding time [140]

no marked change in the dispersion of the product (a_s' decreases due to agglomeration). Instead, grinding involves mostly a distortion of the crystal lattice, i.e. amorphisation.

The heat of hydration of βC_2S activated by grinding for 90 hours amounted to 243 J g^{-1} (28-day value). This corresponds to 93% of the "total hydration heat" of βC_2S since the hydration heat of completely hydrated βC_2S is 260 J g^{-1} [250]. Complete hydration of non-activated βC_2S only takes place after setting for several

years. A similar tendency applies for the change in the amount of chemically bound water.

A peak at approximately 773 K is diagnostic for the thermal dehydration of $Ca(OH)_2$ but it does not appear on the derivatograms recorded from pastes prepared from samples obtained by mechanical dispersion for 2 hours and 20 hours, respectively (Fig. 5.42, DTA–DTG curves *a* and *b*). There are no well defined steps on the TG

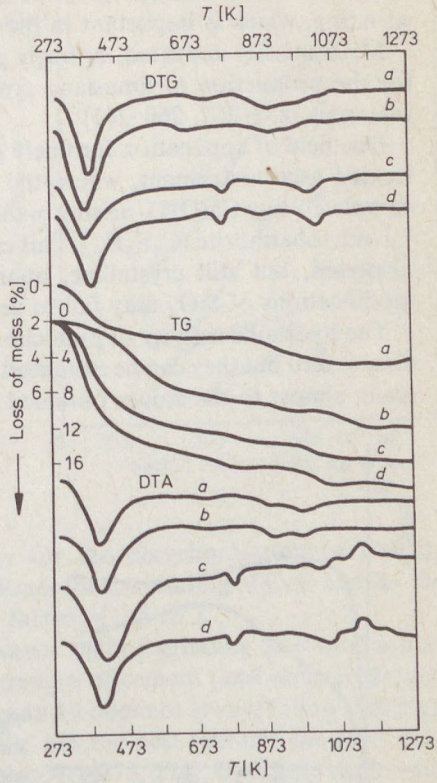

Fig. 5.42. DTA and DTG curves of hydrated βC_2S samples ground for various periods. Grinding times (τ_A): *a*—2 h, *b*—20 h, *c*—60 h, *d*—90 h [140]

curves *(a, b)*. It can therefore, be concluded that not much amorphous $Ca(OH)_2$ was formed by hydration. In contrast the derivatograms of βC_2S ground for 60 hours and 90 hours exhibit endothermic peaks characteristic of the decomposition of $Ca(OH)_2$ (around 773 K) and exothermic peaks characteristic of the transformation of the C_2SH phase to wollastonite (1175 K) (Fig. 5.42, DTA–DTG curves *c* and *d*. The formation of crystalline portlandite and its advanced hydration can also be demonstrated by X-ray diffractometry and by electron microscopy. Mechanical activation resulted in increased strength of βC_2S both in respect of initial (7-day) and final (28-day) values, especially when a surfactant was added to the feed in order to avoid aggregation and agglomeration.

The improvement of the hydration ability of βC_2S and of other clinker minerals by mechanical activation has been discussed by other authors [211–213, 251].

5.3.6. ENHANCEMENT OF ACTIVITY ACHIEVED BY FINE GRINDING HYDRAULITES, INDUSTRIAL WASTES, AND RAW MATERIALS OF THE CEMENT INDUSTRY

Activation by fine grinding to increase reactivity towards calcium hydroxide and materials, which are otherwise hydraulically inert or insufficiently active, can be activated and their reactivity towards calcium hydroxide can be much increased by fine grinding, which is important in the manufacturing of building materials.

Mechanically activated, or finely ground quartz sand can, for instance, be utilised for the production of lime-sand type, normal, and hydrothermally setting binding materials [252–257, 260–265].

One field of application for finely ground quartz is in the production of autoclave-treated asbestos cement, where the main object of applying the quartz is to bind completely any $Ca(OH)_2$ arising in the course of cement hydration by the formation of 1.1 nm tobermorite ($C_4S_5H_5$). This can only be properly achieved by using very finely dispersed, but still crystalline, quartz, since amorphised, or a priori amorphous modifications of SiO_2 may fail to generate 1.1 nm tobermorite [266, 267].

The hydraulic activity of pumicite and its reactivity towards $Ca(OH)_2$ are initially almost zero but they can be enhanced by grinding in a ball mill or in a vibration mill to reach almost to the values obtained for diatomaceous earth (Fig. 5.43).

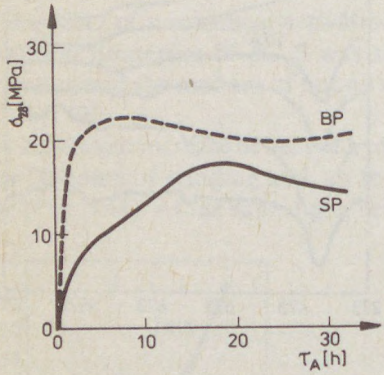

Fig. 5.43. Compressive strength σ_{28} of pumicite-lime hydrate mortars water-cured for 28 days versus grinding time τ_A in a vibrating mill [268]. BP—pumicite from Bodrogszegi, SP—pumicite from Szurdokpüspöki

Mechanically activated pumicite, when blended in a proper ratio with lime hydrate or portland cement, can be used to prepare bonding and plastering mortars and, occasionally, concretes made for special purposes [268, 269].

Mechanical activation offers opportunities for the utilisation of certain industrial wastes in the silicate industry and for the development of waste-free technologies. Thus, it is possible by mechanical activation to produce cements with low, or zero, clinker content in which the percentage of waste material may vary between 20 and 100% [270]. Activation of blast furnace slag by fine grinding is of great importance for the cement industry since, by increasing its fineness, the hydraulic activity of the slag can be much improved (cf., Fig. 5.44). In this way, it is possible to produce cements of both high strength and high cinder content [258]. It has been established that the fine

grinding of blast furnace slag induces deep-seated structural changes in the slag materials [271].

Recently, Meissner and his co-workers [251, 272] have studied the effect of mechanical activation on the technological properties of cement raw materials and on the formation of clinker minerals. Among other things, they found that, because of

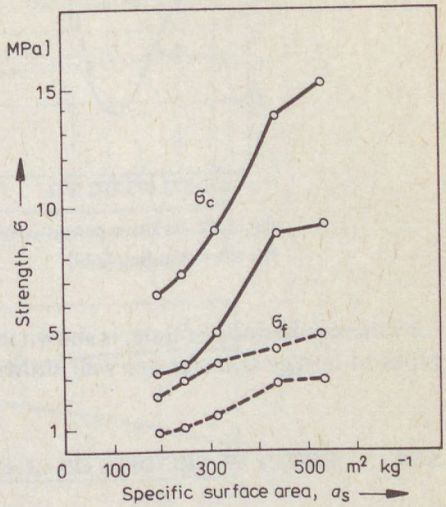

Fig. 5.44. Hydraulic activity of ground slags [274]. σ_c—compressive strength, σ_f—flexural strength

mechanical activation, the activation energy for the decarbonisation of $CaCO_3$ dropped from 160 kJ mol^{-1} to 80 kJ mol^{-1}. Rates for the binding of CaO and for the formation of clinker minerals increased by a factor of 1.5 to 2.

In connection with the technological relevance of fine grinding and mechanical activation, it should be mentioned that the strength of cement (and other hydraulic binding materials) is the result of several factors and it does not always follow that high fineness and the associated high initial activity are the best features for high final strength (cf., problems of "overgrinding" of cement) [273, 274]. Optimum dispersion and activity have to be adjusted to the technology of the application [275] or new technologies for concrete preparation have to be developed which can fully exploit high dispersion and high activity [276, 277].

5.3.7. CHANGES IN THE DIELECTRIC PROPERTIES

The dielectric properties of silicates can be influenced by grinding. The changes in these properties can be characterised by curves exhibiting a minimum, a maximum, or both [278]. A decrease of permittivity can sometimes be observed when the ground product is stored [279].

Changes in the dielectric properties closely follow changes of crystal structure and the morphology of the ground product. For example, the variation of the relative permittivity of bentonite, after heat treatment at various temperatures and grinding

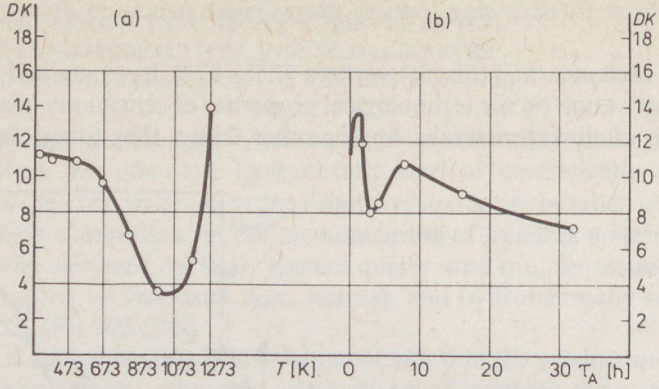

Fig. 5.45. Relative permittivity (*DK*) of bentonite (a) after heating and, (b) after grinding [249]

for different periods of time, is shown in Fig. 5.45. Differences in the effects of the two types of energy transfer are well shown by the change of permittivity.

5.3.8. EFFECT OF GRINDING ON CLAY–WATER SYSTEMS

Experience shows that the properties of aqueous suspensions and hydrogels of clay can be influenced by prior grinding, and that wet and dry grinding have opposite effects [173, 174, 180, 183, 184]. The dispersion of clay–water systems can be increased by wet grinding, while the internal structure remains largely intact. In contrast, even after relatively brief activation by dry grinding, the clay particles aggregate or even agglomerate and, therefore, the dispersion of aqueous suspensions of such material is reduced. Disintegration of the crystal structure and amorphisation also take place.

Thus, wet grinding improves those technological characteristics which are controlled by the degree of dispersion and the structure of the liosphere around particles, i.e. features such as the viscosity and stability of aqueous suspensions and the plasticity of hydrogels. Wet grinding increases the shrinkage on drying; it also increases the tendency of crack formation and deformation during drying, and the drying sensitivity. These experimental data are in accord with the observations that the kneading of clay or the intensive stirring of its suspensions [280, 281] promotes peptisation in water, increases stability and plasticity, and influences viscosity and thixotropy. Kneading, i.e. repeated plastic transformation of clay hydrogels, is one of the important technological processes in the ceramics industry for improving the plasticity of clays and raw pastes.

The quality of clay cannot be much improved by dry grinding and care must even be exercised to avoid its deterioration. Operations which involve intensive mechanical effects acting upon the crystal structure of clay minerals should not be used in the preparation of plastic clays. Although dry grinding is disadvantageous for plasticity, there may be economic reasons or some other special feature of the raw material whereby dry grinding cannot be avoided. For example, when clay is transported over

long distances it has to be stripped from its natural water content at the mine site. However, dried lumps of clay, disintegrate slowly in water and after fine grinding they can be transformed readily to a hydrogel. Therefore, in the dressing plant the drying of clay is usually followed by fine grinding which serves as an activation operation. If, during this process, mechanical dispersion is carried to the stage of mechanical activation, this will result in a deterioration of the plasticity of the clay (Fig. 5.46).

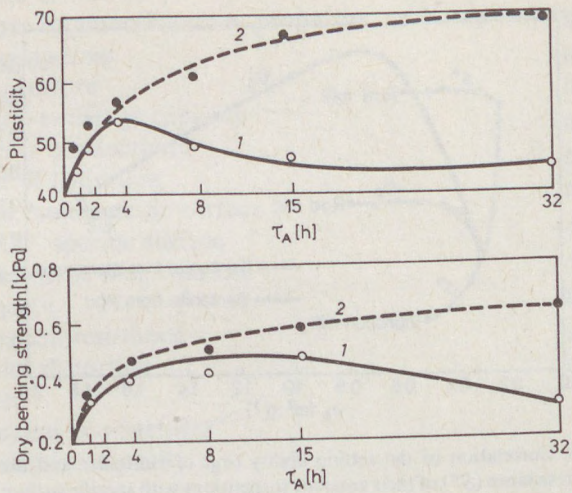

Fig. 5.46. Plasticity and dry bending strength of clays after mechanical activation. *1*—Dry grinding, *2*—wet grinding [97]

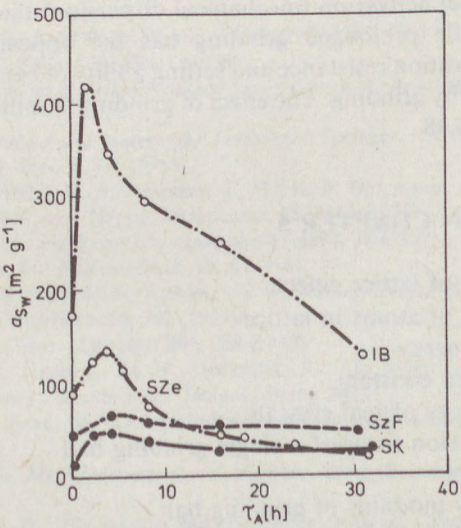

Fig. 5.47. "Methylene blue surface" (a_{SM}) of aqueous suspensions as a function of time for dry grinding [97]. IB = bentonite from Istenmezeje, SZe = zeolite from Suba, SzF = fire-clay from Szegi, SK = kaolin from Sárisáp

Adsorption of methylene blue is often employed [282] for determining the "active" specific surface of clays. This surface represents the surface which is accessible, or is becoming accessible, to the large molecules of the dye. The values obtained may also characterise plasticity and the montmorillonite content of the clay sample. If the other factors which bear on wetability by influencing the liosphere are constant, then the larger the "methylene blue area" the better the plasticity of a clay. From Figure 5.47 it

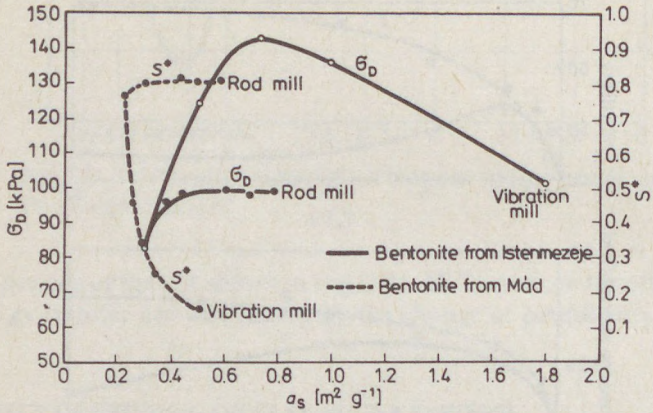

Fig. 5.48. Correlation of the setting ability (σ_D) of bentonite and the filtering resistance (S^*) of their aqueous suspensions with specific surface (a_s) after activation in two different types of mills [97]

is apparent that by brief activation (mechanical dispersion) the methylene blue are can be increased, while prolonged grinding has the opposite effect because c agglomeration. The filtration resistance and setting ability of bentonite-based foundı sands are also changed by grinding. The effect of grinding in mills of different type ca be gleaned from Fig. 5.48.

SYMBOLS IN CHAPTER 5

n	number of lattice defects
N	number of atoms in lattice
E_u	lattice energy
k	Boltzman constant
f	free energy of real crystals
F_g	compression force of a single grinding ball
c, k, m	constants
E	elasticity modulus of grinding ball
ϱ	density
v_a	elevation velocity of balls
α'	Madelung constant depending on the type of lattice
V, V_0, V_2	volume, molar volume

W	work
P	force
D	diffusion rate
A_n	activation energy of the formation of lattice defects
A_d	activation energy of the diffusion of lattice defects
Λ	crystallite size
δ_a/a_0	lattice distortion
RAm	degree of amorphisation, proportion of X-ray amorphous material
τ_A	grinding time
T	temperature
T	cation-exchange capacity
$\varkappa$	electric conductivity
Q	heat of hydration
a_s	"external" specific surface
a'_s	"total" specific surface
a_{s_M}	"methylene blue" surface
$\sigma, \sigma_D, \sigma_C, \sigma_f$	strength
S^*	filtration resistance
G_v	lattice distortion
m	mass
ξ_0	"oxygen compactness"
c_a	adsorptive capacity

REFERENCES

[1] Kittel, C.: *Introduction to Solid State Physics*. Wiley, New York 1961

[2] Naeser, G., Scholz, W.: *Kolloid-Z.*, **156**, 1 (1958)

[3] Smekal, A. G.: in *Proceedings of the International Symposium on the Reactivity of Solids* (ed. Hedvall, J. A.). Cotenburg, 1952

[4] Smekal, A. G.: *Zur Struktur und Materie der Festkörper*. Springer, Berlin 1952

[5] Gaudin, A. M.: *Mining Eng.*, **7**, 531 (1955)

[6] (Boldirev, V. V., Zakrevskij, V. A., Urakaev, F. H.) В. В. Болдырев, В. А. Закревский, Ф. Х. Уракаев: *Изв. АН СССР*, сер. Неорг. материалы, **15**, 2154 (1979)

[7] Schrader, R., Tetzner, G.: *Freiberger Forschungshefte, A*292, 28 (1965)

[8] Schrader, R., Kneschke, G.: *Silikattechnik*, **19**, 6 (1968)

[9] Meyer, K., Polly, F.: *Dechema Monographien. Vol. 57*, Verlag Chemie, Weinheim 1967

[10] Kramer, J.: *Acta Phys. Austriaca*, **10**, 392 (1957)

[11] Jedamzik, J.: *Z. Phys. Chem. (Leipzig)*, **261**, 258 (1980)

[12] Boden, G., Sahre, P., Henning, M. P., Jedamzik, J.: *IX. Symp. für Mechanoemission und Mechanochemie* (Summary). Kammer der Technik, Berlin 1983

[13] Streleckij, A. N.: *IX. Symp. für Mechanoemission und Mechanochemie* (Summary). Kammer der Technik, Berlin 1983

[14] Krell, A.: *IX. Symp. für Mechanoemission und Mechanochemie* (Summary). Kammer der Technik, Berlin 1983

[15] Bowden, F. F., Teabor, D.: *The Friction and Lubrication of Solids*. Clarendor. Press, Oxford 1964

[16] Peters, K.: *1. Europ. Symp. Zerkleinern* (ed. Rumpf, H.). Verlag Chemie, Weinheim, VDI Verlag, Düsseldorf 1962

[17] Lin, I. J., Nadiv, S., Grodzian, D. J. M.: *Mineral Sci. Eng.*, **7**, 313 (1975)

[18] Juhász, Z., Wojnarovitsné, I.: *Ber. Dtsch. Keram. Ges.*, **61**, 131 (1984)

[19] Huhn, H. J., Heegn, H.: *Silikattechnik*, **29,** 376 (1978)
[20] Boldirev, V. V.: *Banicke Listy*, VEDA Bratislava 1982
[21] Menyhárt-Kocsis, M., Domsa, K.: *Chem. Tech.*, **20,** 630 (1968)
[22] (Urakaev, F. H., Boldirev, V. V., Pozdnjakov, O. F., Regely, V. P.) Ф. Х. Уракаев, В. В. Болдырев, О. Ф. Поздняков, В. Р. Регель: *Кинетика и катализ*, **18,** 350 (1977)
[23] (Urakaev, F. H., Pozdnjakov, O. F., Boldirev, V. V., Savintsev, Ju. P.) Ф. Х. Уракаев, О. Ф. поздняков, В. В. Болдырев, Ю. П. Савинцев: *Кинетика и катализ*, **19,** 1442 (1978)
[24] Carey Lea, M. C.: *Phil. Mag. & J. Sci.*, **37,** 470 (1894)
[25] Krauth, A.: *Ber. Dtsch. Keram. Ges.*, **45,** 622 (1968)
[26] Tkačova, K., Heegn, H.: *Silikaty*, **4,** 321 (1976)
[27] Bernhardt, C., Heegn, H., Ilgen, S., Reinsch, E.: *Banicke Listy*, VEDA Bratislava 1982
[28] Migasaka, K., Senna, M.: *Termochemica Acta*, **83,** 225 (1985)
[29] Heegn, H.: In: Untersuchungsmethoden zur Charakterisierung mechanisch aktivierter Festkörper (ed. Juhász, Z.) *BME Tudományos Közlemények*, **13,** KÖZDOK, Budapest 1978
[30] Machida, M., Senna, M.: *J. Phys. Chem.*, **89,** 313 (1985)
[31] Fuerstenau, D. W., Venkataraman, K. S.: *Proceedings of International Symposium on Powder Technology '81*. The Soc. of Powder Techn., Kyoto 1982
[32] (Ljahov, N. Z., Boldirev, V. V.) Н. З. Ляхов, В. В. Болдырев: *Изв. СО АН СССР* **12,** серия хим. наук (1982)
[33] Ljahov, N. Z.: *Banicke Listy*, VEDA, Bratislava 1982
[34] (Pavljuhin, Ju. T., Marikov, Ju. Ju., Boldirev, V. V.) Ю. Т. Павлюхин, Ю. Ю. Мариков, В. В. Болдырев: *Изв. АН СССР*, **12,** серия хим. наук (1983)
[35] (Budnikov, P. P., Ginstling, A. M.) П. П. Будников, А. М. Гинстлинг: *Реакции в смесях твердых тел*. Госстройиздат, Москва 1961
[36] Schleede, A., Gantzchow, G.: *Z. Phys.*, *A***15,** 15 (1923)
[37] Mill, G.: *Acta Cryst.*, **9,** 21 (1956)
[38] Imamura, K., Senna, M.: *Mat. Res. Bull.*, **19,** 59 (1984)
[39] Bredig, M. A.: *J. Phys. Chem.*, **46,** 801 (1942)
[40] Kochanowska, A., Satawa, V.: *Ber. Dtsch. Akad. Wiss.*, Berlin 1959
[41] Northwood, D. O., Lewis, D.: *Am. Mineral*, **53,** 2089 (1968)
[42] Rendon, J. L., Cornejo, J., Arambarri, P.: *J. Colloid & Interface Sci.*, **94,** 546 (1983)
[43] Hall, H., Kitschingman, W.: *Nature (London)*, **180,** 1067 (1957)
[44] Tilley, C. E.: *Mineralog. Mag.*, **22,** 77 (1929)
[45] Eitel, W.: *Physikalische Chemie der Silikate*. Leipzig 1941
[46] Frenkel, J.: *Z. Phys.*, *A***37,** 572 (1926)
[47] White, V. B.: *J. Am. Ceram. Soc.*, **44,** 170 (1961)
[48] Naeser, G., Scholz, W.: *Ber. Dtsch. Keram. Ges.*, **39,** 106 (1962)
[49] Boehm, M., Hofmann, Z.: *Z. anorg. u. allgem. Chem.*, **278,** 58 (1955)
[50] Anst, R. B., Drickauer, M. G.: *Science*, **140,** 817 (1963)
[51] Liebold, R.: *Technik*, **7,** 113 (1952)
[52] Dachille, F., Roy, R.: *Nature (London)*, **186,** 34 (1960)
[53] Bridgman, P. W.: *J. Chem. Phys.*, **15,** 311 (1974)
[54] Náray-Szabó, I.: *Inorganic Chemistry* (in Hungarian). Tankönyvkiadó, Budapest 1957
[55] Schrader, R., Hoffmann, B.: *Z. anorg. u. allgem. Chem.*, **369,** 41 (1969)
[56] Bruns, J. M., Bredig, M. A.: *J. Chem. Phys.*, **25,** 1281 (1956)
[57] Jameson, C., Goldsmith, F. R.: *Amer. Mineral.*, **45,** 818 (1960)
[58] Sterzel, W.: *Angew. Chem.*, **77,** 16 (1965)
[59] Juhász, Z.: *Acta Geol. Acad. Sci., Hung.*, **25,** 247 (1982)
[60] Senna, M., Iguchi, Y.: in *Reactivity of Solids* (eds: Barret, P., Dufour, L. C.). Amsterdam 1985
[61] Schrader, R., Weigelt, D.: *Z. anorg. u. allgem. Chem.*, **372,** 228 (1970)
[62] Imamura, K., Senna, M.: *J. Chem. Soc. Faraday Trans.*, **78,** 1131 (1982)
[63] Neff, M.: *Grundlagen und Anwendung der Röntgen-Feinstruktur-Analyse*. R. Oldenbourg, München 1962
[64] Kochendörfer, A.: *Z. Kristallogr.*, **105,** 393 (1944)
[65] Fricke, R., Gwinner, E.: *Z. Phys. Chem.*, **183,** 3 165 (1939)
[66] Ohlberg, S., Stricker, D.: *J. Am. Ceram. Soc.*, **45,** 170 (1962)

[67] Patzak, I.: *Ber. Dtsch. Keram. Ges.*, **43**, 77 (1966)
[68] Ludwig, G.: In: Untersuchungsmethoden zur Charakterisierung mechanisch aktivierter Festkörper (ed. Juhász, Z.) *BME Tud. Közl.*, **13**, KÖZDOK, Budapest 1978
[69] Ziegler, G.: *Keram. Z.*, **33**, 10, 602 (1981)
[70] Arkel, A. C.: *Physica*, **5**, 208 (1925)
[71] Goucher, S. S.: *Phil. Mag.*, **2**, 289 (1929)
[72] Burgers, W. G.: *Nature (London)*, 1037 (1935)
[73] Wassermann, G.: *Z. Metallk.*, **28**, 262 (1936)
[74] Paudert, R., Liebscher, S., Körlin, P., Trinks, W.: *Chem. Tech.*, **20**, 276 (1968)
[75] Dehlinger, V.: *Z. Kristallogr.*, **65**, 615 (1927)
[76] Hess, K., Stener, E., Fromm, N.: *Kolloid-Z.*, **98**, 148 (1942)
[77] Talbot, J. M., Kempis, E. B.: *Nature (London)*, **197**, 166 (1963)
[78] (Barambojm, N. K.) Н. К. Барамбойм: *Механохимия высокомолекулярных полимеров*. е. изд. химия, Москва 1978
[79] (Boldirev, V. V.) В. В. Болдырев: *Наука (Сибирское отделение)*, **64**, 42 (1983)
[80] Heinicke, G.: *Tribochemistry*. Akademie Verlag, Berlin 1984
[81] Steinicke, K., Ebert, J., Geissler, H., Hennig, H. P., Kretzschmer, U.: *Krist. & Tech.*, **13**, 597 (1978)
[82] Steinicke, U., Kretzschmer, U., Barsova, L., Jurik, T., Hennig, H. P.: *Cryst. Res. & Tech.*, **16**, 971 (1981)
[83] Kretzschmer, U., Ebert, I., Steinicke, U., Hennig, H. P.: *Cryst. Res. & Tech.*, **16**, 949 (1981)
[84] Steinicke, U., Barsova, L., Kretzschmer, U., Jurik, T.: *Banicky Listy*, VEDA, Bratislava 1984
[85] Schmalzried, H.: *Festkörper-reaktionen*. Akademie Verlag, Berlin 1971
[86] Juhász, Z.: *MTA Kémiai Közlemények*, **43**, 225 (1975)
[87] Arai, Y., Yasue, T.: *Kogyo Kwagaku Zasshi*, **73**, 2603 (1970)
[88] Juhász, Z.: Mechanical activation of raw materials in industry of building materials (in Hungarian). DSc Thesis, Budapest 1979
[89] Fischer, F., Peters, K., Warnecke, A.: *Brennstoff-Chem.*, **13**, 209 (1932)
[90] Grohn, H., Paudert, R., Bisinger, H. F.: *Z. Chem.*, **2**, 88 (1962)
[91] Heinicke, G., Harenz, H.: *Z. anorg. u. allgem. Chem.*, **329**, 185 (1963)
[92] Jamieson, J. G., Goldsmith, J. R.: *Am. Mineral.*, **45**, 818 (1960)
[93] Hüttig, G. F., Simm, W., Glawitsch, G.: *Mech. Chem.*, **85**, 1124 (1954)
[94] Menyhárt-Kocsis, M., Domsa, K.: *MTA Kémiai Közlemények*, **35**, 9 (1971)
[95] Smekal, A. G.: *Naturwissenschaften*, **39**, 18 (1952)
[96] Heinicke, G., Riedl, R., Harenz, H.: *Z. Phys. Chem. (Leipzig)*, **227**, 62 (1964)
[97] Juhász, Z.: Mechanochemical activation of silicate minerals (in Hungarian). PhD. thesis, Budapest 1969
[98] Juhász, Z.: *Acta Chim. Acad. Sci. Hung.*, **114**, 199 (1983)
[99] Gammage, R. S., Glasson, D. R., Hodgson, I. R.: *J. Colloid & Interface Sci.*, **92**, 2, 530 (1983)
[100] Avvakumov, E. G.: *Banicke Listy*, VEDA, Bratislava 1980
[101] Bartha, R., Bruthans, Z.: *Építőanyag*, **15**, 113 (1963)
[102] Thiessen, P. A., Meyer, K., Heinicke, G.: *Grundlagen der Tribochemie*. Akademie Verlag, Verlin 1967
[103] Waenting, P.: *Kolloid-Z.*, **41**, 152 (1927)
[104] Stener, E.: *Chem. Tech.*, **1**, 1 (1943)
[105] Hess, K., Stener, E.: *Z. Phys. Chem. (Wiesbaden)*, **193**, 234 (1943)
[106] Hoffmann, M., Kaufmann, W.: *Chem. Rundschau*, **9**, 13 (1956)
[107] Juhász, K.: Degradation and stabilisation of polymers (in Hungarian). Tankönyvkiadó, Budapest 1964
[108] (Sirokov, Ju. G., Iljin, A. P.) Ю. Г. Широков, А. П. Ильин: *Изв. АН СССР*, серия химических наук, **6**, 34 (1983)
[109] Takahashi, H., Tsutsumi, K.: *Dechema Monographien. Vol. 57*, Verlag Chemie, Weinheim 1967
[110] Schrader, R., Dreier, K., Werner, M. H.: *Chem. Tech.*, **20**, 475 (1968)
[111] Likl, F., Zemsch, P.: *Elektrochem.*, **56**, 979 (1952)
[112] Kiperman, S. L., Bolondin, A. A., Dawidova, J. R.: *Chem. Zentr.*, 4401 (1959)
[113] Adamtschik, K. A.: *Silikattechnik*, **12**, 557 (1952)
[114] Rasch, R.: *Ber. Dtsch. Keram. Ges.*, **40**, 7, 635 (1963)
[115] Tammann, G.: *Z. Elektrochem.*, **35**, 21 (1929)

[116] Hüttig, G. F.: *Zement-Kalk-Gips*, **7**, 151 (1954)
[117] Szánthó, E.: *MTA Műszaki Tudományok Oszt. Közlemények*, **38**, 191 (1967)
[118] Menyhárt-Kocsis, M.: *Építőanyag*, **27**, 348 (1975)
[119] Heinicke, G.: *Z. Chem.*, **2**, 284 (1982)
[120] Naeser, G., Scholz, W.: *Ber. Dtsch. Keram. Ges.*, **39**, 106 (1962)
[121] Köster, A.: *Angew. Chem.*, **69**, 563 (1957)
[122] Beke, B., Opoczky, L.: *Dechema Monographien. Vol. 57*, Verlag Chemie, Weinheim 1967
[123] Lehmann, M., Fahn, R.: *Tonind. Ztg. u. Keram. Rundschau*, **79**, 3 (1955)
[124] Bruckner, Gy.: *Organic Chemistry* (in Hungarian). Tankönyvkiadó, Budapest 1952
[125] Alexander, L. T., Byers, M. G.: *J. Chem. Educ.*, **9**, 916 (1932)
[126] Schaw, M. C.: *J. Appl. Mechanics*, **15**, 37 (1948)
[127] Grohn, H., Friedrich, H., Paudert, R.: *Z. Chem.*, **2**, 24 (1962)
[128] Jenova, L. P.: *Kolloidn. Zh.*, **250**, 186 (1972)
[129] Daniel, H., Gentili, R.: *Helv. Chim. Acta*, **39**, 1586 (1956)
[130] Benson, B. E., Castle, J. E.: *J. Phys. Chem.*, **62**, 840 (1958)
[131] Grohn, H., Paudert, R.: *J. prakt. Chem.*, **11**, 63 (1960)
[132] (Isakov, P. M.) П. М. Исаков: *Качественный анализ руд и минералов методом растирания порошков*. Гос. Изд-во геологической литературы, Москва 1953
[133] Lin, I. J., Somasundaran, P.: *Powder Technol.*, **6**, 171 (1972)
[134] Hristo, C. G.: Mechanism of solid-phase reactions initiated by mechanical activation. DSc thesis, Burgas 1983
[135] Opoczky, L.: Fine grinding processes of brittle materials in silicate industry (in Hungarian). DSc thesis, Budapest 1982
[136] Mehta, P. K.: *Rock Products*, May, 84 (1971)
[137] Coney, J. J.: *Belgische Auslegeschrift*, **623**, 417 (1963)
[138] Schrader, R., Köhnke, K.: *Silikattechnik*, **21**, 47 (1970)
[139] Philipp, O., Schrader, R.: *The VI. International Congress on the Chemistry of Cement. Vol. I*, Moscow Stroyizdat 1976
[140] Opoczky, L., Juhász, Z.: *The VI. International Congress on the Chemistry of Cement. Vol. II*, Moscow Stroyizdat 1976
[141] Juhász, Z.: *MTA Kémiai Közlemények*, **31**, 227 (1969)
[142] Szánthó, E., Lindner, O.: *Dechema Monographien, Vol. 57*, Verlag Chemie, Weinheim 1967
[143] (Adamtschik, K. A.) К. А. Адамчик: *Журнал прикладной химии*, **1**, 13 (1952)
[144] Melland, D. W., Cuming, W. M., Ritchie, P. D.: *J. Appl. Chem.*, **2**, 31 (1952)
[145] (Budnikov, P. P., Mchedlov-Petrosjan, O. P.) П. П. Будников, О. П. Мчедлов-Петросян: *Журнал прикладной химии*, **5**, 645 (1956)
[146] Schrader, R., Wissing, R., Kubsch, M.: *Z. anorg. u. allgem. Chem.*, **365**, 171 (1969)
[147] Bernhardt, C., Heegn, M.: *Építőanyag*, **27**, 321 (1975)
[148] Schneider, U.: *Aufbereitungs-Technik*, **11**, 567 (1968)
[149] Steier, K., Hoffmann, F., Schönert, K.: *Chem. Ing. Tech.*, **46**, 739 (1974)
[150] Chaklader, A. C. D.: *Trans. Brit. Ceram. Soc.*, **63**, 289 (1964)
[151] Flörke, O. W.: *Tonind. Ztg. u. Keram. Rundschau*, **85**, 141 (1961)
[152] Hoffmann, U., Roth, A.: *Z. anorg. u. allgem. Chem.*, **357**, 196 (1968)
[153] Briscoe, M. V. A., Molt, P. F.: *Trans. Int. Min. Metall.*, **46**, 291 (1973)
[154] King, E. J.: *Occupational Med.*, **4**, 26 (1947)
[155] Demster, P. D., Ritchie, P. D.: *J. Appl. Chem.*, **3**, 182 (1952)
[156] Gibb, J. G., Ritchie, P. D., Sharp, J. W.: *J. Appl. Chem.*, **4**, 213 (1953)
[157] Weyl, W. A.: *Structure and Properties of Solid Surfaces*, Chicago 1953
[158] Juhász, Z.: *Építőanyag*, **27**, 337 (1975)
[159] Takamura, T., Yoshida, M., Inazuka, K.: *Kolloid-Z.*, **195**, 12 (1963)
[160] Nagelschmidt, G., Gordon, R. L., Griffin, O. G.: *Nature (London)*, **169**, 539 (1952)
[161] Rehbinder, P. A., Hodakov, G. S.: *Silikattechnik*, **13**, 200 (1962)
[162] Hoffmann, F., Schönert, K.: *Powder Technol.*, **39**, 77 (1984)
[163] Heegn, M., Bernhardt, C.: *Freiberger Forschungshefte, A553*, 57 (1976)
[164] Sakabe, H., Kawai, K., Koshi, K., Soda, R., Hamada, A., Schiman, M., Mayashi, M.: *Bull. Nat. Inst. Indust.* (Japan), **4**, 1 (1960)

[165] Steinicke, U.: *IX. Symp. für Mechanoemission und Mechanochemie* (Summary). Kammer der Technik, Berlin 1983
[166] Steinicke, U., Hennig, H. P., Richter, A., Mendau, J., Kretzschmer, U.: *Cryst. Res & Technol.*, **17**, 1585 (1982)
[167] Hennig, H. P., Ebert, I., Steinicke, U., Geissler, H., Kretzschmer, U.: *Krist. & Techn.*, **15**, 353 (1980)
[168] Hennig, H. P., Steinicke, U., Ebert, I., Geissler, H.: *Banicky Listy*, VEDA, Bratislava 1980
[169] Steinicke, U., Hennig, H. P., Ebert, I.: *Z. Phys. Chem. (Leipzig)*, 266 (1985)
[170] Kelley, W. P., Jenney, M.: *Soil Sci.*, **41**, 367 (1936)
[171] Mackenzie, R. C., Meldau, R., Cramer, V. R.: *Ber. Dtsch. Keram. Ges.*, **33**, 22 (1956)
[172] Rouxhet, P. G., Brindely, G. W.: *Clay Minerals*, **6**, 211 (1966)
[173] Köhler, E., Hoffmann, U., Scharrer, E., Frühauf, K.: *Ber. Dtsch. Keram. Ges.*, **37**, 11 (1960)
[174] Shaw, B. T.: *J. Phys. Chem.*, **46**, 1032 (1942)
[175] Laws, W. D., Page, J. B.: *Soil Sci.*, **62**, 319 (1946)
[176] Perkins, A. T.: *Soil Sci.*, **65**, 185 (1948)
[177] Gregg, S. T., Hill, K. J., Parker, T. W.: *J. Appl. Chem.*, **4**, 631 (1954)
[178] Gregg, S. T.: *Trans. Brit. Ceram. Soc.*, **54**, 259 (1955)
[179] Lehmann, H., Fahn, R.: *Tonind. Ztg. u. Keram. Rundschau*, **79**, 3 (1955)
[180] Wiegmann, J., Kranz, G.: *Silikattechnik*, **8**, 520 (1957)
[181] Wiegmann, J.: *Bull. soc. franç. céram.*, **36**, 49 (1957)
[182] Wiegmann, J.: *Ber. Dtsch. Keram. Ges.*, **34**, 257 (1957)
[183] Haase, Ph., Winter, K.: *Bull. soc. franç. céram.*, **44**, 13 (1959)
[184] Legrand, C., Nicols, J.: *Bull. soc. franç. céram.*, **44**, 61 (1959)
[185] Bartholomä, M. D.: *Ber. Dtsch. Keram. Ges.*, **36**, 28 (1959)
[186] Bartholomä, M. D., Schwiete, M. G.: *Die Ziegelindustrie*, **4**, 97 (1960); **12**, 421 (1960)
[187] Miller, W.: *Silikattechnik*, **19**, 128 (1968)
[188] Schrader, R., Kutzer, M. I., Hoffmann, Br.: *Tonind. Ztg. u. Keram. Rundschau*, **94**, 410 (1970)
[189] Hlavay, J., Jonás, K., Elek, S., Inczédy, J.: *Clay Minerals*, **25**, 451 (1977)
[190] Juhász, Z.: *Acta Mineralogica Petrographica*, **26**, 121 (1979)
[191] Tóth, M.: Proceedings of 10*th* Int. Kaolin Symp. (UNESCO). Budapest 1979
[192] Ocepek, D.: *Dechema Monographien. Vol. 57*, Verlag Chemie, Weinheim 1967
[193] Hahn, H. J., Müller, A.: *J. Thermal Anal.*, **19**, 485 (1980)
[194] Hlavay, J., Inczédy, J.: *Építőanyag*, **29**, 29 (1977)
[195] Parker, T. W.: *Clay Minerals*, **8**, 135 (1962)
[196] Juhász, Z.: *Ber. Dtsch. Keram. Ges.*, **50**, 267 (1973)
[197] Čičel, Kranz, G.: *Clay Minerals*, **16** (1981)
[198] Novak, I., Jakubekova, D., Fatalova, D.: *Silikaty*, **26**, 15 (1982)
[199] Juhász, Z.: *Bull. Hung. Geol. Soc.*, **99**, 22 (1969)
[200] Opoczky, L.: *Fibre Reinforced Cement and Concrete RILEM Symposium*. The Construction Press LPD, London 1975
[201] Opoczky, L.: *Banicke Listy*, VEDA, Bratislava 1980
[202] Opoczky, L.: *Proceedings of International Symposium on Powder Technology '81*. The Soc. of Powder Techn., Kyoto 1982
[203] (Berkovich, T. M.) Т. М. Беркович: *Эффективность использования асбеста при производстве асбестоцементных изделий*. Изд-во лит. по строительству, Москва 1972
[204] Motoi, S.: *J. Ceram. Assoc. (Japan)*, **86**, 92 (1978)
[205] Büssem, W., Schusterius, C.: *Wiss. Veröffentl. Siemens-Werke*, **17**, 59 (1938). In: Eitel, W.: Phys. Chem. Silikate. Leipzig 1941
[206] Opoczky, L.: *Építőanyag*, **18**, 41 (1966)
[207] Opoczky, L.: Investigation of grinding processes of the cement clinker and intensifying them by grinding aids (in Hungarian). Ph.D. thesis, Budapest 1968
[208] Opoczky, L.: *European Symposium on Particle Technology*. Reprints, Vol. A, Dechema, Frankfurt am Main 1980
[209] Opoczky, L.: *Powder Technol.*, **17**, 1 (1977)
[210] Opoczky, L.: *MTA Kémiai Közlemények*, **48**, 235 (1977)
[211] (Kudrjavceva, N. C., Hodakov, G. S.) Н. Л. Кудрявцева, Г. С. Ходоков: *Коллоидный журнал*, **28**, 524 (1966)

[212] (Hodakov, G. S.) Г. С. Ходаков: *Тонкое измельчение строительных материалов*. Изд-во литературы по строительству, Москва 1972
[213] Schrader, R.: *Silikattechnik*, **22,** 344 (1971)
[214] Jannaguis, N., Guinnier, A.: *The VI. International Congress on the Chemistry of Cement. Vol. I*, Stroyizdat, Moscow 1976
[215] Dachille, F., Roy, R.: *Proceedings of 4th International Symposium on the Reactivity of Solids*. Amsterdam 1960
[216] Gout, R., Kra-Kouadio, L., Panis, A.: *Bull. soc. franç. céram.*, **116,** 3 (1977)
[217] Kachalova, L.: *Építőanyag*, **31,** 27 (1979)
[218] Steinicke, U., Barsova, L. J., Kretzschmer, U., Jurik, T.: *Banicke Listy*, VEDA, Bratislava 1984
[219] Hennig, H. P., Ebert, I., Jost, H., Pielert, L., Stork, I., Tkačova, K.: *Banicke Listy*, VEDA, Bratislava 1984
[220] Hennig, H. P., Ebert, I., Tkačova, K., Jost, H., Pielert, L., Stevulova, N.: *Banicke Listy*, VEDA, Bratislava 1984
[221] Schlagel, E., Morgner, J.: *Silikattechnik*, **22,** 48 (1971)
[222] Juhász, Z.: *Periodica Polytechnica*, **22,** 57 (1978)
[223] (Polubojarinov, D. I., Popilskij, D. Ja.) Д. И. Полубояринов, П. Я. Попильский: *Огнеупоры*, **26,** 80 (1961)
[224] Schrader, R., Hoffmann, B., Planitz, H., Henneberger, I.: *Zement-Kalk-Gips*, **5,** 194 (1970)
[225] Osmond, F.: *Ann. Mineral.*, **8,** 5 (1885)
[226] Heyn, E., Bauer, O.: *Mittl. Kgl. Materialprüf. Amt.*, 128 (1909)
[227] Wache, X., Chandron, G.: *Compt. rend.*, **180,** 1495 (1925)
[228] Hess, K., Henman, K. E.: *Ber. Dtsch. Keram. Ges.*, **75,** 1802 (1942)
[229] Puchegger, F.: *Naturwissenschaften*, **39,** 428 (1952)
[230] Paudert, R., Liebscher, S., Trinks, W.: *Chem. Tech.*, **19,** 356 (1966)
[231] Schrader, R., Rumpf, H.: *Z. anorg. u. allgem. Chem.*, **350,** 137 (1967)
[232] Schrader, R., Rumpf, H., Kressner, R.: *Chem. Ing. Tech.*, **39,** 843 (1967)
[233] Schrader, R., Hoffmann, K.: *Chem. Ing. Tech.*, **42,** 38 (1970)
[234] Schrader, R., Arnold, M., Rumpf, H.: *Z. anorg. u. allgem. Chem.*, **350,** 120 (1967)
[235] Szánthó, E.: *VIII. Int. Kongress für Erzaufbereitung*. Leningrad 1968
[236] Juhász, Z.: *Aufbereitungs-Technik*, **41,** 558 (1974)
[237] Schrader, R., Dusdorf, M.: *Krist. & Tech.*, **1,** 59 (1966)
[238] Schmidt, K. G.: *Ber. Dtsch. Keram Ges.*, **31,** 42 (1954)
[239] Juhász, Z.: *MTA Kémiai Közlemények*, **48,** 167 (1976)
[240] Tresswjatskij, S. G.: *Chem. Zbl.*, 4599 (1959)
[241] Sztankovics, L.: *Építőanyag*, **22,** 262 (1970)
[242] (Kajnarskij, I. S., Nazarenko, N. D.) И. С. Кайнарский, Н. Д. Назаренко: *Огнеупоры*, **2** (1956)
[243] (Salkov, K. A., Nevredimova, P. V., Radin, V. V.) К. А. Шалков, П. В. Невредимова, В. В. Радин: *Огнеупоры*, **1** (1956)
[244] (Kajnarskij, I. S., Nazarenko, N. D.) И. С. кайнарский, Н. Д. Назаренко: *Сб. Научных трудов по химии и технологии силикатов*. Промстройиздат, Москва 1956
[245] (Avgustinnik, A. I., Krasninskaja, V. M., Alekseeva, N. S.) А. И. Августинник, В. М. Краснинская, Н. С. Алексеева: *Сб. научных трудов по химии и технологии силикатов*. Промстройиздат, Москва 1956
[246] (Nosova, Z. A., Smirnova, K. A.) З. А. Носова, К. А. Смирнова: *Стекло и керамика*, **4,** 18 (1956)
[247] Lőcsei, B.: *Építőanyag*, **22,** 332 (1970)
[248] Sanyal, J., Lahiri, D.: *Trans. Ind. Ceram. Soc.*, **20,** 11 (1961)
[249] Juhász, Z.: *Tonind. Ztg. u. Keram. Rundschau*, **108,** 449 (1984)
[250] Lerch, W., Bogue, R.: *Bur. Standards J. Res.*, **12,** 645 (1934)
[251] Sulimenko, L., Meissner, St.: *Proceedings of the Siliconf.*, Part III, OMIKK, Budapest 1985
[252] (Loginov, G. I.) Г. И. Логинов: *Труды совещания по применению вибропомола в промышленности строительных материалов*. Промстройиздат, Москва 1957
[253] (Abrosenkova, V. F., Loginov, G. I., Rehbinder, P. A.) В. Ф. Абросенкова, Г. И. Логинов, П. А. Ребиндер: *ДАН СССР*, **115,** 509 (1957)
[254] (Loginov, G. I., Rehbinder, P. A., Abrosenkova, F. V.) Г. И. Логинов, П. А. Ребиндер, В. Ф. Абросенкова: *Коллоидный журнал*, **21,** 442 (1959)

[255] (Hint, I.) И. Хинт: *основы изготовления силикальцитных изделий*. Госстройиздат, Москва 1962
[256] Hint, I.: *Silikattechnik*, **17,** 340 (1970)
[257] (Kornilov, E. G., Kozlev, V. G. et al.) Е. Г. Корнилов, В. Г. Козлев и др.: *Изв. Сиб. Отделения АН СССР*, серия хим. наук, **6,** 15 (1983)
[258] Opoczky, L., Verdes, S., Mrakovics, T. K.: *Proceedings of I. World Congress on Particle Technology*, Part II, NMA, Nürnberg 1986
[259] Kuznecova, T. W., Sulimenko, L. M., Meissner, St.: *Tonind. Ztg. u. Keram. Rundschau*, **6,** 424 (1985)
[260] (Sominskij, D. S., Kornienko, G. G., Komonova, V. V., Hodakov, G. S.) Д. С. Соминский, Г. Г. Корниенко, В. В. Комонова, Г. С. Ходаков: *Научные сообщения ВНИИТИСМ*, **28,** Промстройиздат, Москва 1957
[261] (Hodakov, G. S., Edelman, S. I., Kornyienko, G. G.) Г. С. Ходаков, С. И. Эдельман, Г. Г. Корниенко: *Коллоидный журнал*, **24,** 332 (1962)
[262] *Сборник Трудов ВНИИСМ* **1.** Тонкое измельчение материалов. Госстройиздат, Москва 1959
[263] *Сборник Трудов ВНИИСМ*. **3.** Тонкое измельчение материалов. Госстройиздат, Москва 1960
[264] (Budnikov, P. P., Petrovih, N. V.) П. П. Будников, Н. В. Петровых: *Труды МХТИ*, **24,** Промстройиздат, Москва 1957
[265] (Hodakov, G. S.) Г. С. Ходаков: *Успехи химии*, **XXXII,** 7, 860 (1963)
[266] Opoczky, L., Szatura, L.: *Építőanyag*, **26,** 401 (1974)
[267] Szatura, L.: *Építőanyag*, **31,** 49 (1979)
[268] Juhász, Z.: *Periodica Polytechnica*, **26,** 41 (1982)
[269] Juhász, Z., Zigovics, I.: *Periodica Polytechnica*, **26,** 61 (1982)
[270] Karimov, N., Zaporozsec, L., Tankibaev, M.: *Proceedings of the Siliconf.*, Part III. OMIKK, Budapest 1985
[271] Opoczky, L., Verdes, S., Mrakovics, T. K.: *Powder Technol.*, **48,** 91 (1986)
[272] (Meissner, St.) Ш. Майснер: Влиание механоактивации на свойства цементных сырьевых шихт. Кандидатская диссертация. Москва 1983
[273] Opoczky, L.: *Építőanyag*, **19,** 121 (1967)
[274] Beke, B., Opoczky, L.: *Zement-Kalk-Gips*, **58,** 541 (1969)
[275] Aichenger, K., Jordon, A.: *Zement-Kalk-Gips*, **6,** 451 (1953)
[276] (Mihajlov, N. V.) Н. В. Михайлов: *Основные принципы технологии бетона и железобетона*. Гос. изд-во лит. по строит., архит. и строит. материалам, Москва 1961
[277] (Rehbinder, P. A., Mihajlov, N. V.) П. А. Ребинде, Н. В. Михайлов: *Вестник АН СССР*, **10,** 70 (1961)
[278] Juhász, Z.: *Ber. Dtsch. Keram. Ges.*, **50,** 267 (1973)
[279] Berk, K., Déri, M.: *Veszprémi Vegyipari Egyetem Közleményei*, **9,** 129 (1965)
[280] Buzágh, A., Szepesi, K.: *Acta Chim. Acad. Sci. Hung.*, **5,** 287 (1955)
[281] Barna, J., Marschalko, B.: *Acta Technica*, **XV,** 77 (1956)
[282] Juhász, Z., Kakasyné, J.: *Építőanyag*, **7,** 402 (1958)

Chapter 6

6. EQUIPMENT FOR FINE GRINDING AND THE PROBLEM OF MECHANICAL ACTIVATION

Experience gathered in recent years shows that any size-reduction equipment which is suitable for fine and superfine grinding can also be used, at least in principle, for mechanical activation. Mills employed for the production of fine and very fine powders show a wide variety of sizes and methods of construction.

However, size-reduction machinery, despite their diversity, operate on essentially two principles of energy transfer:

(a) Energy is transmitted by the surfaces of two grinding tools (grinding bodies) moving relatively to each other. This movement may be in any direction between parallel and perpendicular, i.e. energy transmission proceeds by shear, compression, or both. Most of the mills in everday use belong to this type, i.e. ball, roller, and vibration mills.

(b) The kinetic energy of the body to be comminuted is used: i.e. the energy of collision and impact. Centrifugal crushers and mills, where the acceleration is by rotating elements, and jet mills where the acceleration is by a jet of air, gas or steam, belong to this group.

These two effects are combined in hammer crushers and mills.

The selection of appropriate equipment is dictated by the grindability of the feed and the required fineness of the product. However, not only does dispersion increase, but the crystal structure of the feed also changes during fine grinding. In addition, the degree of mechanical activation may depend on the equipment used. Among the problems that arise during the mechanical activation of materials is the high energy demand and the difficulties of achieving continuous operation.

In the following passages the major types of milling equipment will be briefly described with special emphasis on their applicability for the production of very fine and/or highly active products.

6.1. BALL MILLS

Ball mills are most often used in the silicate industry, especially in cement manufacturing, because the grinding equipment must be of large capacity. In these mills comminution is carried out by impact, compression, and friction forces exerted by free-falling grinding bodies. Ball mills are not ideal devices for grinding brittle materials (e.g., clinker), since the compression strength of the materials to be

ground is several times higher than their tensile or bending strength. In principle, such materials could be more economically comminuted by the application of tension and bending forces.

One of the drawbacks of using ball mills for fine grinding is the increase in particle interaction; this is a consequence of the overdoses of energy transmitted by the grinding bodies. The size of grinding bodies in ball mills is adjusted to obtain 80% undersize whilst, at the same time, being capable of fracturing the largest particles in the feed. Consequently, since fine particles are present in every part of the mill the amount of energy is often excessive in respect of these smaller particles. In addition, conditions that favour particle interactions are unavoidable in ball mills, i.e. compression of particles by the grinding bodies, local overheating of the particles, etc.

We have referred earlier to the fact that one of the symptoms of particle interaction (aggregation) is a decrease of the uniformity coefficient (n) of the grind. Figure 6.1 shows the n-plot of the changes of n that occur along the length of the mill. In order to increase the fineness of the cement the mill was loaded with only 13.9 t h^{-1} instead of

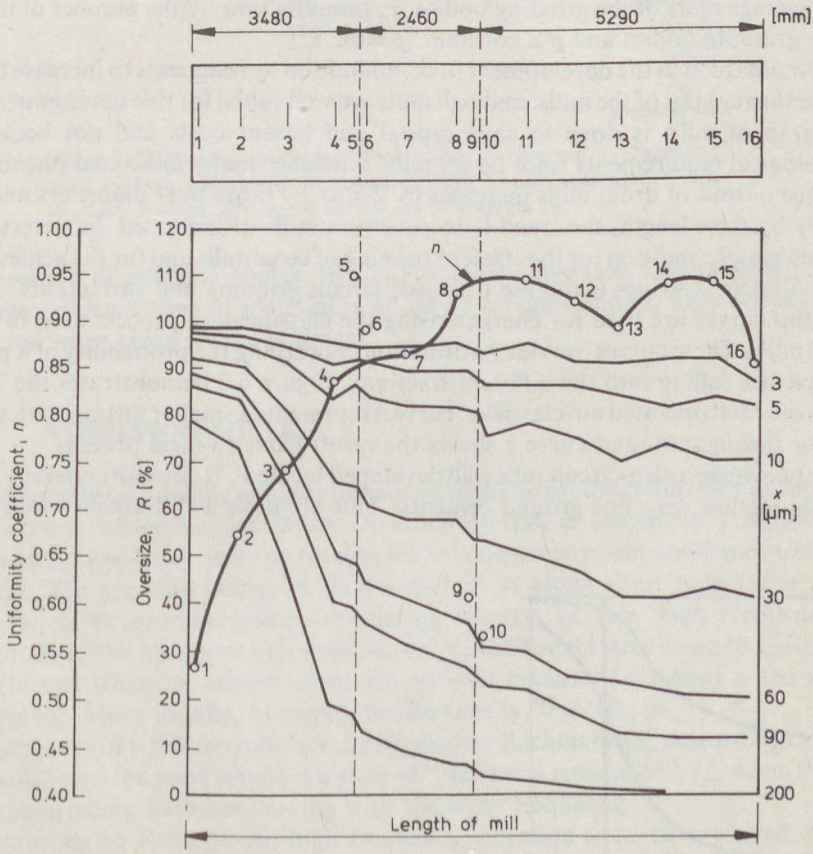

Fig. 6.1. Variation of particle size distribution and uniformity coefficient (n) along the axis of the mill. Dimensions of the mill: ∅ 2.5 × 12 m, capacity 13.9 t h^{-1} [5]

the usual 20 t h^{-1}. The changes of n indicate aggregation in chamber III, and the end-product left the mill in an aggregated state. The characteristics of the product at probe point 14 were: $a_s \cong 0.27$ m^2 g^{-1}, $\bar{x} \cong 38$ μm, $n \cong 1.00$, at point 16: $a_s \cong 0.28$ m^2 g^{-1}, $\bar{x} \cong 34$ μm, $n \cong 0.853$. Modifications of the grinding bodies or the application of grinding aids is often necessary [1–6] to avoid particle interaction.

Beke [1] carried out experiments on cement grinding and proposed the following empirical formulae for correlating the change of the uniformity coefficient (n) with the diameter of the mill, the diameters of the grinding bodies, and the average mass of these grinding bodies:

$$n = f\left(\frac{\tau_A}{Dd^p}\right), \tag{1}$$

and

$$n = f\left(\frac{N}{D^2G}\right), \tag{1a}$$

where D is the diameter of the mill drum, d the average diameter of the grinding bodies, G the average mass of the grinding bodies, τ_A grinding time, N the number of impacts by the grinding bodies and p a constant ($p \approx 6$).

The main trend in the development of comminution techniques is to increase the size and the throughput of the mills, and ball mills are well suited for this development. The scaling-up of mills is done to save capital and labour costs and not because of technological requirements since larger mills introduce many unwanted phenomena. Since the output of drum mills increases by 2.5 to 2.7 times their diameters and only linearly by their length, the trend is to construct mills of increased diameters.

An essential condition for the efficient running of large mills and for the achievement of good fineness values is the use of closed circuit grinding and surfactants.

Tromp curves are used for characterising the classification process used in closed circuit mills. These curves provide information concerning the probability of a particle of given size falling into the different fractions. Figure 6.2 demonstrates the Tromp curves of a well operated air-classifier: curve a represents a smaller throughput, curve b a larger throughput, and curve c shows the result from an ideal process.

The two-stage, open-circuit tube mill developed by the F. L. Smidth company is used to manufacture very fine-ground cements. This employs a "Minipebs" mill in the

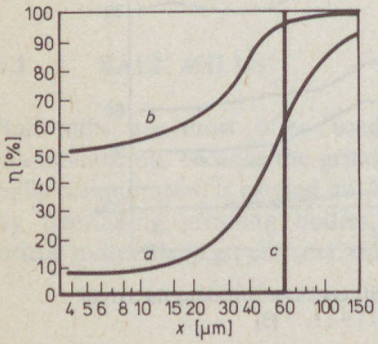

Fig. 6.2. Tromp curve of an air-classifier adjusted a—to coarse and b—to fine grinding; c—the ideal process [7]

second stage which is filled with grinding bodies of 4 to 8 mm diameter. Surfactants are fed into the mill to prevent agglomeration and its inside is cooled with water (Fig. 6.3). Very long grinding times are necessary in order to ensure the required mechanical activation and reactivity in a ball mill. The maximum activity which can be attained is also influenced by mill features such as diameter, density of grinding bodies, and

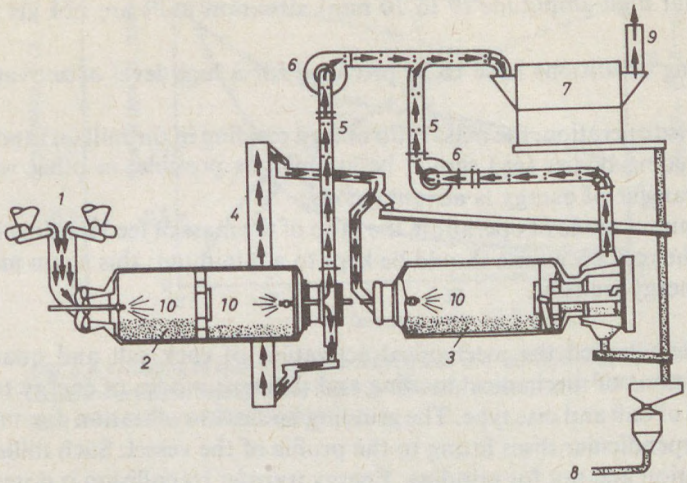

Fig. 6.3. "Minipebs" cement mill. *1*—Feeding, *2*—tube mill, *3*—"minipebs" mill, *4*—bucket elevator, *5*—exhaust, *6*—fan, *7*—dust separator, *8*—final product, *9*—vent, *10*—injection of water or grinding aid

composition of grinding bodies. In a continuously operated, large size ball mill the average residence time of material is about 25 minutes and no high activity can be expected when using such equipment.

6.2. VIBRATION MILLS

Vibration mills are widely used for preparing very fine products and they are especially suitable for mechanical activation. A vibration mill is essentially a supported, or suspended, cylindrical drum or trough-shaped container which undergoes vibrational motion. The grinding bodies in such a mill move along short trajectories and the material to be ground suffers low-energy impacts of very high frequency. The amplitude of this motion is only a few millimetres. Product sizes down to 1–10 μm can be achieved when an appropriately pre-ground material (~1 mm) is fed into the equipment. More usually, however, the fineness is 20 to 40 μm.

The theory of vibration mills was elaborated by Bachmann [8]. According to him the best condition for good results is a state of "statistical resonance", i.e. when the drum and the grinding balls are moving with the same frequency.

According to Rose [9, 10] high frequency vibration is to be preferred and it is essential that the dimensions of the grinding bodies should be adjusted to the strength and particle size of the feed.

In the opinion of Bernhardt and his co-workers [11–14] the amplitude of the vibration mill and the quantity of the feed is of prime importance in mechanical and mechano-chemical activation. Comminution and activation are most efficient at high amplitudes (7 to 10 mm or higher). In such cases, the rotational speed of the drum should also be sufficiently high to ensure the passage of material through the mill. It has to be noted that high-amplitude (9 to 10 mm) vibration mills are not yet available commercially.

The following conditions have to be provided for a high level of activation:

—in batchwise operation, the mass ratio of feed residing in the mill (m) and the mass of the grinding bodies (m_k) should be as small as possible; in other words high specific transfer of energy is advantageous;
—in a continuous mode of operation, the ratio of the mass of feed residing in the mill (m) and the residence time should be kept to a minimum; this again means high specific energy transfer.

Schneider [15] studied the mechanical activation of rock salt and quartz under different conditions of mechanical loading and different modes of energy transfer in vibration mills of ball and disc type. The grinding bodies in a vibration disc mill consist of parallel, perpendicular discs fitting to the profile of the vessel. Such mills are used only for activation and not for grinding. Energy transfer by collision is dominant in a vibration mill loaded with balls while, in a disc mill, shear and friction also contribute to comminution. Because of the more intensive energy transfer and friction the temperatures in a disc mill are higher than those in a ball mill.

Figure 6.4 shows changes of crystallite size, crystal lattice distortion, and intensity of X-ray bands, as functions of time during the grinding of quartz. The intensity of X-ray peaks is given by Schneider as a percentage compared with the values observed after very brief grinding. It can be established that quartz is ground faster in a disc vibration mill and, with prolonged grinding time, the disc mill produces greater fineness than a ball mill. The degree of lattice distortion increases with increasing grinding time and with reduced crystallite size. Crystal distortion attains its maximum value after 25 hours of grinding (0.11%) in a vibration mill loaded with balls; in a disc mill, the corresponding value was 0.19% after 50 hours of grinding.

Differences in the action of the two types of vibration mill are more apparent when lattice distortion and intensity of X-ray peaks are plotted against crystallite size (Fig. 6.5).

It is clearly recognisable that, at average crystallite size, the distortion of the crystal lattice of quartz is more pronounced when vibration grinding is performed in a disc mill than when it is carried out in a vibrating ball mill. When, in turn, the sample was ground to the same crystallite size there was less diminution of the X-ray peaks when a vibrating ball mill was used.

When a very fine or mechanical activated product is desired then vibration mills have several advantages over rotating ball mills.

An investigation of the solubility (on the basis of the percentage of Al_2O_3 dissolved) of different clay minerals that were activated in different types of milling equipment has been shown by Bernhardt and Heegn [16, 17] and that the best value (90%

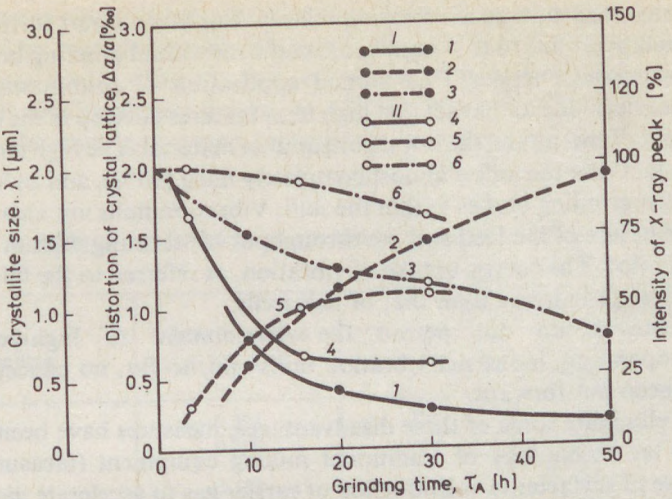

Fig. 6.4. Grinding of quartz in a disc mill (I) and in a ball mill (II) [15]. Curves *1* and *4*—crystallite size; curves *2* and *5*—distortion of crystal lattice; curves *3* and *6*—intensity of X-ray peaks

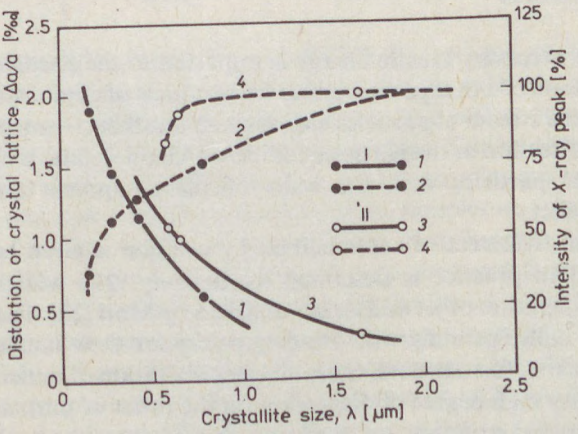

Fig. 6.5. Grinding of quartz in a disc mill (I) and in a ball mill (II) [15]. Curves *1* and *3*—distortion of crystal lattice; curves *2* and *4*—intensity of X-ray peaks

solubility) was shown by a sample activated in a vibration mill for 0.5 hours and with an amplitude of 8 to 9 mm. However, only 52% of the Al_2O_3 content of a clay activated in a ball mill for 8 hours could be dissolved.

Changes in the crystal structure of cement clinker and clinker minerals could only be detected after very long grinding (20 to 30 hours) in a ball mill [18], while a few minutes were sufficient for these effects to be detected when the grinding was performed in a vibration mill [19].

An important disadvantage of vibration mills is their low output; furthermore, the feed must be relatively fine (3 to 5 mm) because the individual grinding bodies impact relatively low impact energies. The limited application of continuously-operated vibration mills is also due to the fact that high temperatures develop in the mill because of the high input of energy and the low throughput of material. The high temperature is caused by the fact that the mill is almost completely filled (90%), and by the complex trajectory of the grinding bodies within the mill. Vibration mills are also sensitive to changes in the nature of the feed and the throughput of vibrating mills at continuous operation is limited. The energy uptake of vibration, as referred to the fill of grinding bodies, is only slightly lower than that of ball mills.

These drawbacks do not permit the development of high-performance, continuously-operating, industrial vibration mills and, so far, no conceptually new designs have been put forward.

In order to eliminate some of these disadvantages, measures have been taken that mainly affect the technology of traditional milling equipment (measures such as cooling, the use of surfactants, introduction of carrier gas to accelerate material flow, application of multistage gears, etc.). These improvements are identical, as regards their essential features, to those employed to improve the efficiency of ball mills.

6.3. JET MILLS

In a jet mill the necessary kinetic energy is imparted to the particles of the feed by a stream of air, steam or other gases, such as the products of combustion. Comminution takes place when a stream of particles collides with another stream of particles moving in the opposite direction or the particles collide with baffle-plates within the apparatus. Impingement of particles with the walls of the equipment also contributes to comminution effect.

The theoretical treatment of comminution by collision is given by Rumpf [20]; the equipment used in practice is described by Bendefy [21], while a comprehensive analysis of the operation of jet mills was published by Mori [22]. The main advantages of jet mills over mills operating with grinding bodies are their simple construction and lack of moving parts, furthermore, more efficient liberation of minerals in rocks due to free collision, very high degree of dispersion (in the order of μm), as well as extensive changes in the crystal structure and mechano-chemical properties. In jet mills there is no compression of particles by grinding bodies. The high air-to-feed ratio, as well as the temperature drop caused by the expansion of the grinding medium (gas or steam), offsets the heat evolved by collision and friction of the particles and reduces overheating.

Grinding by collision provides a more exact control of energy transfer by selecting the correct velocity of collision: agglomeration can be avoided and the preparation of products with a high uniformity coefficient (n) becomes possible. The usefulness of jet mills for the mechanical activation of brittle materials has been proved repeatedly [23–28]. Akunov and his co-workers [25–28] studied the morphology of ground cement brought to the same fineness by grinding in a jet mill with a countercurrent steam jet and in a laboratory ball mill. They found that the product of the jet mill consisted of

particles having sharp edges produced as a result of fracture induced by high velocity impacts. The particle size distribution and the hydraulic activity and strength of cements produced in this way are more uniform and are higher than those produced in a ball mill. On increasing the degree of dispersion the difference in the activity of products obtained by the two processes increases in the favour of jet milling (cf., Table 6.1).

Table 6.1. Strength of cement samples ground to the same fineness in a ball mill and in a jet mill [26]

Mode of grinding	Specific surface a_s [$m^2\ g^{-1}$]	Compression strength [MPa]		
		3	7 days	28
Ball mill	0.294	22.6	34.1	50.7
Jet mill	0.290	31.6	50.5	65.7
Ball mill	0.360	30.4	43.3	54.3
Jet mill	0.357	40.7	54.7	65.2
Ball mill	0.402	33.6	46.5	54.0
Jet mill	0.400	47.0	53.4	70.0
Ball mill	0.452	33.6	47.5	56.3
Jet mill	0.456	49.1	57.2	72.1

Menyhárt-Kocsis [23] tested a Fryma–IMRS–80 type gas-jet laboratory mill for grinding dolomite, limestone, cement clinker, sand, apatite, etc. and demonstrated that, due to exposure to high-velocity collision, the feed suffers deep-seated changes in its crystal structure and, thus becomes highly activated. Similar observations were also made by Hodakov [24] who studied ground cement samples activated in a vibration mill, a ball mill, and a jet mill. The dispersion of the samples was characterised by their "total" specific surface (a_s') and particle size distribution; their activity was characterised by the strength of the cement pulp prepared from them and by the quantity of chemically bonded water. Although the "total" specific surface and the particle size distribution were almost the same, the sample ground in a jet mill showed the highest activity. X-ray diffractometry demonstrated that changes in the crystal structure were most profound in the product from a jet mill; the changes were not so marked in the product from a vibration mill, and were even less obvious in the product from a ball mill.

Jet mills differ according to the energy-bearing medium (air-jets, steam-jets and gas or combustion product jets) and in the properties of the medium (its pressure, temperature) before entering the jet. The pressure of a high pressure jet before the injector is 0.2–1.5 MPa; in low pressure jets the pressure is 0.03 to 0.2 MPa; and in fan-operated types the pressure is 0.02 to 0.03 MPa.

A disadvantage of jet mills, as compared with ball mills, is their higher specific energy consumption. The largest jet mills have an output of a few tons/hour. The development of jet mills is limited by the fact that, on one hand, it is difficult to accelerate larger particles to the required speeds and, on the other hand, that extremely high velocities are required for producing very fine products.

6.4. THE ATTRITOR MILL

Mixers filled with small balls and other grinding bodies are used for producing fine dispersions. Balls and the feed material are placed in a fixed cylindric vessel and are brought into movement by suitable stirring elements. The stirring device in the "attritor" is an axle with rods fixed on it, in a similar manner to a multiarm stirrer. The feed is circulated by means of a built-in pump and the vessel is provided with a heating jacket. The "attritor" is used in the ceramic industry and in the manufacture of pigments and paints. It was first used for fine and superfine wet-grinding, but experiments with iron [29], quartz [30, 31], and limestone [31] proved that the mill is also suitable for mechanical activation and that it may, in same instances, offer certain advantages in comparison to other mills, e.g. vibration mills [31, 32]. Heegn and his co-workers [32, 33] demonstrated that if strontium ferrate is activated in a vibration mill then extensive amorphisation takes place even after brief grinding: this result was detrimental to the later use of the strontium ferrate because of deterioration of its magnetic properties. In contrast, when grinding was carried out in an attritor, the specific surface increased monotonously while crystallinity was either preserved or it decreased much less than on grinding in a vibration mill. This example demonstrates that the technological value of a given product cannot adequately be characterised by its degree of dispersion alone.

6.5. DISINTEGRATORS

Disintegrators belong to the group of high speed mills and they operate in a similar manner to hammer mills. The feed is subjected to impact and shear by rapidly revolving pins and is, at the same time, thrown against the mill lining. Comminution takes place by collision, as with jet mills. Disintegrators operate with a high peripheral velocity and the dimensions of the mill are small. The important difference between ball mills and disintegrators is in the mode of energy transfer. In ball mills the kinetic energy used during fracture is carried by the grinding bodies; in disintegrators the energy is carried by the particles that are being comminuted. Disintegrators produce materials of high fineness and high uniformity; conditions which prevent agglomeration. High performance disintegrators are mainly employed to comminute moderately abrasive materials such as coal.

The application of disintegrators for mechanical activation has been studied by Hint [34, 35]. He developed a special disintegrator, called a dismembrator, which was successfully applied for the mechanical activation of quartz and lime–hydrate–quartz mixtures on an industrial scale. In this mill as, for example, in the Alpine impact-pin mill the feed is ground between two discs which revolve against each other at very high speed. Grinding is affected by the collision of particles which have very high kinetic energy with each other and with the grinding bodies.

High fineness can only be achieved by investing much energy in disintegrators (i.e. by multiple recycling of the feed), but structural changes as measured by changes in specific surface are greater than in other types of mills [33].

Bernhardt, Heegn, and their co-workers [11–14, 29–31, 36, 37, etc] studied the

mechanical activation of quartz, limestone, iron powder, clay, etc. in laboratory mills of various types. Among other mills they included a vibration mill, a ball mill, a disintegrator, a jet mill, and an attritor. The products were characterised by their "total" specific surface (a'_s), by the solubility of quartz in sodium hydroxide (surface solubility), by the heat of dissolution, and by the solubility in hydrogen fluoride (total dissolution of particles). They also followed the changes in the crystal structure of the materials by X-ray diffractometry. The difference in the heat of dissolution (ΔQ), before and after mechanical treatment, was taken as an index for mechanical activation, since this should correspond to the energy accumulated in the solid body as a consequence of mechanical treatment (i.e. dispersion and activation).

They further established that ground quartz prepared in an attritor gave a relatively low value of ΔQ, despite having a larger specific surface. Samples obtained by grinding in a disintegrator exhibited smaller specific surfaces and higher ΔQ values than in the attritor. In Figure 6.6 the correlation $\Delta Q = f(a'_s)$ is demonstrated for quartz and

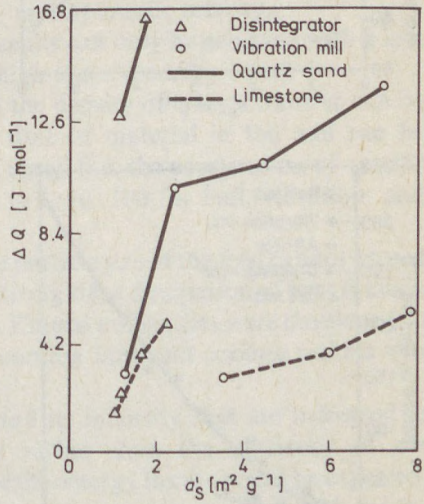

Fig. 6.6. Correlation of "total" specific surface (a'_s) and accumulated energy (ΔQ) [11]

limestone ground in a disintegrator and in a vibration mill. When compared with the vibration mill, the disintegrator gave identical ΔQ values but much smaller specific surface values for both feeds. Figure 6.7 shows that the amorphisation of quartz at identical specific surface value is more extensive in both mills than in other types of equipment. The situation is different if one looks at the solubility of quartz in sodium hydroxide as a function of specific surface (Fig. 6.8). Jet mills and disintegrators apparently affect much less of the surface layers of quartz than other mills. These, and other observations not discussed here, prompted the authors to the conclusion that mills in which energy transfer occurs by collision (disintegrators, jet mills) produce, at relatively low dispersion, more extensive changes in the crystal structure than other mills, i.e. they produce higher ΔQ and X-ray intensity changes. However, surface activation is not substantial in this instance (low solubility in sodium hydroxide). In contrast, in mills in which energy transfer is accomplished by compression, shear, or

both (equipment such as ball mills, vibration mills, and attritors) relatively high dispersion is associated with intensive surface activation but only slight changes in the crystal structure.

Meissner and Sulimenko [38, 39] studied the effect of various modes of mechanical activation (impact, friction, compression) on the technological properties of cement raw meal and clinker formation. The following properties depend on the mode of

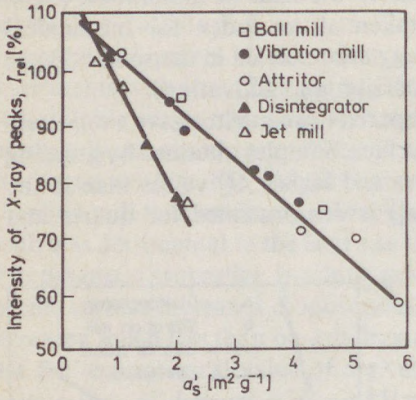

Fig. 6.7. Correlation of the relative intensity of X-ray peaks (I_{rel}) and "total" specific surface (a_s') [11]

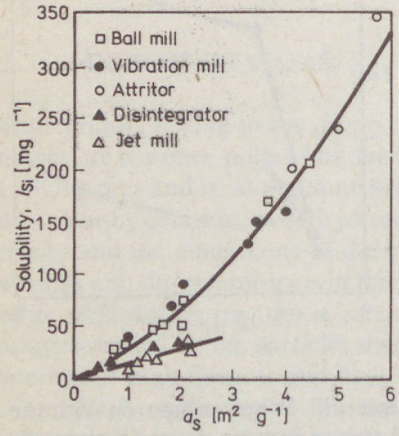

Fig. 6.8. Solubility of quartz in sodium hydroxide (l_{Si}) as a function of the "total" specific surface (a_s') [11]

milling: particle structure, adhesion, particle size, morphology of particle surface, and deformation of the crystal lattice. These features influence the reactivity of the components and the whole disperse system and, thereby, the composition and structure of the clinker. Two-stage milling seems to be the most efficient in the overall technology of clinker production: in the first comminution by impact and compression (autogeneous, ball, or roller mills), while in the second stage collision at velocities exceeding 160 m s^{-1} should be applied (e.g. in a high speed impact mill).

6.6. PLANETARY MILLS

One trend in the design of comminution equipment is to shrink the size of the mills by increasing the frequency of energy transmission. Planetary mills exploit this principle using centrifugal acceleration instead of gravitational acceleration: this allows the preparation of highly dispersed and activated ground products. The development, construction, and operation of planetary mills are extensively covered by the literature [40, 41].

The application of mainly laboratory-scale planetary mills for mechanical activation has been studied primarily by Soviet researchers [42–48]. Their general conclusion was that, by observing certain conditions, these mills produce high activation after a relatively short grinding time. For example, solubility of apatites and phosphates can be increased 6 to 10-fold by mechanical activation in a planetary mill; this procedure is also advantageous in the preparation of periclase and calcium hydrosilicates. These materials underwent deep-seated changes in their crystal structure which resulted in improved solubility and hydraulic activity.

It has to be added, however, that the above results can only be achieved with a low ratio of feed to grinding body mass, i.e. by a high specific energy input.

By increasing the speed of the planetary mill the density of energy transfer can be greatly increased and, thereby, the residence time of material in the mill can be effectively reduced. The effect of an increase of speed (i.e. the acceleration of specific surface increase), under analogous conditions is 1 : 10 : 100 for ball, vibration, and planetary mills, respectively [49].

Because of the small size of planetary mills the particle size of the feed cannot exceed 5 to 7 mm. Also the heating effect is extremely strong since dissipation of heat is much less effective than with drum mills, for example. Finned mill bodies were developed to improve heat transfer and the use of special cooling fans and cooling jackets was recommended.

It is the frequency of energy transmission and its intensity that are increased in planetary mills which use centrifugal force rather than the efficiency of the disintegration process. Therefore, no gain in specific energy input should be expected. On the contrary, the extremely high intensity of energy transfer involves high energy consumption; with calculated values of 504 to 540 J g^{-1} for a specific surface of 0.28 to 0.30 $m^2 g^{-1}$ (a_s). An increase of energy input per unit volume by a factor of approximately 1000 resulted in accelerated wear by about the same factor. Thus, although this approach is interesting from a theoretical point of view and provides an enhancement of the efficiency of grinding, it is not anticipated that planetary mills will acquire a practical importance in the silicate industry.

However, remarkable efforts have been made by Soviet researchers to develop planetary mills and to promote their applicability in mechano-chemical technology and for the construction of special mill-activators [48].

SYMBOLS IN CHAPTER 6

a_s	"external" specific surface
a'_s	"total" specific surface
D	diameter of mill
d	average diameter of grinding bodies
τ_A	grinding time
N	number of impacts by grinding bodies
n	uniformity coefficient
η	efficiency
λ	crystallite size
m	quantity of material residing in the mill
G, m_k	average mass of grinding bodies in the mill
Q	heat of dissolution
I_{rel}	relative intensity of X-ray lines
l_{Si}	solubility of quartz in sodium hydroxide
$\Delta a/a$	crystal lattice distortion
p	constant
$\bar{x}$	fineness number

REFERENCES

[1] Beke, B.: *Zement-Kalk-Gips*, **11**, 529 (1958); *Építőanyag*, **11**, 113 (1959)
[2] Kolostori, J.: Aufbereitungs-Technik *10*, 511 (1976); *Építőanyag*, **24**, 407 (1977)
[3] Opoczky, L.: *Keram. Z.* **31**, 390 (1979)
[4] Opoczky, L.: *InterCeram*, **30**, 387 (1981)
[5] Opoczky, L., Mrákovics, T. K.: *Silikattechnik*, **32**, 104 (1981)
[6] Scheibe, W.: I. World Congress on Particle Technology Part II, NMA, Nürnberg 1986
[7] Beke, B.: *Építőanyag*, **25**, 47 (1973)
[8] Bachmann, D.: *Verfahrenstechnik, Beih. Z. VDI*, **84**, 43 (1940)
[9] Rose, H. E., Sullivan, R. M.: *Vibration Mills and Vibration Milling*. Constable & Co. Ltd, London 1961
[10] Rose, H. E.: *Symposium Zerkleinern*, Verlag Chemie, Weinheim, VDI Verlag, Düsseldorf 1962
[11] Bernhardt, C., Heegn, H.: *Építőanyag*, **27**, 343 (1975)
[12] Bernhardt, C., Heegn, H.: *Banicke Listy*, VEDA, Bratislava 1976
[13] Gottschalk, I., Bernhardt, C.: *Freiberger Forschungshefte*, *A***553**, 155 (1976)
[14] Heegn, H., Bernhardt, C.: *Freiberger Forschungshefte*, *A***553**, 155 (1976)
[15] Schneider, U.: *Aufbereitungs-Technik*, **11**, 567 (1968); *Aachener Blätter*, **18**, 1/2 (1968)
[16] Bernhardt, C.: In: Untersuchungsmethoden zur Charakterisierung mechanisch aktivierter Festkörper (ed. Juhász, Z.). *BME Tud. Közlemények*, KÖZDOK, Budapest, **13**, 1978
[17] Bernhardt, C., Heegn, H.: *Silikattechnik*, **29**, 373 (1978)
[18] Opoczky, L.: *Építőanyag*, **18**, 41 (1966)
[19] (Kudrjavceva, N. L., Hodakov, G. S.) Н. Л. Кудрявцева, Г. С. Ходаков: *Коллоидный журнал*, **28**, 524 (1966)
[20] Rumpf, H.: *Chem. Ing. Tech.*, **31**, 323 (1959)
[21] Bendefy, I.: *Magyar Kémikusok Lapja*, **21**, 633 (1966)
[22] Mori, V.: *Symposium Zerkleinern*. Verlag Chemie, Weinheim, VDI Verlag Düsseldorf 1962
[23] Menyhárt-Kocsis, M.: *Építőanyag*, **27**, 348 (1975)
[24] (Hodakov, G. S.) Г. С. Ходаков: *Тонкое измельчение строительных материалов*. Изд-во литературы по строительству, Москва 1972

[25] (Akunov, V. I.) В. И. Акунов: *Струйные мельницы*. 2-3 Изд-во. Машиностроение, Москва 1967; *Труды НИИЦемента*, **26**, Москва 1973
[26] (Desko, Ju. I., Akunov, V. I. et al.) Ю. И. Дешко, В. И. Акунов и др.: *Цемент*, **11**, 16 (1976)
[27] Kuznecova, T. V., Dimitrieva, V. A., Judovics, B. E., Makasev, S. D., Akunov, V. I., Albaz, V. M., Ciskina, I. D.: *Zerkleinern und Klassieren, Freiberg*. Preprint. Kammer der Technik, Berlin 1981
[28] Akunov, V. I., Kuznecova, T. V., Pankratov, V. L.: *Zerkleinern und Klassieren, Freiberg*, Preprint. Kammer der Technik, Berlin 1981
[29] Husemann, K., Bernhardt, C., Heegn, H.: *Powder Technol.*, **14**, 41 (1976)
[30] Bernhardt, C., Heegn, H.; *Dechema Monographien. Vol. 79*, Verlag Chemie, Weinheim, VDI Verlag Düsseldorf 1976
[31] Heegn, H., Bernhardt, C., Gottschalk, J.: *Chem. Tech.*, **26**, 696 (1974)
[32] Heegn, H., Bernhardt, C., Ludwig, G.: *Bahicke Listy*, VEDA, Bratislava 1980
[33] Heegn, H., Bernhardt, C.: *Zerkleinerung und Tribochemie, Freiberg*. Preprint. Kammer der Technik, Berlin 1981
[34] (Hint, I.) И. Хинт: *Основы изготовления силикокальцитных изделий*. Госстройиздат, Москва 1962
[35] Hint, I.: *Silikattechnik*, **17**, 340 (1970)
[36] Bernhardt, C., Gottschalk, J., Heegn, M., Husemann, K.: *Silikattechnik*, **25**, 183 (1974)
[37] Husemann, K., Bernhardt, C., Gottschalk, J., Heegn, M.: *Silikattechnik*, **25**, 238 (1974)
[38] (Meissner, St.) Ш. Майснер: Влияние механоактивации на свойства цементных сырьевых шихт. Кандидатская диссертация. МХТИ, Москва 1983
[39] Sulimenko, L. M., Meissner, St.: *Proceedings of the Siliconf.*, Part III, OMIKK Budapest 1985
[40] Bradley, A. A.: *3. Europ. Symp. Zerkleinern (Cannes)*. in *Dechema Monographien. Vol. 65*, 1971
[41] Voch, F.: *3. Europ. Symp. Zerkleinern (Cannes)*. in *Dechema Monographien, Vol. 65*, 1971
[42] (Busuev, L. P.) Л. П. Бушуев: Известия вузов. *Горный журнал*, **3**, Свердловск 1960
[43] (Busuev, L. P.) Л. П. Бушуев: Известия вузов. *Горный журнал*, **3**, Свердловск 1965
[44] Boldyrev, V. V., Kolosov, A. S., Csajkina, M. V., Avvakumov, E. G.: *VI. Symp. für Mechanoemission und Mechanochemie* (Summary). Kammer der Technik, Berlin 1977
[45] Jusupov, T. S., Cherbakov, M. Ju., Kochegarov, G. G., Koroleva, S. M.: *Banicke Listy*, VEDA, Bratislava 1980
[46] (Logvinenko, A. T., Savinkina, M. A., Logvinenko, V. A.) А. Т. Логвиненко, М. А. Савинкина, В. Л. Логвиненко: *Изв. Сибирского филиала АН СССР*. серия хим. наук, **3**, 140 (1972)
[47] Savinkina, M. A., Logvinenko, A. T.: *VI. Symp. für Mechanoemission und Mechanochemie* (Summary). Kammer der Technik, Berlin 1977
[48] (Kozlov, V. J., Kozirev, S. A., Redykin, B. F.) В. И. Козлов, С. А. Козырев, Б. Ф. Редькин: *Изв. Сибирского отделения АН СССР*, **12**, серия хим. наук. **5**, 25 (1983)
[49] Husemann, K., Jäckel, H. G.: *Banicke Listy*, VEDA, Bratislava 1980

SUBJECT INDEX

acetone 120, 122
acetylene 174
acid(s) 116, 193–195
additives 105, 117–121, 123, 188
adherence 93, 105–106, 109, 122, 138
adhesion 13, 67, 89, 93, 103, 105–109, 120–122, 124, 126, 133, 137
– forces 168, 184, 224
adsorption 13–15, 29, 33–36, 73, 100, 105, 107, 115–118, 120, 122–123, 129, 131–137, 157, 161, 169, 179, 197–198, 207
– enthalpy 132, 134–135
– isotherms 33–35, 131–133, 137
"adsorptive decrease of strength" 115, 122
agglomeration (agglomerates) 13, 18, 20, 77, 81, 89, 92–94, 96–98, 100–101, 103, 109, 110, 122–123, 127–128, 138, 147, 150, 152, 155–156, 161, 168–169, 171, 198–200, 204, 217, 220, 222
aggregations (aggregates) 13, 18, 20, 81, 87, 89, 92–94, 96–98, 101, 103, 109, 120, 122–123, 127, 138, 165, 201, 215–216
alcohol(s) 116, 119, 122, 165
aliphatic fatty acids 121
alite, alite clinkers 83, 85–86, 91, 105–106, 166
alizarin red 119
aluminium chloride, $AlCl_3$ 116, 119–120, 164
– hydrosilicates 44–45, 78
– hydroxide 188
– oxide, Al_2O_3 83, 116, 166, 188–191, 193, 195, 219
– powder 123
amine(s) 120, 122–123, 165
amorphisation 14–15, 21, 25, 39, 73, 98, 124, 127–128, 150–151, 153–157, 161, 170–179, 182, 184, 188, 194, 196, 200, 204, 222–223
amorphous material(s), system(s) 13, 15, 52, 65–66, 153, 159, 173, 193
anatase 189
andalusite 45
andesite 123
Andreasen pipette 20
anhydrite 157
aniline 116
ankerite 157
anthracene 108
apatite 78, 80, 222, 226
aplite 80, 91, 170–171, 194, 198
aragonite 153–154, 157, 196
argon, Ar 34, 174, 191–192
asbestos 123, 178–184
asbestos cement 184, 202
attritor mill 222–224

ball mills 71, 81–82, 93, 110, 113–114, 119–120, 122–124, 166, 184, 202, 214–217, 219, 221, 224, 225
barite 116
barium carbonate, $BaCO_3$ 167–168
– oxide, BaO 85, 159
basalt 162
bauxite (minerals) 188, 193
bayerite 190, 192
BDDT classification 33–34
belite, belite crystals, belite clinkers 83, 85–87, 91, 105–106, 184–185
bentonite 170–171, 175, 177, 179–180, 194, 196–197, 199, 204–206
benzene 120
BET-equation (methods) 34, 36, 132
biotite 175–176, 198
black coal 71
böhmite 188–191, 193
Boltzmann's constant 147
bonding energy 13–14, 157
– spectrum of Hüttig 71–72
Bond's method 81–82
– "third theory" 81, 111
– "work index" 81, 110
boron carbide 71
– oxide, B_2O_3 185

brittle material(s) 49, 63, 66–67, 69–70, 83, 87, 89, 93, 115–16, 123, 214, 220
brucite 179
bulk porosity 32
– stability 38
– structure 17
Burgers vector 61, 63
butylamine 122, 137

cadmium selenide, CdSe 152
- sulphide, CdS 152, 165
calcite 64, 69, 71–72, 78, 80, 103, 116, 119, 123, 128, 131–133, 149, 153–154, 157–159, 165–166, 184, 193, 196
calcium aluminate 166
– carbonate, $CaCO_3$ 98–99, 107, 137, 152, 158, 165–167, 184, 193, 203
– fluoride, CaF_2 117
– hydrosilicates 225
– hydroxide, $Ca(OH)_2$ 50, 158, 162, 166, 183–184, 201–202
– metasilicate 98, 152, 165–166
– oxide, CaO 83, 158, 166, 193–194, 203
– stearate 123
– sulphate, $CaSO_4$, $CaSO_4 \cdot 0.5\,H_2O$ 156–157
capillary condensation 35–36, 156, 166–167
– reactions 166
carbides 150, 164
carbonates 39, 52, 157, 158, 159, 160, 163, 165, 166, 167
carbon black 105
– chlorides, CCl_4, C_2Cl_6, $CHCl_3$ 120, 164
– dioxide, CO_2 153, 157–159, 163–166, 168, 174, 191
– monoxide, CO 163
– powder 119
cassiterite 193
catalysis 162
cation-exchange capacity 40, 169, 197–200
cellulose 12, 155, 161, 164
cement, cement clinker, clinker 23–26, 34–37, 69–70, 85–87, 88–90, 96, 104–106, 114, 116, 120–137, 155, 157, 162, 164, 166, 183–185, 193, 200, 202–203, 214–216, 218–219, 221, 224
cement raw material 166, 202–203
changes in crystal structure (structural changes) 21, 39, 92, 99, 138, 147, 150–152, 154–155, 170, 184, 186–193, 203, 219, 221
chemi-hesion 168–169
chemi-sorption 13, 74, 132, 135–137, 161, 169
chemo-mechanical effects 117–118
chlorides 12, 162, 164, 166
chlorine, Cl_2 164
chlorite 170, 175–176, 194, 196, 199
chromite 123
chrysotile (asbestos) $Mg_3Si_2O_5(OH)_4$ 179, 181–183
clays, clay minerals 166, 176–177, 204–206
clay-water systems 204
clinker minerals 34, 83–87, 88, 121, 184, 186, 200, 201, 203, 219
brownmillerite, C_4AF 83–85, 184–186, 187
dicalcium silicate, C_2S, $2CaO \cdot SiO_2$ 83–85, 93, 106, 130, 137, 184, 185–186, 200–201
tricalcium aluminate, C_3A, $3CaO \cdot Al_2O_3$ 83–85, 87, 106, 184–185, 187
tricalcium silicate C_3S, $3CaO \cdot SiO_2$ 83–85, 106, 184–186
clino-enstatite 152
clinoptiolite 170, 196
coal 119, 121, 159, 222
cobalt sulfate, $CoSO_4$ 165
co-crystallisation 13, 93, 109, 151
coherent systems 18
cohesion forces 49, 55
colloid carbon 121
colour tests 165
colsite 45
compaction factor 19
– work 38
compactness 18, 32, 97, 109
compression 70, 75
cordierite 197
corundum 78, 119, 123, 188–190, 193
Cotrell model 68
covalent bond(s), bonding 78, 105, 115, 149, 172
crack(s) 28, 67–73, 79, 83, 87–88, 115–118, 122, 130, 204
cristobalite 45, 152, 170–171, 173, 196–197
crystalline boron 71
crystallite size 21, 39–40, 154, 171–172, 176–178, 191–192, 218–219
cupric oxide, $CuO \cdot 2H_2O$ 166, 168
– sulphate, $CuSO_4$, $CuSO_4 \cdot 5H_2O$ 119, 156, 166–168
cyclohexane 116, 122, 152
cyclosilicates 53

de-activation 52
de-aggregation 33, 41
decomposition of polymers 161
"decrease of strength by adsorption" 115, 122
defect site theory 67
deformation 11–12, 44–47, 49–52, 56–66, 69, 70, 73–74, 77, 93, 107, 115, 117, 147, 150–152, 157, 161, 163–164, 167, 172–173, 177–179, 204
degree of dispersion 15, 17, 91–93, 96, 98, 101, 105, 122, 147, 151, 162, 174–175, 179, 193, 204, 221
Derjagin–Talaev correlation 31
diamond 78
diaspore 188, 190

dicalcium silicate 34, 35, 71, 83–84, 92–93, 97, 124, 126–131, 133. 137, 200
dickite 175
dielectric properties 40, 203
diethylene glycol 121
diffusion 50, 67, 150, 165
disintegrators 111, 114, 222, 224
dislocations 58–66, 68, 71, 74–75, 115, 117–118, 138, 147, 150, 152–153, 162, 165, 171–173
disperse system(s) 12–13, 15, 17, 20, 27, 36, 93, 98, 105–106, 109, 113, 168
dissociation 12, 157–159, 184
dissolution 50–51
dodecyl ammonium chloride 120
dolomite 119, 158–159, 221

edge mill 123, 179, 181
efficiency of grinding 14, 92, 112
elastic deformation 44–47, 50–51, 55, 58, 63, 65–66, 68, 108, 110, 112
elasticity modulus 45, 55, 67–68, 110–111, 138, 148
electrical phenomena 74
electric potential 49
electron emission 74, 149
electrostatic charges 105, 117
– forces 107, 109
electrovalent bonds 105
energy of elastic deformation 68
– transforms 113, 151
enstatite 152, 184, 196
enthalpy of adsorption 134–135
equilibrium states of grinding 89, 101–104
ethanolamines 122
ethene, C_2H_4 174, 191–192
ethylene glycol 122, 137
ethyne, C_2H_2 191
"external" specific surface (area) 28–29, 79–80, 84–85, 93–94, 100–101, 124–126

Fáy–Zhelev's plot 26
Fáy–Zhelev's re-normalised log–normal distribution 27, 29
feldspar 52, 57, 123, 170, 175, 196
ferric chloride, $FeCl_3$ 116
– oxide, Fe_2O_3 83, 123, 149, 152, 159, 163–164, 193, 196
– sulphate, $Fe_2(SO_4)_3$ 165
ferrous carbonate, $FeCO_3$ 159
– oxide, FeO 163
– sulphide, FeS 163
fineness number 24–25, 94, 96, 127, 129
fire-clay 157, 170, 175–178, 196, 198, 205
Flotigan 119
fluorides 117, 148–149, 153, 197
fluorite 78
fly-ash 171
forsterite 181, 196
fracture 12, 37, 44, 49, 56–58, 67–73, 77, 79, 87–88, 96, 101, 105–106, 111, 115–117, 121–122, 139, 147–150, 152, 161–162, 173, 178–179, 198, 221
Frank–Read sources 62
Frenkel equation 64

Gaudin–Schuhmann–Andreev equation (plot) 23–24, 29
gel(s) 65–67, 157, 159, 161, 170–171, 179
gibbsite 188
Giprocement's method 81–82
glass(es) 49–50, 52, 65–67, 69, 71–73, 105, 116, 120, 123, 170–171
gliding of layers 56, 57, 61
glycol(s) 121–123
granite 119, 123
graphite 119, 153
Griffith's length 67
Grinard reactions 164
grindability 37, 77, 79–88, 96, 102, 119–120, 123, 137–138, 214
grinding aids 93, 105, 118–125, 129, 137
– energy 110, 114
– rate 101–104, 119–120, 127, 130
– work 14, 79
gypsum 78, 80, 121–123, 149, 156, 166

Hagen–Poiseuille rule 32
Hardgrove's method 79, 81–82, 112, 119, 139
hardness 72, 77–79, 82–85, 93, 107–109, 115–117, 138
HEA 121
heat effects 39, 58, 73
hematite 120, 196
hexane 120
high temperature reactions 194
Hooke's law 45, 56
hydrargillite 188, 190
hydraulites 202
hydrogel 204–206
hydrogen, H_2 174, 192
– bonds 78
– chloride, HCl 164
– oxide, H_2O 163–164, 168, 181, 199
– sulphide, H_2S 158, 163–164
hydroxides 157, 159, 188

ideal crystals 52, 54, 58
illite 170, 175–176, 196
incoherent systems 18, 39
inosilicates 53–54, 57, 184
interaction energy 107–109
– of particles (particle interactions) 12–13, 77, 83, 88–89, 91–94, 96, 98, 101, 105–109, 112, 120, 123, 137–138, 169, 215

intermediate phase 83, 85–88, 91
"internal" specific surface (area) 28–29, 36
internal symmetry 53
iodides 12
ion-exchange capacity 40, 169, 176, 178, 197–200
ionic bond, bonding 55, 71, 78, 115, 172
iron, iron powder 105, 223
isoamyl alcohol 116

Jet mills 164, 214, 220, 224

kaolin, kaolinite 15, 157, 166, 169–171, 175–179, 195–196, 198–199, 205
Kelvin's equation 36
Kirpichov–Kick law 110
Knudsen diffusion 30–32
Kolmogorov's log–normal distribution 23, 25, 27, 29
Kozeny–Carman equation 30
krypton, Kr 34

Langmuir's equation 132
laser sedimentometer 21
lattice defects 12, 22, 39–40, 58–60, 63, 96, 147, 150, 153, 159, 162, 170–171, 174, 179, 192, 195
– deformation, distortion 21–22, 85, 147, 150, 153–154, 165, 170–172, 174, 179, 181, 184, 191–193, 200, 218–219
– energy 13–15, 78, 148
lignin sulphonic acid 120–121
lime 124–125, 166, 202, 222
limestone 23, 35, 71, 79–80, 82, 85, 93–96, 98–100, 105, 119–121, 123–125, 157, 165, 221–223
"limiting grain size" 71
"– particle size" 70
litharge 152–153
lithium fluoride, LiF 149
lizardite 179
London-dispersion forces 13, 93, 107, 109

macrocrack(s) 87
magma–plasma model 64
magnesite, $MgCO_3$ 119, 123, 157–159, 167, 170, 196
magnesium chloride, $MgCl_2$ 176
– oxide, MgO 85, 106, 117, 149, 159, 166, 191–195
– silicate, $MgSiO_3$ 166
magnetite 193
manganese carbonate, $MnCO_3$ 159
– fluoride, MnF_2 153
marble 71, 120
massicot 152–153
MAVEKLIN 124, 128
Maxwell's equation 48
mechanical activation 11–13, 71, 74, 100–101, 114, 138, 148–150, 156, 159, 164, 166, 170–172, 175, 179–180, 183, 188–189, 195–198, 202–203, 205, 217–218, 220, 222–225
– dispersion 12, 15, 22, 88, 150, 193, 201, 203, 206
– twin formation 64
mechano-chemical activation 15, 44, 73, 113, 147, 152–153, 156, 161, 170
– dissociation 157, 159
– reactions 11, 13, 39–40, 52, 92–93, 98–99, 109, 147, 150–151, 155, 163–169, 179
mechano-chemistry 11
medium 20, 112, 114–115, 117–118, 120, 122, 151, 167, 182, 193, 221
melt bridges 109–110
mercuric oxide, HgO 153
metallic bonding, bonds 55, 115
metals 12, 52, 105, 107, 123, 150, 154, 162–164
methane 164
methanol 119
methyl chloride 162
methylcyclohexane 120
methylene blue surface 205–206
micas 148–149, 175, 198
microcrack(s) 63, 67–68, 79, 87, 115, 122
microhardness 63, 77–79, 83, 85, 109, 116, 139
microplasticity 63
Minipebs-mill 216–217
Mittag's method 81–82
Mohs scale 78
molecular tensile strength 67, 69, 74
montmorillonite 170, 175, 179, 196–199, 206
mordenite 170
mullite 123, 196–197
muscovite 175–176, 198

naphthene soap 121
naphthene-sulphonic acid 121
nesosilicates 53–54, 184
nickel, Ni 155
– carbonate, $NiCO_3$ 158, 163
– oxide, NiO 158, 163
– sulphide, NiS 163
nitrides 150
nitrogen, N_2 34, 51, 98, 120, 165
nitromethane 120

obsidian 123
oleic acid 120–122
organic compounds 155, 164, 193
– vapour 116, 120
ores 119, 148, 152, 155, 193
orthoclase 72, 78
Ostwald's rule 152
overlapping effect 13, 168, 169
oxidation 163
oxides 52, 85, 116–117, 119–120, 152–153, 157, 159, 163, 166, 178, 188, 191–194, 196

oxygen, O_2 174, 191
oxygen compactness 170–171

paramagnetic centres 149, 192
particle interaction (see interaction of particles)
– porosity 18, 33, 99, 139
– size 12–13, 20–21, 23–25, 27–31, 36, 69–70, 81, 87–89, 94, 96, 98–99, 101–104, 110–111, 116, 128–130, 138, 162, 168, 173, 191, 193, 224–225
– – distribution 15, 17, 23–27, 29, 86, 92–93, 95–96, 109, 111, 128, 215, 221
passivation 148
penetrometry 36
periclase 72, 106, 193, 196, 225
perlite 171, 196
permeability 30–32
petroleum ether 120
phosphates 155
phyllosilicates 53–54, 57, 175
piezo-electricity 74
pigments 222
planetary mills 225
plastic deformation 47–49, 51, 56–58, 60, 63, 65, 67–70, 72, 77, 78, 84, 107–109, 111–112, 115, 117, 147, 150, 152, 154–155, 165, 173–174, 177–178
– materials 47
plasticity 204–205
plumbic carbonate, $PbCO_3$ 153, 163
– hydroxide, $Pb(OH)_2$ 163
– oxides, PbO, PbO_2, Pb_2O_5 85, 149, 152–153, 163, 188
– sulphate, $PbSO_4$ 163
Poisson's coefficient, constant 48, 148
polycrystalline materials 65, 78, 83
polymer(s) 52, 66, 155, 161
polymorphic modification 150, 153
– transformation 12, 39, 151–153, 155–156, 184–185
polyvinyl chloride 164
pore size, pore size distribution 36–37, 95, 128
– system 18
porosimeter 37
porosity 18, 30, 37, 83, 85, 87, 99–101, 107
porous bodies 18, 37
– disperse bulks 18, 32
portlandite 157, 201
potassium oxide, K_2O 188, 193
– sulphate, K_2SO_4 149
Prandtl's equation 47
primary (mechano-chemical) processes 12, 67, 147, 161
proto-enstatite 152
pumicite 99–101, 175, 193, 202
pyrite 116
pyrophyllite 170–171, 175–176

quartz, quartzite 23, 44–45, 50, 52, 63, 69, 71–72, 74, 78–80, 82, 92–96, 98–102, 105, 112–113, 115–117, 119–120, 123, 148–149, 152–153, 164–166, 170–174, 184, 193–196, 198, 202, 218–219, 222–224

real crystals 58, 71
re-crystallisation 13, 147, 154–156, 162, 167, 171–172, 190
recycling factor 124
reduction 164
Rehbinder effect (theory) 114–120, 122
relaxation 45–46, 48, 50, 69, 74, 147, 157
re-ordering 155–156
Reynolds number 20
rhodochrosite 159
rigid materials 47
Rittinger's law, equation, theory 14, 79, 81, 89, 94, 96, 110, 112
– stage 92, 97
Robinson–Köhn pipette 20
rock salt 71, 159, 218
rod mill 206
Rosin–Rammler–Sperling–Bennett's (RRSB) equation 23–25, 29, 94, 96, 111, 116

Schuhmann's scattering, module 23
screening 20, 27
secondary mechano-chemical processes 12, 147, 161, 168
sedimentation 20–27, 123
sedimentometers 21
selenides 152
sericite 123, 152, 159, 165
siderite 159
silicate(s) 12, 34–35, 44, 51–54, 57, 65–66, 71, 74, 83–84, 92–93, 97–98, 116, 123–124, 126–131, 133, 137, 152, 155–157, 159, 161–166, 170–171, 175, 184, 195–200, 203, 225
silicon chloride, $SiCl_4$ 164, 169
– dioxide, SiO_2 149, 153, 166, 181, 184, 193–194 196
silicones 119, 123
silicon tetroxide anion, SiO_4^{4-} (tetrahedra) 53–54, 65, 78, 84, 105, 162, 177, 197
sillimanite 45
silver sulphate, Ag_2SO_4 165
sintering 151
slags 121–122, 203
Smekal's view 14, 112
soaps 116, 121
sodium carbonate, Na_2CO_3 119, 158, 166
– chloride, NaCl 63, 71, 149, 159
– fluoride, NaF 116
– hydrogen carbonate, $NaHCO_3$ 158
– hydroxide, NaOH 116, 119

sodium carbonate, Na_2CO_3
– oleate 116, 119
– oxide, Na_2O 188
– silicate 116
– stearate 121
solid bodies 18
solubility 51, 160, 169, 173, 178, 184, 193, 218, 222–225
Sorel-cement 193
sorosilicates 53–54
specific grindability 78–80, 84
– surface (area) 13–15, 27–36, 80–81, 84–87, 89, 91–93, 98, 100, 110–112, 119–120, 123–124, 127, 132, 138, 151, 169, 173, 181, 188, 197, 199, 206, 221–222, 225
– surface (free) energy 13–14, 68, 73, 92, 98, 106, 112, 115–116, 138, 151, 223
sphalerite 152
spinel 196–197
SPV system 17–19, 31–33, 38, 99–101
Stoke's law 20
strength 11, 49–50, 57–58, 66–67, 69, 71, 77–79, 83, 107, 109–110, 115–116, 121–122, 196, 202–203, 205, 214–215, 217, 221
stress 44–52, 55–57, 61, 66–67, 69–70, 73–74, 148, 150, 152
– analysis 44, 46, 49–50, 52
structural changes in crystals (see changes in crystal structure) 147, 150, 154–155, 171, 174, 178–179, 184, 188, 189
sulphates 116, 156, 163, 165–166, 168–169
sulphides 116, 152–153, 163–165
surface activation 15, 161–163, 224
– active agents, surfactant 13, 105, 108, 114–117, 119–127, 130, 137–138, 201, 217, 220
symmetry of crystals 52–53

talc 78, 123, 170–171, 175–176, 194–196, 200
tantalum carbide 150
tectosilicates 53–54, 171
"third" theory by Bond 81, 111
thixotropy 204
titanium 155
– chloride, TiCl 116
– oxide, TiO_2 193–194
tobermorite 157, 202
topaz 78
"total" specific surface 14, 28–29, 33, 36, 94, 98, 100, 124, 127, 179, 221, 223–224
translations 57
tribo-chemistry 11, 163
tribo-luminescence 74, 149
tridymite 45
triethanolamine (TEA) 120–122, 124, 128–137
Tromp curves 216
turbidimetry 29

uniformity coefficient (factor) 24–25, 29, 94, 96–98, 111, 127, 129, 214–216, 220

vanadium carbide 150
van der Waals forces 13, 55, 93, 107–109
vaterite 152
vibration mill 13, 15, 55, 71, 93, 99–100, 107–109, 113–114, 120, 122, 148–150, 156, 158–159, 164, 166, 170–171, 174, 176, 178–182, 193–194, 198, 202, 206, 214, 217–218, 220–225
Vicker's hardness 78
Vinsol 123
viscous solids 47
voids 18, 28, 32, 40
"volume" theory by Kirpichov and Kick 110

wastes 202
water 14–15, 34, 39, 44–45, 52, 119–121, 123, 156–158, 162, 173, 179, 182, 188, 190, 193, 197, 199–200, 204, 205, 217
– vapour 34–35, 98, 100, 116, 120, 158, 167, 197
whiskers 58, 71
wollastonite 123, 201
work of deformation 47
wurtzite 152

xerogel 66, 178

yield point 46, 48, 50, 55

Zeisel's method 79–84
zeolites 170, 175, 196, 198, 205
zeta potential 117, 120
zinc 154, 162
– carbonate, $ZnCO_3$ 157
– oxide, ZnO 157, 162, 164
– sulphide, ZnS 152–153, 164
zirconium nitride 150
– dioxide, ZrO_2 153, 184

Bibliotheca Academiae Scientiarum Hungaricae * MAGYAR TUDOMÁNYOS AKADÉMIA KÖNYVTÁRA *

61

Mechanical activation of minerals by grinding: pulverizing and morphology of particles

by A. Z. JUHÁSZ and L. OPOCZKY

The mechano-chemical aspects of minerals and grinding are discussed on the basis of a critical review of the literature and own experimental results. Phenomena accompanying grinding (particle interactions, changes in crystal structure, mechano-chemical reactions) and their effect on the quality of the product and the energy requirement of size reduction are dealt with in detail. A new morphological classification of disperse systems is presented as well as the mechanism of the action of surface active agents, the application of grinding aids, the methods of characterization of disperse systems, and a description of the most widely used grinding-activating equipment.

The book will be of interest for those engaged in teaching, research and production in the following fields: size reduction in the silicate, pharmaceutical, food and pigment industries, ore, coal and mineral dressing, etc.

ISBN 963 05 5329 5

Akadémiai Kiadó, Budapest

Juhász and Opoczky

MECHANICAL ACTIVATION OF MINERALS BY GRINDING

pulverizing and morphology of particles

1.5.6.4.1.9